To my Dad who taught me honesty and perseverance

To my Mum who always lifted me up when I fell

To my nephews for whom I set an example and for whom I try to be the best

To all my amazing family because family means that no one is abandoned or forgotten

To Sean my rock and my love of today and hopefully of the rest of my life…

"Risk-taking is the cornerstone of empire."

Estée Lauder

"Great minds discuss ideas, average minds discuss events, small minds discuss people."

Eleanor Roosevelt

"When I thought I couldn't go on, I forced myself to keep going. My success is based on persistence, not luck."

Estée Lauder

"In the old days, you had a lot of ideas, but you didn't have enough craft and experience"

Carlos Benaim

Acknowledgements

I would like to start by thanking Dr Tatiana Bernardi who was the first person I worked with during my PhD and who trained me in new subject areas with great professionalism but maintained an outstanding human profile and kindness. She has always been extremely respectful towards me and my work and always provided me guidance in the best possible way, being open to all my suggestions and ideas and helping me, with her experience, to understand when they were good and when they weren't, without ever taking over. She is someone who revealed to be a person I can rely on even after we completed our project together, a friend, thank you Tati.

I want to thank Prof. Stefano Manfredini who accepted me in the PhD giving me opportunities to grow through the challenges he set me along the way and for always being able to break the tension with a funny joke. Dr Anna Baldisserotto for help and training on the work with the dermatophytes and Dr Elisa Andreotti.

I want to thank Dr Biagia Musio who helped me out particularly in the final part of the project that I designed and developed in Cambridge and for being able to overcome our personal differences and support me. She cared for me as a big "rompi palle" sister and I know you will miss my "intimidating e-mails…."

I have to also thank Sabine ("Bine"), Sonja and Sean for all the morning chocolate they left on my desk, the dinners together and the stupid jokes in the lab. Thanks are also due to Guy my bay/desk lab mate for the conversations and the unexpected sense of humour. He is someone who set the example for me to follow as a scientist and has gained my deep respect for his honesty and his genuine kindness.

I will bring a piece of you along all my life. Thanks so much guys!

I would also like to acknowledge all the external collaborators I worked with during my PhD. I especially want to thank Prof. Andreas Bender and Prof. Oliver Werz who joined the project with enthusiasm as soon as I contacted them, but, more than everything, for the incredible respect they treated me with and for being willing to discuss ideas with me although I was new to their respective fields. Thanks to this opportunity, I gained the chance to widen my knowledge and to investigate fields I had no prior experience in which also enabled me to shape my project in a more complete way.

I want to thank my proof-readers Dr Tatiana Bernardi, Dr Anna Baldisserotto and especially Dr Sean Newton who has been forced to proof read all the work (given he is a native English speaker).

Enormous thanks go to my three crazy friends Silvia, Marta and Enrica – it is nice to know that no matter where we are in the world or what challenges we will be face, we are always there for each other.

The biggest thanks go to my loving family and especially to my nephews (Elena, Massimo and Leonardo) that I love with all my heart. Without their support I would not be at this point in my life and would not have been able to cope with the challenges I have faced over the past few years. It makes me incredibly proud knowing they look up to me and that I can inspire them, even just a little, and knowing that Massimo wants to become a chemist and Elena a botanist. This thesis is dedicated to them, with the wish they will be able to follow with commitment their passions.

Finally, I want to express my incredible gratitude to Steve for the opportunity to work in his group for 18 months during my PhD and for the incredible generosity he has shown to myself and everyone in the group. I want to thank him for turning me from a pharmacist into a little chemist as well for all the support and for trying to make me understand that my project was good (even if it wasn't Spirodienal A).

TABLE OF CONTENTS

Abbreviation and Acronyms

A	Selectivity factor
AA	Amino acids
A.C	*Artheroderma cajetani*
AMD	Automated Multiple Development
ARA	Arachidonic acid
ARE	Antioxidant responsive element
BTF	Trifluorotoluene
CuAAC	Copper catalysed azide–alkyne cycloaddition
COX	Cyclooxygenase
DCC	Dicylohexylcarbodiimide
DCM	Dichloromethane
DMAP	Dimethylaminopyridine
DETAPAC	Diethylenetriaminepentaacetic acid
DMSO	Dimethyl sulfoxide
DIPEA	*N*,*N*-Diisopropylethylamine
DMPD	Dimethyl-4-phenylenediamine
DPPH	2,2-Diphenyl-1-picrylhydrazyl
DPPH•	2,2-Diphenyl-1-picrylhydrazyl radical
ε°	Power of adsorption
EC	Endothelial cells
EC_{50}	Half maximal effective concentration
EDTA	Ethylenediaminetetraacetic acid
EETs	Epoxy-eicosa-tetraenoic acids
E.f	*Epidermophyton floccosum*
eq.	Equivalents
ET	Single electron transfer
FAO	Food and Agriculture Organization
FBS	Foetal Bovine Serum
FCR	Folin–Ciocolateau
FDA	Food and Drug Administration

FLAP	5-Lipoxygenase activating protein
FOS	Fructo-oligosaccharides
FRAP	Ferric reducing antioxidant power
GSH	Glutathione peroxidase
HAT	Hydrogen atom transfer
HETP	Equivalent Height of Theoretical Plates
HPLC	High Performance Liquid Chromatography
HPTLC	High Performance Thin Layer Chromatography
HRMS	High Resolution Mass Spectrometry
IE-HPLC	Ion Exchange High Performance Liquid Chromatography
IC_{50}	Half maximal inhibitory concentration
IOU	Inhibited Oxygen Uptake
K	Partition coefficient
k’	Retention factor
k	Velocity constant
LG	Leaving group
LXs	Lipoxines
5-LO	5-Lipoxygenase
Log P	Partition coefficient
LTs	Leukotrienes
mPGEs	Microsomal associated prostaglandine E synthase
M.c	*Microsporum canis*
M.g	*Microsporum gypseum*
MOM	Methoxymethyl
N	Number of theoretical plates
NOS	Nitric oxide synthase
OPLC	Over Pressured Layer Chromatography
ORAC	Oxygen Radical Absorbance Capacity
P’	Polarity parameter
PEC	Planar Electro Chromatography
PBP	Polar Bonded Phase

PMNL	Human polymorphonuclear cells
r	Optimisation parameter
R_f	Retention factor
RPC	Rotation Planar Chromatography
RP-HPLC	Reverse Phase High Performance Liquid Chromatography
ROS	Radical Oxygen Species
RNS	Reactive Nitrogen Species
Rs	Resolution
rt	Room temperature
S	Separation factor
SAR	Structure–Activity Relationship
SEM	[2-(Trimethylsilyl)ethoxy]methyl
SDA	Sabouraud Dextrose Agar
SOD	Superoxide dismutase
TBS	*tert*-Butyldimethylsilyl
TE	Trolox Equivalent
TEAC	Trolox Equivalent Antioxidant Capacity
TIPS	Triisopropylsilyl
TLC	Thin Layer Chromatography
TPTZ	2,4,6 tripyrididyl-s-triazine
TRAP	Total Radical Antioxidant trapping Parameter
T.m	*Trichophyton mentagrophytes*
T.r	*Trichophyton rubrum*
T.t	*Trichophyton tonsurans*
T.v	*Trichophyton violaceum*
XOS	Xylo-oligosaccharide

Abstract

The term *phytochemicals* refers to chemical compounds derived from plants, (*phyto* derives from ancient greek meaning *plant*), able to exert a beneficial effect on human health.

Phytochemical is a definition that was made up from pharmaceuticals and nutrition[1] and they are contained mainly in edible plants, thus they can also be defined as food or part of food that improves human health preventing or healing disease.[2] Classes of phytochemicals include alkaloids, phenolic compounds, carbohydrates, organic acids and vitamins and they are used in the nutraceuticals industry as components in food supplements.

They have gained an increasing amount of attention over the last few years given their recognised health benefits, their availability from sustainable sources and the fact that in the food supplement market, where they are largely employed, it is not necessary to gain the approval of the FDA to commercialise them.

This opens up an issue related to fraudulent products with a non-defined or fake composition.[3]

In the work herein presented, two of the main classes of phytochemicals were considered:

- Soluble fibre (carbohydrate polymers such as fructo-oligosaccharides) and their novel characterisation methods
- Polyphenols derived from consumable sources: structure–activity relationship (SAR) studies of their semi-synthetic analogues

The application and development of innovative methods for the characterisation of bio-polymers (soluble fibre) is crucial, primarily for the food and nutraceutical industry given the lack of rapid and efficient analytical methods for the quality control of those phytochemicals in foodstuff.

It is a compelling issue especially giving that the presence of soluble fibre is used to claim prebiotic activity for the food product. It is worth mentioning that the term *soluble fibre* is specific to certain structures classes e.g. inulins and fructo-oligosaccharides etc.

Characterisation of such materials, up until now, has been done by mass difference. However, it is clear that this cannot be sufficient to support their presence and the claims associated with it in nutraceuticals and foodstuff and so precise analytical methods and more precise characterisation is essential.

Thus the first part of this work focuses on the application of a novel High Performance Thin Layer Chromatography (HPTLC) based method which was developed using samples of *Adansonia digitata* fruit pulp to demonstrate this approach given the reported prebiotic activity of this essential food.

The second part of this thesis focuses instead on structure–activity relationship studies of food phytochemicals and their semisynthetic analogues on selected targets. Within that research line new polyphenol analogues were designed, synthesised and evaluated on different targets in order to determine their potential as multi-target compounds.

Polyphenols have attracted great interest in the field of medicinal chemistry considering their reported anti-cancer, anti-inflammatory, anti-oxidant, anti-artherosclerotic properties, as well as neuro- and cardio-protective activities. They have been used in prebiotics, pharmaceuticals, cosmetics, nutraceuticals and can be extracted from renewable sources such as tea leafs, grapes, cocoa seeds and vegetables. Unfortunately, due to their poor solubility properties in aqueous media and rapid in vivo metabolic breakdown they are yet to be exploited to their full potential.

The fact that they have not exploited to their full potential yet, make this class of phytochemicals interesting to work on, in order to try to solve the discussed issues related with them and to expand the project scope further.

1. Introduction to Novel Characterisation Methods in Phytochemicals

1.1. History of Chromatography

Until the 1930's, adsorption chromatography technique conceived by Tswett (1872-1919), was the method commonly used in the analysis of natural extracts. The necessity of having a quick method to identify the different components of the mixture under analysis led to the invention, by Izmailov and Shraiber in 1938, of an "open" chromatographic method – thin layer chromatography (TLC). In 1944 Consden et al. changed the approach to partition chromatography using paper,[4] which from that moment onwards quickly became universally used as stationary phase. In 1951, Kirchen and coworkers then introduced a fluorescent indicator in the stationary phase, which led to silica gel becoming the new preferred stationary phase for TLC. The term *thin layer chromatography* was created by Stahl in 1956 and from there Merck created other kind of thin layers to be used as stationary phase, such as aluminium oxide layers. It is at the end of the 1970's that High Performance Thin Layer was commercialised and thus the technique HPTLC started to develop from 1987 when Geiss published the manual "*Fundamentals of Thin-layer Chromatography"* and in 1988 the *Journal of Planar Chromatography* was born.

1.2. Chromatography Theoretical Principles

The first principle underlying chromatography is the "affinity" that the analytes contained in the samples move in the system in relation to their affinity towards the mobile and stationary phase. Each analyte in a given chromatographic system has a partition coefficient K (Equation 1.2.1) that is the ratio between the substance concentration in the stationary phase (C_s) and the mobile phase (C_m).

$$\mathbf{K = C_s / C_m}$$

Equation 1.2.1 Calculating the partition coefficient.

Assuming that the sample provided is soluble in both phases, it would distribute itself between the two until reaching the partition equilibrium. Although it can appear that the substances move with a different speeds, in reality and in accordance with the solubility of each analyte in the mobile phase, some substances will leave the column faster than others (most soluble in the eluent are less retained by the stationary phase). This results in shorter retention times in High Performance Liquid Chromatography (HPLC) or advancing to higher

retention factor, R_f,[†] values on TLC plates. Substances which possess higher solubility in the eluent, migrate less often per unit time.

In thin layer chromatography several factors contribute to determine the R_f such as:

1. Dimension and model of the chamber
2. Composition and dimension of the thin layer
3. Flux direction of the mobile phase
4. Volume and composition of eluent
5. Humidity
6. Sample preparation

The most relevant mechanism in TLC are the following:

1.2.1. *Adsorption*

The stationary phase is generally a solid (although it can occasionally be an immobilised layer of liquid) and on the surface the analyte interacts either specifically or non-specifically. The degree of retention depends on the functional groups on each analyte and on their steric structure. In "normal phase chromatography" the mobile phase is less polar than the stationary. There are two models explaining the mechanism of adsorption chromatography. According to the model of Snyder[5] and Soczewinskithe,[6] the mobile phase competes with the analytes to be retained by the thin layer and the samples displace the eluent molecules from the adsorption site on the stationary phase. The model of Scott and Kucera,[7] instead, shift the focus on the interaction between the mobile phase and the sample. Both models are valid mainly depending on the composition of the eluent.

1.2.2. *Partition*

Partition chromatography is based on the different solubility of the substances in the samples in two immiscible liquid phases. The stationary liquid phase is immobilised on a solid usually porous support, either by absorption or chemical bonds. In the case of using *polar bonded phase* (PBP) such as a diol bonded phase (useful for carbohydrates) the mechanism is more complicated and adsorption must be considered as well.

[†] R_f is defined as the difference between the substance position on the TLC plate and the eluent front.

1.2.3. *Complex Formation*

The retention principle is another possible mechanism and it is based on the reversible formation of coordinated complexes between Lewis acids and bases. This system is particularly useful in separating compounds according to the degree of saturated bonds or steric effects (chiral compounds can also be separated through complex formation). In this type of chromatography, the stationary phase can be impregnated with Lewis acids, such as metal ions. Other separation mechanism include:

- Ion-exchange chromatography
- Size exclusion chromatography
- Inclusion chromatography

1.3. Thin Layer Chromatography

1.3.1. *Planar Chromatography*

High Performance Thin Layer Chromatography (HPTLC) is the most recent application of planar chromatography and together with column chromatography is a developing field. The stationary phase in TLC is a thin layer of solid material immobilised on a plain support.

Is common to place the TLC plate vertically in the TLC closed chamber with the eluent – the mobile phase exploits the capillary forces to proceed on the stationary phase and move the analytes along it until the plate is removed from the chamber. Capillary forces are weak and generated by the eluents decrease in free energy when it starts interacting with the porous matrix of the TLC plate.

The research on TLC has recently produced new technologies (Figure 1.3.1) to enable the technique not only to become more reproducible and efficient but also to enable quantitative as well as qualitative analysis. The stationary phase, sample deposition, elution and detection are critical points and thus several tools to better control these steps have been introduced, such as:

- High performance thin layer plates which have the same characteristic of stationary phase of HPLC columns
- Automated tools for sample deposition
- New elution systems

- New techniques for plate analysis, such as densitometry (which also enables quantitative analysis)

The main innovations in terms of elution phase has been AMD (Automated Multiple Development) in which the developing chamber is hermetically sealed and the environment is controlled under an atmosphere of nitrogen. This is in order to avoid the contact with oxygen which could induce the eventual oxidation of the analytes. Furthermore, this controlled atmosphere prevents the eventual adsorption of water on the thin layer (due to humidity) which could affect the separating ability of the thin layer. This technology also enables very high efficiency through the possibility of realising multi-step gradients as the one presented in this dissertation.

Another innovation in modern TLC is given by the *forced flow* systems that enable the user to increase the speed of the flow or to keep it constant.

OPLC (Over Pressured Layer Chromatography) was introduced in the 1980's. In this technique, an inflatable cushion exerts an adjustable pressure on the TLC plate and a pump pushes the mobile phase through the stationary. This enables optimisation of the flow speed and removal of the vapour phase from the system.

HPTLC (High Performance Thin Layer Chromatography) use the pressure to move the mobile phase.

In **RPC** (Rotation Planar Chromatography), the plate of the stationary phase is round. The sample can also be applied inline with the mobile phase besides applying it before the development as in the other TLC technique. The development mode can proceed from the centre of the plate outwards or from the outside towards the centre.[8]

Among the forced flow methods **PEC** (Planar Electro Chromatography) should be mentioned as another recent development. It is based on an *electroosmotic flow* technique generated applying an electric field along the chromatographic system. To date, this is used only in the characterisation of ideal mixture.[9]

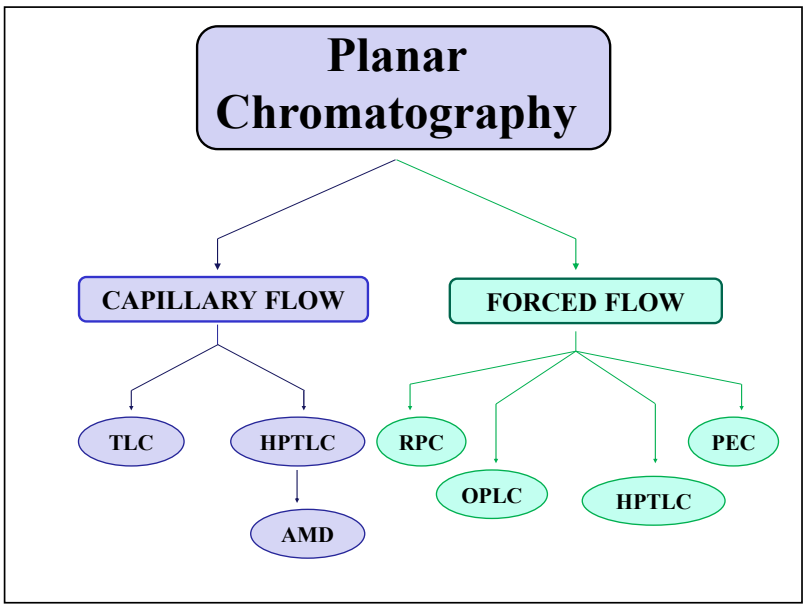

Figure 1.3.1 Planar Chromatography techniques: TLC (Thin Layer Chromatography); HPTLC (High Performance Thin Layer Chromatography); AMD (Automated Multiple Development); RPC (Rotation Planar Chromatography); OPLC (*O*ver Pressure Thin Layer Circular Chromatography); PEC (Planar Electro Chromatography); RPC (Rotation Planar Chromatography).

1.3.2. *Chromatographic Parameters*

Some of the fundamental parameters in TLC, beside the retention factor R_f are:

- Partition coefficient **K**
- Retention factor **k'**
- Selectivity factor **α**
- Separation efficiency
- Equivalent height of theoretical plates (**HETP**)
- Number of theoretical plates (**N**)
- Resolution **Rs**
- Separation factor (**S**)
- Optimisation parameter **r**
- Velocity constant **k**

The partition coefficient **K** is a thermodynamic constant which describes the partition equilibrium between the mobile phase and the stationary phase of a given analyte **A** (Equation 1.3.1).

$$\mathbf{K} = [A_{stationary}]/[A_{mobile}]$$

Equation 1.3.1 *Equation for the partition coefficient.*

The retention time **k'** is, instead, a kinetic constant, which can be experimentally determined. It describes the speed of analytes along a chromatographic system. It is defined as the ratio between the time that the solute spends in the mobile phase and the time it spends in the stationary phase. It can also be described as the ratio between the amounts of solute in the two phases in a precise moment.

In planar chromatography, to efficiently separate two compounds, the chromatographic system must be selective and the compounds need to be retained to a different extent. This means that the partition coefficients of the species under analysis have to be sufficiently different to result in a selectivity factor higher than 1.

The selectivity factor **α** is described as the ratio between the partition coefficient of the two species under analysis, and $K_1 > K_2$ (Equation 1.3.2). Thus factor α is always > 1.

$$\alpha = K_1 / K_2$$

Equation 1.3.2 *Equation for the selectivity factor α.*

The separating efficiency in chromatography, also depends on the band widening – the wider the band the lower the separation efficiency. Band widening is a phenomenon dependent on several factors such as turbulent and molecular diffusion, mass transfer effects and retention mechanism of solute that is specific of any system mobile phase/solute/stationary phase.

Each of the effects mentioned above are more or less determined according to the characteristic of the chromatographic system.

The band widening in TLC means an increase of the surface area of the spots, in capillary flow conditions the determining factors are connected to the dimensional distribution and the average size of the stationary phase. If the particles have an average size around 12 μm and are characterised by irregular shape and distribution, the band widening depends on the packing quality, related to the turbulent movements and to the mass transfer process that are particularly slow. The efficiency in this case is limited by the entity of those effects.

In stationary phases characterised by smaller particle size, with homogenous distribution and steric shape (high performance thin layers) and short migration distances the phenomenon is regulated only by the particle size (optimal particle size are around 5-6 μm).

The development of high performance thin layers has enabled thin layer chromatography to discuss separation efficiency through the following concepts: **HEPT** the height of the theoretical plates[‡] and the number of theoretical plates (Equation 1.3.3).

$$\mathbf{N} = \frac{L}{\mathrm{H}}$$

Equation 1.3.3 *Number of theoretical plates as ratio between migration distance of mobile phase L, and height of theoretical plates H.*

The theoretical plate number depends on the migration distance of the mobile phase, migration distance of solute and on the amplitude of the spot in the direction of the development. The packing and the particle size of the stationary phase are critical for band broadening during analysis. HEPT can also be seen as the ability of the system to reduce band broadening giving narrow bands.

Fundamental in chromatography is the Van Deemeter Equation (Equation 1.3.4) as it links the different factors contributing to band broadening.

$$\mathbf{H} = \frac{\mathrm{A} + \mathrm{B}}{u + \mathrm{C}} \cdot u$$

Equation 1.3.4 *Van Deemeter equation.*

In the above equation, **H** is the height equivalent to a theoretical plate, **A** is constant term dependent on the average particle size and homogeneity of the stationary phase and **C** is constant and is related to longitudinal diffusion (it becomes less relevant with the increase of u which is the flow speed in cm/s). The term **C** instead is related to stationary phase mass transfer.

Given that in HPTLC the particle size is reduced and homogeneity increased compared to a conventional TLC plate, the band broadening is reduced (Figure 1.3.2).

[‡] The height of theoretical plates (HETP) is the ability of a chromatographic system to generate sharp peaks

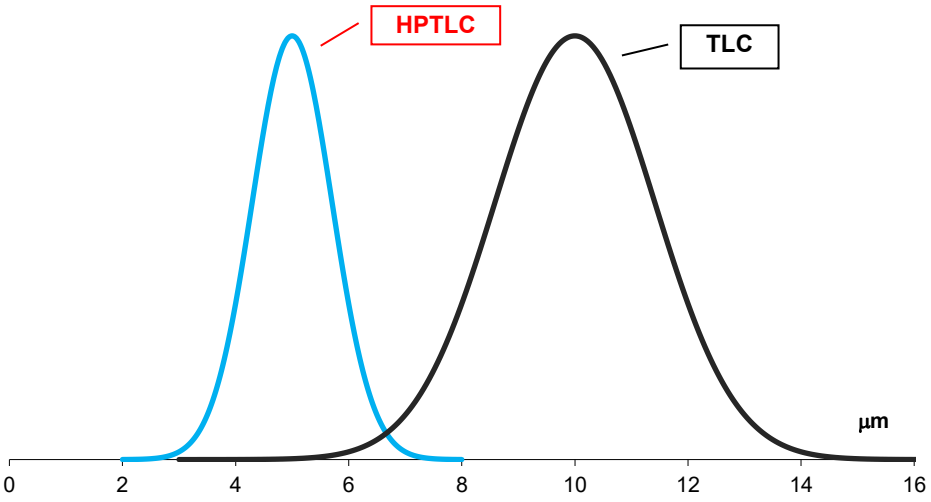

Figure 1.3.2 *Particle size distribution of the stationary phase in HPTLC and TLC.*

The flow also depends on the stationary phase as well as the characteristic of the mobile phase and for this reason, the effect of varying the mobile phase has on the eluent strength is studied in the optimisation of the gradient.[10]

Another parameter to take into account is the resolution $\boldsymbol{R_s}$ between two peaks in the chromatogram, which express the separation between two compounds.

It depends on selectivity factor **α**, plate number **N** and **k**' capacity factor (Equation 1.3.5). In general, it is the combination of stationary and mobile phase to determine the system resolution.

$$\mathbf{R}_s = {}^1/_4\,(\alpha - 1)N^{1/2}({}^{k'}/_{1+k'})$$

Equation 1.3.5 *Equation for the resolution* $\boldsymbol{R_s}$.

1.3.3. *Stationary Phase*

In thin layer chromatography, the stationary phase involves two principles: adsorption and partition. In adsorption chromatography, the two main factors determining the activity of the stationary phase are the dimension of the area of the activated surface and the surface energy for surface unit. The activated area affects the number of adsorption process that can happen, all together, and effect of the deactivators on separation. The wider the activated area the lower the deactivators. For hydrophilic stationary phase (as for silica gel or alumina), the main deactivator is water.

Variation in the activated surface area can affect:

- Spots dimension
- Rf values
- Selectivity
- Speed migration of eluent front
- The position relative to multiple fronts that are often formed when the mobile phase is constituted of several solvents

The surface energy affects the strength of the adsorption interaction and it is generally assumed that this value is independent from the surface activated area. However, its average value for surface unit decreases with increasing the deactivation's effect. The surface energy reaches a stable value when 20 to 50% of the active sites have been deactivated. The highest energetic sites are the ones that are deactivated first. The Snyder equation relates the activities of stationary phase with characteristics of the analyte and solvent.[11]

It shows that separation efficacy is strongly dependent on:

- Particle size (μm)
- Specific surface area (m^2/g)
- Diameter (Å) and pores volume (mL/g)

The most common adsorbing material used (~80% of cases) is silica gel. Its activated surface contains free silanol groups (-Si-OH), which are responsible for the polar characteristics of silica layer, and siloxanes groups (-Si-O-Si-). Silica 60 most widely used and has an average pore diameter of 60 Å.

Alumina is another stationary phase commonly used (normally for acid sensitive compounds) and. It is highly polar and possesses characteristics of both cationic and anionic exchange. Stationary phase for partition chromatography are generally modified (Figure 1.3.3).

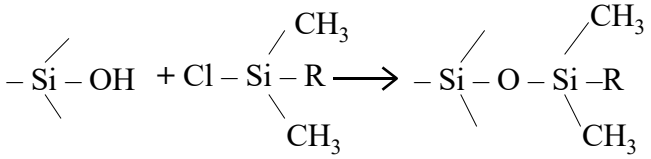

Figure 1.3.3 *Modified stationary phase.*

R can either be an alkyl group, for hydrophobically modified (reversed phase , RP) layers, or a substituted alkyl group in the case of hydrophilic thin layers.

The main alkyl groups in reversed phase are methyl, octyl, dodecyl, octadecyl. The hydrophobic character of those phases depends on chain length and on substituent R, the longest the less polar, and from the degree of modification of the support (its degree of porosity affects the efficiency of substitution).

The R of the hydrophilic modified thin layers instead are functional groups of different polarity, such as the ciano (– C_2H_4**CN**), the diol (– $C_3H_6OCH_2CH$**OH**CH_2**OH**) and the amino groups (– C_3H_6**NH₂**)[12].

1.4. Development Solvent

The characteristics that the development solvent should possess are purity grade, chemical stability, low viscosity and easy handling. During the solvent selection process, its strength and selectivity must be considered. Solvent strength is defined by three main parameters: Hildebrand solubility parameter (**δ**), power of absorption (**ε°**), and polarity parameter (**P'**).

Hildebrand solubility parameter δ constitutes a measure of the degree of molecular interaction (Van Der Waals) of the solvent. It represents the density of cohesive energy (**c**) of the solvent and is experimentally obtained through Equation 1.4.1, in which ΔH is the vaporisation heat, R the fundamental gas constant, T the boiling point of the solvent, V_m the molar volume of the solvent.[13]

$$\delta = \sqrt{c} = \sqrt{\frac{\Delta H - RT}{V_m}}$$

Equation 1.4.1 *Hildebrand solubility parameter.*

The power of absorption ε° is the main parameter to consider in adsorption chromatography. Snyder defined in Equation 1.4.2, where $\mathbf{E_{Sa}}$ refers to the adsorption energy and $\mathbf{A_s}$ is the molecular surface occupied by the solvent.

$$\varepsilon^\circ = \frac{E_{Sa}}{A_S}$$

Equation 1.4.2 *Equation for the power of absorption factor* $\boldsymbol{\varepsilon^o}$.

In Snyders definition it is assumed that the adsorbent surface is completely occupied with solvent (S) and solute (X) and compete with one another according to the equilibrium reported in Equation 1.4.3. In Equation 1.4.3, $\mathbf{X_a}$ and $\mathbf{S_a}$ refer to adsorbed molecules of solute and solvent respectively, whereas $\mathbf{X_m}$ and $\mathbf{S_m}$ refer to molecule that have not been adsorbed of solute and solvent respectively.

$$n\ S_a + X_m \leftrightarrows X_a + n\ S_m$$

Equation 1.4.3 *Adsorption equilibrium.*

The overall retention equation in adsorption chromatography is shown below (Equation 1.4.4).

$$Rm = \log\left(Va\frac{Wa}{Vm}\right) + \alpha \cdot \left(X^{\circ} - A_X \varepsilon^{\circ}\right)$$

Equation 1.4.4 *Retention equation used in adsorption chromatography.*

The highest interactions between the solute and the adsorbent will result in a higher *Rm* and consequently the constant **k'**, and lower *Rf*. The optimal value for **k'** is between 2 and 5 for a bi-component sample and between 0.5 and 20 for a multi-component sample.

The parameter most widely used in partition chromatography (although it is also used in adsorption chromatography) is the polarity parameter **P'**, experimentally defined as the sum of the solubility's in the solvent under examination of three standard molecules: ethylic alcohol (hydrogen donor), dioxane (hydrogen acceptor) and nitromethane (high dipole moment). It can range between -2 and 10.2 (which is water polarity).

It is common practice to use a mixture of solvents in order to adjust the eluent strength for specific applications. **P'** in a mixture of **n** components is defined according to Equation 1.4.5, where Φ is the volume fraction of the compounds and $\mathbf{P'}_i$ is the mean of the polarity of the pure components.

$$\sum_{i=1}^{n} P'_i \cdot \Phi_i$$

Equation 1.4.5 *Equation for the mean polarity of pure components.*

It is worth mentioning that the solvent strength depends on the interactions with the stationary phase and it increases with its polarity in normal phase chromatography (instead in reverse phase it decreases).[14,15]

Solvent selectivity is determined by molecular interactions and can affect the separating efficiency power through polarity and hydrogen bonds. The dispersion forces cause fluctuant polarisation constantly moving on the molecular surface, which induce weak attractive forces. These are the only components of the molecular interaction of polar solvents. The degree of polarity that the temporary dipoles confer to a molecule are related to the surface area, thus the bigger the molecule the bigger the interactions.

Hydrogen bonds can instead be evaluated from the point of view of the interactions between electron-donors and electron-acceptors and the reactivity can be described of Lewis acid-base. A practical method to represent the total composition is the construction of a selectivity triangle.

Assuming that the Hildebrand value **δ** is the same for all substances it can also be assumed that the solubility characteristic of compounds are determined not from the differences in the total value of **δ**, but from the contribution related to the three interactions forces that compose it.

$$\delta_T = \delta_D + \delta_P + \delta_H$$

Equation 1.4.6 *Hildebrand total parameter.*

In Equation 1.4.6, δ_T is the Hildebrand total parameter, δ_D is the dispersion component, δ_P polar component and δ_H hydrogen component. Based on this hypothesis, the fractional parameters ***f*** (Equation 1.4.7) which represent the percentage contribution to the three components are reported on the side of a triangle.

$$f_D = \frac{\delta_D}{\delta_D + \delta_P + \delta_H} \qquad f_P = \frac{\delta_P}{\delta_D + \delta_P + \delta_H} \qquad f_H = \frac{\delta_H}{\delta_D + \delta_P + \delta_H}$$

Equation 1.4.7 *Equations for the three components.*

In this way, it is possible to obtain a selectivity triangle in which each spot of the area represent a precise force composition. The Teas triangle (Figure 1.4.1) has a theoretical meaning more than a practical one. This because solvents are not all equivalent and so the solvents localisation in the triangle needs to be adjusted with experimental results. The triangle is mainly an empirical system.

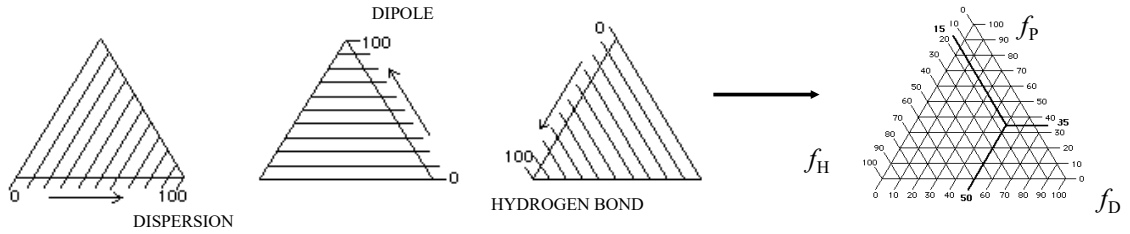

Figure 1.4.1 *Teas triangle.*

Snyder has described a triangular selectivity of solvents as well. Its definition takes into account the dipolar interaction, proton-acceptor and proton-donor characteristics, which are the parameters that define the polarity parameter P'. Relating to these parameters the fractional values x that locate the solvents on the triangle are xd, xa and xn (Equation 1.4.8).

$$x_d = \frac{\text{ethanol solubility (H - donor)}}{P'}$$

$$x_a = \frac{\text{dioxane solubility (H - acceptor)}}{P'}$$

$$x_n = \frac{\text{nitro - solubility - methane (dipol)}}{P'}$$

Equation 1.4.8 *Synders equations for solvent selectivity.*

Snyder also classified the solvents into eight selectivity classes**Error! Bookmark not defined.** (Figure 1.4.2).

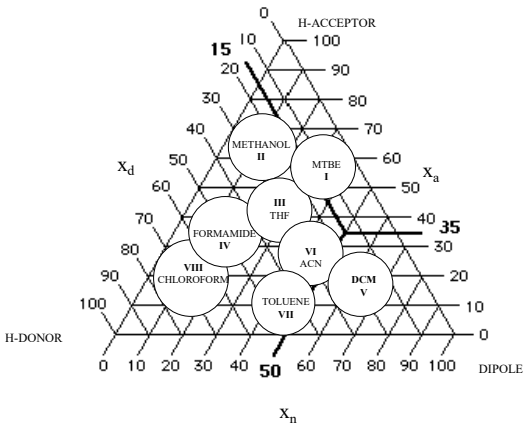

Figure 1.4.2 *Synders classification of solvents.*

In order to choose the correct solvent mixture for a separation, the optimal strength is detected and subsequently the selectivity of the solvents is considered.

1.5. Modern Planar Chromatography

As previously mentioned, critical steps in Thin Layer Chromatography are: sample deposition, elution, derivatisation and detection. With modern planar chromatography techniques, these steps are automated which enables optimisation and reproducibility of the technique.

Deposition happens by means of a microsyringe which enables the deposition of thin bands which are characterised by fixed length and homogenous distribution, small amount of sample (1-5 µL), thus avoiding overloading of the samples that would affect resolution and efficiency. This deposition method is a "*spray-on*" method (the solvent completely evaporates during the process) and deposition of samples through this automated method make the separation efficacy independent from the nature of the solvent. This also enables the operator to deposit multiple times along the same band if needed, which is very useful especially if the standard's addition method mast be used.

Figure 1.5.1 *Linomat 5 apparatus.*

Another advantage of using the automated depositor CAMAG Linomat 5 (Figure 1.5.1) is the opportunity to start from a single diluted solution and deposit different traces at different concentrations, generating multi-level calibrations with a noteworthy time saving. The sample deposited through the CAMAG Linomat 5 is nebulised in nitrogen flux. The dimension of the band, the volume of the deposited sample, the distance between the borders of the plate and the traces can be selected and saved to be reproduced iterative times.

In the elution process, using the Automated Multiple Developer (Figure 1.5.2) offers several advantages. The TLC plate is placed in an isolated and closed chamber under nitrogen atmosphere. This avoids the condensation of molecules of mobile phase on the thin layer affecting the development and it enables the speed of solvent front to become independent from the saturation degree of the vapour phase. Operating in controlled atmosphere also

enables to avoid the deactivation effects exerted by water molecules due to humidity and it enables better separation efficiency and higher reproducibility.

Figure 1.5.2 *AMD apparatus.*

The main advantage of the AMD is the possibility of ameliorating the resolution through band concentration. It enables the automated development following a multi-step gradient, in which the solvent strength decrease increasing the number of elution and this decrease is combined with an increase of the development distance.

The separating ability of this technique is comparable with HPLC methods and separation can be refined for each segment of the chromatogram. In planar chromatography it is possible to perform mono and bi-dimensional separations. In the first case, the TLC plate is developed up to a chosen length for chosen times before the development is stopped and solvent removed (the elution process takes place several times). This strategy, used in the separation of complex matrices, allows the variation of experimental parameters such as plate length, mobile phase composition in each development and the number of developments.

Weak eluents are necessary to separate substances that are less retained whereas components strongly retained are separated using stronger eluents.

Figure 1.5.3 *Immersion device III.*

An important characteristic of the development process is the concentration mechanism of the bands, which increase the efficiency of the layer counteracting the diffusion process of the zone. Each time the stationary phase compress the spot in the direction of the development, the spots that are initially round in shape, gradually turns to oval and eventually turns to be a thin band. This happens because the mobile phase firstly interacts with the molecules in the bottom portion of the spot, starting moving them, when the eluent front surpass the concentrated spot, this migrates and enlarge according the same mechanism common to thin layer chromatography.

The derivatisation of the plates is performed through Chromatogram Immersion Device III from CAMAG (Figure 1.5.3) which is an instrument composed of a dipping apparatus controlled by a timer which dips the TLC plate in a dipping chamber, enabling an homogenous and more reproducible method for derivatisation compared to the spray method normally used.

As a detection system, modern chromatography utilises densitometry scanning, which is a technique that enables not only qualitative but also quantitative determination. The instrument used is a CAMAG TLC Scanner 3 (Figure 1.5.4) interfaced with the software winCATS. According to the signals registered (absorbance or fluorescence) it produces a densitogram which is similar to a chromatogram where the peak maximum corresponds to the maximal density of the spot on the plate.

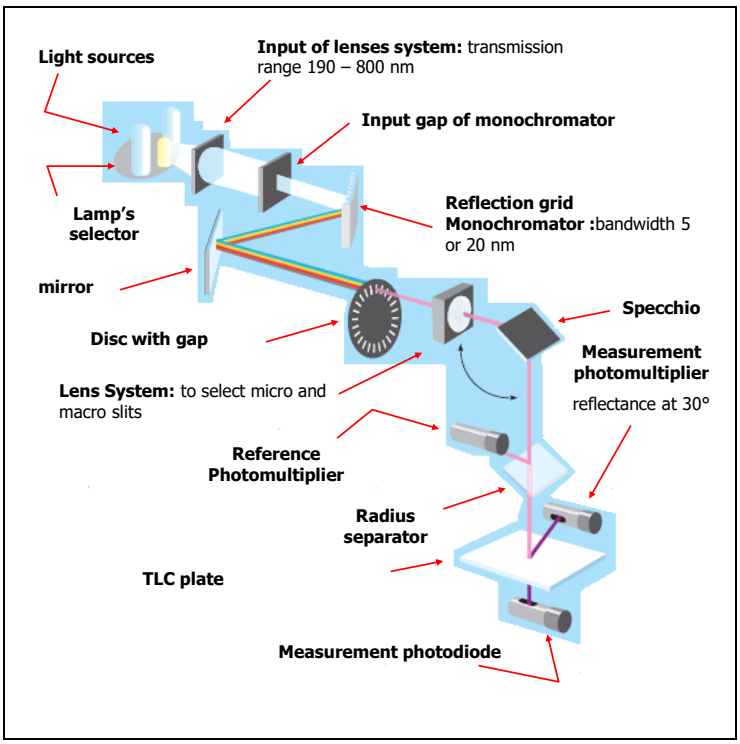

Figure 1.5.4 *Scheme of action mechanism of Scanner 3D.*

Taking into account that samples are adsorbed and dispersed in a solid matrix are able to cause light scattering, the instrument generally works by reflectance and not through transmittance. The Beer–Lambert linear expression is not usable. Normally the non-linear Kulbeka–Munk is used in HPTLC, (Equation 1.5.1) where $\mathbf{R_\infty}$ is the reflectance of an opaque layer infinitely thick, **S** is the scattering coefficient, **ε** is the molar adsorption coefficient of analyte and **c** is the analyte concentration.[16,17]

$$\frac{(1-R_\infty)}{2R_\infty} = \frac{2.303 \cdot \varepsilon \cdot C}{S}$$

Equation 1.5.1 *Kulbeka-Munk equation.*

The fluorescence measurement has a low background noise and the signal is a linear function of the quantity of sample in a concentration range between two and three orders of size. The equation in this case is shown in Equation 1.5.2, where **F** is defined as the intensity of fluorescence, **φ** is the quantum yield, $\mathbf{I_0}$ is the excitation source, **ε** is the adsorption coefficient, **b** is the TLC thickness and **c** is the sample quantity.

$$\mathrm{F} = \varphi \cdot \mathrm{I_o} \varepsilon \cdot b \cdot C$$

Equation 1.5.2 *Equation for fluorescence measurement.*

1.6. *Adansonia Digitata* and Prebiotics

The African Baobab *(A. digitata)* is a tree that belongs to the *Bombacaceae* family, gender *Adansonia*, specie *Digitata* and it spontaneously grows in Africa (one species), in Australia (one species) and in Madagascar (six species). The various species differ in the morphological characteristics of the flower. The *Adansonia digitata* fruit pulp is mainly used as food due to its high nutritional properties, (energetic value 200 kcal/100g and 836 kJ/100g). Baobab fruit pulp is 10-45 cm long and 8-15 cm large and it is covered by a hard shell (the shell has an ovoid or cylindrical irregular shape).

It is composed of a ligneous, hard and capsule-shape epicarp and it is also covered by green-yellow hair, the endocarp of the fruit constitutes its pulp.

The endocarp of ripe Baobab fruit appears off-white dehydrate and powdered and it has a characteristic acidic taste due to the presence of organic acids such as: citric acid, tartaric acid, malic acid and succinic acid. Several parts of it are used daily in the diet of rural communities in West Africa as reported by Brady (2011).[18] To support its use and as proof of Baobab relevance as multi-purpose specie, it is worth mentioning that the Forestry Department of the Food and Agriculture Organization (FAO) of the UN has reported information on *A. digitata* (FAO 1988).[19] The main reason for its use as a nutritional foodstuff and the relevance for the food industry, resides in its high nutritional values, due to the high fibre content, carbohydrates and high antioxidants content.[20,21]

The fruit pulp is also used in the traditional medicine for its prebiotic activity.[22] The term prebiotic refers to a non-digestible food ingredient able to beneficially affect the host by selectively stimulating the growth and/or activity of a limited number of bacteria in the colon leading to improvement of the host's health.[23]

Roberfroid[24] revisited the concept and concluded that prebiotics should be evaluated according to three criteria:

- Non-digestibility,
- Fermentation by intestinal microflora,
- Selective stimulation of microflora leading to health benefits.

Increasing the assumption that Baobab dry pulp leads to an increase of bifidobacteria population and lactic bacteria,[25] the gut microflora is capable of using complex sugars such

as oligosaccharides[§] such as inulins and fructo-oligosaccharides[**] (Figure 1.6.1) and xylo-oligosaccharides[††,26] (Figure 1.6.2) as a source of carbon.

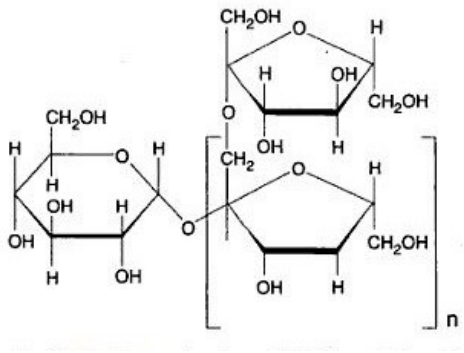

Figure 1.6.1 *Fructo-oligosaccharide structure.*

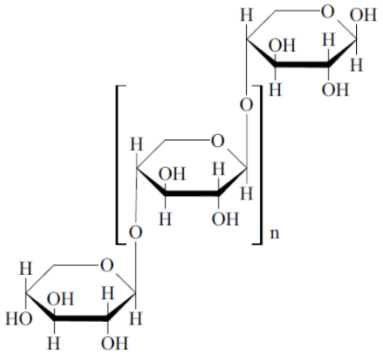

Figure 1.6.2 *Xylo-oligosaccharide structure.*

[§] Oligosaccharides are carbohydrates with a polymerisation degree ranging from 2 to 10 monomeric units.

[**] Fructo-oligosaccharides (FOS) are carbohydrates composed of glucose and fructose subunits with a polymerisation degree between 3 and 10.

[††] Xylo-oligosaccharides (XOS) are xylose polymers connected through β-1-4 composing the hemicellulose of the plants cell wall. They have a polymerisation degree between 2 and 10 and they are known as xylobiose, xylotriose, and so on. Xylobiose (DP = 2) is considered to be a xylo-oligosaccharide in food applications.

2. Novel Characterisation Methods Applied to Phytochemicals: Aims and Background

This first portion of this dissertation focuses on novel characterisation methods applied to phytochemicals. In particular, a new approach to bio-polymer (soluble fibre) determination was developed by means of High Performance Thin Layer Chromatography (HPTLC). Quality control is an important issue in the food industry; however, the lack of rapid and efficient analytical methods often hinders adequate and efficient characterisation of foodstuffs. The aim of this research was to apply a recently developed precise, reliable and green method for the qualitative characterisation of oligosaccharides in complex plant matrices, using *Adansonia digitata* as a case study.

In the food industry, it is common practice to provide technical data sheets wherein information on soluble fibre is given as a difference in mass from other components (fat, proteins, etc.). Identifying the presence of certain soluble fibres in foodstuffs is important as this is often used to claim prebiotic activity for the product.

Considering that the expression "soluble fibre" is used to refer to specific structures such as inulins, fructo-oligosaccharides, xylo-oligosaccharides etc. it is clear that the characterisation by mass difference, alone, cannot be used to support such a claim and more specific analytical methods are required.

To demonstrate the application of our novel high performance thin layer chromatography (HPTLC) method, a sample of *Adansonia digitata* fruit pulp due was used due to its previously reported prebiotic activity. High performance liquid chromatography (HPLC) was used in order to validate the results before and after hydrolytic treatment, obtained by HPTLC. Widely accepted solvent and solvent/ultrasound assisted based extraction methods were used or adapted for preparation of the samples.

In a second study, the samples were submitted to enzymatic digestion and, after optimisation of the enzymatic conditions, the polymer obtained was submitted to acid hydrolytic treatment in order to specifically identify their constituent components and confirm the results previously obtained.

3. Results and Discussion

3.1. Novel Characterisation Methods in Phytochemical Analysis

Adansonia digitata dry fruit pulp was chosen as the sample in this study due its previously reported prebiotic activity and given the relevance it has in the support of rural community in Africa. De Caluwé et al. previously showed that increasing concentrations of baobab dry pulp led to an increase in the population of bifido-bacteria and lactic bacteria because the gut microflora is able to use complex sugars such as fructo-oligosaccharides and xylo-oligosaccharides etc. as a source of carbon.[27]

Furthermore, the Forestry Department of the Food and Agriculture Organization (FAO) of the UN has reported information on *Adansonia digitata*[28] and the International Centre for Research in Agroforestry (ICRAF) continues to promote its use as a multipurpose species. It is worth mentioning that materials having low pH, high nutritional value and a relatively high content of antioxidants[29] are often promoted as a nutritious foodstuffs. Up until the start of our investigations, no detailed analyses of *Adansonia digitata* dry fruit pulp were reported in the literature – the determination was always performed by mass difference.

Initially, the aim was to apply our newly developed method to the specific characterisation of the oligosaccharides composing the *Adansonia digitata* dry pulp and to validate the method on this case study.

The detailed analysis presented herein started with the extraction of one gram of accurately weighted baobab dried pulp following (or adapting) methods previously reported by Davis et al.[30] and Wei et al.[31] or Jaime et al.[32] Samples for analysis were prepared through extraction with cold or hot water under magnetic stirring, with or without the assistance of ultrasound (Table 3.1.1).

Ultrasound has been reported as one of the most effective tools to extract polysaccharides, such as inulins, from various plants tissues,[31] whereas extractions with a mixture of methanol/water 62.5% v/v[30] and pre-treatment with acetonitrile are reported to be useful for the removal of free sugars.[33] Extraction with ethanol/water in a ratio of 70/30 was also employed.[32] Centrifugations were performed using an ALC 4242 centrifuge at 3500 rpm.

Table 3.1.1 *List of samples obtained with different extracting procedures.*

Entry	Samples	Concentration	Extraction	Further processing before supernatant collection
1	**A1**	0.97 g/100 mL distilled water	12 h stirring	30 minutes centrifugation.
3	**A3**	1.02 g/100 mL distilled water	15 mL distilled water heated to 60 °C for 30 minutes, 15 minutes ultrasound at 20 °C 30 mL distilled water heated to 60 °C for 30 minutes,15 minutes ultrasound at 20 °C 30 mL distilled water heated to 60 °C for 30 minutes, 15 minutes ultrasound at 20 °C 25 mL distilled water heated to 60 °C for 30 minutes,15 minutes ultrasound at 20 °C	After each step 30 minutes centrifugation. Supernatant collected and subsequent draws were made on the bottom body, collecting all supernatant fractions.
4	**A4**	1.00 g /100 mL distilled water	45 minutes ultrasound at 75 °C	
5	**PTA5**	1.00 g/50 mL acetonitrile (PTA5)	Pretreatment: 10 minutes stirring, ultrasound assisted extraction after 15 minutes.	30 minutes centrifugation.
6	**PTA5, A5**	1.00 g/50 mL acetonitrile (PTA5)	Pretreatment: 10 minutes stirring, ultrasound assisted extraction after 15 minutes. Vacuum evaporation of the bottom body from pretreatment and extraction with mixture methanol/water 62.5% under stirring. Ultrasound extraction at 55 °C for 15 minutes and vortex agitation every 5 minutes for 20 seconds.	Pre-treatment: 30 minutes centrifugation. Supernatant collected. 10 minutes centrifugation (6000 rpm).
7	**A6 EtOH**	1.0 g/250 mL ethanol 70%, 50 mL water	50 mL ethanol 70% heating 100 °C for 10 minutes. 30 minutes centrifugation collecting supernatant on the bottom body extraction with ethanol, repeated 3 times.	30 minutes centrifugation after each extraction test.

			Final extraction with water at 80 °C for 10 minutes. EtOH fraction collected	
8	**A6 H_2O**	1.0 g/250 mL ethanol 70%, 50 mL water	50 mL ethanol 70% heating 100 °C for 10 minutes. 30 minutes centrifugation collecting supernatant on the bottom body extraction with ethanol, repeated 3 times. Final extraction with water at 80 °C for 10 minutes. H_2O fraction collected	30 minutes centrifugation after each extraction test.

Refractive index (Brix index) was used to determine the dry substance, in the aqueous samples, expressed as the calculated % in w/v for the samples which were in aqueous solution. The results of analytical determinations for samples A1 (26%), A3 (32%) and A4 (21%) are reported in (**Error! Reference source not found.**).

Table 3.1.2 *Brix index for water extract solutions*.

Samples	Brix index (% w/v)
A1	26
A3	32
A4	21

The values obtained from the brix index measurements for samples A1 and A4 correspond to the certified concentration of soluble fibres content (Figure 3.1.1), reported by the analysis certificate of the baobab dry fruit pulp used to prepare the samples presented in this work (Table 3.1.1). The value registered was slightly higher for sample **A3** but it did not exceed the amount of soluble fibre plus sugar content according to the analysis certificate (Figure 3.1.1**Error! Reference source not found.**) ranges between 28.3 % and 31 %.

Dietary Fibers
Average values per 100g of fruit pulp.

Soluble dietary fibers	21.6-23 g / 100 g.
Insoluble dietary fibers	21-22.9 g / 100 g.

SUGARS
Average values per 100g of fruit pulp.

Glucose	3.4-3.7 g / 100 g.
Fructose	3.3-3.8 g / 100 g.

***Figure* 3.1.1** *Dietary fibre and sugar content by analysis certificate of the dry fruit pulp used.*

After this first evaluation and some preliminary trials, samples obtained through the extraction procedures described in (Table 3.1.1) were loaded onto the diol HPTLC plate at volume of 1-5 and 10 µL.

Figure 3.1.2 shows the developed plate in which solutions of the standards at 1000 ppm were prepared in a solvent mixture acetone: water in ratio 2:1, applied and compared to samples loaded at 1 µL. The samples deposited at 5 and 10 µL were "overloaded" and subsequently, the traces showed significant tailing, thus they are not presented herein.

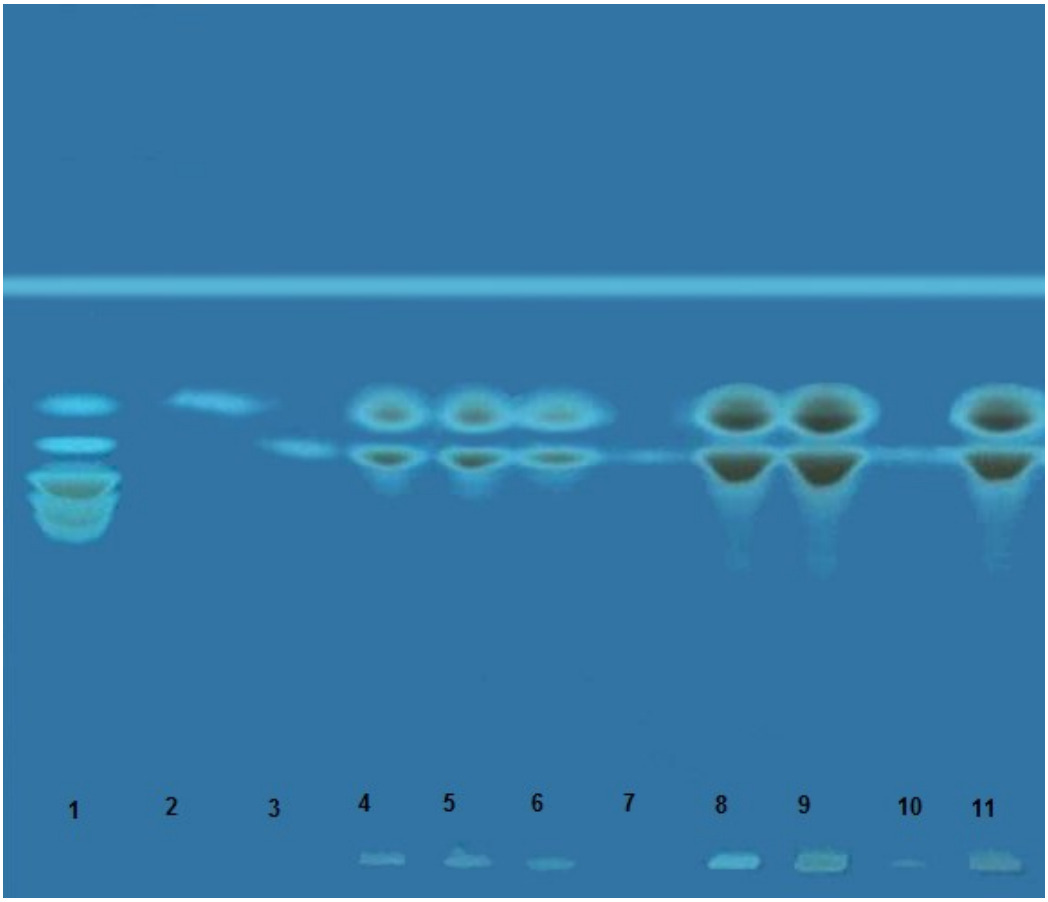

Figure 3.1.2 *Derivatised plate for visualisation of sugars mixtures extracted.*

Trace one (Figure 3.1.2) corresponds to Actilight®, trace two to a mixture of glucose/fructose in a ratio 1:1 respectively and traces three, seven and ten correspond to sucrose. Fructose and glucose, when deposited in separate solutions with the method herein described, showed the same Rf value of 0.5. Sucrose instead had an Rf of 0.47, but at this point of our study, it was not of interest to discriminate between glucose and fructose, because the main objective was to detect and separate the oligosaccharide components and not the monomeric moieties.

1 µL of the Actilight® solution was applied at a 2% (w/v) concentration. Actilight® is composed of dietary fibre and contains short chain fructo-oligosaccharides (FOS) which is

a prebiotic ingredient. The standard oligosaccharides observed in trace one, include a range that goes from 0.5 µg for sucrose to 8.5 µg for nystose. Actilight standard solution was prepared at a different concentrations, in respect to other sugars taking into account that it is the result of the enzymatic synthesis process, thus the substances contained in it are not at the same concentration. A 2% w/v solution is a concentration we knew would have allowed us to visualise sucrose, the lowest concentrate substance in Actilight®. Next to the standard traces, the samples are shown: **A3** in trace four, **A4** in trace five, pre-treated **A5** in trace six, **A5** in trace eight, **A6 ethanol** fraction in trace nine and **A6 aqueous** in trace eleven. The method sensitivity is around 10 ppm for each sugar, as previously reported by Vaccari et al.,[34] the detection limit has previously been extensively explained by our group with statistic data.[35]

The chromatogram (Figure 3.1.2) clearly shows the absence of oligosaccharides with higher molecular weight than sucrose and, as can be seen, the differences in intensity of the traces suggest that the different extraction methods used here affects only the quantitative analysis but not the qualitative extraction. The chromatograms as a result after analysis of the traces following acquisition with Camag Visualizer and data processing performed using Wincats Comparison Viewer and Camag Scanner III, confirmed what was suggested by Figure 3.1.2. The chromatograms confirmed, with no doubt, that the different extraction procedures used influence the extractive efficiency with respect to glucose, fructose and sucrose. And none of the samples showed the presence of any fructo-oligosaccharides with a molecular weight higher than sucrose. The densitogram of Actilight® (Figure 3.1.3, a) shows every sugar component peak with good resolution whereas the densitogram of traces 5 (sample A4) (Figure 3.1.3, b) and 9 (sample A6 water fraction) (Figure 3.1.3, c) further demonstrate that no peaks at a molecular weights higher than sucrose are present. No relevant amount of oligosaccharides (>10 ppm) were detected with the extracting procedures mentioned above.

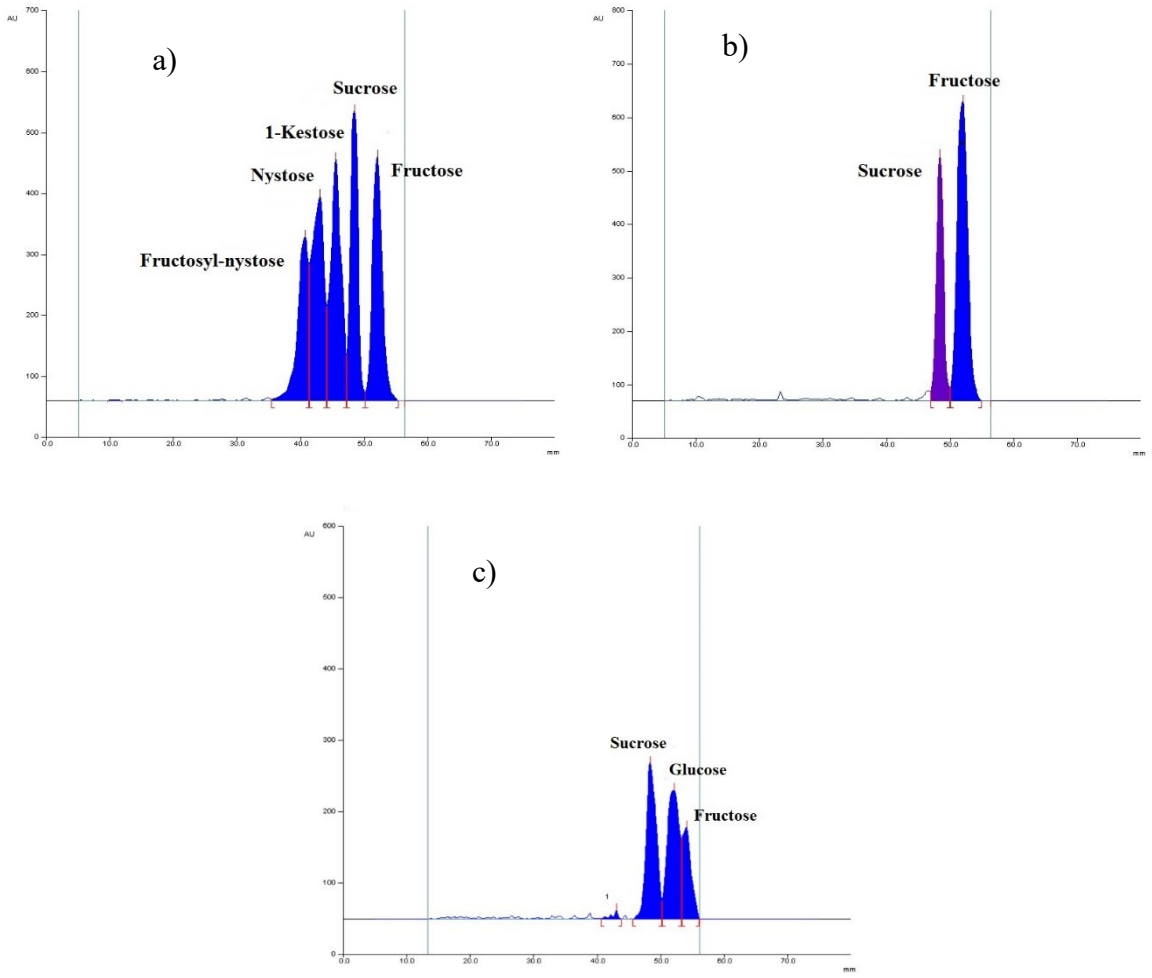

Figure 3.1.3 *Densitograms over Camag Scanner III: a) Actilight® standard; b) trace 5, sample A4; c) trace 9, sample A6 water fraction.*

It was then considered necessary to compare the results obtained by means of HPTLC alongside HPLC analysis, matching all the samples before and after hydrolytic treatment, in order to provide further analysis on the free and bonded monosaccharide. This investigation was necessary to evaluate the concentrations of glucose and fructose before and after acidic treatment and verify the absence or presence of oligo-saccharides of higher molecular weight than sucrose through the fructose/glucose calculated ratio. This was used to confirm if the monomers derived after hydrolytic treatment were derived solely from the breakdown of sucrose (and thus confirm or disprove the results obtained with the application of our HPTLC method). In order to confirm the absence of oligosaccharides, as revealed by HPTLC analysis, the ratio between fructose and glucose obtained should be approximately one-to one. A higher ratio would instead signify the presence of oligosaccharides and gave a measure of their medium chain length.

The samples were analysed in triplicate and calibration curves were obtained by injection of sugar standards of glucose, fructose and sucrose in concentrations ranging from 0.01% to 0.3%. In order to verify the stability of the instrument response for inter-day reproducibility one of the standards was daily injected. Table 3.1.3 details the concentrations of sugars found in the samples together with their standard errors after acid hydrolysis of the samples.

Table 3.1.3 *HPLC results pre-hydrolysis and post-hydrolysis with their relative uncertainty.*

Samples	Pre-hydrolysis			Post-hydrolysis	
	Sucrose%	**Glucose%**	**Fructose%**	**Total Glucose %**	**Total Fructose%**
A1	0.1636±0.0268	0.0570±0.0025	0.0469±0.0031	0.1408 ± 0.0029	0.1487±0.0034
A3	0.1844±0.0268	0.0639±0.0025	0.0717±0.0031	0.1470 ± 0.0026	0.1617±0.0034
A4	0.1216±0.0260	0.0465±0.0025	0.0380±0.0032	0.1070±0.0026	0.1131±0.0033
A5	0.7112±0.0270	0.0703±0.0024	0.0148±0.0032	0.2715±0.0027	0.3270±0.0035

The variation of the monomeric sugar concentrations, highlighted by the HPLC analysis performed, between the samples obtained through different extracting procedures, clearly confirmed the different efficiency of the extracting strategies adopted from a quantitative evaluation perspective.

This observation was further confirmed by the data reported in Table 3.1.4, the calculated fructose/glucose ratio values in the samples (which gives the medium length of the oligosaccharides eventually extracted) ranges between 1.1:1 and 1.5:1 supporting once more the absence of oligosaccharides with chain length longer than sucrose. These results confirmed the outcomes obtained through our HPTLC method and provided evidenced that all the fructose obtained after hydrolytic treatment was a result of sucrose breakdown.

Table 3.1.4 *HPLC results after hydrolysis and average length evaluation of carbohydrates chains*.

Samples	Glucose% generated by hydrolysis	Fructose% generated by hydrolysis	Fructose/Glucose Ratio
A1	0.08	0.10	1.2:1
A3	0.08	0.09	1.1:1
A4	0.06	0.07	1.1:1
A5	0.20	0.31	1.5:1

These preliminary outcomes highlight the need to develop a more accurate and precise method to characterise soluble fibre through the direct determination of oligosaccharides rather than by difference in mass. The method by mass difference commonly used in the food industry does not allow for an accurate attribution of the nutritional value of the product, and in this specific case study of *Adansonia digitata* we demonstrated the that this method led to an incorrect attribution of the known prebiotic activity of the baobab dry fruit pulp. The absence of oligosaccharides suggested that the prebiotic activity largely reported for baobab dry pulp must be attributed to other components rather than of the soluble fibre. Perhaps the simple monosaccharides or the flavonoids, which are present in high quantity, could account for this nutritional value.[36] The direct comparison with HPLC validated the HPTLC method previously developed in our laboratory (see experimental section for method details) and applied to our current case confirmed the method to be suitable on real samples from complex matrices.

Taking into account that the gut microbiota possess hydrolytic enzymes such as β-fructosyl-furanosidase[‡‡] and enzymes able to digest and use as carbon source the "insoluble fibre" present in plant matrices such as endo-xylanase[§§] (hemicellulase) it was decided to expand the study further by processing samples of *Adansonia digitata* samples with enzymatic treatments that could mimic the activity of gut microbiota. The aim was to verify if the lack of detectable oligosaccharides was due to the extracting procedures used. We speculated that the high complexity of the cell wall of the *Adansonia digitata* dry fruit pulp may be contributing to the lack of oligosaccharides identified through simple extraction. To investigate this, enzymatic treatments of the cell wall were applied and the samples analysed for its composition to determine the hemicellulose components herein present were any of the oligosaccharides preferred by gut microflora as carbon sources, such as xylo-oligosaccharides, in order to address the prebiotic activity of the baobab fruit pulp with certainty.

In order to evaluate the optimal enzymatic conditions, several variables were evaluated including type of enzymes and associations at different ratios. The optimal conditions for processing the bottom bodies were identified as a 1:1 mixture of cellulase and hemicellulase.

[‡‡] Inulinase is able to selectively breakdown terminal fructose units, breaking down inulins, FOS and raffinose, they do not attack α-glycosidic bonds or residues different from fructose
[§§] Enzymes that randomly breakdown xylan and xylo-oligosaccharides which are constituents of hemicellulose building cell walls in plant

The enzymatic hydrolysis was carried out in a sodium acetate/acetic acid buffer solution at pH 5.00 at 37 °C for 12 hours in bath shaker.

Several conditions to process bottom bodies before digestion with enzymatic treatments were also screened. Among those the following method was selected: to one gram of accurately weighted *Adansonia digitata* dried pulp 50 mL of acetonitrile were added. The mixture was stirred for ten minutes under mechanical force and 15 minutes with ultrasound. The resulting mixture was centrifuged for 30 minutes and the resulting bottom body was separated from the supernatant, dried under reduced pressure (Samples **1a-1f**) and submitted to enzymatic treatment. Samples **1a-1f** were compared with samples **2a-2f** in which *Adansonia digitata* dry pulp was directly submitted to enzymatic digestion.

As previously, mentioned pre-treatment with acetonitrile is useful for the removal of free sugars[33] whereas ultrasound is widely used as an effective method to extract sugars from different plants tissues.[31] Centrifugations were performed with an ALC 4242 centrifuge at 3500 rpm. After processing the samples through enzymatic digestion (

Table ***3.1.5***), AMD-HPTLC separation was performed in order to evaluate the result of breaking the cell wall prior to detection of oligosaccharide content.

Table 3.1.5 *Cellulase/hemicellulase hydrolytic treatments.*

Entry	Samples name	Bottom bodies (mg)	Cellulase (mg)	Hemicellulase (mg)
1	1a	51.6	/	51.8
2	1b	49.3	/	24.9
3	1c	54.5	/	19.6
4	2a	55.7	/	52.9
5	2b	58.0	/	25.0
6	2c	54.4	/	19.6
7	1d	52.1	25.0	.24.9
8	1e	53.2	13.0	12.7
9	1f	56.7	8.9	8.7
10	2d	52.8	25.2	25.9
11	2e	51.2	12.6	12.4
12	2f	54.9	8.0	7.8

Entries 1 to 6 (samples **1a-1c** and **1a-1c**) are samples treated just with hemicellulase to illustrate the difference between unoptimised and optimised treatment. The results after enzymatic digestion of the samples are shown below (Figure 3.1.4).

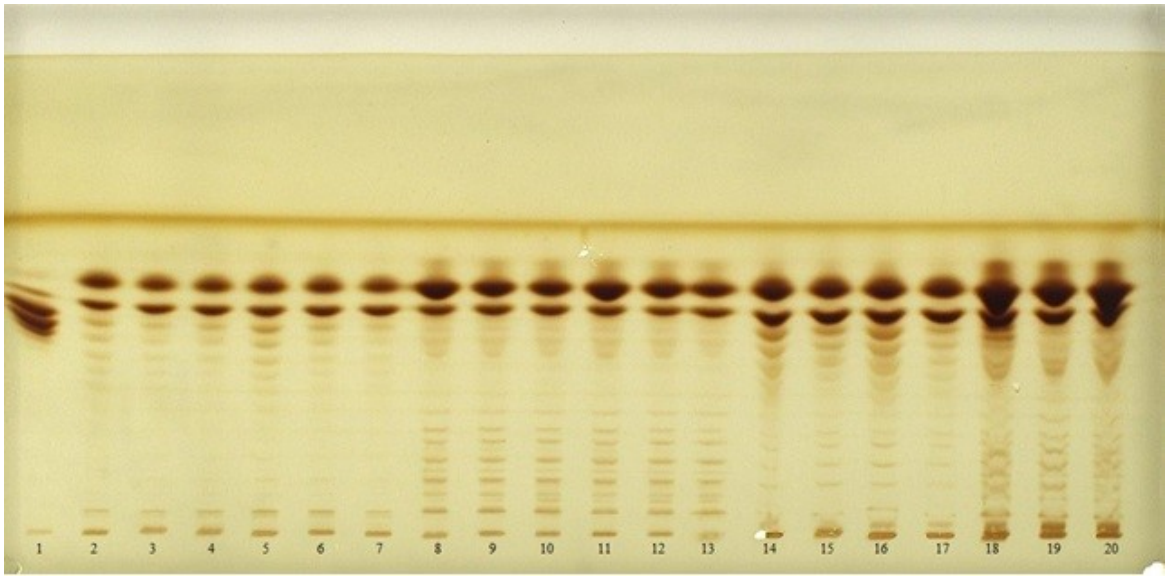

Figure 3.1.4 *AMD-HPTLC separation of baobab pulp fruit samples after enzymatic treatment (cellulase and hemicellulase) deposited from 1 to 3 µL.*

The first trace on the HPTLC plate (Figure 3.1.4) corresponds to an Actilight® solution 2% standard that was deposited at 1 µL. Traces from 2 to 7 correspond to samples **1a, 1b, 1c, 2a ,2b** and **2c** at 1 µL. Traces from 8 to 13 correspond to samples **1d,1e,1f, 2d, 2e** and **2f** at 1 µL. Traces from 14 to 17 correspond to samples **1a, 1c, 2a** and **2c** at 3 µL. Finally, traces from 18 to 20 samples **1d, 1e** and **2d** at 3 µL. Each sample deposited on the diol plate showed the presence of saccharides with higher molecular weight than sucrose. It should be highlighted that samples deposited from trace 2 to 7, which were treated with just hemicellulase, produced more intense spots at lower molecular weights. The samples displayed between traces 8 and 13, which are the result of the optimised enzymatic treatment with hemicellulase and cellulase in a ratio 1:1, produced instead a larger variety of polymers. Samples displayed between traces 8 and 13 also showed a wider range of molecular weights suggesting that the association of enzymes was more efficient. In these traces polymers with higher molecular weights can be detected in addition to the lower molecular weights ones displayed when the samples were treated just with hemicellulase traces 2 to 7.

The linear gradient herein used to develop the TLC plate was performed with decreasing polarity on the polar stationary phase diol layer. This was to allow the most polar substances to run higher than the heavier ones. In Figure 3.1.5, a densitogram of track 11 corresponding to sample **2d**, is shown as representative example of the excellent separation obtained of the many analytes produced after enzymatic hydrolysis, following application of our HPTLC based method (refer to experimental section for details) .

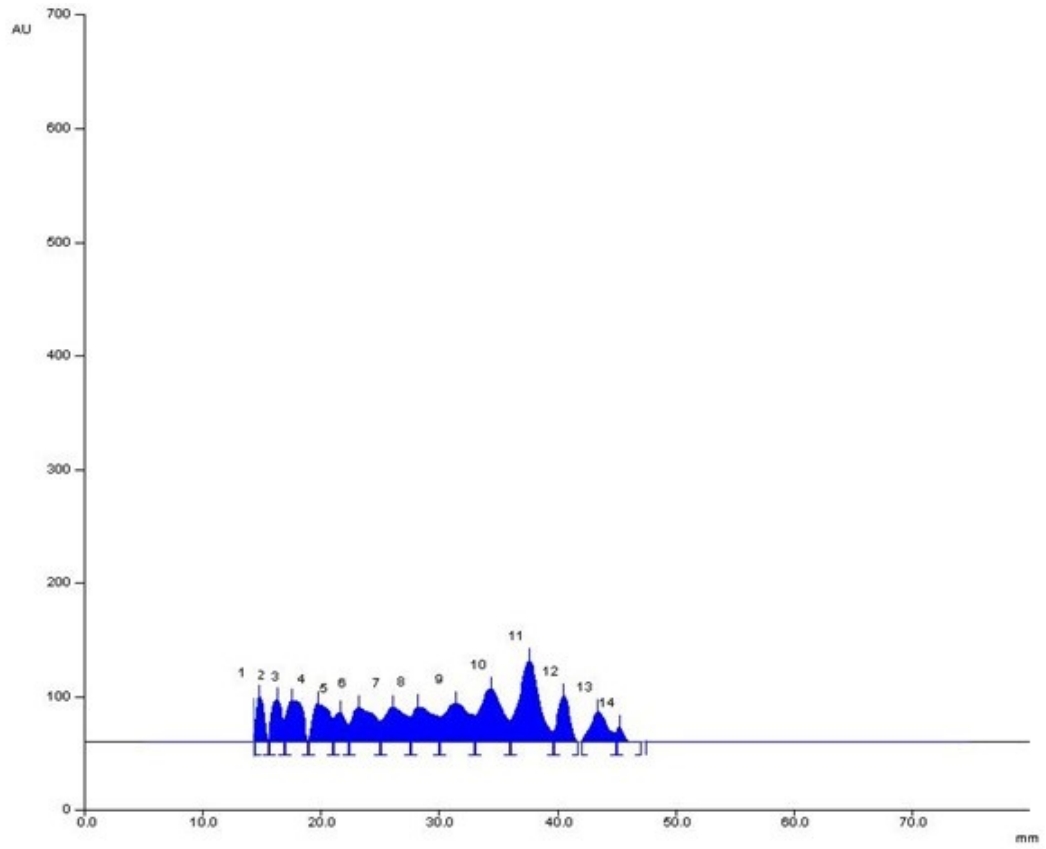

Figure 3.1.5 *Densitogram of HPTLC-AMD developed diol layer track 11 sample 2d at 1 µL.*

At this point it was considered necessary to verify if the polymers obtained and evidenced on the HPTLC plate contained oligosaccharides of interest to help the gut microflora to grow from the lag phase to the exponential phase. To achieve this, it was necessary to submit the samples to successive chemical hydrolysis in order to analyse their monosaccharide building blocks.

Our strategy was to perform complete degradation with hydrochloric acid and to evaluate techniques to allow for good separation of the analytes. It is common use to utilise HPLC as convenient method to analyse non-complex mixtures of saccharides. The results obtained from the HPLC analysis and the relevant retention times are presented below (Figure 3.1.6).

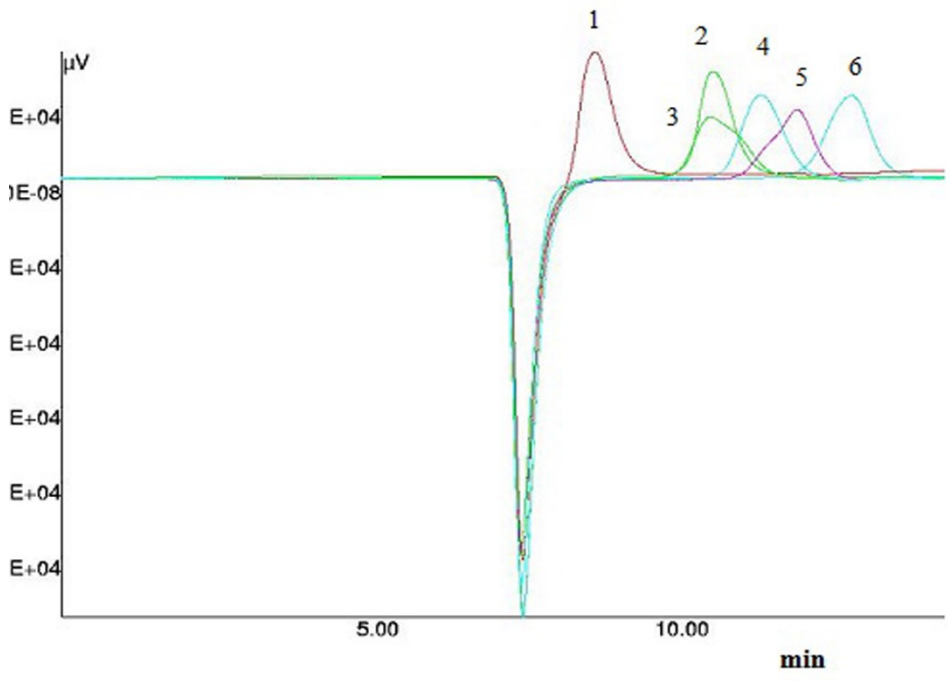

Figure 3.1.6 *HPLC separation of monosaccharides expected from our hydrolysed samples with retention times: (1) galacturonic acid 8.7 min; (2) glucose 10.6 min; (3) rhamnose 10.6 min; (4) xylose 11.4 min; (5) fructose 12.0 min; (6) arabinose 12.9 min.*

Under these HPLC conditions (experimental section) rhamnose and glucose appeared to have the same retention times and xylose, fructose and arabinose were also not well resolved (Figure 3.1.6). Considering that HPTLC is quicker, more green and reliable as a technique, we decided to investigate if our HPTLC method would allow for separation and resolution of the sugars that in the HPLC method, used herein, overlapped. Before switching to HPTLC we attempted to investigate if some of the sugars that overlapped, might be present after acid hydrolytic treatment but due to the poor resolution the results were inconclusive. To highlight this, a chromatogram of one of the samples submitted to acid hydrolysis after enzymatic digestion is shown below (Figure 3.1.7).

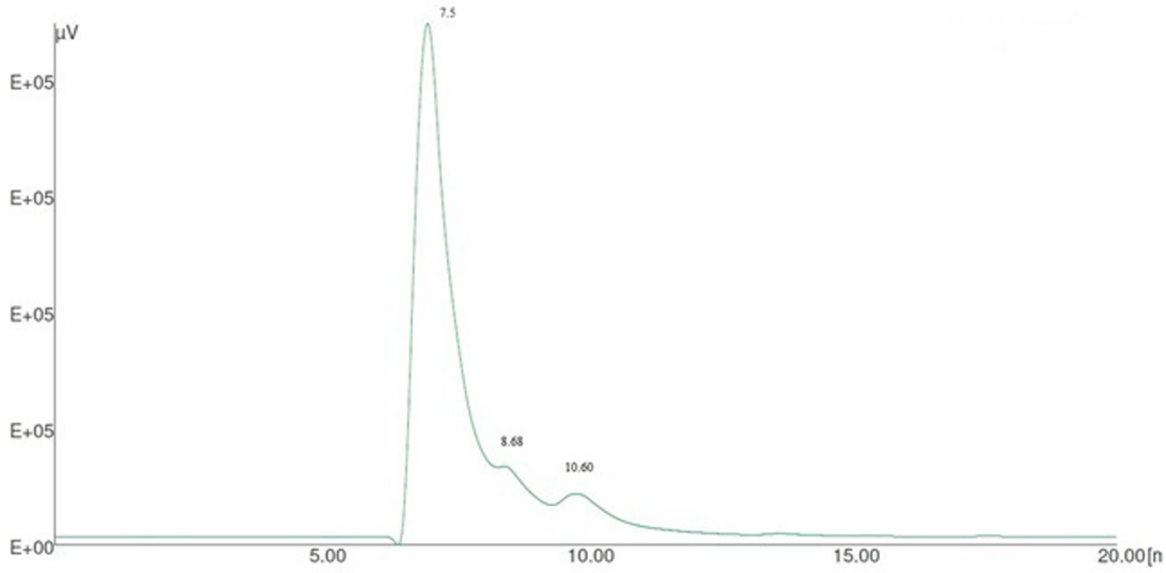

Figure 3.1.7 *A representative HPLC trace after chemical hydrolysis of a typical sample.*

A representative HPLC chromatogram (Figure 3.1.7) of these samples is characterised by a high peak of chlorides at 7.5 minutes that interferes with peaks at 8.6 and 10.6 minutes. However, some useful information was gained from this data such as the complete absence of fructose and arabinose in our hydrolysed sample, which was evident from the lack of peaks at the corresponding retention times (12.0 and 12.9 minutes, respectively). However, this complex pattern (as well as the overlapping peaks of the sugars of interest in the HPLC chromatograms) was a driver for us to turn to the HPTLC technique, without further attempts to optimise the HPLC method. This also provided an opportunity to further evaluate the potential of HPTLC as an efficient separations technology.

In the baobab case study herein presented, determination of standardised sugar R_f values was realised using standard mixtures of galacturonic acid, glucose, arabinose, xylose and rhamnose. The densitograms of the standardised sugar solutions obtained through HPTLC are shown below.

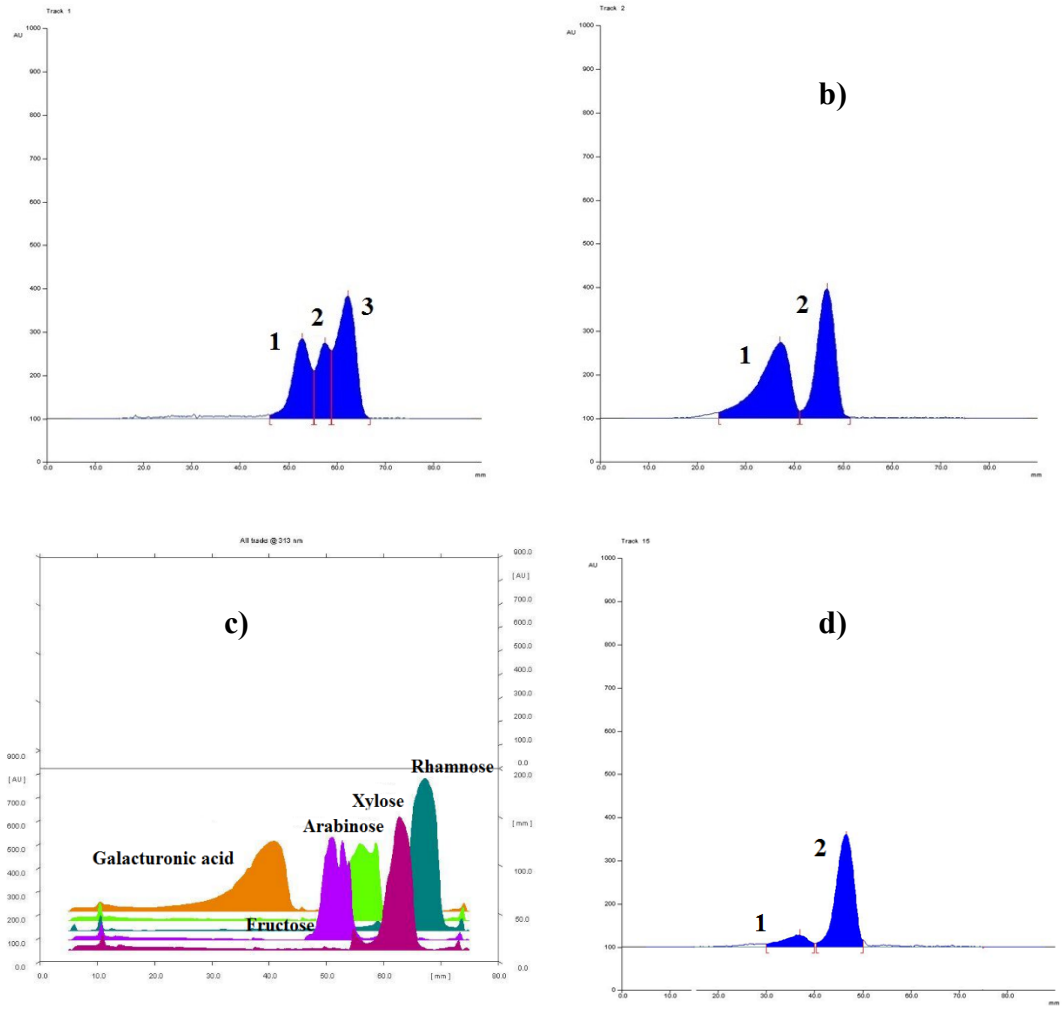

Figure 3.1.8 *HPTLC densitograms of standards a) Standard Mixture 1:1:1 arabinose, xylose, rhamnose; b) Standard mixture 2:1 galacturonic acid, glucose; c) Two dimensional HPTLC standard separation of (1) galacturonic acid, (2) fructose, (3) arabinose, (4) xylose, (5) rhamnose; d) Representative sample* ***2d****, after acid hydrolysis, diluted 1:10 and deposited 5 µL.*

From Figure 3.1.8 it is evident that rhamnose and glucose show significantly different R_f values and are well resolved (rhamnose $R_f = 0.69$ and glucose $R_f = 0.52$). The excellent resolution is further demonstrated through the comparison of the standards and the two dimensional depiction of the HPTLC sample **2d** after acid hydrolytic treatment (Figure 3.1.8) where galacturonic acid (peak 1) and glucose (peak 2) were detected and well separated. Considering that our HPTLC method proved to be effective in clearly separating and discriminating between the different sugars, we proceeded with the characterisation of the monosaccharides deriving from the acid hydrolysis of all the samples described above (

Table ***3.1.5***).

Separations with representative samples were then performed using the original concentrations of standard mixtures. The concentrations of monosaccharides were evaluated with a Camag Visualizer by comparison of the spots density.

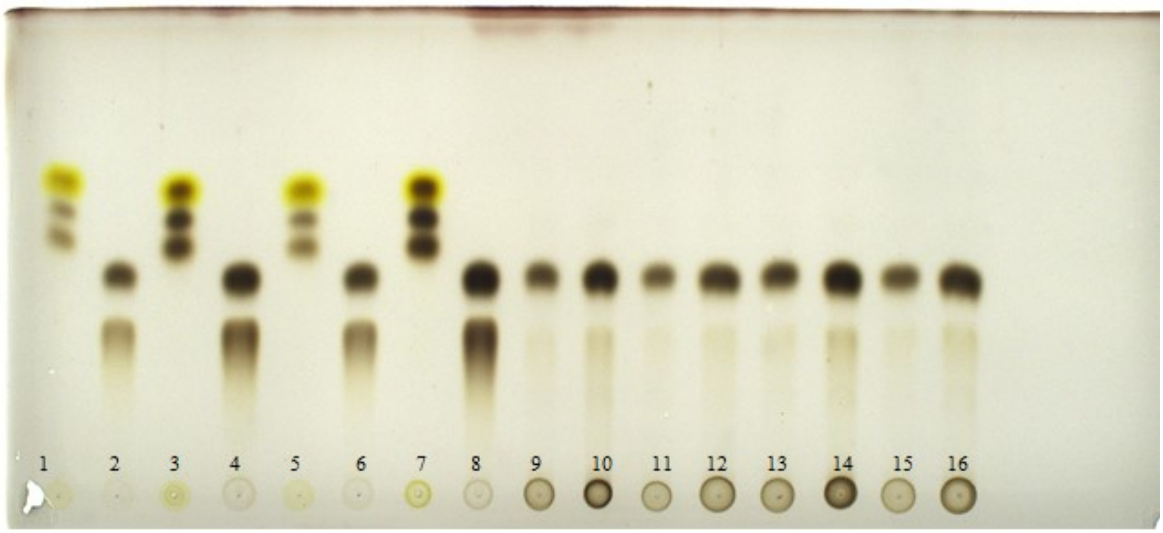

Figure 3.1.9 *HPTLC monosaccharides evaluation. Traces 1-8 standard solutions deposited at increasing volumes, traces 9-16 representative samples that had been submitted to enzymatic and subsequently to chemical hydrolyses.*

On traces 1, 3, 5 and 7 were deposited arabinose, xylose and rhamnose 1000 ppm standard mixture at 4, 8, 5 and 10 µL respectively. On traces 2, 4, 6 and 8 were deposited a 1000 ppm standard solutions of glucose and galacturonic acid at 4, 8, 5, 10 µL respectively. Traces 9 to 16 were samples that had been submitted to enzymatic treatment with cellulase and hemicellulase at known concentrations (optimised conditions

Table ***3.1.5***). No other monosaccharides, besides glucuronic acid and glucose, were detected.

Processing the Visualizer evaluation (Figure 3.1.9) gave the concentrations of galacturonic acid and glucose found after chemical degradation with hydrochloric acid and their ratio (galacturonic acid was present in 0.7% and glucose in 10.0% so the ratio between the two was 14.0).

4. Conclusions

The work presented here, on the characterisation of *Adansonia digitata* dry pulp, extended our groups previous research through the application of a modern instrumental HPTLC technique that provided a determination of different oligosaccharides at the nanogram level. It also confirmed that this technique allowed for a rapid screening of sugar-containing samples simultaneously (16 traces were deposited simultaneously in this work, Figure 3.1.9, but up to 24 traces can be run), with minimal solvent waste produced in the development process. The method herein described, not only was validated on a real case study, proving to be as efficient as the most common HPLC method in the first part of the study, but has also proven to be equally efficient and reliable in separating and discriminating between monosaccharides in a complex mixture, without need of further optimisation. The HPTLC method developed through this research, along with Isocratic and Automated Multiple Development (AMD), was used as an alternative to common and widespread analytical methods. It was used to rapidly analyse complex mixtures containing a broad variety of monosaccharides thus allowing to save the time that would have been instead necessary to adapt the HPLC method to the case study.

Furthermore, and very noteworthy, this study represents a specific and accurate analysis of the soluble and insoluble fibre components compared to what previously done. The results obtained, demonstrated the absence of inulin and FOS which are the soluble fibre to which is usually accredited the prebiotic power of baobab, and highlighted that the calculation of soluble fibre by mass difference from the other nutrients is not sufficient. For this reason a direct determination of the oligosaccharides content should be required and performed in order to accurately attribute the nutritional value of a food product, especially taking into account that this constitutes a very important issue for food industry.

It should the responsibility of the food industry to guarantee the values of nutrient substances, in particularly those that selectively stimulate growth and/or biological activity of protective microflora of the human intestinal tract and contributing, if consumed systematically to the maintenance of its normal content and biological activity. It was demonstrated that our HPTLC method is suitable for this purpose and enabled a rapid and simultaneous screening of food extracts and was equally efficient in the separation of sugar polymers and monosaccharides and could be adopted as more accurate and informative characterisation of food products.

From this study, baobab fruit pulp was confirmed as a good source of carbohydrates, useful for nutrition; however, it was impossible to detect significant amounts of oligosaccharides responsible of the well-known prebiotic activity in the soluble fibre fraction.

Furthermore, after many different enzymatic treatments were performed on dry pulp samples in order to identify the optimal processing conditions in terms of degradation product type and numbers an enzymatic treatment with the contemporary contribution of cellulase and hemicellulase enzymes were selected. The aim of these enzymatic digestions was to evaluate if, for some unclear reason, in our case, the commonly used extraction procedures failed to extract the soluble fibre and also to evaluate the composition of the dry pulp cell wall. Characterising the components of the cell wall such hemicellulose, could have helped to justify the prebiotic activity reported for baobab dried pulp after the presence of any soluble fibres such as inulins and FOS were excluded.

The results obtained by processing the samples with enzymatic digestions and subsequently submitting them to acidic hydrolysis to characterise the monomeric building blocks of the polymers detected (Figure 3.1.4) unequivocally excluded the presence of fructo-oligosaccharides (FOS). The oligomeric products from cell wall degradation were found to be composed of 10% glucose and 0.7% of galacturonic acid expressed over 100 grams of dry pulp, confirming once more that the method by mass difference (commonly used to attribute the nutritional value of the food product) does not lead to accurate attribution. No xylo-oligosaccharides attached to the cell wall were detect either along with no other oligomers normally preferred by the gut microflora.

From our studies, we believe that the components at the base of the widely reported prebiotic activity of *Adansonia digitata* may be either the monosaccharides largely present (i.e., sucrose, glucose, and fructose) or the flavonoids.[36] These components may influence the microflora and have an impact on colonic health,[37] which can bring the microorganism into an exponential phase of growth.

To further confirm these hypotheses for the *Adansonia digitata* fruit pulp, different samples of dry pulp could be processed (following the protocols herein described) and analysed through our HPTLC method, alongside fresh baobab fruit pulp. The analysis on the effect of different processing methods on the content of oligosaccharides in *Adansonia digitata* dry pulp could, in the future, also provide further evidence for the prebiotic activity.

5. Experimental Protocols

All reagents and solvents were of analytical grade. Acetone, acetonitrile, ortho-phosphoric acid, acetic acid, ethanol, methanol, and hydrochloric acid were purchased from Merck (Darmstadt, Germany). The *Adansonia digitata* dried fruit pulp used to prepare the samples analysed in this study was obtained from Baobab Fruit Company Senegal (Thies, Senegal). The water used for chromatography, standards, and sample solutions was of ultrapure grade. D-(+)-Glucose (lot no. 9434820009 J. T. Baker Deventer, Holland), D-(+)-fructose (Carlo Erba reagent RP), sucrose (J. T. Baker Deventer, Holland), and pure fructo-oligosaccharides (FOS: 1-kestose 33.1%, nystose 42.5%, fructosilnystose 11.3%, and sucrose 2.4%, Actilight® C.F.M. Milano). Standards were dissolved in a mixture of water/acetone (2:1) to give Actilight® solution 2 % w/v, D-(+)-glucose, D-(+)-fructose, sucrose, xylose, rhamnose, arabinose and galacturonic acid 1,000 ppm stock solutions for HPTLC applications. Dilution of the stock solutions with water yielded the working solutions applied at concentrations of 100 ppm only for daily use and only for R_f evaluation. Standard stock solutions can be stored at –18 °C and used for at least one month. For HPLC analysis, the standards were dissolved in ultrapure water to give 5% standard stock solutions. Subsequently, samples were diluted with distilled water between 0.01 and 0.3 % (working solutions) for calibration curves in HPLC determinations.

5.1. Hydrolytic Treatment of Samples

5.1.1. *Acid Hydrolysis*

The hydrolytic treatment procedure was optimised in our laboratories and has been successfully applied to FOS extracts (Icumsa Lane-Eynon method 1994).[38] To each sample, HCl 6.3 M was added and the mixture was kept at 60 °C for 15 minutes. Samples were then cooled down to 0 °C in an ice bath and subjected to quantitative determinations. It is important to mention that the pH of each solution needed to be adjusted to neutral value after hydrolytic treatment, in order to avoid degradation of the silica thin layer of the plate.

5.1.2. *Enzymatic Hydrolysis*

After several experimental trials, the optimal conditions to process our dry pulp were identified in a mixture with a 1:1 ratio of cellulase and hemicellulase. The enzymatic hydrolysis was carried out in a sodium acetate/acetic acid buffer solution at pH 5.00 at 37 °C for 12 hours in bath shaker.

5.1.3. *HPTLC Protocols*

HPTLC gradient (Table 5.1.1) was performed with decreasing polarity in controlled humidity and temperature conditions. A 15-step gradient was performed using a Camag AMD apparatus following the conditions described below. The mixing of the eluent solutions (acetone/acetonitrile (1:1) and ultrapure water) was fully automated in the Camag AMD2 apparatus, until 70 mm of solvent front.

Table 5.1.1 *Elution conditions AMD2 with four solvent mixtures for 15 gradient steps. Solution Ace/ACN was in a ratio 1:1 (Ace = acetone, ACN = acetonitrile).*

Step	(Ace/ACN)/H_2O (75/25)	(Ace/ACN)/H_2O (80/20)	(Ace/ACN)/H_2O (85/15)	(Ace/ACN)/H_2O (85/15)	Eluent front (mm)
1	100.0	0.0	0.0	0.0	12.4
2	81.4	18.6	0.0	0.0	16.5
3	52.6	47.4	0.0	0.0	20.0
4	34.0	66.0	0.0	0.0	24.9
5	22.0	78.0	0.0	0.0	29.1
6	14.2	67.2	18.6	0.0	32.8
7	9.2	43.4	47.4	0.0	36.3
8	5.9	28.1	66.0	0.0	41.1
9	3.8	18.1	78.1	0.0	45.3
10	2.5	11.7	85.8	0.0	48.3
11	1.6	7.6	72.2	18.6	51.1
12	1.0	4.9	46.7	47.4	52.9
13	0.7	3.2	30.1	66.0	56.1
14	0.4	2.0	19.5	78.1	59.2
15	0.3	1.3	12.6	85.8	64.9

The gradient shape (Figure 5.1.1) shown below was performed on 20 cm × 10 cm diol HPTLC plates (Merck) for oligosaccharides samples detection. Instead, separation was

performed on silica plates 10 × 20 mm for monosaccharides detection after acid hydrolysis treatment.

Samples were loaded on the appropriate HPTLC plate by means of Linomat V Camag as 4 mm bands, 12 mm from the side edge and 10 mm from the bottom edge. The delivery rate for deposition was 15 µL/s. Runs were performed with 80 mm of eluent front (acetonitrile/acetic acid/water 63/33/5 mL) in a twin through-chamber without any precondition time.

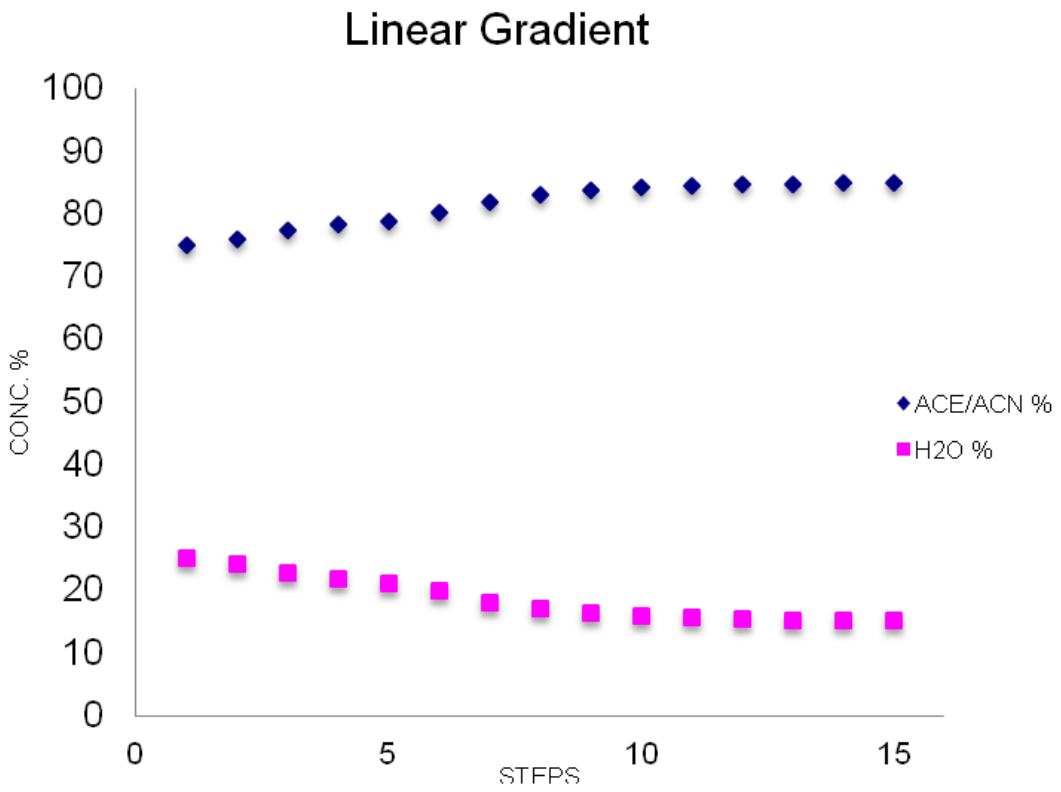

***Figure* 5.1.1** Profile of fifteen-step AMD linear gradient for oligosaccharides separation.

5.1.4. *Derivatisation and Scanning*

The HPTLC plates loaded with samples **A1-A6** and **B**, after development, were derivatised with 4-aminobenzoic acid (2 g), anhydrous acetic acid (36 mL), water (40 mL), 85% phosphoric acid (2 mL) and acetone (120 mL)[39] by means of Camag dipping apparatus with an immersion time of 2 seconds. This derivatisation was made with 4-aminobenzoic acid to display only the sugars. This solution can be kept for 2 weeks at –18 °C with no loss in reactivity. The derivatised layers were dried at 115 °C for 15 minutes in a convection heater.

HPTLC plates loaded with samples **1a-1f** and **2a-2f** were derivatised with 10% sulfuric acid in ethanol[39] by means of Camag dipping apparatus and an immersion time of 9 seconds,

subsequently, the immersion plates were dried at 100 °C for 3 minutes. The solution can be stored for 2 weeks at –18 °C without deterioration.

The derivatised layers were scanned with a Camag Scanner III interfaced with a personal computer using WinCats version 1.2.6. evaluation software, in fluorescence with a Hg lamp at 366 nm for samples and 400 nm. Layer images were acquired with Camag Visualizer and the results from different plates were compared using Wincats Comparison Viewer. The silica plates, for isocratic monosaccharides separation, were also scanned at 400 nm.

HPLC was used for quantification of glucose and fructose in the same samples before and after acid hydrolysis. An Aminex HPX-87H (Biorad®) column and a refraction index detector was used in HPLC-IE.

For HPLC analysis, each solution was filtered through a 0.45 µm filter before injection. All stock solutions of sugars were prepared at 5% w/v (50000 ppm) and were stored in the dark at –18 °C and used within one week. External calibration curves were obtained using ultrapure water and preparing working solutions which were plotted as standard peak areas against relative concentrations (fig. 2). Calibration curves (Figure 5.1.2) revealed good linearity with correlation coefficient R^2 values between 0.9993-0.9999 (below**)** and were obtained utilising three replicates of seven solutions between 0.01-0.3% w/v (100-3000 ppm). Samples were diluted with pure water or injected as prepared.

Table 5.1.2 *Linear regression parameters for calibration curves of targeted sugars*.

Standards	Slope	Intercept	Correlation (R^2)
Sucrose	5889394	2577	0.9999
Glucose	6386612	-49006	0.9998
Fructose	5288958	40593	0.9993

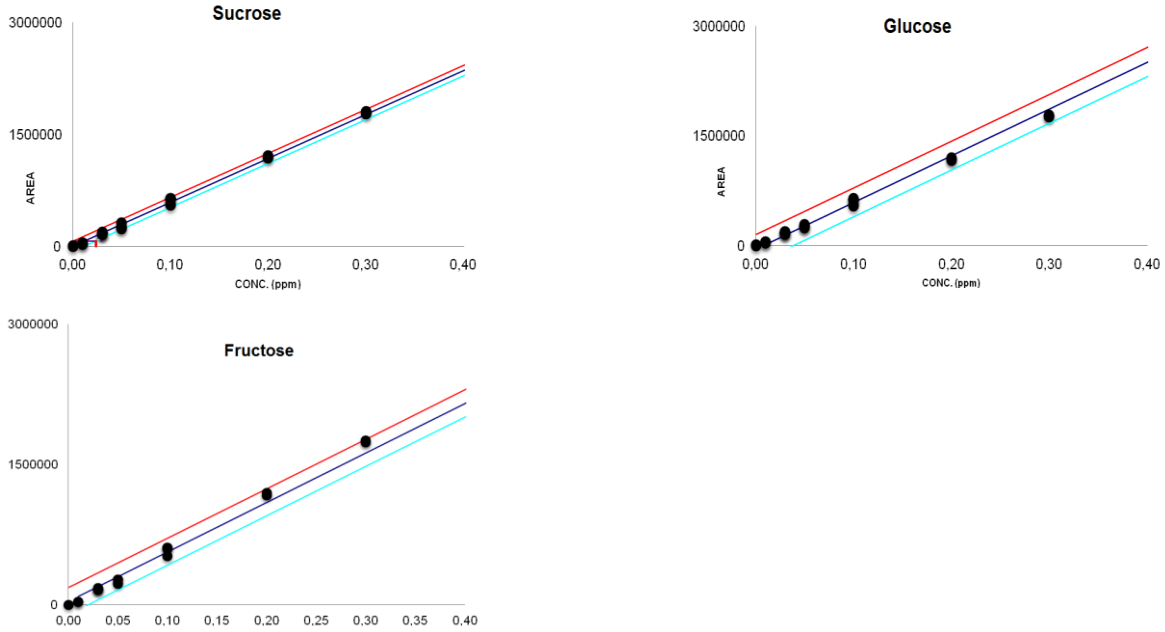

Figure 5.1.2 *Calibration curves for sucrose, glucose and fructose in pure water and confidence limits at 95%.*

Calibration curves for xylose, rhamnose, arabinose and galacturonic acid are not shown considering that we moved away from HPLC, when all those sugars needed to be characterised at the same time, for the characterisation of such complex mixtures.

6. Introduction

6.1. Polyphenols

Polyphenols are secondary metabolites of higher plants and are among the most abundant and ubiquitous. There are obtained from renewable sources including plant materials[40] (blueberries, apples, grapes, cocoa beans, tea leaves etc.) and consequently widely consumed in the human diet. This has contributed to their widespread use in pharmaceuticals, cosmeceuticals and nutraceuticals.[41]

They are from a class of heterogeneous molecules exerting different functions in plants such as mechanical supports. They are from a family of lignins and are a class of biopolymers constituted by random polymerisation of units of phenolic alcohols (e.g. *p*-cumaryl alcohol, sinapyl alcohol and coniferyl alcohol), and those from the family of phyto-alexins offer protection against animals and pathogens. Furthermore, they can act as pollinator attractors and considering their antioxidant activity, are able to offer protection against UV-radiation, such as polyphenols from the class of flavonoids (Figure 6.1.1**Error! Reference source not found.**).

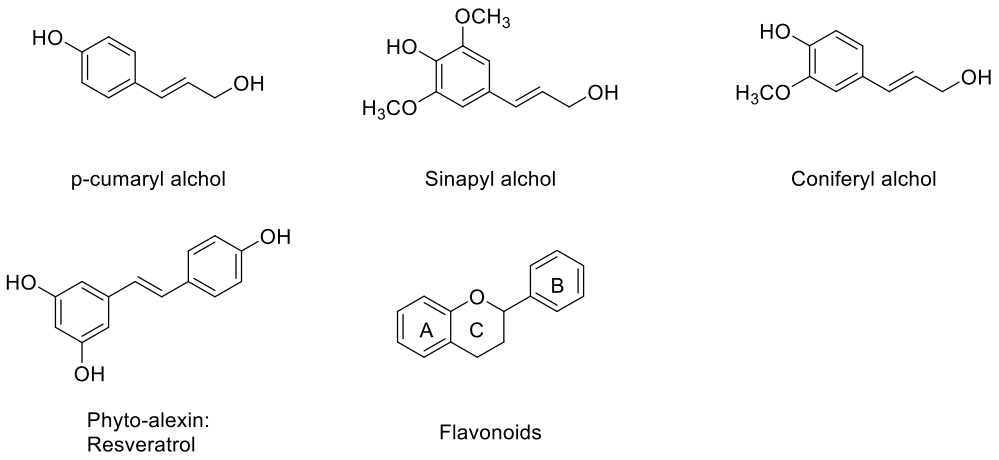

Figure 6.1.1 Selected examples from the families of polyphenols.

The antioxidant properties of polyphenols is related to the number of hydroxyl groups it possesses and their position in the aromatic ring. Previous reports have shown that they can exert beneficial effects on a wide range of diseases from cancer to infections, inflammation, allergic reactions, hepato-protection etc. Yet they are often characterised as having poor solubility issues and rapid metabolic degradation. They are metabolised in the human body through methylation, sulfonation and glucuronidation pathways.[42]

6.2. Antioxidants

The term "antioxidant" has a number of different definitions depending of the scientific field being considered. In general, an antioxidant may be a synthetic or natural compound (or mixture of compounds) capable of scavenging free radicals and inhibiting reactions promoted by these highly reactive species. As well as preserving the health of animal tissues, minimising the reactions of free radicals impacts materials such as plastics and rubbers and foodstuffs.[43]

They can belong to different classes, each with different mechanistic actions, and can be metal chelators, oxidative enzyme inhibitors, antioxidant enzyme cofactors or free radical chain inhibitors. Free radicals are physiologically produced in the biological systems and they exert a dual role as both beneficial and harmful species. They can be divided in two main classes: reactive oxygen species (ROS) and reactive nitrogen species (RNS), which include also some non-radical species. From the reactive oxygen species include: superoxide anion radical ($O_2^{-}\cdot$), elemental oxygen (O_2), hydroxyl radical ($OH\cdot$), hydrogen peroxide (H_2O_2) and lipid peroxyl radical ($LOO\cdot$). Reactive nitrogen species include: nitric oxide radical ($NO\cdot$) and nitrogen dioxide radical ($NO_2\cdot$).

They are generated during cell metabolic activity through the regulation of enzymes such as NADH/NADPH or NOS (NO synthase). Under physiological conditions, they are present in low concentrations and activate signalling pathways to protect from e.g. infectious agents, but if homeostasis is disturbed and their concentration increases they can cause damage. High concentrations of ROS and RNS damage cell structures such as proteins, lipids, membranes and DNA.

It is interesting to note that several ROS-mediated actions that happen under normal physiological conditions are actually to protect cells against ROS-induced oxidative stress and to maintain or re-establish the "redox balance". In fact, ROS are involved in the signalling pathway that contributes to maintain the oncogenic phenotype but they can also induce senescence and apoptosis acting as anti-tumorigenic agents.[44]

More commonly, free radical species have been reported to be involved in inflammation processes, aging, cardiovascular disease, atherosclerosis, rheumatoid arthritis, hypertension, ischemia/reperfusion injury, cancer, diabetes mellitus and neurodegenerative diseases (e.g. Alzheimer's and Parkinson's). The mechanism of radical-mediated reactions can be

summarised as shown in (Scheme 6.2.1) where the cascade of radical reactions is shown for the lipid peroxidation.

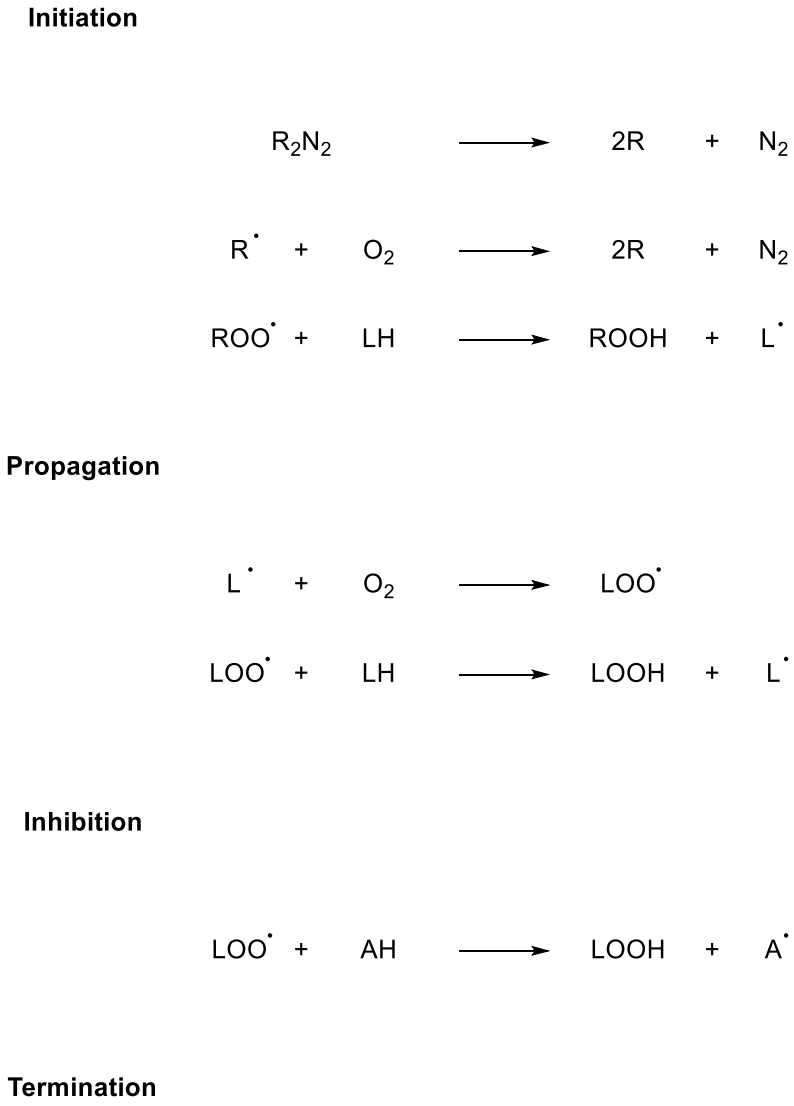

Scheme 6.2.1 *Mechanism of radical oxidation process. LH = substrate, AH = antioxidant.*

Based on the above mechanism, it can be assumed that one mole of antioxidant scavenges two radicals and that molecular oxygen is present in a large excess. Antioxidants can be divided in two main classes: *preventive antioxidants* and *chain breaking antioxidants*.

6.2.1. *Preventive Antioxidants*

Preventive antioxidants intercept the oxidising species before they can do the damage. They include metal deactivating compounds such as ethylenediaminetetraacetic acid (EDTA), diethylenetriaminepentaacetic acid (DETAPAC), polyphenols, transferrin, ferritin and

enzyme scavenging hydroperoxides e.g. glutathione peroxidase (GSH), superoxide dismutase (SOD), catalase and species able to quench singlet oxygen atoms such as β-carotene etc.

Metals are able to promote the oxidation processes through generating hydroxyl radicals (OH·) which act as catalysts reactions such as the Fenton and the Haber–Weiss reaction (Scheme 6.2.2).

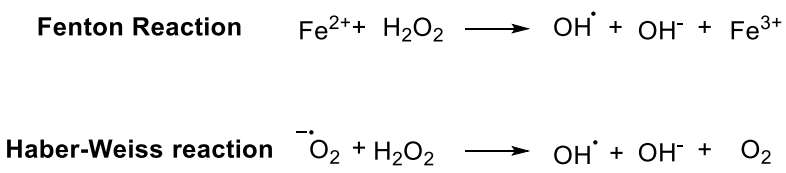

***Scheme* 6.2.2** *Fenton and the Haber–Weiss reaction.*

Iron and copper are present in biological tissues and are produced in the normal turnover of cells or in tissues lesions. They need to be quickly scavenged to avoid oxidative stress. The micro-organism herein prepossess plasmatic proteins such as transferrin, lactoferrin and ceruloplasmin that act as metal chelators and transporters in order to avoid oxidation stress due to those metals.

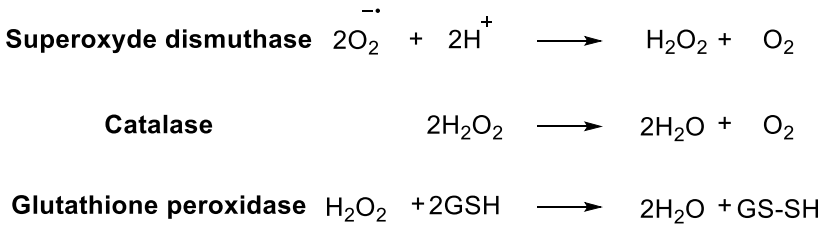

Scheme 6.2.3 *Intracellular scavenging enzymes.*

Enzymes that scavenge hydroperoxide are endogenous antioxidants resources.[45] Superoxide dismuthase (SOD) accelerates the dismutation of superoxide anions into water and elemental oxygen whereas catalase converts hydrogen peroxide molecules also into water and oxygen. Glutathione peroxidase (GSH) is a tripeptide constituted of glycine, cysteine and glutamic acid that contains selenium. It scavenges hydrogen peroxide by converting it into water (Scheme 6.2.3).

6.2.2. *Chain Breaking Antioxidants*

This type of antioxidant act on the chain, after the oxidation process has already begun, by retarding or stopping the oxidative process, intercepting the chain-carrying radicals such as

the peroxide radical ROO·. The ability to react with alkoxyl radicals can be significant to prevent the formation of cytotoxic agents.[46] A characteristic property of an efficient chain breaker is the ability to react with the radicals more quickly than their substrate and that the generated antioxidant radical A· is stable enough to not react further (or react very slowly) with the substrate. Polyphenols, discussed later, has this characteristic. This category of antioxidants can be divided in two sub-classes: *donor chain breaking antioxidants* e.g. vitamin E (α-tocopherol), vitamin C (L-ascorbic acid) and β-carotene and *sacrificial chain breaking antioxidants* such as NO (nitric oxide).

Donor chain breaking antioxidants donate hydrogen to form a radical on the phenolic hydroxyl group which is more stable due to resonance (Scheme 6.2.4). Polyphenols belongs to that class of antioxidants and structures such as ascorbic acid, are hydrosoluble donor chain braking antioxidants or biophenols as α-tocopherol are instead liposoluble donor chain breaking antioxidants.

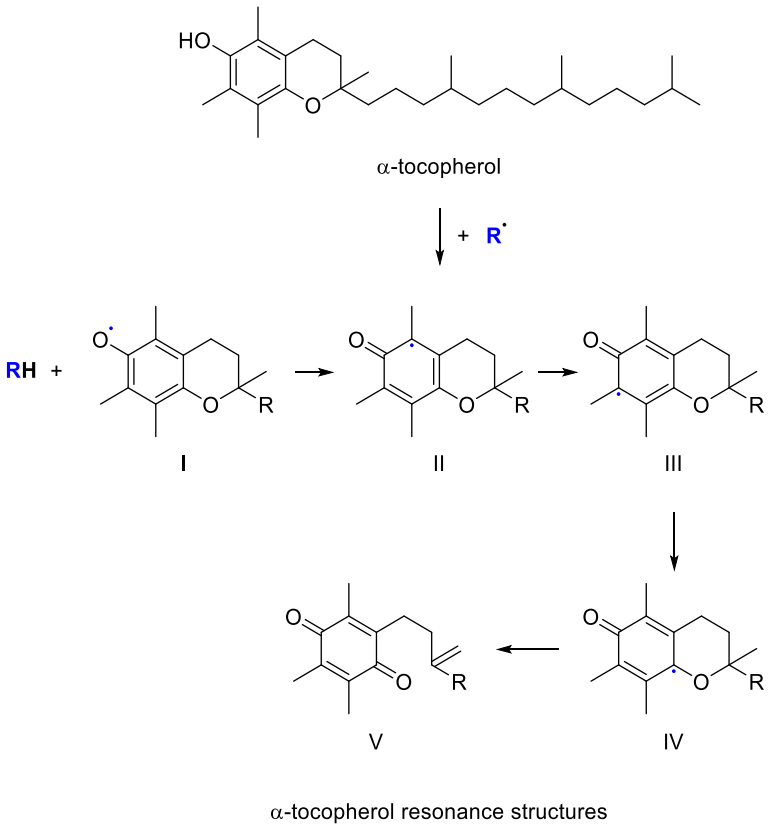

Scheme 6.2.4 *Donor chain breaking antioxidant, α-tocopherol, radical scavenging mechanism.*

The vitamin E family includes both tocopherol and tocotrienol which are characterised by a chroman heterocycle that can differ in the number and position of methyl groups, and an hydrophobic phytol terpenoid chain. This chain is fully saturated in the case of tocopherol and a triene in the tocotrienols.

Other donor chain breaking antioxidants belonging from the polyphenol family include L-ascorbic acid, quercitin, gallic acid and caffeic acid (Figure 6.2.1).

Depending on their reduction potential, they can act in a synergistic way and recycle each other as is the case for L-ascorbate (+282 mV) which is able to regenerate α-tocopherol (+480 mV).[47]

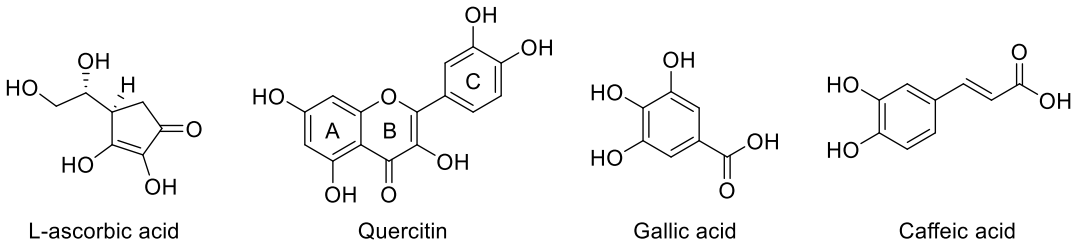

Figure 6.2.1 *Examples of donor-breaking chain antioxidants*.

Antioxidants such as nitric oxide (NO) are sacrificial chain breaking antioxidants as it acts as a chain terminator reacting with chain-carrying peroxy radical (Scheme 6.2.5).[48]

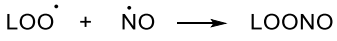

Scheme 6.2.5 *Nitric oxide acting as chain terminator*.

6.2.3. *Antioxidants Assays*

Considering that the action mechanism differs with each antioxidant active, several types of assay have been developed. It is important to note that "the antioxidant activity measured by an individual assay reflects only the chemical reactivity under the specific conditions applied in that assay, thus is inappropriate and misleading to generalize the data as indicators of total antioxidant activity".[1]

The assays can be divided in two major categories depending on the chemical reactions involved: single electron transfer (ET) and hydrogen atom transfer (HAT) assays.

HAT-based assays monitor competitive reaction kinetics, and the kinetic curves provide the data necessary for quantitative analysis. They are generally composed of a synthetic free radical generator, an antioxidant and an oxidisable molecular probe. ET instead involves a redox reaction with the oxidant, which also constitutes the probe, to monitor the reaction. Both classes of antioxidant assays measure the scavenging capacity of an antioxidant rather than its preventive ability.

ET methods includes Folin–Ciocalteu (FCR), ferric iron reducing antioxidant power (FRAP) assay, the Trolox equivalent antioxidant capacity (TEAC), *N*,*N*-dimethyl-*p*-phenylendiamine (DMPD) assay and the Cu(II) reduction capacity assay.

They are based on the assumption that the antioxidant capacity is equal to the reducing capacity.[49] They do not involve any oxygen-based radicals in the assay and there are no competitive reactions involved. In these type of assay, the oxidant also act as probe and it extracts electrons from the antioxidant. Analysis is determined by a change in colour (the reaction ends when the colour change stops). The change in absorbance (ΔA) registered is plotted against the antioxidant concentration to give a linear curve.

HAT methods includes oxygen radical capacity methods (ORAC), total radical trapping antioxidant parameter (TRAP), inhibited oxygen uptake (IOU), inhibition of LDL oxidation, inhibition of linoleic acid oxidation and Crocin bleaching assay. These assays are more relevant to the chain breaking antioxidant activity, considering that they quantify the hydrogen atom donating power of the antioxidant under analysis, which is a key step in the radical chain reaction.

There are also other types of antioxidant assays that do not fall into one of the categories mentioned above such as H_2O_2 scavenging capacity assay, hydroxyl radical ($OH\cdot$) scavenging assay, singlet oxygen scavenging capacity and peroxynitrite scavenging capacity assay.

6.3. Multi-Target Approach in Drug Design

The heterogeneous class of polyphenols is known for its wide range of activity, they have been reported to prevent and counteract numerous diseases, as mentioned before, but the most interesting characteristic of those molecules and the reason underlying their recent rediscovery by medicinal chemists worldwide is that they are natural multi-target actives. One of those natural occurring molecules can efficiently target multiple pathways, leading to no off targets. A better understanding of the action mechanism of those multi-target phytochemicals, and the optimization of these natural occurring lead compounds can open up to new strategies in medicinal chemistry. Two famous examples of natural multi-target polyphenols are curcumin that has been reported to inhibit COX-1, 5-LO,[50] NF-kb,[51] melanoma and other cancer cell line,[52] and caffeic acid which has been demonstrated to be

hepatoprotective, act as 5-LO[53] inhibitor, be efficient in inhibiting several kinds of tumours e.g. colon and fibrosarcoma,[54] and reducing aflatoxin*** production.[55]

Over the last two years the scientific community has begun to realise the advantages of a multi-target drug design compared to the traditional site-specific approach, going upstream compared to what was done over the past few decades from the medicinal chemistry community. The benefits from such an approach include not only a better balance between activity and side effects but also a reduction in cost and time to develop and reach the market.[56]

Several of the main advantages of poly-pharmacology over the site-specific target approach and combinatorial therapies include:[56]

1. Superior efficacy against advanced stage diseases compared to single target specific molecules, due to minimisation of efficiency of the body compensatory effect.
2. More predictable pharmacokinetic profile compared to multiple drug administration in combinatorial therapies.
3. Minor chances to develop target-based resistance.
4. Lower risk of side effects compared to combinatorial therapy.
5. More facile administration - simultaneous presence of the multi-target active principle where it is required.
6. A multi-target active could potentially be easier to develop as the regulatory requirements to demonstrate safety and activity, compared to a combinatorial treatments, would be less arduous.

It is possible to think of the multi-target concept as being dualistic. A multi-target drug can be designed to act on different locations of the same pathways. This was demonstrated by Werz and co-workers in 2014 through the development of new prenylated pyrazol-curcuminoids as anti-inflammatory analogues capable of targeting 5-lipoxygenase (5-LO) alongside with microsomal prostaglandin E synthase (mPGES-1).[57]

Alternatively, it is possible to think of multi-target strategies as a way to design molecules that can act on targets that are unrelated (or distantly related). This creates the opportunity to target different pathologies, as the case of methotrexate which has activity against target relating to cancer, psoriasis and rheumatoid arthritis.

*** Aflatoxin is a myco-toxin produced by *Aspergillus Flavus* and *Aspergillus Parssiticus*, fungi phatogenic fungi which attack trees and grains.

A major challenge in poly-pharmacology is to avoid excessive promiscuity in order to avoid side effects due to the interaction with anti-targets. For this reason, particular care should be addressed to try and optimise, during the design stage, the profiles of activity towards the selected targets in order to minimise the likelihood of side effects.

In practice, multi-target structure–activity relationship (SAR) studies is therefore a primary necessity but it is still considered far from routine, mostly due to the fact that poly-pharmacology, and the rational design of multi-target actives in itself, it is still in its infancy.

Presented in this thesis, a library of compounds was designed with specific features that could lead to interaction with multiple targets. Three main targets were chosen for the compounds presented in this work, of which two are involved in human inflammation processes. The first selected target was 5-lipoxygenase, a crucial enzyme of the arachidonic acid (AA) cascade and involved in the first two catalytic reactions of the biosynthesis of leukotrienes (LTs).[58] It has been established that the role of LTs as inflammatory mediators play a pathophysiological role in different diseases (asthma, allergic rhinitis, cardiovascular diseases and certain types of cancer).[59] The second target was transcription factor Nrf2, which is responsible of recognising the antioxidant response element (ARE) regulating a number of cytoprotective genes. The significance of the Nrf2-regulated cytoprotective adaptive response has been demonstrated in animal models of electrophilic and oxidative toxicity, carcinogenesis, inflammation-associated carcinogenesis, and acute inflammation.[60] (This target will not be discuss in the present work, giving that the molecules herein presented are still under investigation for this target).

The final target selected was 14 α-lanosterol demethylase a cytochrome P450 enzyme common to all dermatophytes. 14 α-Lanosterol demethylase is the target enzyme of azoles such as ketoconazole, miconazole and fluconazole. It is an enzyme involved in the synthesis of ergosterol, an important component of the dermatophytes cell wall. Considering that the mortality associated with dermatophytosis as reported by the World Health Organization (WHO) in sub-Saharan African region in 2001 was found to be similar to that attributed to gout, endocrine disease, panic disorders and war-related injuries and considering the increasing number of resistant strains, research in this area is still topical.

It is also noteworthy that dermatophytosis caused a higher mortality risk in patients affected by HIV. Furthermore, taking into account that mycosis is commonly associated with inflammation, it is easy to understand the relevance and reasoning behind our research

towards multi-target actives that are able to act both on the inflammation process and dermatophyte infections.

6.4. Arachidonic Acid Pathway

Arachidonic acid (ARA) is a fatty acid stored in membrane phospholipids, especially in phosphatidylcholine,[61] and is released from the phospholipids through the action of phospholipase A_2 where it is subsequently utilised by three major enzymes: cyclooxygenase (COX), lipoxygenases (5, 12 and 15-LO) and the cytochrome P450 monooxygenase.

Among the lipid mediators generated by those pathways is possible to discriminate two main classes of mediators: pro-inflammatory/non-resolving and anti-inflammatory/ pro-resolving (Scheme 6.4.1).

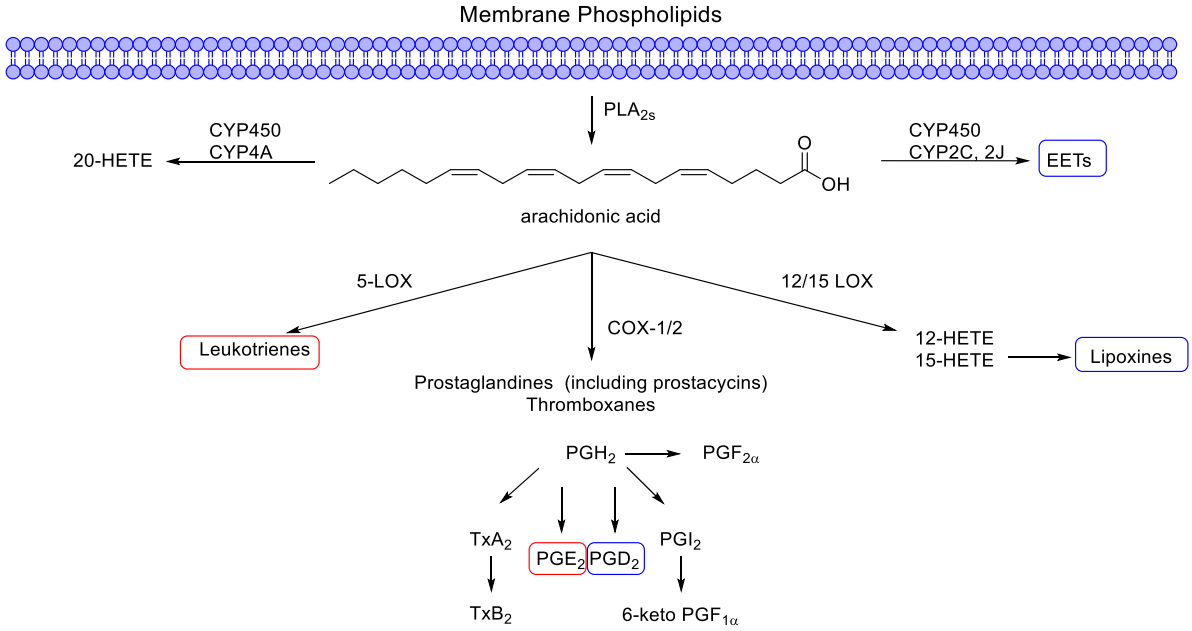

Scheme 6.4.1 *Summary of arachidonic acid pathways: pro-resolving/anti-inflammatory mediators (blue) and pro-inflammatory/non-resolving (red).*

A significant challenge in targeting the inflammation cascade is to decrease the formation of pro-inflammatory lipids mediators, such as PGE_2 and LTB_4, without affecting the level of the anti-inflammatory ones, such as PGD_2, lipoxins (LXs) or epoxy-eicosa-tetraenoic-acids (EETs). This can be realised by targeting the enzymes isoforms responsible for the production of pro-inflammatory mediators. The class of non-steroidal anti-inflammatory drugs known as Coxib (e.g. Etericoxib, Celecoxib), for example, specifically target the isoform COX-2 which is the one induced during inflammation processes, responsible for the

production of inflammatory prostacyclin. The market has been saturated over the years with drugs targeting COX on the arachidonic acid pathway. Another important target is represented by 5-lipoxygenase (5-LO) but despite efforts to find drug candidates targeting 5-LO, the only inhibitor to reach the market so far has been zileuton.[62]

Although 12- and 15-lipoxygenase have been shown to be involved in inflammation processes, they are also responsible of the synthesis of resolving mediators such as lipoxins. For this reason, it is more desirable to specifically target 5-LO among the lipoxygenase isoforms. The only products of 5-LO pathway are, in fact, leukotrienes which are pro-inflammatory mediators. Leukotrienes have been shown to be connected not only with pathologies such as asthma and allergic rhinitis as well as cardiovascular diseases but also with certain types of cancer.[63] Thus it is important to avoid their formation in order to counteract the inflammation response.

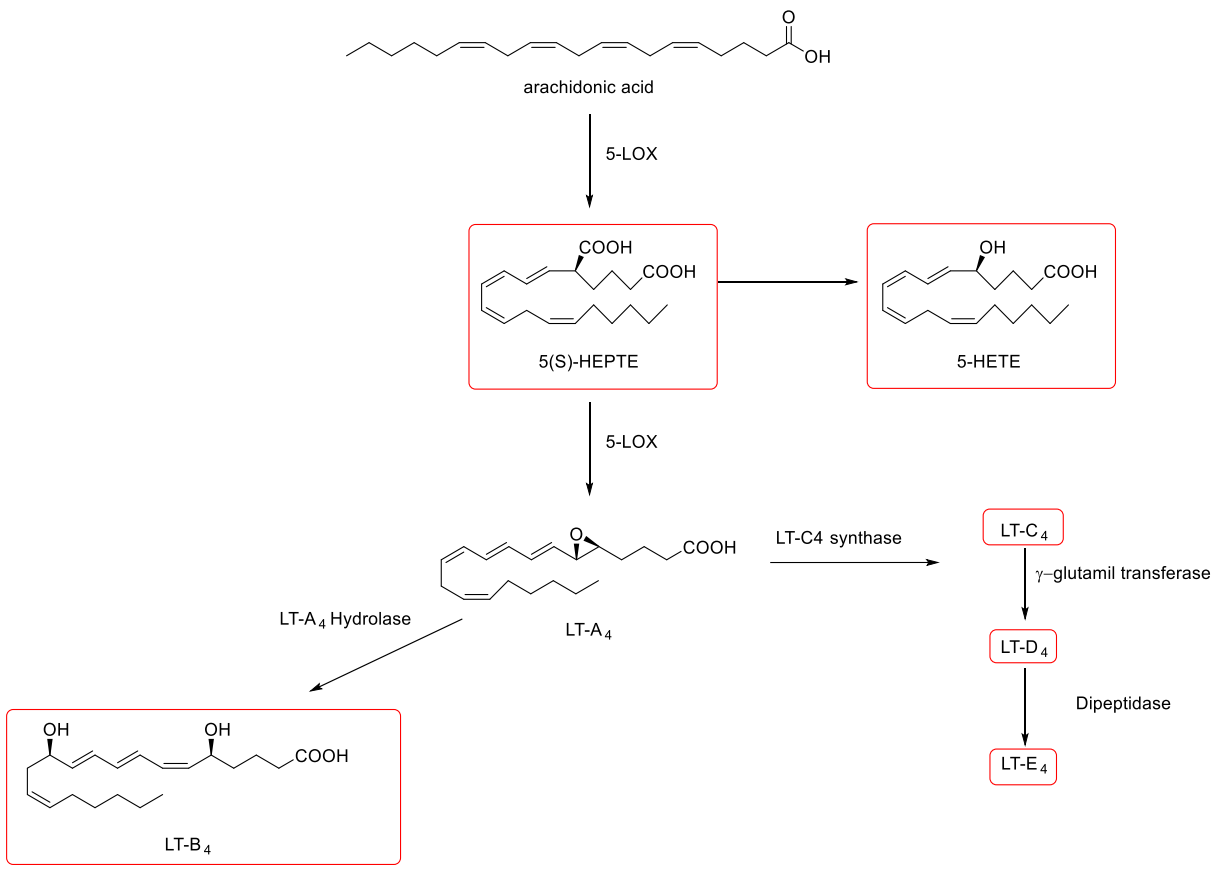

Scheme 6.4.2 *5-Lipoxygenase pathway*.

Leukotrienes (LTs) are paracrine lipid mediators that bind to rhodopsin-like G protein–coupled receptors which has various roles in inflammation and immunological function.

Among the leukotrienes, LTB_4 is a potent chemotactic agent for inflammatory cells including neutrophils, macrophages and eosinophils alongside with the Cys-LTs, LTC_4, LTD_4, and LTE_4 which are potent constrictors of airway smooth muscles leading to bronchoconstriction which is formed by the intervention of 5-LO on arachidonic acid (ARA). These LTs increase leukocyte tissue infiltration and play an important role in immune reactions by enhancing the release of pro-inflammatory cytokines by macrophages and lymphocytes and are involved in immediate hypersensitivity reactions. Cys-LTs are also responsible for the increase of vascular permeability leading to oedema through contraction of endothelial cells (EC) in the microvasculature. LTs can also interact with sensory nerve fibres, leading to changes in their excitability and enhanced release of tachykinins. Therefore they are important inflammatory mediators in a number of different inflammatory diseases and allergic disorders.[64]

5-Lipoxygenase is one of six isoforms of lipoxygenase present in humans and it is expressed in different leukocytes poly-morphonuclear leukocytes (neutrophils and eosinophils), mast cells, monocytes/macrophages, B-lymphocytes, dendritic cells and foam cells. It is a monomeric enzyme containing 672/673 AA. Its structure is characterised by an N-terminal β-sandwich and a C-terminal catalytic domain binding the prosthetic iron that is ferrous (Fe^{2+}) for purified recombinant 5-LO treatment with lipid hydroxides such as 5-HPETE which transforms it into ferric (Fe^{3+}). It utilises two co-factors, Ca^{2+} (fundamental for 5-LO activity) that binds to a C2 domain on the N-terminal β-sandwich and adenosine triphosphate (ATP).[65] It seems that ATP has a stabilising role on the enzyme and its hydrolysis is not needed. The affinity between 5-LO and the ATP is used in the purification processes of the enzyme, although the precise binding site of ATP has not been determined yet.[66] 5-LO also utilises 5-LO activating protein (FLAP), a member of the Membrane-Associated Proteins in Eicosanoid and Glutathione metabolism (MAPEG) family, through protein-protein interactions for catalytic activity. FLAP appears to facilitate the transfer of ARA to 5-LO, a hypothesis which is supported by the evidence that when FLAP is inhibited (or not expressed) the transformation of endogenous amino acid into 5-LO products is blocked.[67] Interestingly, ARA supplied from the exogenous environment is able to be metabolised even when the FLAP activity is inhibited. 5-LO can be stimulated through phosphorylation by kinases, in particular p38 mitogen activated protein kinase (p38 MAP kinase) on Ser-271, serine kinase ERK2 on Ser-663 and cAMP-dependent protein kinase PKA catalytic subunit

on Ser-523. Regarding polymorphonuclear leukocyte (PMNL), evidence has shown that p38 MAP kinase and ERK2 were important for ARA-induced 5-LO product formation.67

As shown in Scheme 6.4.2, the metabolism of arachidonic acid (ARA) by 5-LO starts by generating 5-(*S*)-HPETE, which is subsequently either reduced to the corresponding alcohol, 5-HETE, or to the short lived epoxy-leukotriene, LTA_4. The latter is further metabolised to release a series of LTs either via the hydrolysis of its epoxide by LTA_4 hydrolase (LTA4H) to the corresponding diol, LTB_4, or its metabolism to the cysteine-adduct LTC_4 from which other cysteinyl-LTs (Cys-LTs), LTD_4 and LTE_4, are sequentially formed from LTC_4.[68]

Strategies to counteract the pro-inflammatory activity of the product of 5-LO have involved blocking the leukotrienes receptors (montelukast and zafirlukast), direct inhibitors of 5-LO of which the only representative on the market up to date is zileuton.

Given the recent findings on the multiple factors that influence the regulation of leukotriene formations such as FLAP, ERK2, p38 MAP kinase and Ca^{2+} etc. more focus is being placed nowadays on targeting these as well (e.g. licofelone FLAP inhibitor), in order to achieve a

larger success chance on the intact cell environment. Multi-target strategies that attempt to inhibit the arachidonic acid pathway at different sites are starting to be explored.

The 5-lipoxygenase inhibitors can be classified based on the stage they are interacting at:

- Direct 5-LO inhibitors:[69]
    - Iron ligand inhibitors[70] (zileuton)
    - Redox inhibitors (polyphenols)
    - Non redox competitive inhibitors (they compete with arachidonic acid to bind to the enzyme active site)69
- Inhibitors of LTA_4 hydrolase[71]
- FLAP inhibitors (Licofelone)[72]
- Leukotriene receptor inhibitors (Montelukast, Zafirlukast)

Among the direct 5-LO inhibitors, despite the 25 years of research on the topic, the only commercial compound, as previously mentioned, is *N*-[1-(1-benzothien-2-yl)ethyl]-*N*-hydroxyurea (zileuton) (Figure 6.4.1).

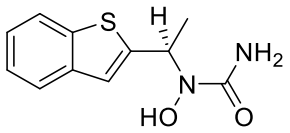

Figure 6.4.1 *Structure of zileuton.*

The *N*-hydroxyurea portion of the molecule acts by chelating to iron in the active site of 5-LO preventing it from oxidising and thus entering the catalytic cycle. It also possesses weak reducing properties auxiliary to the inhibitory activity towards 5-LO.[73] It has various drawbacks such as short half-life and liver toxicity which is due to irreversible inhibition of glutathione *S*-transferase through alkylation.

Among the redox inhibitors, it is worth mentioning a few polyphenols including curcumin, resveratrol, baicalin, catechin, quercitin and caffeic acid (Figure 6.4.2). Their antioxidant potential is well-known, thus they interact with 5-LO avoiding the oxidation of ferrous iron present in the catalytic site.

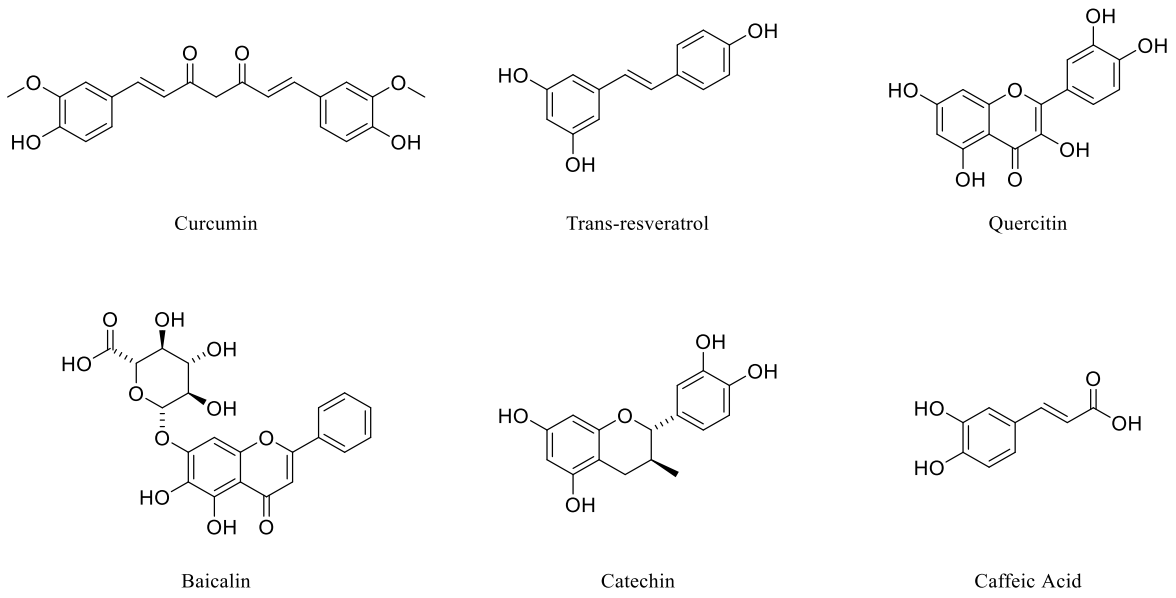

Figure 6.4.2 *Examples of polyphenols targeting 5-LO product formation.*

A combination of baicalin and catechin, known as Flavocoxid (Limbrel), is currently under clinical development for the treatment of osteoarthritis.[74] Other polyphenols such as curcumin are effective in inhibiting 5-LO product formation and inflammation processes, not only because of its antioxidant properties but also due to its ability to interact at different locations of the arachidonic acid pathway. They are a natural lead compound towards the development of multi-target actives with proven safety and activity.62

Another site on the arachidonic acid pathway that is emerging as good target in anti-inflammatory therapy is FLAP. Licofelone (Figure 6.4.3) is an active that was developed as dual COX/5-LO inhibitor and has been proven to target FLAP.[75] It is currently undergoing phase III clinical trials for therapy of osteoarthritis.72

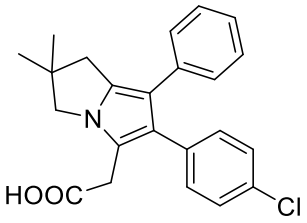

Figure 6.4.3 *FLAP inhibitor in phase III clinical trials.*

The mode-of-action of licofelone targeting FLAP was first evidenced by the fact that the compound showed only weak inhibition of 5-LO in cell free assays and instead, showed high inhibition power on PMNL, highlighting that licofelone needed the intact cell environment

to exert its function. In the intact cell environment, FLAP is present thus Fisher et al. investigated its interference with FLAP, finding in this interaction the reason of its activity.

Another strategy to counteract the inflammatory response catalysed from the 5-LO pathway is to inhibit the leukotriene receptors. This is the action mechanism of clinically approved montelukast and zafirlukast (Figure 6.4.4), which inhibit the cysteinyl-leukotrienes on the CysLT1 receptors.

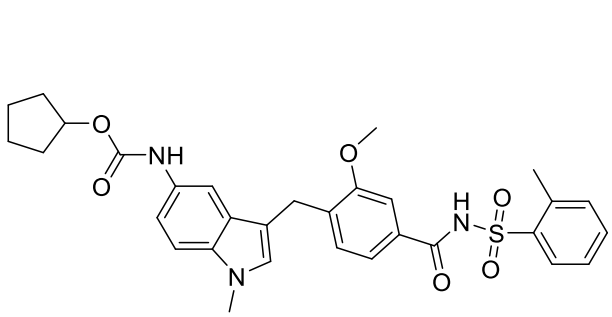

Zafirlukast

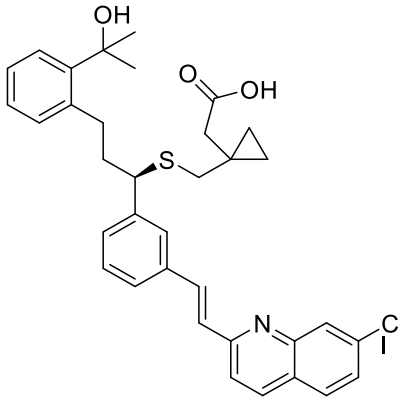

Montelukast

Figure 6.4.4 *Cysteinyl-leukotrienes inhibitors used in asthma therapy*.

6.5. Dermatophytes

Fungi can be classified as either pathogens or non-pathogens, depending on their ability to cause pathological states or not. The majority of fungi are non-pathogens. Dermatophytes are fungi that invade and grow in dead keratin. They are hyaline separate molds. The hyphae of these mycelial organism are able to penetrate the stratum corneum of nails and skin and they possess keratinolytic proteases, which enable the microorganism to entry the living cells.[76] A wide number of the known keratinolytic fungi belong to either the family of *Arthrodermataceae* (which include genera *Epidermophyton, Microsporum* and *Trichophyton*) or *Onygenaceae* from the phylum *Ascomycota*.[77] They are spore shooter microorganisms, the spores generate the mycelium. These families are generally homogeneous with respect to appearance, physiology, taxonomy, antigenicity, basic growth requirements, infectivity and diseases they cause. They tend to grow outwards on skin producing a ring-like pattern – hence the term 'ringworm'. They are very common and affect different parts of the body causing dermatophytosis.[78] They can affect nails leading to

onychomycosis a general term that denotes any fungal nail infection[79] (*tinea unguium* specifically describes a dermatophytic invasion of the nail plate, *Tricophyton rubrum* is the dermatophyte that is generally responsible), onychomycosis generally leads to destruction and deformity of toe and fingernails, nail thickens, change colour, split and lift from the nail bed.[80]

Dermatophytes can also affect the scalp (tinea capitis, *Tricophyton* and *Micosporum* genera are mainly responsible) they cause patches on the scalp of hair loss, sometimes associated with a "black dot" pattern, accompanied by inflammation, swelling, itching, pustules and scaling. *Tricophyton tonsurans* and *Tricophyton violaceum* are examples of dermatophytes causing scalp dermatophytosis.

Furthermore, they can affect skin, causing scaling, crusting, sometimes blister-like lesions, rushes and the classic round spots pattern, typical of ringworm lesions, it can be associated with inflammation, an example of microorganism responsible for this dermatophytosis is *M. canis.*

The mycosis generated by dermatophytes can be separated in localised and profound dermatophytosis,[81] although with the clinically approved drugs it is possible to obtain high success rates, systemic mycosis are much more difficult to treat which is why continued research into antimycotic actives for systemic application is essential. One of the difficulties of treating a systemic dermatophyte infection is the fact that dermatophytes tend to attack tissues poorly vascularised and thus are more challenging for the delivered drug to reach the site of infection. Furthermore, there is a problem in selectively targeting the dermatophytes towards the fungi cells rather than the human forms.

Systemic mycosis mainly affect, and are a main concern for, people with a compromised immunosystem, such as patients with HIV or cancer, in which the dermatophytes grow and develop quicker and easily. These infections, in immuno-depressed subjects can degenerate to cause fatality. Other factors that can enhance the risk of dermatophytosis are prolonged hospitalisations, alcohol abuse, radiotherapy, haemodialysis and serious burns.

6.5.1. *Targets for Dermatophyte Therapy*

All dermatophytes are characterised by an unusual cell structure. It is important to know the dermatophyte strain in order to understand in which way different antimycotic drugs exert their function.

The cellular membrane, also known as cytoplasmic membrane, covers the cytoplasm with all its components and forms a barrier between the cell environment and its components. If the membrane is damaged, all the cytosolic components are released leading to the death of the cell.

The cell wall that protects and shapes the cell membrane in dermatophytes, is made up of a dense network of fibrils of chitin (β-1-4 polymer of *N*-acetyl-glucosamine).

The cell membrane is primarily composed of lipids (phospholipids), among which sterols ergosterol and lanosterol are the most important, and their synthetic pathways are preferred targets in the antimycotic therapy. Ergosterol is synthesised from lanosterol and is fundamental to keep the homeostatic equilibrium of the cell membrane and its integrity.

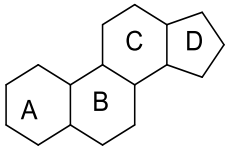

Figure 6.5.1 *Steroidal backbone.*

Sterols are compounds characterised by a fused tetracyclic motif (Figure 6.5.1). Natural hormones belonging from the sterols class such as cortisol, estrogens, testosterone, or actives such as cortisone and its derivative possess have this tetracyclic in common.

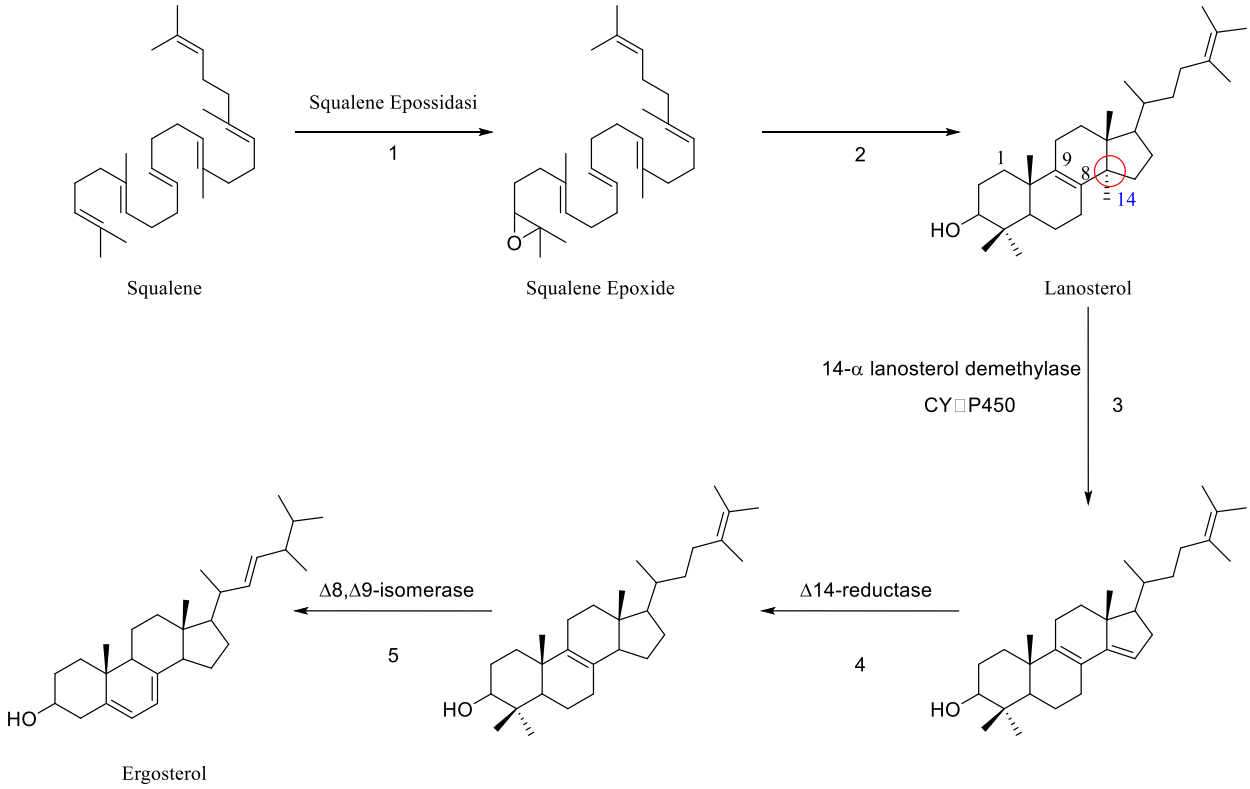

Figure 6.5.2 *Synthesis of cell membrane in dermatophytes.*

The synthesis of ergosterol provides a privileged target for antimycotic drugs. Different classes of molecules act at different levels, for example, allylamine (amorpholine and its derivatives) act by blocking the squalene epoxidase (Figure 6.5.2) azole-containing derivatives act against 14 α-lanosterol-demethylase (Figure 6.5.2), morpholines target, instead, Δ14-reductase and Δ8, Δ9 isomerases 4 and 5 (Figure 6.5.2).

6.6. Azole-containing derivatives

Azole-containing antimycotic drugs include structures containing imidazole or triazole rings which possess the same antimycotic action mechanism.

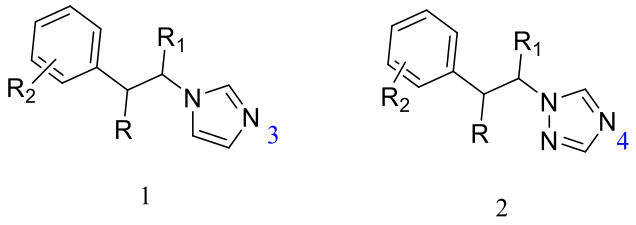

Figure 6.6.1 *Azole-containing derivatives general structures, 1 imidazole, 2 triazole.*

The activity demonstrated by azole-containing derivatives is due to the heteroaromatic ring (imidazole or triazole) and to the tetrahedral symmetry to which the heterocycle is bound.[82]

All the azole-containing derivatives act by inhibiting the 14 α-lanosterol demethylase through the basic nitrogen of the heterocycle which binds the haem group of CYP450 in the position normally occupied by oxygen. The remaining portion of the molecule interacts with other parts of the apo-protein and allows the active compound to specifically recognise that enzyme among all the CYP450 ones. Blocking the activity of 14 α-lanosterol demethylase leads to a backlog of sterols still bearing the methyl at the 14 α-position, which changes the membrane permeability making it less efficient and altering the functionality of membrane's proteins.[83]

Studies on *Saccharomices Cervisiae* indicate that two nitrogen atoms of the azole ring structures, nitrogen in position 3 for imidazoles, and nitrogen in position 4 in triazoles, is necessary to stabilise and to complex the ferric ion of the haem group. The other portion of the azole-containing molecules, such as the alkyl substituents R and R_1 in the molecules are important in determining the binding interactions with it (Figure 6.6.2).[84]

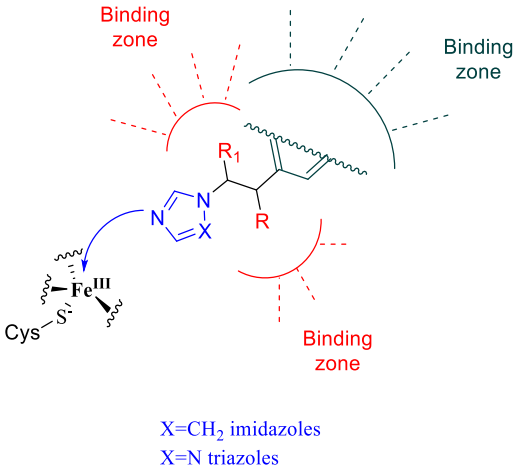

Figure 6.6.2 *Interaction of the azole rings with* 14 α-*lanosterol demethylase of S. Cervisiae.*

Among the azole-containing examples of drugs used in localized infections are miconazole and econazole, and for systemic therapy, ketoconazole, voriconazole and fluconazole (Figure 6.6.3).

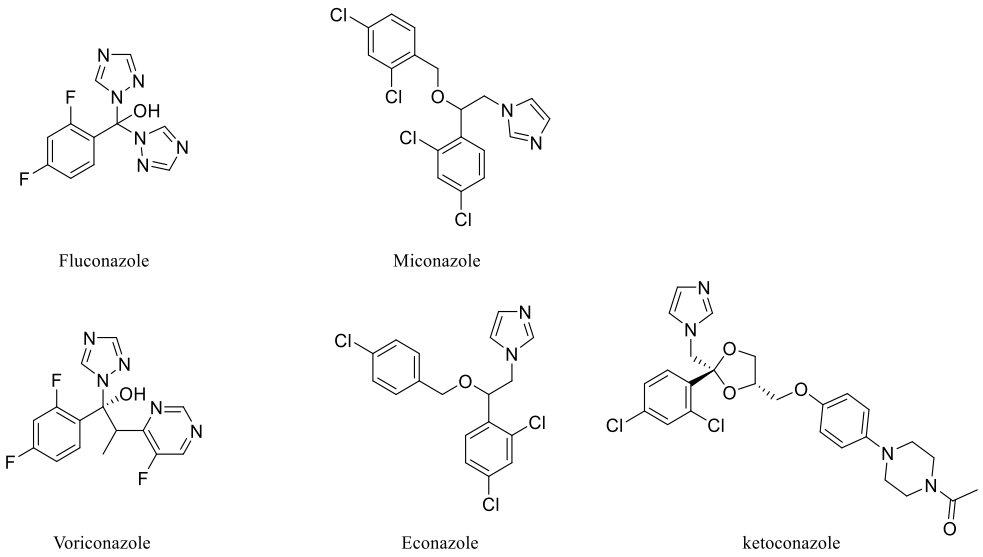

Figure 6.6.3 *Examples of azoles antimycotic drugs.*

Is important to mention that triazoles, compared to imidazoles, have a slower metabolic breakdown pathway and are more specific towards the CITP450 of the dermatophytes over the human one.

7. Project aims and background

7.1. Novel Semi-Synthetic Polyphenol Analogues and Related SAR Studies

The originally proposed project centred on the design of semi-synthetic polyphenol analogues. The aim was to find new carriers for those natural compounds and to enhance their bioavailability, half-life in the blood, facilitate their transport across cell membranes and consequently result in an increase in their biological activity.

Initially, it was believed this could be achieved through the syntheses of polyethylene glycol (PEG)-linked conjugates or sugar derivatives - changing the type and position of the sugars. Evidence in the literature supported this proposal, particularly research from Jun Li et al.[85] on PEG-derivatives of curcumin, Kunihiko et al.[86] on glycosyl-curcuminoids and of L. Biasutto et al.[87] on resveratrol. Based this precedence, efforts were focused to achieve the pegylation of curcumin.

Curcuminoids and polyphenols, in general, have attracted a strong interest because of their versatility in terms of biological activities, applications and available sources. These classes of compounds demonstrate anti-cancer, anti-inflammatory, anti-oxidant, anti-artherosclerotic properties, as well as neuro- and cardio-protective activities. They have been used in prebiotics, pharmaceuticals, cosmetics, nutraceuticals and can be extracted from renewable sources such as tea leaves, grapes, cocoa beans and vegetables.[88]

After preliminary studies inherent to these classes of molecules, efforts were re-directed to consider alternative ways to enhance the performance of the polyphenols of interest. The focus of the project was, consequently, redirected. New linkers were chosen that not only could act in a similar way to polyethylene glycol, i.e. increasing water solubility through hydrogen bond interactions, but could also serve as active pharmacophores, thereby no more acting just as simple passive connection units. It was thought that this would expand the activity profile of the synthesised analogues and enable the introduction of molecular diversity. To achieve this, linkers based on a triazole core were targeted as building blocks (Figure 7.1.1).

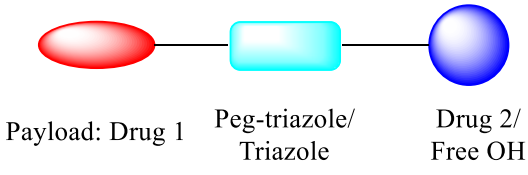

Figure 7.1.1 *General scheme for the library of compounds.*

Triazoles are known to act as pharmacophores, capable of interacting with a broad range of targets. They have been attributed to the activity in several antifungal, antibacterial and anticancer agents, HIV protease inhibitors[89] and anti-inflammatory compounds.[90]

From a synthetic standpoint, an advantage of incorporating the triazole motif into the linker is the relatively simple and inexpensive method of preparation: the copper catalysed azide–alkyne cycloaddition (CuAAC) better known as "click chemistry". Modifications to the azide and alkyne coupling fragments facilitate the introduction of molecular diversity.[91]

This choice of linker also opened the scope of the project to the concept of poly-pharmacology, which is an area of increasing interest amongst the medicinal chemist community. There are several benefits of a multi-target approach which include not only a better balance between activity and side effects but also a reduction of costs and time of development to reach the market.[92]

When considering the concept of a multi-target approach it is possible to think about it as dualistic. A multi-target drug can be designed to act on different levels of the same pathways, as demonstrated by Werz and co-workers[93] by the development of new prenylated pyrazole-curcuminoids as anti-inflammatory analogues able to target 5-LO alongside with mPGES-1. Alternatively, it can be thought of as a way to design molecules that can act either on un-related or distantly related targets in order to reach different pathologies, as is the case of methotrexate which is used in treatment therapies from cancer to psoriasis to rheumatoid arthritis.

A major challenge in poly-pharmacology is to avoid excessive promiscuity in order to limit the side effects as much as possible caused by interaction with anti-targets. For this reason, particular care should be during the optimisation process, the synthetic-design stage and the activity profiles towards the selected targets. In the field of medicinal chemistry, multi-target structure–activity relationship (SAR) studies is therefore a primary necessity but it is still far from routine mostly due to the fact that poly-pharmacology, and the rational design of multi-targets active as a science, is still in its infancy. Therefore, further research into this area is required to fully understand the value of this concept.

Three main targets were chosen for our library of compounds of which two are reported to be involved in the human inflammation process. The first of which was 5-lipoxygenase, a crucial enzyme of the arachidonic acid (AA) cascade and involved in the first two catalytic reactions of the biosynthesis of leukotrienes (LTs).[94] It has been established that the role of

LTs as inflammatory mediators play a pathophysiological role in different diseases, for example, asthma and allergic rhinitis as well as cardiovascular diseases and certain types of cancer.[95] The second target was transcription factor Nrf2, which is responsible of recognising the antioxidant response element (ARE) regulating a number of cytoprotective genes. The significance of the Nrf2-regulated cytoprotective adaptive response has been demonstrated in animal models of electrophilic and oxidative toxicity, carcinogenesis, inflammation-associated carcinogenesis, and acute inflammation.[96] (This target will not be discuss in the present work, giving that the molecules herein presented are still under investigation on this target).

The final target selected was 14 α-lanosterol demethylase a cytochrome P450 enzyme common to all dermatophytes. Dermatophytes are fungi that enter and grow in dead keratin tissue. Several species commonly invade human keratin and these belongs to the *Epidermophyton*, *Micosporum* and *Trichophyton* genera. They tend to grow outwards on skin producing a ring-like pattern, hence the term 'ringworm'. They are very common and can affect different parts of the body.[97]

14 α-Lanosterol demethylase is the target enzyme of azoles such as ketoconazole, miconazole and fluconazole. It is an enzyme involved in the synthesis of ergosterol, an important component of dermatophytes cell wall. This enzyme is targeted by a number of triazole-containing fungicide drugs. Considering that the mortality associated with dermatophytosis as reported by the World Health Organization (WHO) in Sub-Saharan African region in 2001 was found to be similar to that attributed to gout, endocrine disease, panic disorders and war related injuries and considering the increasing number of resistant strains, research in this area is still topical.

It is also noteworthy that dermatophytosis cause a higher mortality risk in patients affected by HIV. Furthermore, taking into account that mycosis is commonly associated with inflammation, it is easy to understand the relevance and reasoning behind our research towards multi-target actives that are able to act both on the inflammation process and dermatophytes infections.

8. Results and Discussion

8.1. Preliminary Studies Toward Curcumin Analogues

The substrate initially chosen within the polyphenol family was curcumin, given its known multi-target activity. It is, in fact, largely reported to be an anti-oxidant, anti-cancer[1] (against, for example, melanoma, pancreatic cancer etc.) and anti-inflammatory active.[9] Some of the main problems connected with the use of polyphenols include their poor solubility in organic media, rapid metabolic clearance and issues associated with *in vivo* delivery which overall leads to poor bioavailability. In the past numerous synthetic strategies were adopted to overcome these issues including pegylation,[1] liposomes[98] and glycosylation (a chemical modification used in nature to protect polyphenols from enzymatic oxidation enhance their half-life in cells).[99]

Based on this precedence, analogue **1** was initially set as a target to evaluate the possibility of synthesising a new family of semi-synthetic curcuminoids (Figure 8.1.1).

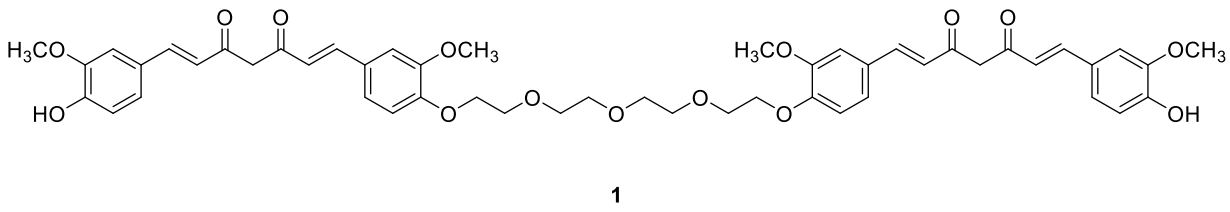

1

Figure 8.1.1 Semi-synthetic analogue of curcumin.

Starting materials **2** and **3** (Figure 8.1.1) were prepared *via* known procedure before the *O*-alkylation reaction was investigated (

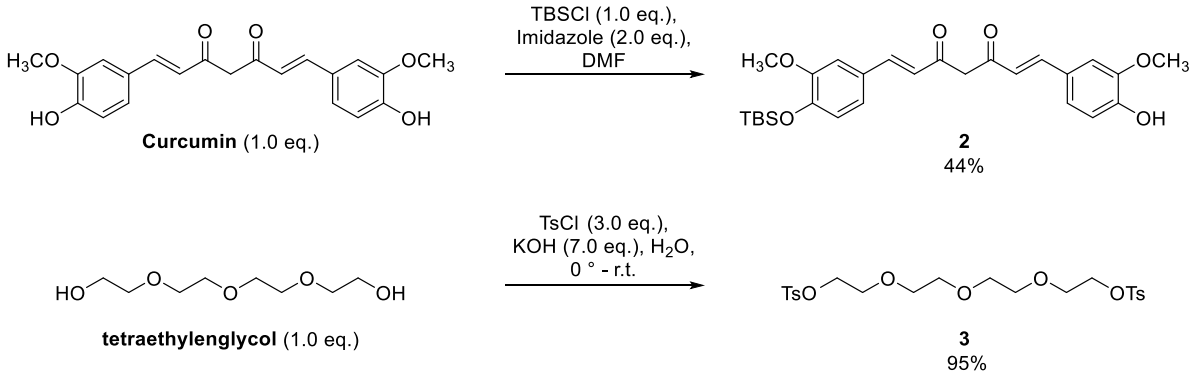

Scheme **8.1.1**).

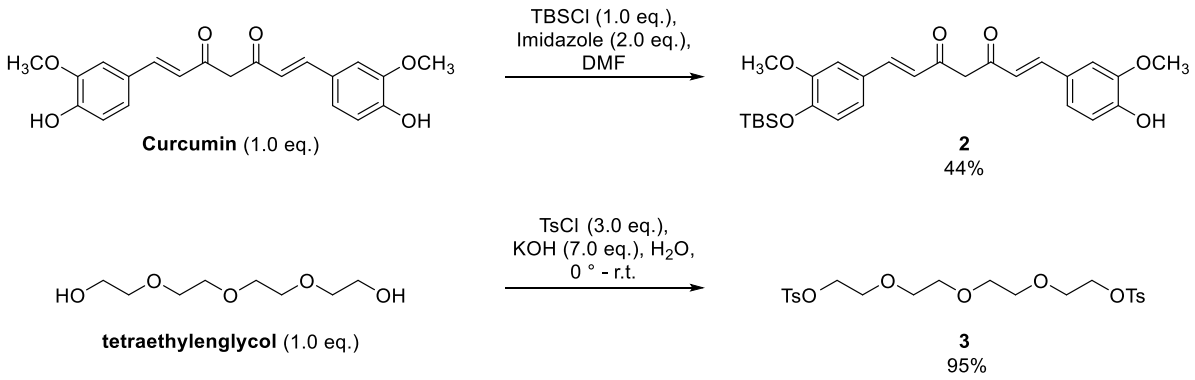

Scheme 8.1.1 *Syntheses of silyl-protected curcumin (**2**)*[100] *and tosyl-protected tetraethylene glycol (**3**).*[101]

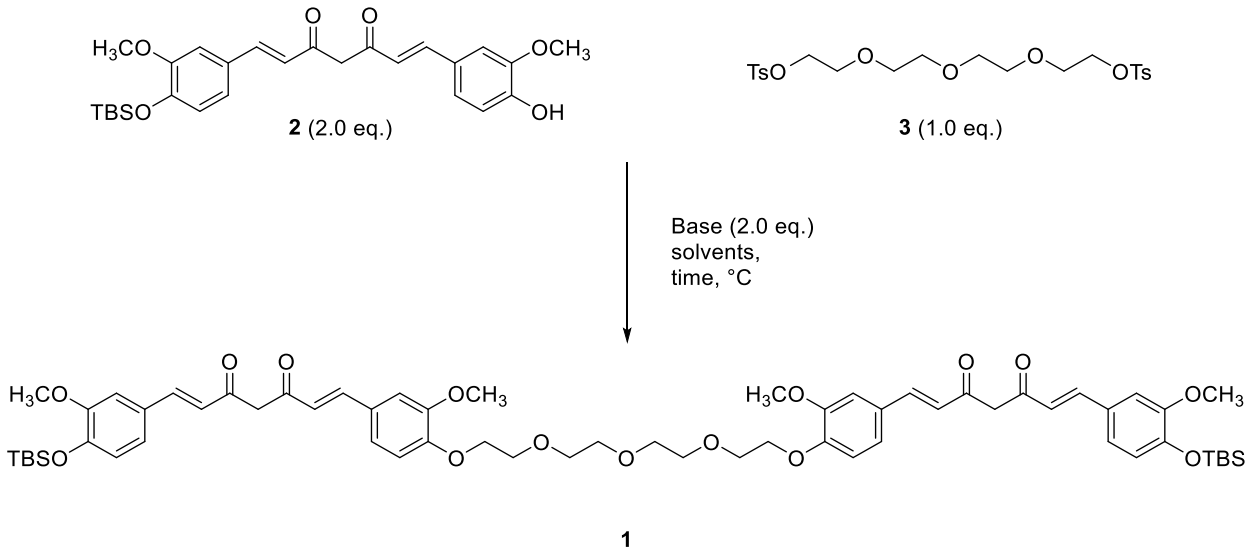

Scheme 8.1.2 *O-Alkylation between silyl-protected curcumin (**2**) and bis-tosylated tetraethylene glycol (**3**).*

Initial screening of the *O*-alkylation reaction lead to no product formation (**Error! Not a valid bookmark self-reference.**). Instead, the reaction mixtures indicated the conversion of mono-protected curcumin **2** back to curcumin.

Table 8.1.1 *Reaction conditions for O-alkylation. DMF = dimethylformamide.*

ENTRY	BASE	SOLVENT	TEMP. [°C]	TIME [HOURS]
1	K_2CO_3	DMF	80	12
2	K_2CO_3	DMF	20	12

The *tert*-butyldimethylsilyl (TBS) protecting group revealed to be unexpectedly unstable under basic conditions and we thus decided to perform a more detailed screening of the stability of mono-protected curcumin **2** under different combinations of solvent and base (

Table **8.1.2**).

Table 8.1.2 *Stability test of mono-protected curcumin **2** under different solvent/base combinations. The stability was monitored by thin layer chromatography. DIPEA = diisopropylethylamine; DMF = dimethylformamide; DCM = dichloromethane; THF = tetrahydrofuran; DMSO = dimethyl sulfoxide; NMP = N-methyl-2-pyrrolidone; MTBE = methyl tert-butyl ether.*

Entry	***Base***	***Solvent***	***Comments***
1	K_2CO_3	DMF	Curcumin recovered
2	NaH	DMF	Curcumin recovered
3	DIPEA	DMF	Curcumin recovered
4	Cs_2CO_3	DMF	Curcumin recovered
5	Cs_2CO_3	DCM	TBS-protected curcumin 2 was stable under these conditions
6	Cs_2CO_3	Acetone	Curcumin recovered
7	Cs_2CO_3	THF	TBS-protected curcumin 2 was stable under these conditions
8	Cs_2CO_3	Dioxane	TBS-protected curcumin 2 was stable under these conditions
9	Cs_2CO_3	DMSO	Curcumin recovered
10	Cs_2CO_3	NMP	Curcumin recovered
11	Cs_2CO_3	Methanol	Curcumin recovered
12	Cs_2CO_3	MTBE	TBS-protected curcumin 2 was stable under these conditions
13	Cs_2CO_3	Ethanol	TBS-protected curcumin 2 was stable under these conditions
14	Cs_2CO_3	Acetonitrile	Curcumin recovered

The conditions in entry 7 were used for subsequent *O*-alkylations of mono-protected curcumin **2** as it was noted that these conditions had a better solubility profile than those used in entries 8, 12 and 13. However, it was found that under these conditions, when proceeding with the *O*-alkylation a complex mixture of products was formed and it proved difficult to isolate and/or characterise the desired product. It was thought that the complex

mixture formed may have been caused by the nature of the protecting group and so a variety of mono-protected curcumin analogues were prepared and screened under the optimal *O*-alkylation conditions (Scheme 8.1.3).

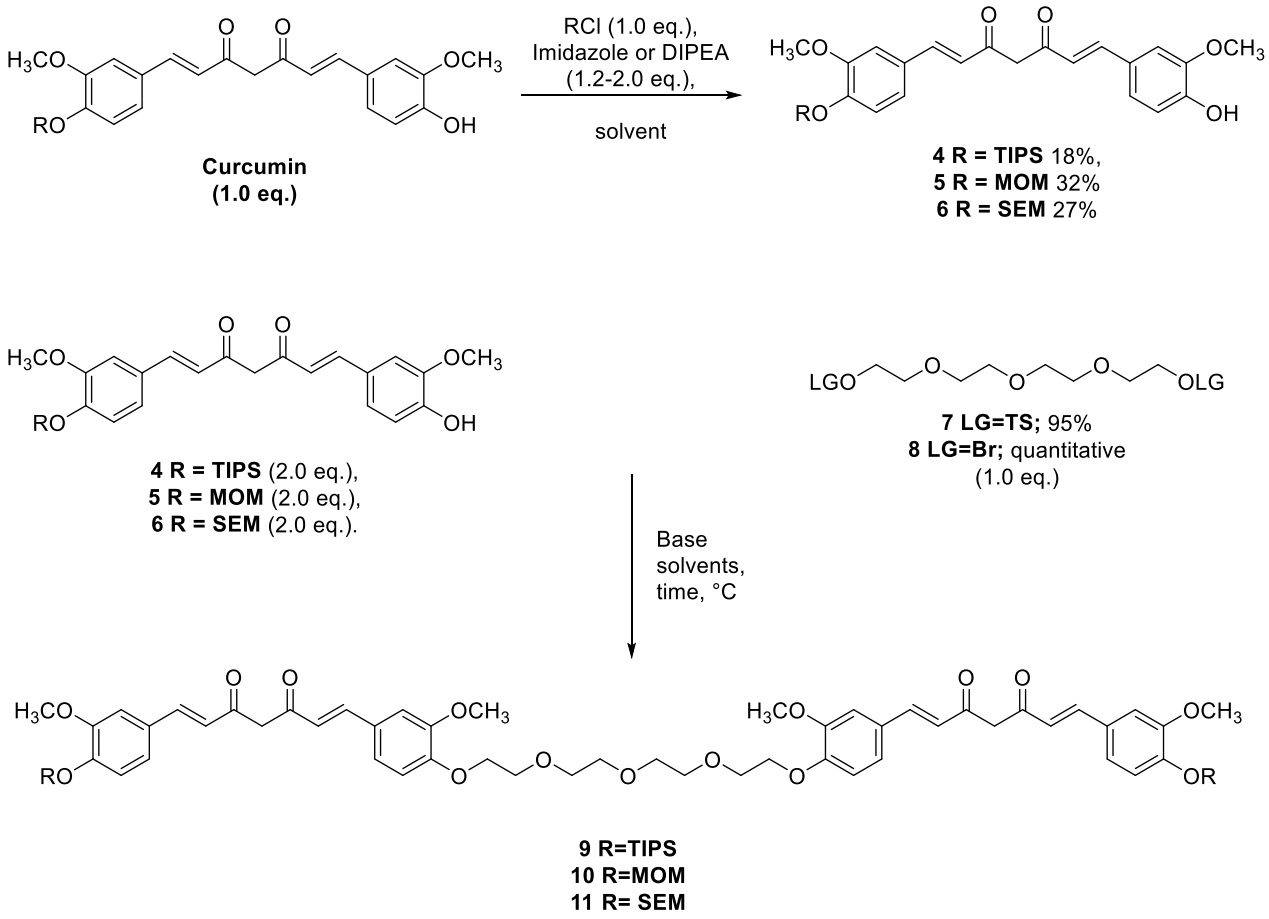

Scheme 8.1.3 *Synthesis of mono-protected curcumin analogues **4**, **5** and **6** were achieved following procedures previously reported in the literature.*[15,102,103]

Table 8.1.3 *Reactions between differently mono-protected curcumin and bis-tosylated PEG 7. DMF = dimethylformamide.*

ENTRY	MONO-PROTECTED CURCUMIN	PEG ANALOGUE	BASE [EQ.]	SOLVENT	TEMP. [°C]	RESULT
1	4	7	Cs_2CO_3 (4.0)	DMF	20	Curcumin recovered
2	5	7	Cs_2CO_3 (4.0)	DMF	20	Complex mixture
3	6	7	Cs_2CO_3 (4.0)	DMF	20	Complex mixture

Despite changing the protecting group on curcumin, it was not possible to afford the desired product and again, the silyl protecting group (triisopropylsilyl) proved to be unstable in basic conditions furnishing only curcumin (entry 1,

Table **8.1.3**). It was then hypothesised that a possible issue for the lack of product formation could be due to the slow reactivity of the tetra-ethylene glycol intermediate. And so, *bis*-bromo tetraethylene glycol **8** was prepared and used in the *O*-alkylation reaction (Table 8.1.4).

Table 8.1.4 *Reactions between mono-protected curcumin **6** and bis-tosylated PEG **8**. DMF = dimethylformamide; THF = tetrahydrofuran.*

ENTRY	MONO-PROTECTED CURCUMIN	PEG ANALOGUE	CATALYST	BASE [EQ.]	SOLVENT	TEMP. [°C]	RESULTS
1	6	8		Cs_2CO_3 (4.0)	DMF	20	Complex mixture
2	6	8	NaI	Cs_2CO_3 (4.0)	DMF	20	Complex mixture
3	6	8		Cs_2CO_3 (4.0)	THF	20–70	Complex mixture
4	6	8		NaH (4.0)	THF	60	Complex mixture
5	6	8		K_2CO_3 (4.0)	Acetonitrile	120	Complex mixture

Despite these variations, it was never possible to isolate the desired *O*-alkylated product. Due to these persistent difficulties, it was decided to reshape the project to employ alternative linkers and substrates.

8.2. Library Planning Strategy Assisted Through *In Silico* Evaluation

8.2.1. *Molecular Modelling Studies*

The design of the synthesised compounds was assisted by molecular modelling studies, which were performed in collaboration with the group of Prof. Bender from Cambridge University. The preliminary docking screen performed, directed the choice of the linkers backbone.

Computational studies, on the proposed targets, were performed on human 5-lipoxygense (5-LO) PDB: 3O8Y, and on 14 α-lanosterol demethylase from *S. Cerevisiae* PDB: 4K0F.

Docking studies on Nrf2 were not performed because of insufficient data on the amino acid composition of the active site.

Caffeic acid and zileuton were docked and used as references as they are known binding ligands of 5-LO. Caffeic acid is stabilised in the 5-LO binding pocket through the formation of hydrogen bonds with Ala424, blocking the binding site of the arachidonic acid in 5-LO. In a similar way, the binding site of zileuton, a well-known potent inhibitor of 5-LO, is located within the inner part of the binding pocket and is stabilised by the formation of a network of hydrogen bonds with the main chains of Leu420 and Ala424 and the side chain of Asn425, as can be noted in Figure 8.2.1.

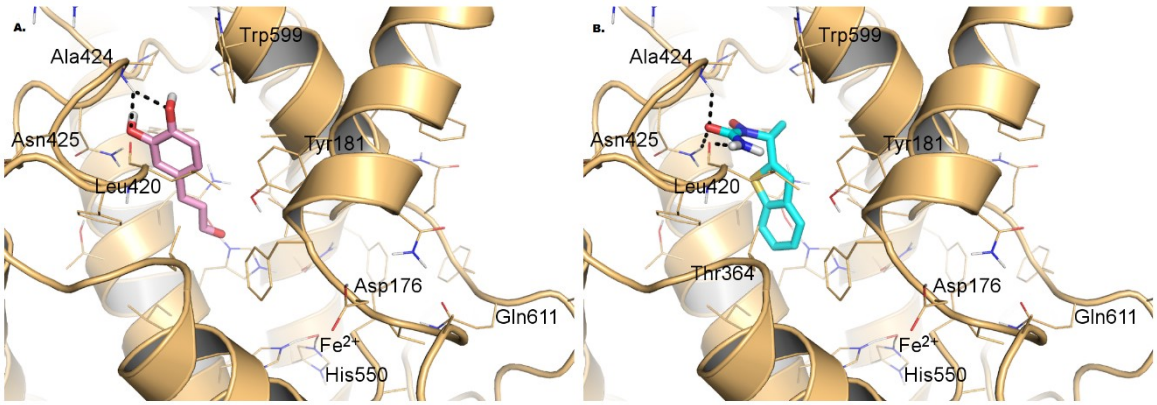

Figure 8.2.1 *Caffeic acid (left) and Zileuton (right) bound into the 5-LO arachidonic acid binding site.*

To validate the docking procedure in 14 α-lanosterol demethylase, fluconazole was docked into the protein and used as a reference. Fluconazole is stabilised in the binding cavity through π-π interactions between one of its triazoles ring and Tyr126 as can be noted Figure 8.2.2. It is known that the main interaction of triazole-containing antimycotic actives is its interaction with the iron of the HEME group.

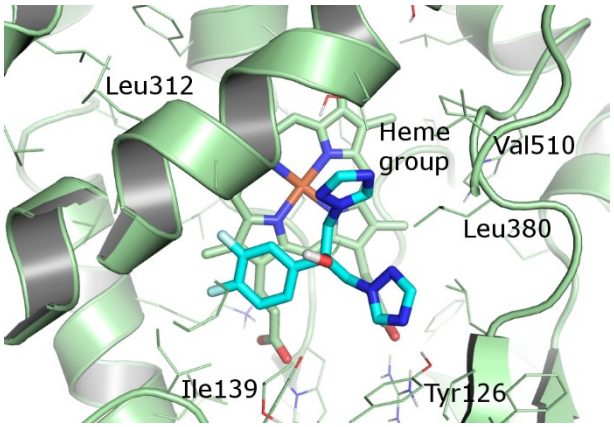

Figure 8.2.2 *Fluconazole stabilised in the binding cavity of* 14 α*-lanosterol demethylase.*

The general structures of the two initially designed classes of compounds are shown in Figure 8.2.3.

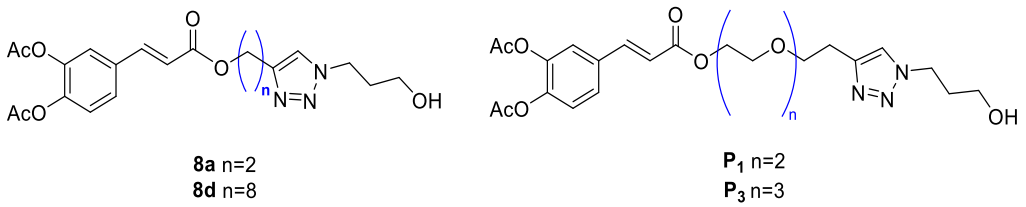

Figure 8.2.3 *General structures of the alkyl triazoles (left) and polyethylene-glycol triazoles (right) families.*

The preliminary docking studies suggested that the alkyl linker presents better interaction in the hydrophobic binding site of 5-LO with respect to the peg-triazole linkers. Binding energies for the alkyl triazole linkers were generally lower compared to the polyethylene glycol analogues. Considering that zileuton has a lower binding energy than caffeic acid (–8.8 kcal/mol and –6.5 kcal/mol respectively) and is known to be a better inhibitor of 5-LO, the difference in the binding energies between the alkyl triazole linkers and the peg-triazole linkers suggested a significant outcome.

Compounds bearing the polyethylene-glycol chain, **P1** (binding energy –9.00 kcal/mol) and **P3** (binding energy –8.4 kcal/mol) showed a binding energy comparable to the clinically approved zileuton (binding energy –8.8 kcal/mol). They have shown a stronger binding interaction, in our predictions, compared to the relatively poor inhibitor caffeic acid (–6.5 kcal/mol), although, the compounds bearing the alkyl linkers have generally shown lower binding energies (**8a** –9.4 kcal/mol and **8d** –9.5 kcal/mol) than the polyethylene-glycol ones.

Furthermore, it was observed that the polyethylene-glycol chain of compound **P3** sits at the limit of the binding site. Inhibitors with a longer linker chain cannot enter completely into the binding site of 5-LO, thus the binding energy starts to increase. The portion that remains out with the binding site plus the interaction with the solvent can increase the entropy of the complex (e.g. **P4** n=6, –7.0 kcal/mol). Figure 8.2.4 shows the comparison between compounds **8a, 8d, P1** and **P3** , where it can be noted that **P3**, compared to the other molecules, is at the limit of the binding site.

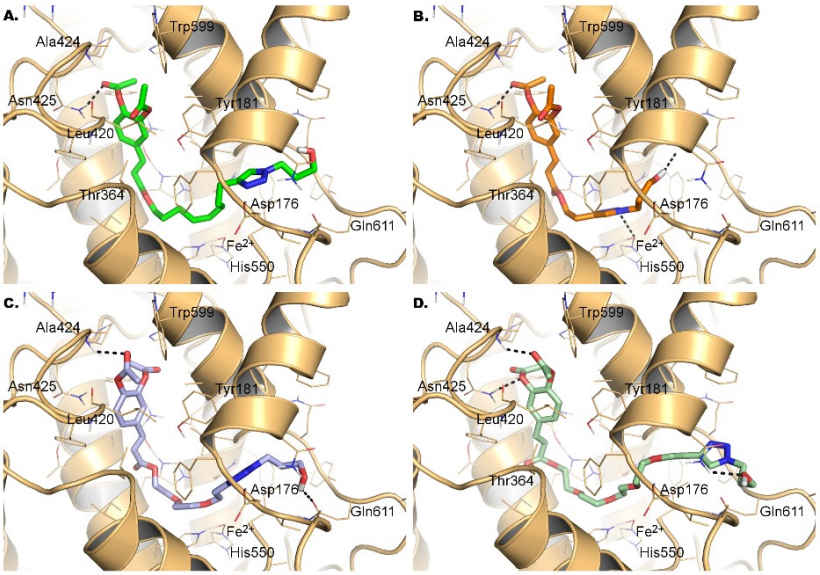

Figure 8.2.4 *Predicted binding images for* ***8d*** *(A),* ***8a*** *(B),* ***P1*** *(C),* ***P3*** *(D) on 5-lipoxygenase.*

Instead, on 14-α-lanosterol demethylase, the polyethylene-glycol analogues form hydrogen bonds with His381 favouring a different orientation of the molecule and of the triazole ring. Alkyl triazole **8d** is oriented towards the iron of the HEME group, similar to fluconazole. Instead, with polyethylene-glycol analogues, **P1** and **P3** the triazole ring is oriented in the opposite direction (Figure 8.2.5). This difference in orientation did not translate into a relevant difference in binding energy. Considering that the action mechanism of triazole-containing antimycotic drugs involves the interaction between the basic nitrogen atom of the heteroaromatic ring and the iron of the HEME of the CYP450 (thereby preventing the enzyme from oxidising its normal substrate[104]), the different orientation observed between the two families might lead explain the difference in the *in vitro* activity.

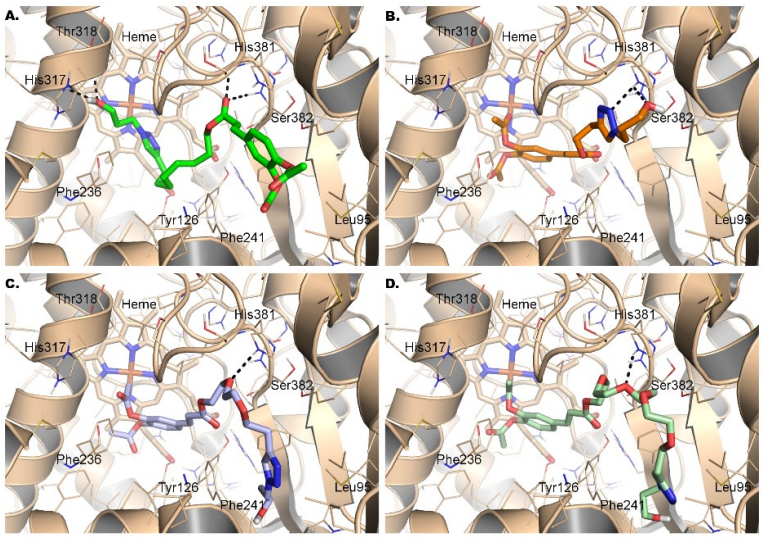

Figure 8.2.5 *Predicted binding orientations of* ***8d*** *(A),* ***8a*** *(B),* ***P1*** *(C),* ***P3*** *(D) on 14 α-lanosterol demethylase.*

Therefore, the simple triazole core was selected as common feature to all our final compounds and it has been synthesised *via* a copper(I) catalysed alkyne-azide cycloaddition - a modern version of the Huisgen 1,3 dipolar cycloaddition also known as "click chemistry".[105]

8.2.2. *Molecular Modelling Parameters*

The structure of all compounds herein presented were optimised using the MMFF94x force field. The torsional root and branches of the ligands were chosen using AutoDockTools (version May_03_13),[106] allowing flexibility for all rotatable bonds of the ligand. Subsequently, AutoDockTools was used to assign Gasteiger–Marsilli atomic charges to all ligands. On the other hand, all water molecules were removed from the 5-LO and 14 α-lanosterol demethylase crystal structures (PDB ID: 3O8Y and 4K0F, respectively). It is worth mentioning that this structure of 5-LO was crystallised without any ligands. In order to obtain an active conformation of this enzyme, the coordinates of arachidonic acid were extracted from crystal structure 3V99 and docked in 3OY8 using a rigid docking approach. The complex obtained was then submitted to a structure optimisation using the MMFF94x force field and the resulting protein structure was used to perform the calculations presented in this study (Figure 8.2.6). AutoDockTools was also used to merge all non-polar hydrogen atoms and to assign Gasteiger charges for each atom of the macromolecule.

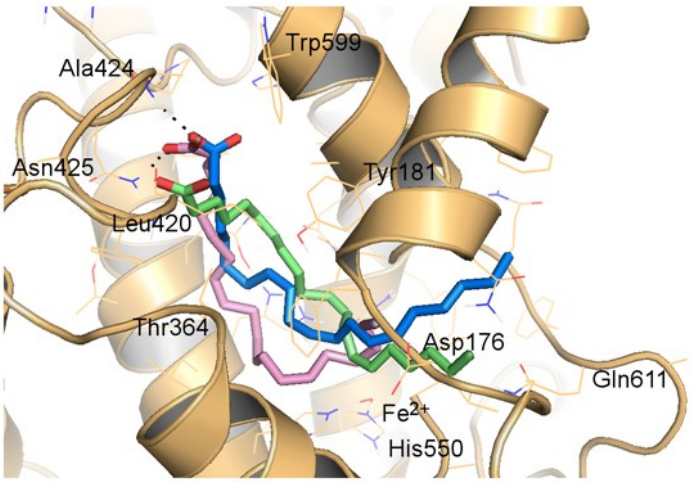

Figure 8.2.6 *Predicted binding conformations of arachidonic acid.*

Figure 8.2.6 shows the arachidonic acid of crystal structure 3V99 overlapped on crystal structure 3O8Y (green); the result of the rigid docking of arachidonic acid on 3O8Y (blue); and the result of the flexible docking of the same molecule after the structure optimisation of the protein (pink).

Docking calculations were performed with AutoDock Vina 1.1.2 software.[107] The searching area was defined by a box of 30 × 20 × 30 Å centred at the coordinates of the catalytic Fe^{2+} for 5-LO and a box of 30 × 25 × 25 Å centred at 17.39, 11.13 and 16.78 in the 14 α-lanosterol demethylase crystal structure. The conformational search of the ligand was performed using and exhaustiveness value of 8 to generate maximum 9 binding modes with a maximum energy difference of 4 kcal/mol between the best and worst conformations. The conformation with the lowest predicted binding energy was used for further analysis. In order to maintain the reproducibility of this study, all the calculations were performed using a seed equal to 1.

8.3. Design and Synthesis of the Compound Library

8.3.1. *Rationale Behind the Design*

The synthesised library of compounds was based on the readily available polyphenol caffeic acid. In order to determine the key features for the anti-inflammatory and fungicide activities associated with this family of compounds, strategic structural modifications were conceived. Focus was placed on the substitution of the aromatic portion (**A**), the type of linker (**B**), the chain length (**C**) and functionalisation of the hydroxyl group (**D**) (Figure 8.3.1).

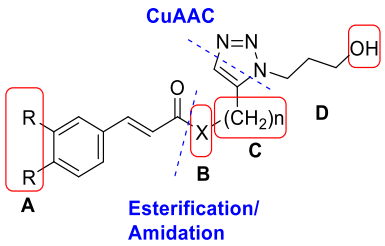

Figure 8.3.1 *Generic structure of the synthetic triazole-containing analogues.*

The synthesis of these compounds relies on an initial esterification or amidation of caffeic acid which also installs either the alkyne or azide fragment prior to formation of the triazole ring through a copper(I) catalysed azide-alkyne cycloaddition (CuAAC).

A fundamental objective for this library of compounds was to obtain a certain degree of molecular diversity, through a concise and expedient synthetic approach, in order to explore the structure–activity relationship (SAR) on the selected targets. Initially, the effect of the chain length of the linker fragment between the polyphenol and the triazole core was investigated (Figure 8.3.2). This variable was considered relevant for both of the considered targets. 5-Lipoxygenase consists of a relatively large binding site and it is not yet well known

what are the key structural features that are required for an efficacious drug candidate. This is highlighted by the fact that zileuton is still the only molecule on the market that is prescribed as a specific inhibitor of 5-lipoxygenase.[9]

Instead, on the 14 α-lanosterol demethylase, the chain length of the linkers could be an important feature that influences the efficacy of the new molecules, not just for the binding interactions at the active site, but also because increasing lipophilicity could affect their ability to pass through the dermatophytes cell wall, thereby increasing the potential to exert their antifungicide function. In both cases, maintaining a certain degree of lipophilicity is important to facilitate efficient intestinal adsorption and to achieve a reasonable oral bioavailability for systemic treatment.[108]

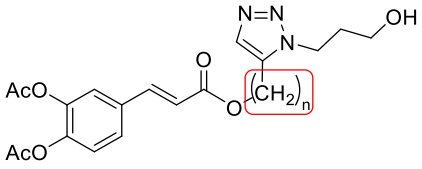

8a n = 2;
8b n = 4;
8c n = 5;
8d n = 8;

Figure 8.3.2 *Synthetic analogues with varying chain lengths between diacetyl caffeic acid and the triazole ring.*

Substitution of the ester with an amide group was also examined (Figure 8.3.3) in order to determine the effect the ester group has on the activity of these compounds whilst also evaluating the effect of the more metabolically stabile amide group.[109]

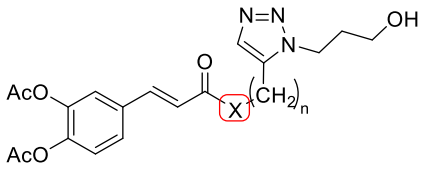

8e X=NH; n = 2;

Figure 8.3.3 *Substitution of the ester functionality with an amide group.*

Alternate functionality to the aromatic acetate groups was also considered (Figure 8.3.4). Replacing the acetate groups with fluorine could lead to a weaker interaction with the binding site of 5-lipoxygenase or 14 α-lanosterol demethylase but, on the other hand, could also lead to improved pharmacological properties. Fluorine has been widely used in pharmaceutical compounds for enhancing biological activity through hydrogen bonding interactions (I added this but check this if correct).[110] In 2008, the US Food and Drug

Administration (FDA) approved 238 fluorine-containing drugs. From this data, fluorine emerges as the second most-widely used heteroatom in drug design and synthesis behind nitrogen.[111]

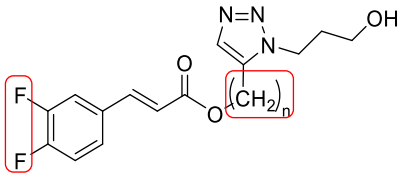

8f n = 2;
8g n = 8;

Figure 8.3.4 *Substitution of the diacetyl groups on the aromatic ring with fluorine atoms at chain lengths n = 2 (**8f**) and n = 8 (**8g**).*

An isomer of analogue **8a** was also prepared (**8h**) (Figure 8.3.5) to evaluate if the different mobility arising from the isomer resulted in a significant change in the activity.

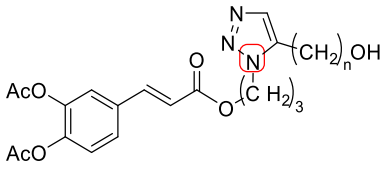

8h n = 2;

Figure 8.3.5 *Triazole isomer of compound 8a.*

Finally, taking into account that the terminal hydroxylalkyl chain could affect the activity against the selected targets, or the passage through the cellular membrane, the last variation of the compound library examined the derivatisation of this group (Figure 8.3.6).

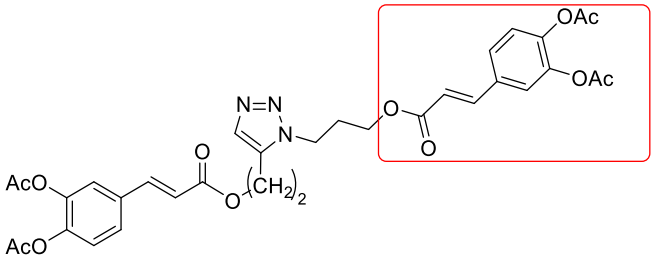

9;

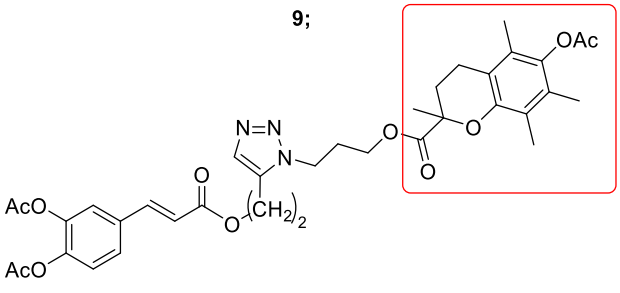

10;

Figure 8.3.6 *Orthogonal derivatives with caffeic acid (**9**) and trolox (**10**).*

8.3.2. *Synthesis of the Library*

Following optimisation (Table 8.3.1), 3-azido-1-propanol was prepared one step from commercially available 3-bromopropan-1-ol through an S_N2 reaction (Scheme 8.3.1).[†††]

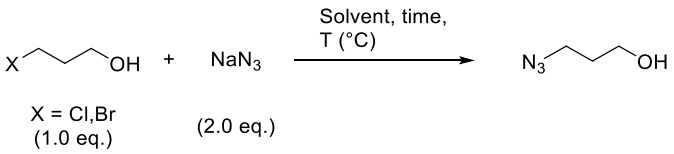

Scheme 8.3.1 *Synthesis of 3-azido-1-propanol.*

[†††] 3-Azidopropan-1-ol is commercially available it was more cost effective to prepare it in-house

Table 8.3.1 *Reaction optimisation of 3-azidopropan-1-ol.*

ENTRY	X	SOLVENT	TIME [H]	TEMP [°C]	CONV (%)†††
1‡‡‡	Br	DMF	24	60	100
2‡‡‡	Br	H_2O	24	60	100
3‡‡‡	Cl	H_2O	30	75	30**Error! Bookmark not defined.**
4ERROR! BOOKMARK NOT DEFINED.	Br	H_2O	30	75	86**Error! Bookmark not defined.**
5ERROR! BOOKMARK NOT DEFINED.	Br	H_2O	15	75	83**Error! Bookmark not defined.**
6ERROR! BOOKMARK NOT DEFINED.	Br	H_2O	45	75	97**Error! Bookmark not defined.**
7ERROR! BOOKMARK NOT DEFINED.	Br	H_2O	30	120	100**Error! Bookmark not defined.**
8ERROR! BOOKMARK NOT DEFINED.	Br	DMF	30	120	100

The optimal conditions to prepare azido-propan-1-ol are shown in entries 1, 2 and 7 (Table ***8.3.1***). Going forward, the conditions reported in entry 1 were used to prepare 3-azidopropan-1-ol. The syntheses of intermediates **3a, 3b, 3c, 3d, 3f, 3g** and **5** (Scheme **8.3.2**) were realised *via* an esterification reaction between α,β-unsaturated acids **1a-b** and terminal alkynes **2a-d** or azide **4** as reported in the literature.[112] The reactions proceeded smoothly in moderate to good yields. The same conditions used for the esterification were also suitable for the formation of amide **3e** from **1a** and **2e** in good yield.

††† Conversion was calculated by ^{1}H-NMR
‡‡‡ These reactions were performed in batch mode
Error! Bookmark not defined. These reactions were performed in microwave mode
Error! Bookmark not defined. Trace amounts of by-product (~5%) was determined by NMR

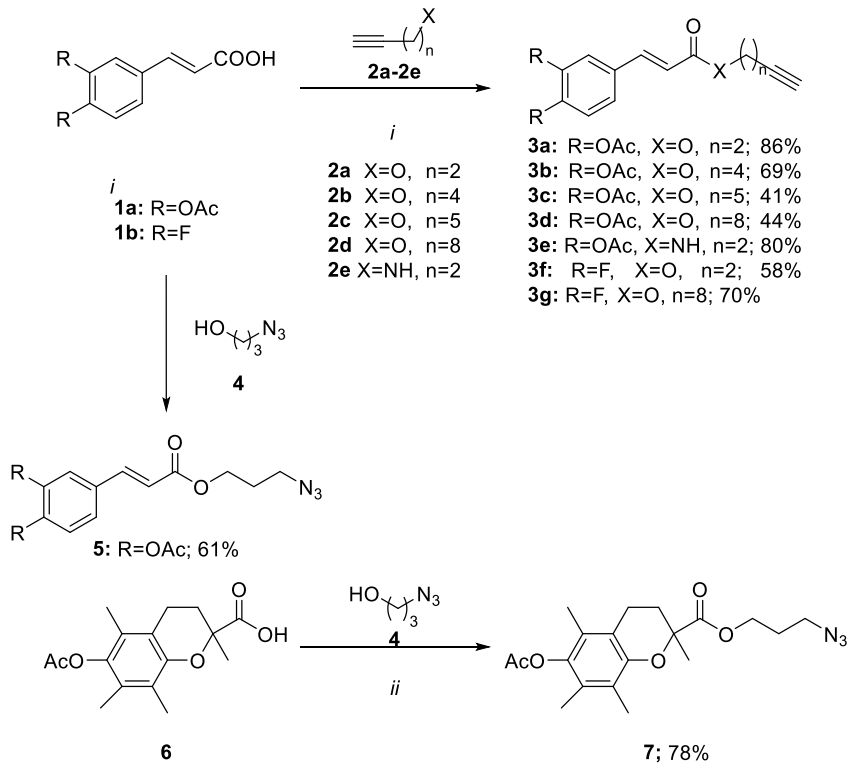

Scheme 8.3.2 *Synthetic procedures for esters (**3a**–**3f**, **5**, 7). Reagents and conditions: (i) thionyl chloride (25 eq.), **1a**–**1b** (1.0 eq.), DMF (1.2 eq.), benzene, Δ, then pyridine (1.2 eq.) and **2a**–**2e** or **4** (1.2 eq.), r.t. (ii) DCC (1.0 eq.), DMAP (1.0 eq.), **6** (1.0 eq.), DCM, r.t., then **4** (1.0 eq.), r.t. DMF = dimethylformamide; DCC = dicyclohexylcarbodiimide; DMAP = dimethylaminopyridine; DCM = dichloromethane*.

To prepare azide **7**, the esterification protocol was changed. It was necessary to submit 6-acetoxy-2,5,7,8-tetramethylchromane-2-carboxylic acid (Trolox) to milder esterification conditions. Steglich esterification conditions were used for this reason (Scheme 8.3.2). In the Steglich esterification reaction, the carboxylic acid is activated with dicyclohexylcarbodiimide (DCC) instead of generating the acyl chloride. Attempts to perform the esterification of **6** under the same conditions used for the esterification of **1a** and **1b** led to consumption of starting material but it proved impossible to isolate the desired product through column chromatography. Figure 8.3.7 shows the NMR overlay between the esterification of Trolox to afford compound **7** with method (i) (Figure 8.3.7 a), and Steglich esterification method (ii) (Figure 8.3.7 b). It can be seen at 3.68, and 3.45 ppm (Figure **8.3.7** a) there is a singlet and a triplet, respectively, not belonging to the desired product, which proved impossible to separate from the product through column chromatography. Instead, this by-product is not observed when submitting compound **6** to the esterification method (ii) (Figure 8.3.7 b).

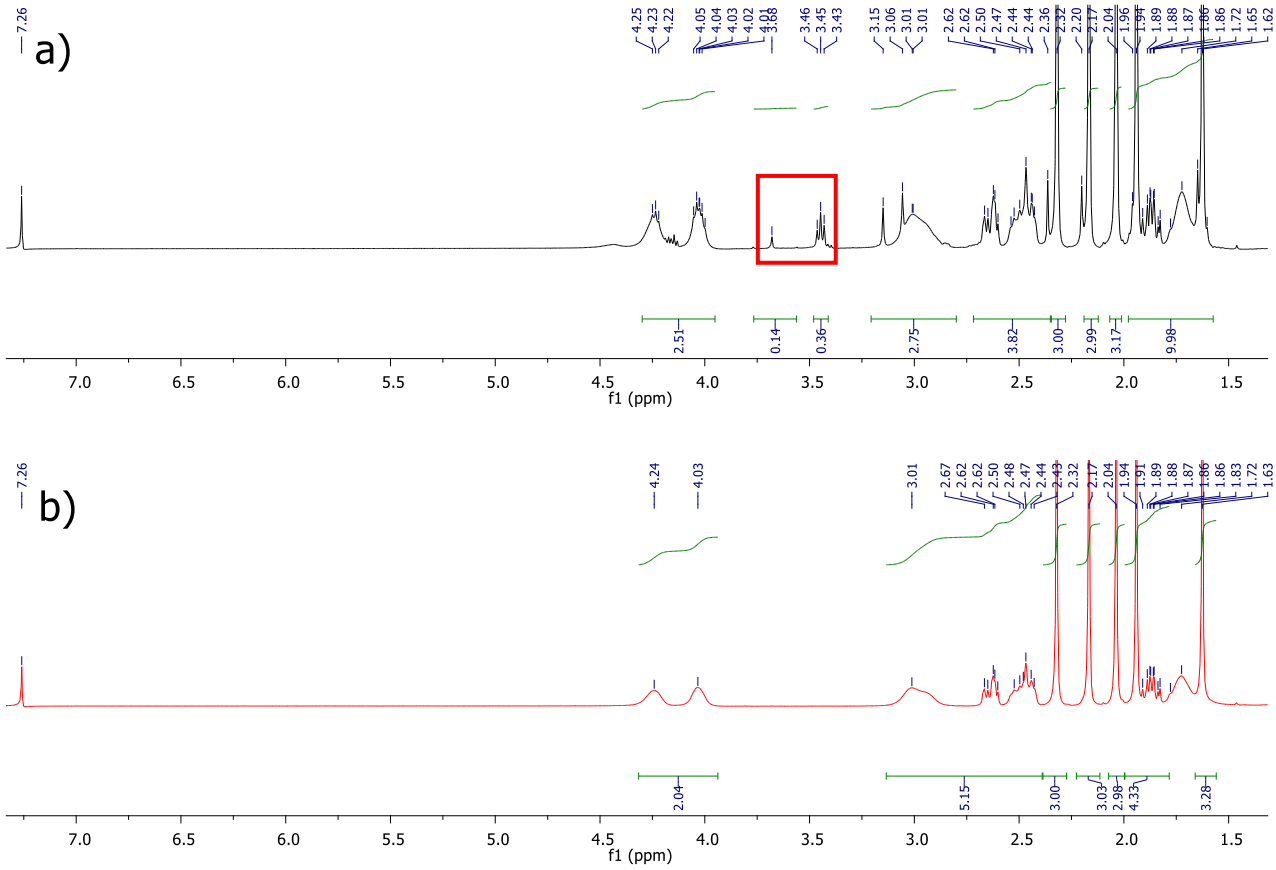

Figure 8.3.7 *Comparison of the crude [1]H-NMR spectra resulting from esterification method (i) (**a**) and method (ii) (**b**) on Trolox* **6**.

The intermediates were then submitted to the copper catalysed 1,3-dipolar azide-alkyne cycloaddition, also known as click chemistry, to afford the final analogues **8a–8h**, **9** and **10**. Click chemistry is a powerful tool to quickly generate molecular diversity and chemoselectivity (the 1,4-isomer is afforded using a copper catalyst and the 1,5-isomer is prepared using a ruthenium catalyst), however, there are many conditions reported. For the formation of the 1,4-regioisomers, the most commonly employed catalyst is used $CuSO_4$ with a co-reagent such as metallic copper or sodium ascorbate, to produce copper(I) in situ. This method for directly generating copper(I) in situ is generally preferred given the air-sensitive nature of the isolated salts.[113] Although, copper(I) species can also be used in aqueous media. Preliminary reactions were performed on a model system (Scheme 8.3.3) to determine which strategy should be employed (Table 8.3.2).

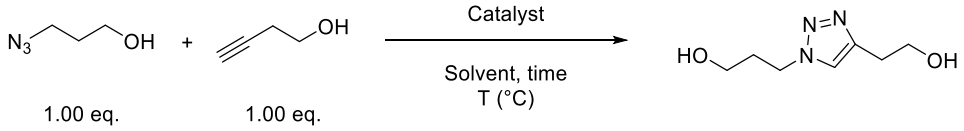

Scheme 8.3.3 *Model reaction to optimise the copper(I) catalysed azide–alkyne cycloaddition step.*

Table 8.3.2 *Reaction condition optimisation of the copper catalysed azide-alkyne cycloaddition reaction.*

ENTRY	CATALYST [MOL%]	SOLVENT	TIME [H]	TEMP. [°C]	CONV [%]
1	$CuSO_4$ [20] and Cu [80]	H_2O–t-BuOH (1:1)	15	125	>90%
2	CuI [10]	H_2O–t-BuOH (1:1)	15	125	>90%

Under both reaction conditions, full conversion was achieved which was evident through comparison of the ^{1}H-NMR spectra of 3-azidopropan-1-ol (Figure 8.3.8 a), the crude reaction mixture (Figure 8.3.8 b) and 3-butyn-1-ol (Figure 8.3.8 c).

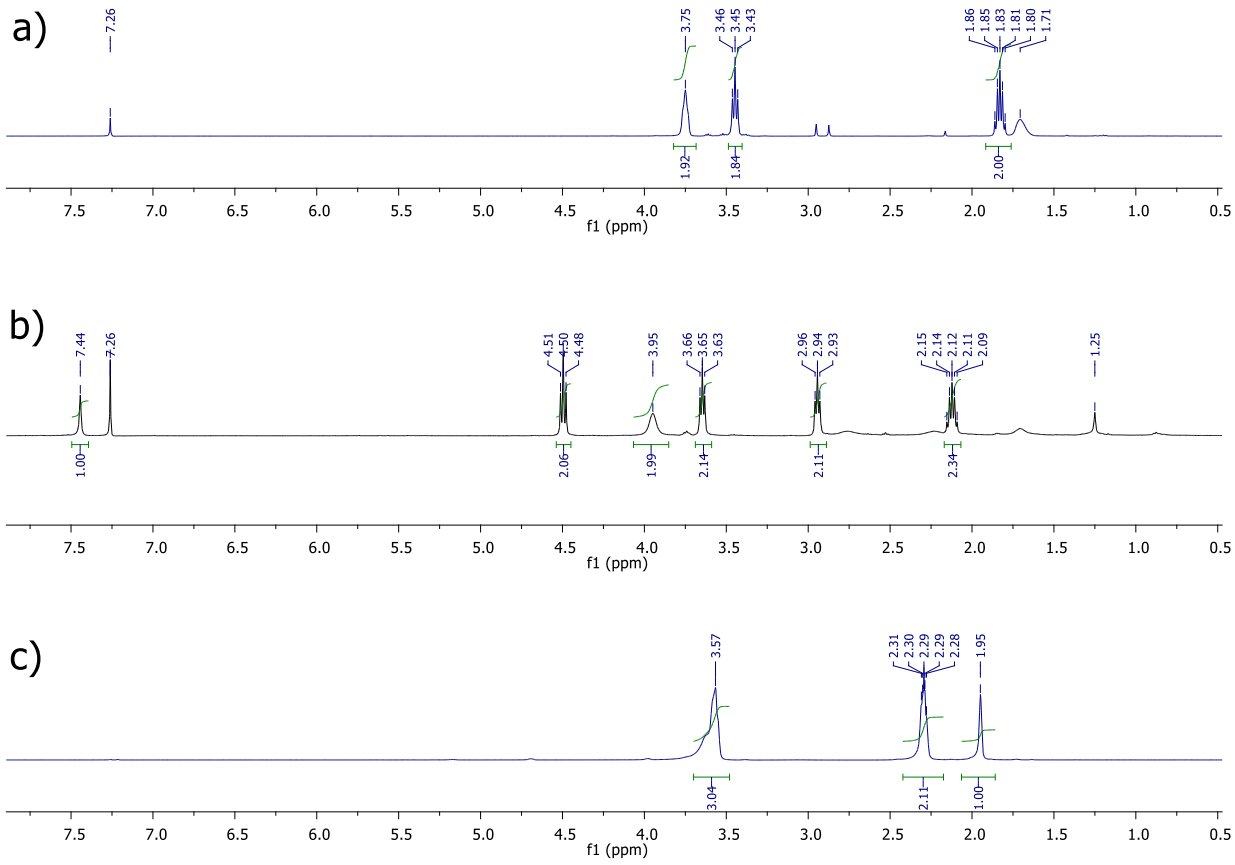

Figure 8.3.8 *Comparison of the ^{1}H NMR spectra of (a) 3-azidopropan-1-ol; (b) crude reaction mixture from entry 2 of Table 8.3.2; and (c) 3-butyn-1-ol.*

Although both reactions proceeded to full conversion, the reaction in which copper(I) was generated in situ proceeded in a less clean manner than the reaction that used a direct source of copper(I). From Figure 8.3.9, the presence in the NMR spectra of trace amounts of by-products formed when using the conditions from entry 1 (Figure 8.3.9 a) is evident whereas these impurities are instead absent in the NMR spectra obtained from the reaction conditions used in entry 2 (Figure 8.3.9 b).

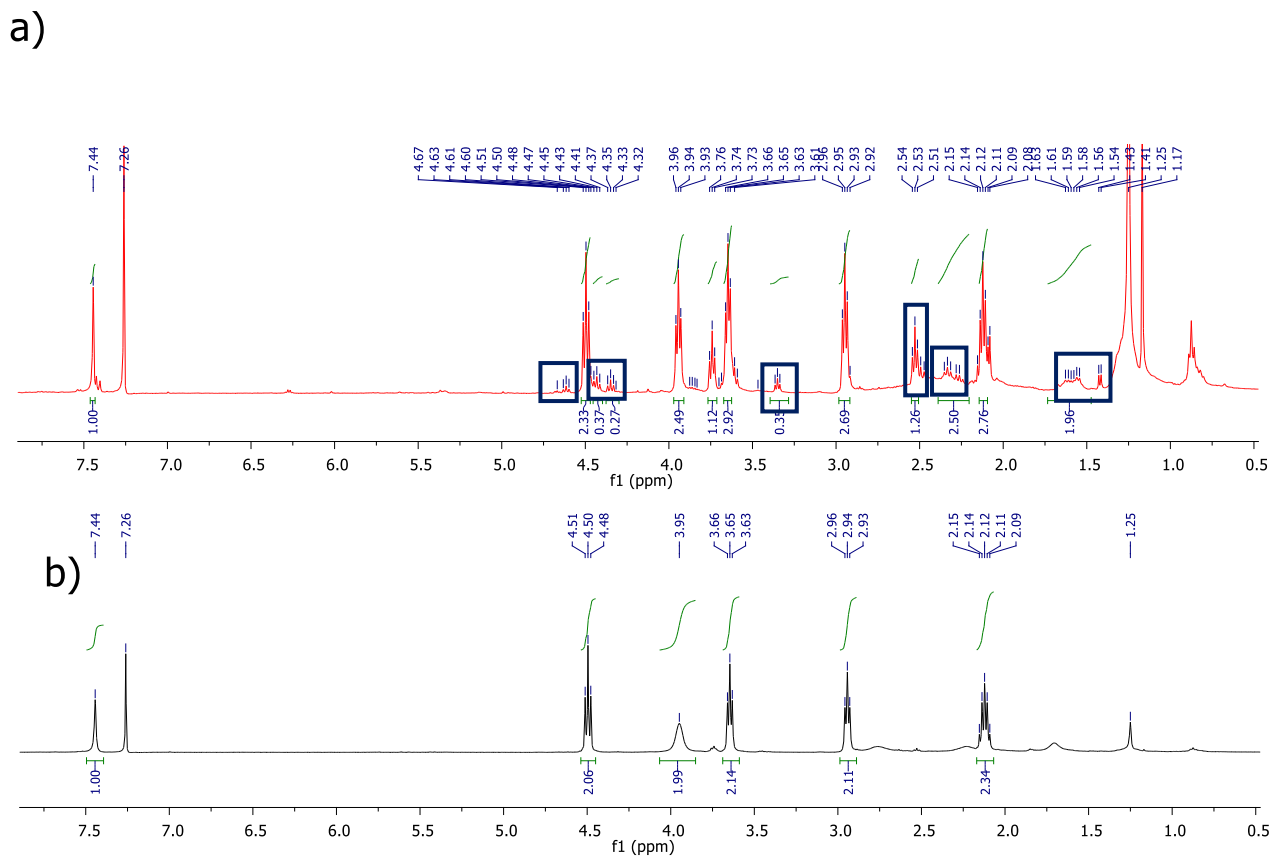

Figure 8.3.9 *Comparison of the NMR spectra obtained from the reaction conditions used in (a) entry 1 Table 8.3.2 and (b) entry 2 Table 8.3.2.*

It was therefore decided to proceed using copper(I) iodide to perform the cycloaddition. However, attempts to synthesise triazole **8a** using the optimised conditions lead to no conversion. The reaction time was increased to 75 minutes and the ratio of **3a** to 3-azidopropan-1-ol was changed from 1:1 to 1.2:1. The reaction was carried out in both microwave and standard batch mode. Both gave conversions to the desired product higher than 95% and no significant differences were observed in the crude NMR spectra.

For convenience and future scale up considerations, it was decided to continue with the synthesis using standard thermal conditions. Compounds **3a-g**, **5** and **7** were subsequently submitted to copper catalysed cycloaddition reaction with **4, 2a** and **3a** respectively, which

afforded the final target compounds **8a-g**, **9** and **10**. The reaction conditions for the cycloaddition revealed to be suitable to prepare all the desired triazole derivatives. The reactions proceeded to completion and gave moderate to good isolated yields (Scheme 8.3.4 and Scheme 8.3.5).

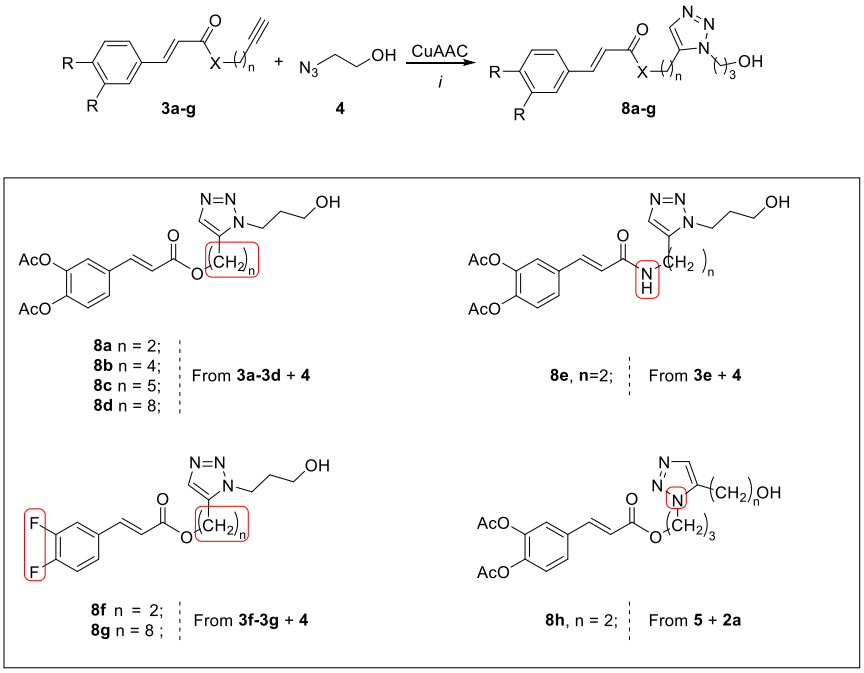

Scheme 8.3.4 *Synthetic procedures for the preparation of triazoles (**8a-h**). Reagents and conditions: (i) t-BuOH–H_2O (1:1), **2a** or **3a-g** (1.2 eq.), **4 or 5** (1.0 eq.), CuI (0.1 eq.), 125 °C.*

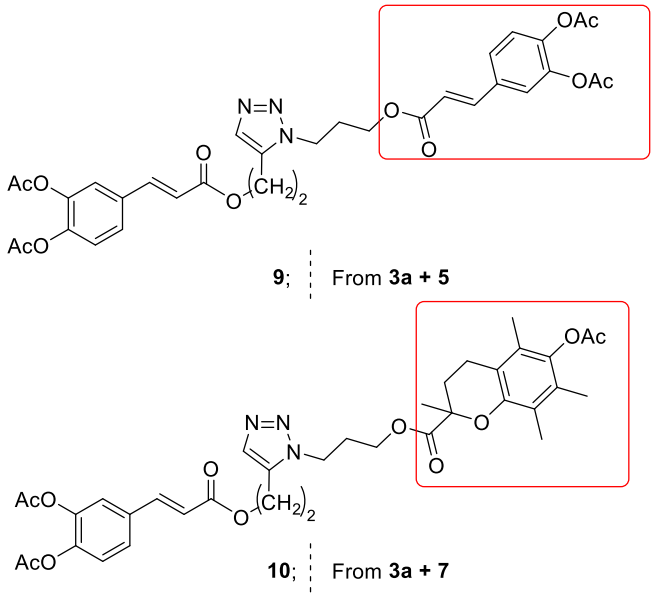

Scheme 8.3.5 *Synthetic procedures for the preparation of triazoles **5** and 7. Reagents and conditions (i) t-BuOH–H_2O (1:1), **3a** (1.2 eq.) **5** or 7 (1.0 eq.), CuI (0.1 eq.), 125 °C.*

8.4. Reaction Mechanisms of the Key Steps

8.4.1. *Steglich Esterification*

The Steglich esterification is a reaction that allows the conversion of acids into esters and amides under mild conditions using dicyclohexylcarbodiimide (DCC) as a coupling agent and 4-dimethylaminopyridine (DMAP) as catalysts. Compared to other methods, the Steglich esterification method works efficiently for more sterically hindered substrates.

The first step involves the activation of the carboxylic acid through the formation of *O*-acylisourea (**I**) (Scheme 8.4.1). This intermediate **I** provides a similar reactivity to the corresponding carboxylic acid anhydride and is more susceptible to nucleophilic attack. The alcohol then adds to the activated carboxylic acid to form the desired ester and dicyclohexylurea (DHU) as a stable by-product.

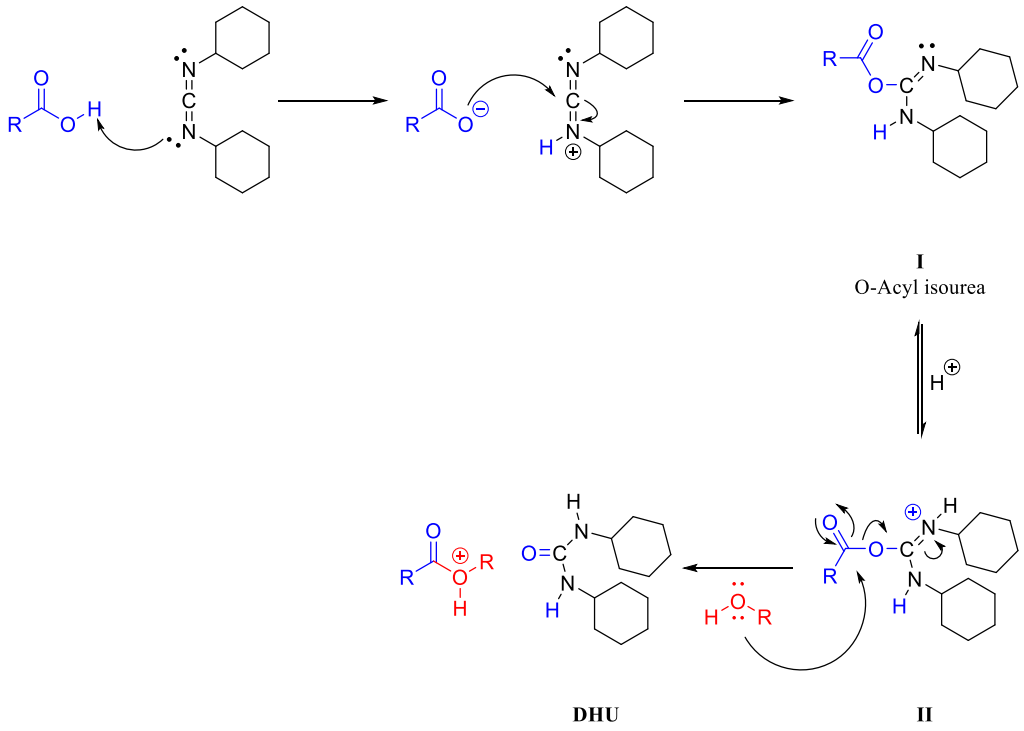

Scheme 8.4.1 *Proposed mechanism of the Steglich esterification.*

N-Acylisoureas (Scheme 8.4.2) are the side products of an acyl migration that takes place slowly, and could be quantitatively isolated in the absence of any nucleophile. The reaction with strong nucleophiles such as amines proceeds fast and so this side product is not observed.

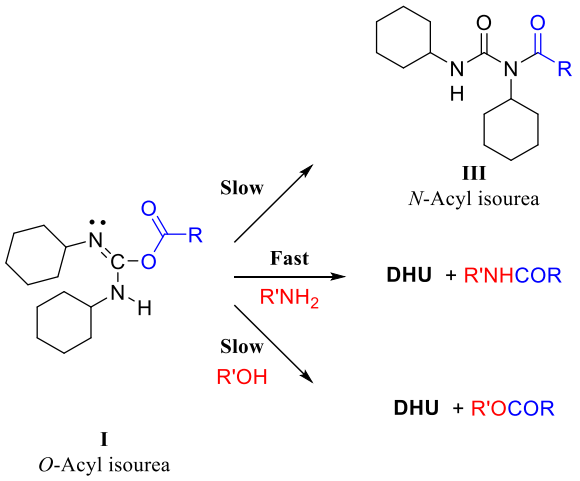

Scheme 8.4.2 *Reactivity of the O-acylisourea intermediate **I**.*

The reaction between amines and carboxylic acids in the presence of DCC leads to amides generally without too many problems. For the efficient formation of esters, the addition of 5 mol% of 4-dimethylaminopyridine (DMAP) is crucial.

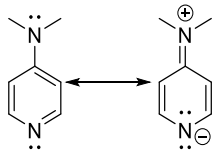

Figure 8.4.1 *Both the nucleophilicity and basicity of the pyridine nitrogen are increased due to the electron-donating effect of the dimethylamino group.*

The acceleration of the reaction with the alcohol accomplished using DMAP, is due to the fact that. DMAP is a stronger nucleophile than the alcohol and so reacts with the protonated *O*-acylisourea (**I**) leading to a reactive amide. This more reactive intermediate is then susceptible to attack from the alcohol. Formally, DMAP acts as an acyl transfer reagent and subsequent reaction with the alcohol gives the ester.

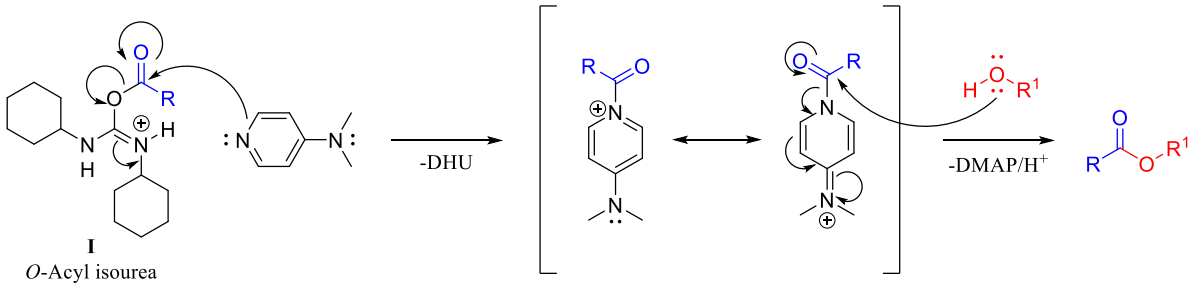

Scheme 8.4.3 *Mechanism of the DMAP catalysed esterification.*

8.4.2. *Copper(I) Catalysed Azide–Alkyne Cycloaddition (CuAAC).*

"Click Chemistry" is a stereospecific, high yielding, wide-in-scope reaction. It can be conducted in green and easily recyclable solvents. It is used extensively in material sciences (polymers and dendrimers formations), in pharmaceutical industry and biological sciences (Inc., 2009).[114]

Sharpless introduced the term "click chemistry" in 2001. It is an optimisation of the Huisgen 1,3-dipolar cycloaddition which, differently from the method developed by Sharpless and co-workers, required elevated temperatures and so was generally not suitable for chemical biology or any thermally unstable substrates. Moreover, it produces a mixture of the 1,4- and 1,5-regioisomers. The copper catalysed cycloaddition method, instead, makes it possible to discriminate between the two regioisomers based on the catalyst choice. Copper(I) catalysts make it possible to exclusively obtain the 1,4-regioisomer, whereas ruthenium catalysts access the 1,5-regioisomer.

The first step involves the activation of the alkyne through a π–bond with copper(I) forming the key intermediate acetylide **I** (Scheme 8.4.4). Afterwards, the azide coordinates to the copper dissociating a ligand L and forming the intermediate **II** that turns into a 6-membered copper(III) metallacycle **III**. The 6-membered ring formation is then followed by the contraction of the ring to give **IV** a triazoyl-cuprate which undergoes protonolysis to afford the final product **V** - the 1,4-substituted triazole ring.

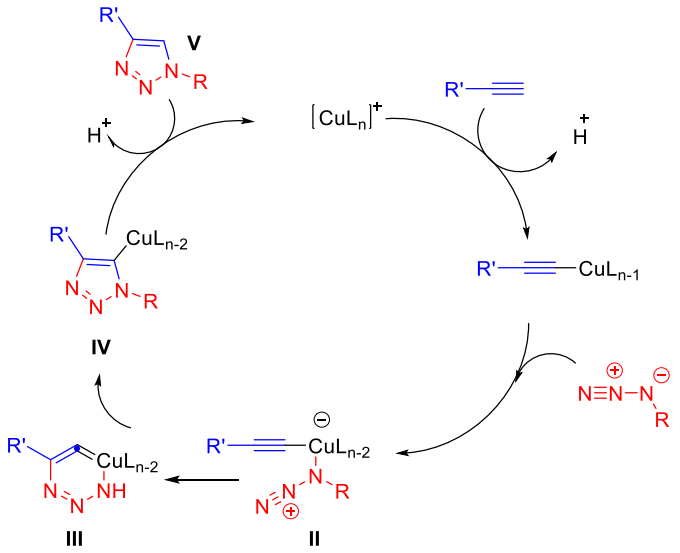

Scheme 8.4.4 *Copper catalysed azide–alkyne cycloaddition.*

The ruthenium catalysed azide–alkyne cycloaddition proceeds through an oxidative coupling of azide and alkyne to give a six membered ruthenium cycle. In this case, the first bond is formed between the most electronegative atom of the alkyne and the terminal azide. This step is followed by the reductive elimination that leads to the triazole formation. The reductive elimination step is the rate-determining one according to DFT (Density Functional Theory) calculations.

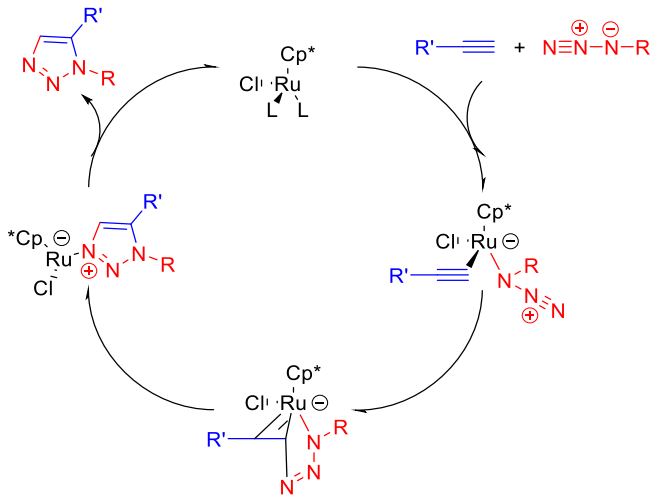

Scheme 8.4.5 *Ruthenium catalysed azide–alkyne cycloaddition*.

8.5. In Vitro Assays

8.5.1. *Antioxidants Evaluation*

The compounds synthesised herein (Figure 8.5.1) were tested for their antioxidant capacity by means of DPPH (2,2-diphenyl-1-picrylhydrazyl radical) and FRAP (Ferric Reducing Antioxidant Power) testing (Table 8.5.1).

It is important, whenever screening the antioxidant capacity of a compound, to perform the testing on different assays, in order to understand the radical scavenging selectivity. The different radical that can be encountered in biological systems has different reactivity profiles, thus one molecule can be selective towards one radical species over another.

It was particularly relevant for our study to check the performance of the newly synthesised compounds against FRAP considering that the active site of both our selected targets contain iron and, in particular, the action mechanism of zileuton against 5-LO is known to involve the reduction of the iron in the active site.

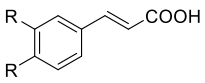

1a: R=OAc
1b: R=F

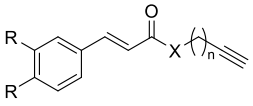

3a: R=OAc, X=O, n=2
3b: R=OAc, X=O, n=4
3c: R=OAc, X=O, n=5
3d: R=OAc, X=O, n=8
3e: R=OAc, X=NH, n=2
3f: R=F, X=O, n=2

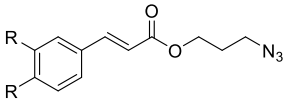

5: R=OAc

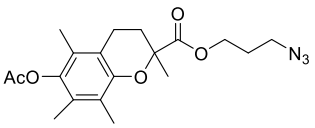

7

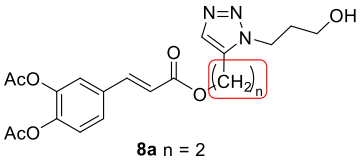

8a n = 2
8b n = 4
8c n = 5
8d n = 8

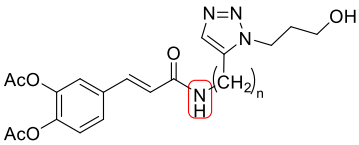

8e, **n**=2

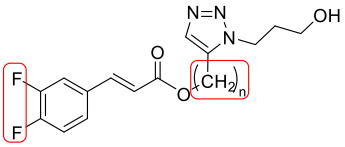

8f n = 2

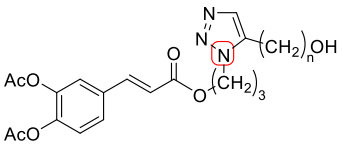

8h, n = 2

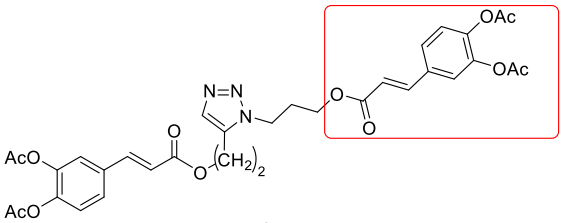

9

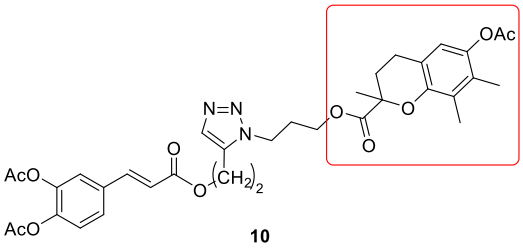

10

Figure 8.5.1 *Summary of compounds synthesised and tested on their antioxidant power.*

Table 8.5.1 *Antioxidant assay results expressed in µmol of Trolox unit for gram of sample*.

Entry	Compound	DPPH (µmol Trolox/g)	FRAP (µmol Trolox/g)
1	Zileuton		755.95 ± 1.9
2	Caffeic Acid	396.10 ± 0.5	9273.49 ± 2.2
3	1a	5.43 ± 0.3	8.07 ± 0.8
4	3a	248.52 ± 2.9	64.71 ±1.1
5	3b	129.59 ± 1.7	104.38 ± 1.3
6	3c	191.39 ± 0.5	65.03 ± 0.7
7	3d	77.32 ± 0.6	31.81 ± 1.5
8	3e	59.38 ± 0.3	29.15 ± 0.6
9	3f	<LOQ[§§§]	54.42 ± 1.2
10	5	92.81 ± 0.9	3,87 ± 0.2
11	7	<LOQ	91,47 ± 1.1
12	8a	131.8 ± 1.2	2738.55 ± 3.4
13	8b	48.75 ± 0.4	598.58 ± 1.6
14	8c	117.40 ± 0.8	32.13 ± 1.2
15	8d	185.36 ± 1.1	98.90 ± 2.1
16	8e	553.27 ± 0.8	391.81 ± 1.3
17	8f	<LOQ	<LOQ
18	8h	157.2 ± 1.7	322.45 ± 1.8
19	9	472.74 ± 1.4	93.74 ± 0.7
20	10	341.22 ± 2.1	42.77 ± 0.8

Protecting the phenolic hydroxyl group on caffeic acid as in compound **1a** leads to almost complete loss of antioxidant activity, as expected (for DPPH tests from 396.10 to 5.43 µmol Trolox/g, for FRAP from 9273.49 to 8.07 µmol Trolox/g). The esterification of **1a** to afford

[§§§] Quantification limit

terminal alkyne compounds **3a-3d** recovered a reasonable amount of the antioxidant activity on both the assays tested, but the elongation of the alkyl chain going from **3a** to **3d** decreased the antioxidant power (in DPPH **3a** 248.52 µmol Trolox/g, **3d** 77.32 µmol Trolox/g; FRAP **3a** 64.71 µmol Trolox/g, **3d** 31.81 µmol Trolox/g). The decrease in activity that follows the chain elongation does not seem to be linear and this effect will be investigated in the future. Compound **3f**, in which the two phenolic hydroxyl groups have been substituted with two fluorine atoms does not show any activity against DPPH but showed some activity in the Frap test (although considered negligible 54.42 µmol Trolox/g) possibly due to the interaction between the terminal alkyne and the iron radicals.

It is interesting to note that the response of the chain elongation in the compounds bearing the triazole linker core is different in the two assays. Increasing the chain length going from compound **8a** to **8d**, the DPPH test demonstrated significant improvement in activity, whereas the results in the FRAP assay exhibited a decrease in antioxidant capacity (Entries 12-15, Table 8.5.1), the intermediate length between **8a** and **8d** do not sow a linear relationship between the chain length and the antioxidant power. Experiments to investigate the reasons behind this behaviour are currently undergoing.

Substituting the ester bond for an amide linkage between the caffeic acid moiety and the linker as in compound **8e** enhances the antioxidant ability on DPPH but lowers its potency against FRAP (Entry 16, Table 8.5.1). The orthogonal derivatives **9** and **10** instead had negligible activity on the FRAP assays but they maintained a good activity profile in DPPH assays with compound **9** exceeding the antioxidant ability of its parent compound, caffeic acid (396.10 µmol Trolox/g of caffeic acid, 472.74 µmol Trolox/g for compound **9**). Compound **10** preserved an activity profile (341.22 µmol Trolox/g) comparable to its parent compound caffeic acid (396.10 µmol Trolox/g).

To summarise these results, the most interesting compounds for their antioxidant activity in DPPH assays were found to be **8e** and **9** which exceeded the activity of their parent compound caffeic acid by 157.10 µmol Trolox/g and 76.64 µmol Trolox/g respectively. With respect to the FRAP analysis, the compound of highest interest was **8a** that, although was less powerful than caffeic acid, exceeded the scavenging power over iron radicals of 1982.6 µmol Trolox/g compared to zileuton, currently the leading commercial compound for directly inhibiting 5-lipoxygenase.

8.5.2. *Antimycotic Assays*

The molecules presented herein were tested for their antimycotic activity against eight strains of dermatophytes, which are responsible for the most common dermatomycosis: *M. canis* (M.c.), *M. gypseum* (M.g.), *T. violaceum* (T.v.), *T. mentagrophytes* (T.m.), *T. tonsurans* (T.t.), *T. rubrum* (T.r.), *E. floccosum* (E.f.) and *A. cajetani* (A.c.)at two concentrations 20 µg/mL and 100 µg/mL.[****]

Fluconazole was used as a reference material (Table 8.5.2). Its IC_{50}, expressed in µg/mL, was checked on all the dermatophytes considered in this study (Table 8.5.3) and it was shown that on *A. cajetani* fluconazole is inactive (IC_{50} >200 µg/mL).

Table 8.5.2 *Percentage of growth inhibition at 20 µg/mL and 100 µg/mL of reference compound on the chosen dermatophytes strains.*

Compounds	**Fluconazole**								
	Microorganism	**M. g.**	**M. c.**	**T. v.**	**T. m.**	**T. t.**	**T. r.**	**E. f.**	**A. c.**
Concentrations tested	20 µg/mL	56.35	38.10	46.51	99.14	51.11	39.42	100.00	+
	100 µg/mL	79.37	79.37	89.39	103.45	66.67	67.31	102.27	5.35

Table 8.5.3 *IC_{50} of reference compounds Fluconazole and Econazole on the dermatophytes of interest.*

Compounds	**Fluconazole**							
Microorganism	**M.g**	**M.c**	**T.v**	**T.m**	**T.t**	**T.r**	**E.f**	**A.c**
IC_{50} [µg/mL]	18.5	29.6	31.03	3.53	19.41	37.16	0.08	> 200

The compounds were tested following the diffusive method in Sabouraud Dextrose Agar (SDA), using DMSO as solvent. The growth inhibition of the compounds tested on the microorganism are reported in Table 8.5.4 and Table 8.5.5 at 20 µg/mL and 100 µg/mL. The compounds were initially tested at concentrations 20 µg/mL and 100 µg/mL to evaluate, by comparison with the results obtained for the clinically approved wide spectrum antimycotic

[****] Given our available resources, we proceeded with the testing on the live microorganism. Our laboratories are currently in the process of acquiring the capabilities and expertise to run the testing on the isolated 14 α-lanosterol demethylase which will verify if the obtained results are influenced by the interaction with the dermatophytes cell environment.

drug, fluconazole, at the same concentrations, if there a compound within our library which showed potential to investigate further in terms of IC_{50} and MIC.

Table 8.5.4 *Percentage of growth inhibition intermediates.*

Microorganism	[µg/mL]	Caffeic Acid	1a	3a	3b	3c	3d	3e	3f	5	7
M. gypseum	20 µg/mL	+	4.76	8.41	4.76	26.67	10.83	1.89	+	11.21	13.33
	100 µg/mL	1.06	10.48	64.49	29.52	37.50	5.83	3.77	46.22	47.66	28.57
M. canis	20 µg/mL	+	+	24.14	29.55	23.61	18.87	1.37	20.73	22.41	21.64
	100 µg/mL	6.32	2.78	68.97	42.42	31.94	16,98	15.07	50.61	56.03	28.36
T. violaceum	20 µg/mL	0	+	50.00	33.33	32.26	13.33	+	28.26	0.00	13.79
	100 µg/mL	62.5	12.90	93.33	66.67	25.81	15.56	13.79	63.04	46.15	20.69
T. mentagrophytes	20 µg/mL	1.23	+	29.90	25.81	28.95	10.17	0.00	18.33	4.04	10.20
	100 µg/mL	2.47	+	78.35	66.67	39.47	8.47	+	49.17	36.36	26.53
T. tonsurans	20 µg/mL	2.50	2.38	2.38	19.51	21.82	+	7.32	14.86	40	+
	100 µg/mL	12.50	57.14	57.14	29.27	32.73	+	7.32	45.95	40	2.63
T. rubrum	20 µg/mL	+	22.22	26.47	45.45	30.95	20.83	+	12.50	35.71	16.67
	100 µg/mL	54.55	33.33	67.65	42.42	33.33	12.50	6.82	43.75	60.71	30.56
E. floccosum	20 µg/mL	+	+	27.27	52,08	59.02	13.56	+	16.22	20.00	+
	100 µg/mL	0.00	13.51	69.70	83,33	68.85	6.78	+	47.30	91.11	+
A. cajetani	20 µg/mL	+	4.23	10.94	16,28	41.67	4.42	6.25	3.91	20.00	+
	100 µg/mL	9.41	8.45	53.13	44,19	50.00	+	13.28	30.47	26.67	12.00

Table 8.5.5 *Percentage of growth inhibition final compounds.*

Microorganism	[μg/mL]	Caffeic acid	8a	8b	8c	8d	8e	8f	8h	9	10
M. gypseum	20 μg/mL	+	0.00	+	11.40	32.32	+	8.74	8.60	4.39	9.84
	100 μg/mL	1.06	0.00	+	22.81	34.34	5.94	21.36	8.60	3.51	9.84
M. canis	20 μg/mL	+	1.09	0.00	0.89	22.22	7.21	+	+	1.27	0.00
	100 μg/mL	6.32	1.09	5.37	16.96	34.34	8.11	12.61	1.32	2.55	2.53
T. violaceum	20 μg/mL	0	0.00	2.50	9.09	14.81	+	+	++	+	0.00
	100 μg/mL	62.5	11.76	5.00	21.21	14.81	9.09	0.00	++	+	7.69
T. mentagrophytes	20 μg/mL	1.23	5.88	1.83	6.80	24.18	+	2.53	7.29	2.65	8.85
	100 μg/mL	2.47	8.82	2.75	15.53	34.07	+	13.92	7.29	1.77	+
T. tonsurans	20 μg/mL	2.50	10.34	6.45	18.18	4.65	+	3.13	+	14.75	+
	100 μg/mL	12.50	13.79	9.68	18.18	9.30	1.92	9.38	4.0	4.92	+
T. rubrum	20 μg/mL	+	25.0	10.42	+	27.03	3.85	+	+	0.00	6.12
	100 μg/mL	54.55	31.25	25.00	0.00	37.84	38.46	0.00	8.0	+	2.04
E. floccosum	20 μg/mL	+	4.35	+	16.22	20.51	11.11	+	+	10.29	4.48
	100 μg/mL	0.00	21.74	+	18.92	33.33	22.22	+	+	20.59	5.97
A. cajetani	20 μg/mL	+	6.06	17.65	5.63	24.62	0.00	+	1.49	1.25	1.33
	100 μg/mL	9.41	7.58	29.41	7.04	30.77	0.00	+	0	5.00	2.67

Although it was not possible to draw a clear profile in the relationship between the structures and the activity profile, one main conclusion was evident from this pool of data. Unexpectedly, the compounds that revealed to be more promising were not the ones bearing the triazole core. Compound **3a** (Table 8.5.4) showed the broadest activity profile, at a concentration of 100 μg/mL and exhibits inhibitions at >50% on all the dermatophytes strains herein considered. Compound **3a** was also the one that showed the strongest inhibition values among all the compounds with the exception of *E. floccosum* in which compound **3b** at 100 μg/mL shows a slightly higher growth inhibition value (83.33%) compared to the same concentration of **3a** (69.70%).

Among the compounds bearing the triazole core (Table 8.5.5), the only one that gave moderate inhibition growth was **8d** with the best inhibition values for this class of compounds ranging between 30% and 40% at concentration of 100 μg/mL. None of the compounds synthesised showed more promising activity over the reference compound, Fluconazole. Only **3a** gave, in some cases, similar results compared to fluconazole e.g. against *T. rubrum* and *T. violaceum* with inhibition values of 67.75% and 93.33% respectively compared to 67.31% and 89.39% for Fluconazole.

Taking into account, that Fluconazole proved to be inactive on *A.cajetani*, it would be valuable to consider further investigations, in the future, on the compounds showing growth inhibition higher than 40% at 100 μg/mL. From this category, the actives that performed well are **3a**, **3b** and **3c**.

It is also worth mentioning, that the compounds **3a-g**, **5** and **7** as a general trend showed higher inhibitory power on the dermatophytes investigated compared to their parent compound caffeic acid (Table 8.5.4).

8.5.3. *5-Lipooxygenase Activity Studies*

The compounds presented above were tested for their ability to inhibit leukotriene formation on purified 5-lipoxygenase (5-LO) in cell-free assays and in intact cells polymorphonuclear leukocyte (PMNL). It is important to evaluate the inhibitory power both in cell-free assays and in intact cells, due to the more complex pathways involved in the intact cells that can interact with the actives before reaching the sight of action.[115] To study the ability of the compounds to inhibit the 5-LO product formation in intact cells, human neutrophils stimulated by means of Ca^{2+} ionophore A23187 with exogenous AA at 20 μM were used.[116,117] The commercially available zileuton served as a reference compound and the analysis of the products formed from 5-LO (LTB_4, its two trans-isomers and 5-H(P)ETE) was performed with reverse-phase high-performance liquid chromatography (RP-HPLC). Preliminary experiments were carried out at 10 μM concentration and the concentrations used to evaluate the IC_{50} of the compounds were 0.1 μM, 0.3 μM, 1 μM and 3μM (Table 8.5.6).††††

†††† These studies were possible thanks to the collaboration with Professor Oliver Werz from the Department of Pharmaceutical/Medicinal Chemistry, Institute of Pharmacy, University of Jena, Germany.

Table 8.5.6 *IC_{50} values on PMNL and isolated 5-LO.*

Internal compound number	*Entry*	*Comp.No*	*5-LO in PMNL IC50 in μM (% remaining activity)*	*Isolated 5-LO IC50 in μM (% remaining activity)*
Caff	**1**	**Caff.**	>10 (104 ± 4.0)	8.5 ± 0.6
CA	**2**	**1a**	>10 (84.7 ± 3.5)	>10 (90.3 ± 1.6)
St A1	**3**	**3a**	1.8 ± 0.2	>10 (50.2 ± 3.7)
St A2	**4**	**3b**	0.92 ± 0.34	>10 (84.3 ± 1.8)
St A3	**5**	**3c**	0.47 ± 0.15	>10 (70.7 ± 4.7)
St A4	**6**	**3d**	0.18 ± 0.01	>10 (71.8 ± 4.6)
St E1	**7**	**3e**	8.23 ± 0.15	>10 (53.5 ± 3.1)
St F	**8**	**3f**	>10 (88.2 ± 3.9)	>10 (52.6 ± 3.0)
St B1	**9**	**5**	1.3 ± 0.4	>10 (73.9 ± 8.2)
St C1	**10**	**7**	2.6 ± 0.1	>10 (86.3 ± 4.8)
A1	**11**	**8a**	9.9 ± 1	7.4 ± 0.5
A2	**12**	**8b**	6.1 ± 0.5	7.6 ± 0.3
A3	**13**	**8c**	3.1 ± 0.6	6.7 ± 0.3
A4	**14**	**8d**	0.2 ± 0.03	3.2 ± 0.2
E1	**15**	**8e**	>10 (103.7 ± 4.3)	> 10 (53.6 ± 14.3)
F	**16**	**8f**	>10 (101.4 ± 6.6)	> 10 (90.3 ± 9.7)
B1	**17**	**8h**	> 10 (75.1 ± 4.3)	7.6 ± 3.0
D1	**18**	**9**	0.6 ± 0.09	> 10 (81.3 ± 10.4)
C1	**19**	**10**	0.16 ± 0.01	> 10 (60.5 ± 8.2)

The data highlighted a clear profile in the structure–activity relationship (SAR). Initially, we protected the phenolic hydroxyl groups of caffeic acid and, as expected, the activity on the isolated enzyme decreased (IC_{50} from 8.5 μM to >10 μM). Although in the cell environment, **1a** has a better inhibitory profile on the formation of leukotrienes than caffeic acid, the

residual leukotrienes formed after incubation with **1a** is 84% against 104% when incubated with caffeic acid. We expect that the acetyl group is facilitating the transit across the cell membrane over the free hydroxyl derivatives similar to the case reported by Biasutto et al.[118]

First of all, the chain length appears to play a critical role in the activity profile, both on isolated enzyme and on intact cells, as can be seen in Figure 8.5.2 and Figure 8.5.3**.**

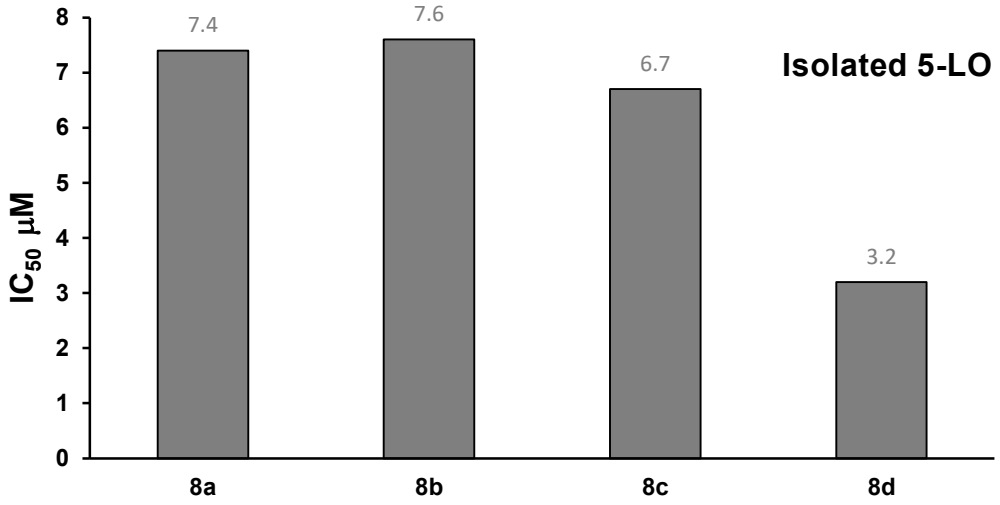

Figure 8.5.2 *Chain elongation effect on IC_{50} values on isolated 5-LO.*

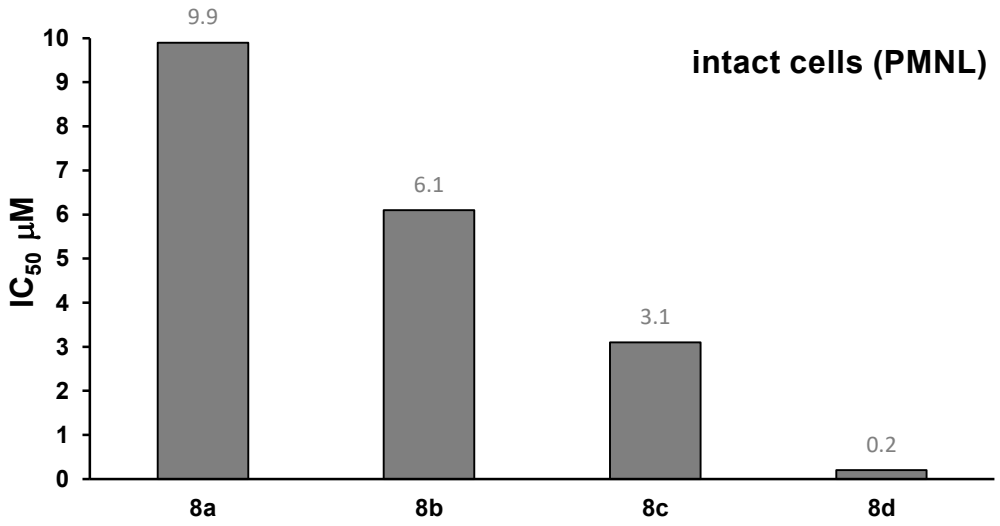

Figure 8.5.3 *Chain elongation effect on IC_{50} values against PMNL.*

Elongating the chain length leads to a decrease in the IC_{50} values (**8a>8b>8c>8d**) on both the isolated enzyme and intact cells. The effect of the chain elongation is more evident in intact cells where the ΔIC_{50} between **8a** and **8d** is 9.7 µM compared to 3.2 µM on the isolated

5-LO. However, the activity profiles on the isolated enzyme and on the cell based assays are comparable in compounds **8a-8d**, confirming that they specifically targeting 5-LO in the leukotriene pathway.

Intermediates **3a-3d** did not show relevant activity on the isolated enzyme (residual activity at all concentrations checked was higher than 50%, IC_{50} >10 μM), but they demonstrated a good activity profile on the intact cells with IC_{50} between 1.8 and 0.18 μM (compounds **3a** and **3d** respectively). The chain length seems to play a role in this case as well (Figure 8.5.4) although less significant – the ΔIC_{50} from **3a** to **3d** is 1.0 μM.

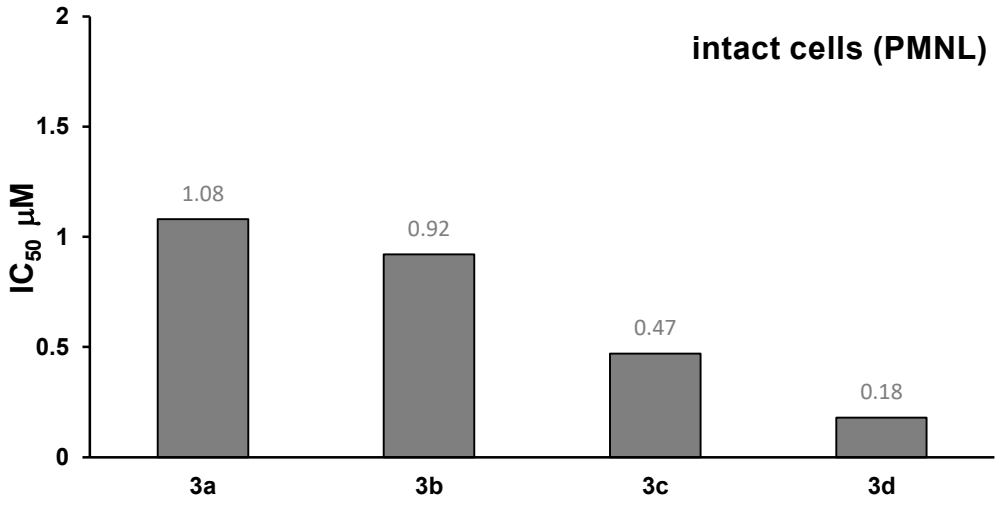

Figure 8.5.4 *Effect of increasing the chain length of the active compounds (**3a-3d**) on PMNL.*

It can be speculated that this lower impact of the chain length on the activity against 5-LO for intermediates **3a-3d** compared to **8a-8d** could be due to the fact that their mode of action on the intact cells is mainly due to interactions with other targets involved in the leukotrienes formation, and only partially interacts on 5-LO. The hypothesis that compounds **3a-3d** interact mainly with other targets in the leukotrienes pathway, is supported by the difference in the IC_{50} values between intact cell environment and isolated 5-LO, where compounds **3a-3d** show IC_{50} values between 1.8 and 0.18, and higher than 10 μM respectively. The IC_{50} values higher than 10 μM in the isolated enzyme verify that compounds **3a-3d** do not inhibit, to a significant extent, the 5-LO activity, and thus the anti-inflammatory effect evidenced in PMNL could be mainly due to interactions with other targets involved in the leukotrienes pathway.

The isomer of triazole **8a** (i.e. **8h**) led only to a slight decrease in the activity profile against 5-LO on both cell based (**8h** IC_{50} >10 μM; **8a** 9.9 μM) and cell free assays (**8h** IC_{50} 7.6 μM; **8a** 7.4 μM).

The corresponding amide **8e** of ester **8a** was inactive in cell based assays (IC_{50} >10 μM and 9.9 μM respectively) and cell-free assays (IC_{50} >10 μM and 7.4 μM respectively). A similar decrease in the activity profile is observed for intermediate **3e** compared to the corresponding ester **3a** (Table 8.5.6). Substituting the acetoxy groups of **8a** with fluorine in **8f** led to an inactive derivative. The same trend is evidenced in intermediate **3a** compared to its fluorine derivative **3f**.

The orthogonal derivatives **9** and **10** failed to significantly suppress the activity of isolated 5-LO, but potent inhibition of 5-LO in intact cells was evident with IC_{50} values of 0.6 μM and 0.16 μM, respectively. Compounds **9** and **10**, along with **3d** are inhibitors of cellular 5-lipoxygenase products, but they are inefficient on isolated 5-LO, suggesting a possible interaction of these compounds with other targets on the leukotriene pathways that requires the intact cell environment to be suppressed such as FLAP.[119]

Experiments to validate this hypothesis have been carried out in transfected HEK (Human Embryonic Kidney cells) cell with or without FLAP, on representative compounds **3a**, **9** and **10** among the molecules showing good inhibition in intact cells (PMNL) but no 5-LO inhibition on the isolated enzyme. The results highlighted that the inhibitory activity of the compounds are slightly better in HEK cells expressing just 5-LO compared to HEK cells expressing both 5-LO and FLAP. This suggests that the compounds need the intact cellular environment to act as strong inhibitors of 5-LO product formations, but the action mechanism does not involve interaction with FLAP. Hypothesis and experiments to clarify how the action mechanism changes in parallel to the structural modifications are ongoing.

Compounds **3d**, **9** and **10** turned out to be the most potent inhibitors of cellular 5-LO activity with IC_{50} values 0.18 μM, 0.6 μM and 0.16 μM respectively. The lead compound against 5-LO in cell free and cell based assays is **8d** with IC_{50} value of 0.2 μM and 3.2 μM in cell based and cell free assays respectively.

8.5.4. *Cytotoxicity Assays*

U937 cell line are characterised by monocytic-like properties and represent a good cell standard for EC(ATCCCRL1593.2) 50 evaluation.‡‡‡‡ U937 were used to determine if the decrease in the cell 5-LO lines was a consequence of a possible cytotoxic effect of the synthesised compounds.

The incubation of U937 for 24 hours with representative compounds from the library was performed to evaluate if the cell viability expressed as EC_{50}, which is the concentration required to inhibit MTT (3-(4,5-Dimethylthiazol-2-yl)-2,5-Diphenyltetrazolium Bromide) - reducing mitochondrial dehydrogenase activity by 50%, adheres to this hypothesis (Figure **8.5.5**).

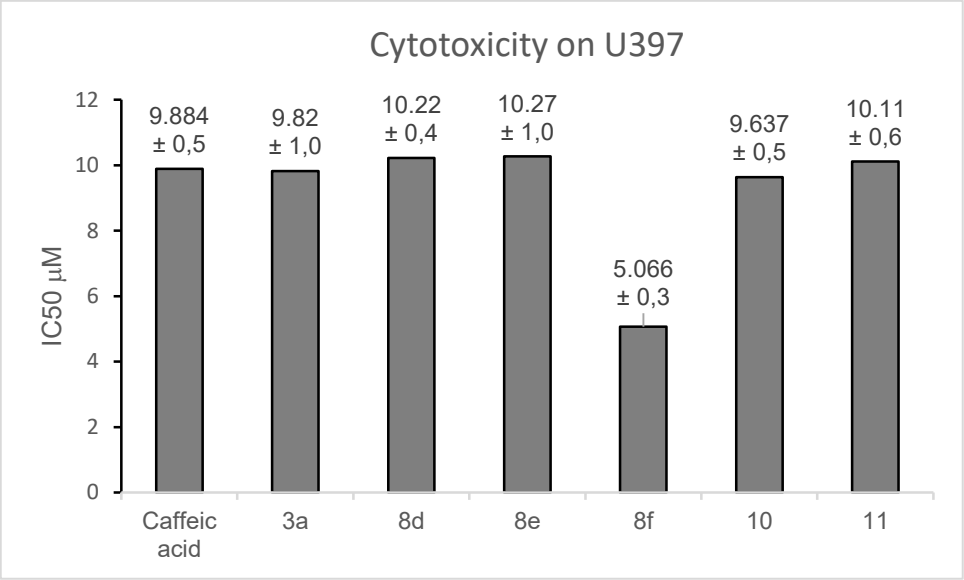

Figure 8.5.5 *EC_{50} of representative compounds on U397.*

As is evident from the above results, the representative compounds chosen from the library to evaluate cell viability, caused cytotoxic effects at concentrations similar to caffeic acid. Compound **8f**, which was one of the less active among the compounds tested in biological assays, presented the highest effect on cell viability with an EC_{50} of 5 µM. These data suggest that the inhibition of 5-LO is unrelated to the cytotoxic effects of the compounds in the present library.

‡‡‡‡ Cytotoxicity assays were performed by Dr Roberta Rizzo (Department of Medical Sciences, University of Ferrara, Italy)

9. Conclusions

In this dissertation, a new series of derivatives based on caffeic acid has been designed, synthesised and tested against eight strains of dermatophytes and 5-lipoxygenase free cell and cell based assays. Although a clear profile in the structure–activity relationship (SAR) on the dermatophytes did not emerge, it was, however, possible to obtain some useful information. However, with respect to the 5-LO assays, it was possible to obtain a clear pattern in the SAR's. Concerning the experiments on the dermatophytes, the most promising molecules, unexpectedly, were not those containing the triazole core. Compound **3a** was the most potent and exhibited the widest spectrum of action. Its growth inhibition values exceeded 50% at 100 μM/mL concentration on all the strains considered in this study. It constitutes a remarkable improvement in the activity compared to its parent compound caffeic acid which showed no activity at both concentrations tested on M.c., M.g., A.c., E.f., T.m. and T.t. showing instead a growth inhibition rate of 62.5% on T.v. and of 54.55% on T.r., but also on T.v. and on T.r. compound **3a** set a remarkable improvement with growth inhibition values of 93.33% and 67.65% respectively. The only exception was on *E. Floccosum* in which compound **3b** at 100 μg/mL shows an higher growth inhibition value (83.33%) then **3a** (69.70%). The only analogue to give moderate inhibition growth was **8d** with the best inhibition values ranging between 30% and 40% at concentration of 100 μg/mL. Overall almost none of the compounds synthesised showed more promising activity than the reference compounds Fluconazole and Econazole. Only **3a** gave, in some cases, similar results compared to Fluconazole e.g. against T.r. and T.v. with inhibition values of 67.75 % and 93.33% respectively against the 67.31 % and 89.39 % of Fluconazole.

On the other hand, against the 5-LO assays a clear pattern was evident. Linker length proved to be critical for inhibitory power against 5-LO product formations on both isolated enzyme and PMNL (IC_{50} **8a>8b>8c>8d**). The presence of the triazole ring seemed critical for selectivity towards 5-LO (IC_{50} **3d** on isolated 5-LO >10 μM, **8d** IC_{50} 3.2 μM). The absence of the triazole core (compounds **3a-3e, 5** and **7**) led to very good activity in cell based assays (IC_{50} between 1.8 μM and 0.18 μM) but no activity against the isolated enzyme, suggesting an action mechanism which requires the intact cell environment.

Compound **8d** has been highlighted, among all the molecules tested, to be the lead compound for selective inhibition of 5-LO products formation either on isolated enzyme or on cell based assays with IC_{50} of 3.2 μM and 0.2 μM respectively, with a power exceeding the clinically approved zileuton which has IC_{50} of 3.5 μM and 1.9 μM respectively. Substitution

of the acetoxy substituents on the aromatic ring of caffeic acid with fluorine (compounds **3f** and **8f**) leads to complete loss in activity on both isolated 5-LO and PMNL. Substitution of the ester motif with an amide (compounds **3e** and **8e**) led to significant decrease or total loss of activity (Table 8.5.6). Moreover, rearrangement of **8a** or **8h** impaired the 5-LO activity in PMNL. Instead azide **5** compared to alkyne **3a** maintains the same activity against PMNL suggesting that an electron dense portion could be crucial for inhibition of 5-LO product formation in intact cells (they show no activity against isolated 5-LO). Furthermore, the orthogonal derivatives **9** and **10**, although failing to inhibit 5-LO directly, proved to be more powerful than the clinically approved zileuton in inhibiting leukotrienes formation in PMNL with IC_{50} of 0.6 μM and 0.16 μM respectively. After evaluating compound **3a, 9** and **10** for FLAP interactions, they all resulted in a slightly higher inhibitory activity on HEK cells where just 5-LO was expressed compared to HEK cells where both 5-LO and FLAP were expressed. These findings highlight that the action mechanism of those compounds does not involve FLAP but needs the intact cell environment. Studies to explain the different mechanism taking place with the modifications of the structures in this class of compounds are currently ongoing.

The cytotoxicity test performed excluded the possibility that activity against leukotrienes, for the compounds herein presented was due to a cytotoxic effect.

To summarise, the results obtained in this research enabled the design of a new potential class of 5-LO inhibitors based on caffeic acid and triazole core moiety, identifying key elements necessary to selectively address the activity against 5-LO and drew a clear relationship between structure and activity for the synthesised compounds against this target.

The only compound among those containing the triazoles ring that may be developed as part of a multi-target strategy, capable of blocking 5-LO alongside 14 α-lanosterol demethylase is compound **8d.** In fact, it demonstrated very good activity against 5-LO in both cell free and cell based assays, as mentioned above, and showed a growth inhibition rate on dermatophytes of around 30%. The action against the dermatophytes was not ideal but leaves hope for improvement. The first step to verify its potential as multi-target drug will be to evaluate **8d** against isolated 14 α-lanosterol demethylase in order to evaluate if its moderate inhibition on the microorganism is due to a scavenging mechanism possessed by the fungus and to confirm that its inhibitory activity is not due to some unexpected action mechanism.

Compounds **3a-3d** revealed to be potential multi-target analogues, considering they give good growth inhibition rates on the evaluated dermatophytes strains and they are powerful

against 5-LO product formations in intact cells. Taking into account that these analogues proved to be active in cell environments they will be now screened against isolated enzymes involved in dermatophyte cell growth and enzymes involved in the arachidonic acid pathways, in order to identify their specific targets and understand how to optimise their structure towards a successful multi-target strategy.

10. Experimental Protocols and Compounds Characterisation

10.1. Antioxidants Protocols

10.1.1. *DPPH Test*

The antioxidant assays involving the DPPH· (1,1- diphenyl-2-picrylhydrazyl) free radical is used to measure the scavenging ability of complex mixtures of pure compounds. It is very popular in the measure of the antioxidant power of natural products. Its success is due to the high sensitivity and the simplicity of operation, furthermore the DPPH· radical is one of the few organic nitrogen radical which are stable and commercially available. The theory underlying this assays is that H-donor molecules act as antioxidant toward the DPPH· radical. The action mechanism is shown in Figure 10.1.1. The antioxidant power exerted by the compound/mixture tested is proportional to the disappearance of the DPPH· radical in the solution. Its disappearance is monitored commonly by UV spectrometer considering that the DPPH· radical shows a strong maximum absorption at λ_{max} = 517 nm, which translates to a deep purple colour. The absorbance value, and thus the colour fades, in a proportional fashion with the decrease of the DPPH· radical in solution. The antioxidant power is measured by monitoring the reduction of absorbance at 517 nm. The antioxidant value is expressed in µmol Trolox per g of samples.[120] To standardise the method a calibration curve using trolox is done prior to experiments. Trolox is a commercially available water-soluble vitamin-E portion. Is common practice to express the results of this assay in trolox unit (TE) or as EC50 which is the amount of antioxidant necessary to decrease the DPPH· free radical of 50%. To scavenge 2 moles of DPPH· free radical 1 mole of trolox is necessary. It is important to mention that this method is not appropriate to evaluate the antioxidant activity of plasma due to precipitation of proteins in the alcoholic media.[121]

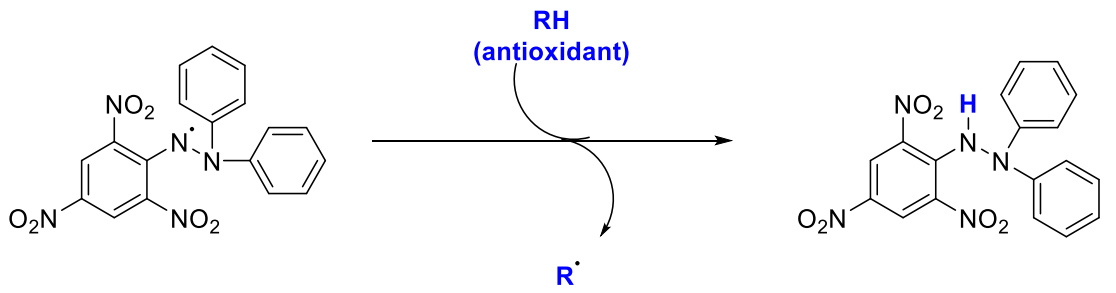

Figure 10.1.1 *DPPH· free radical scavenging mechanism.*

The experimental protocol was adapted from the one reported by Wang et al. (1998)[122]. In 1.5 mL of a 1.0 × 10^{-4} M methanol solution of DPPH·, 0.750 mL of solutions at different concentrations of tested compounds were added. Then the solutions with samples to analyse was shaken vigorously and kept in the dark for 30 minutes. The absorbance of the samples was measured on a spectrophotometer (Beckman Coulter ™, DU® 530, Life Science UV-Vis Spectrophotometer) at λ_{max} = 517 nm against a blank of methanol without DPPH·. The standard for preparation of calibration curve used was trolox. The values are expressed in µmol trolox unit for gram of sample, calculated as linear regression of the results obtained for the samples at different dilution. All tests were run in triplicate and averaged.

10.1.2. *FRAP (Ferric reducing ability of plasma) Test*

Differently from the DPPH· antioxidant test is adequate not only to measure the antioxidant activity of pure compounds or mixtures, but also the plasma antioxidant capacity and for this specific purpose was developed by Benzie and Strain in 1996.[123]

This assays measures the ability to reduce the ferric ion (Fe^{3+}), in acidic conditions, to ferrous ion (Fe^{2+}) in presence of 2,4,6-tripyrididyl-s-triazine (TPTZ) Figure 10.1.2. TPTZ forms a yellow complex with the Fe^{3+} ion, the complex of TPTZ with Fe^{2+} is instead blue. The absorbance increase with the reduction of the ferric iron to the ferrous one. The chemical reaction is reported in Scheme 10.1.1 FRAP action mechanism.

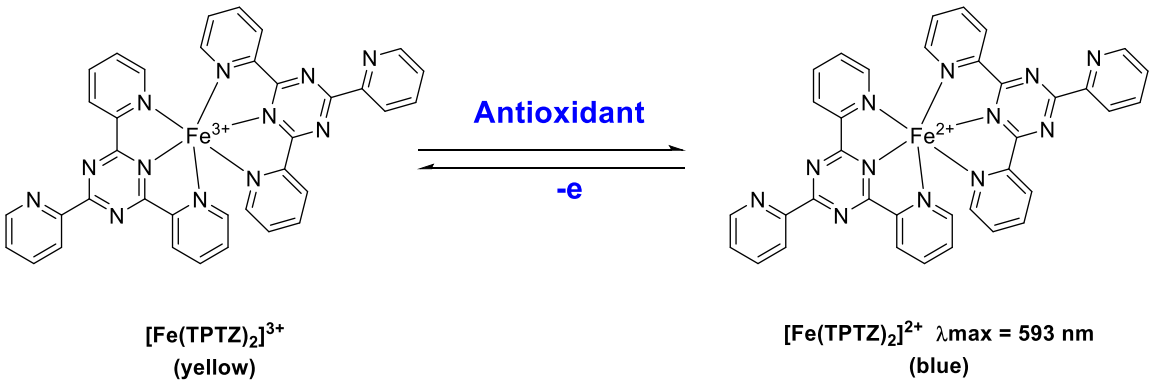

Scheme 10.1.1 *FRAP action mechanism.*

The increase in the absorbance is proportional to the reducing ability of the antioxidant under analysis[124]. The absorbance is measured at the λ_{max} = 593 nm.

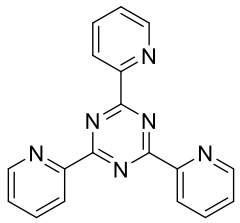

2,4,6-tripyrididyl-s-triazine
(TPTZ)

Figure 10.1.2 *TPTZ structure.*

The reducing power of each standard solution was calculated according to the procedure reported by Xu et al. in 2007.[39] The samples under investigation were dissolved in the selected solvent (methanol and/or water). The FRAP reagent is freshly prepared from the mixing of solutions A:B:C in a ratio 10:1:1 and left at 37 °C for 30 minutes. It needs to be stored at 37 °C while preparing the samples for analysis. Solution A: acetate buffer 0.3 M (pH 3.6), Solution B: TPTZ 10 mM in 40 mmol of HCl, Solution C: $FeCl_3$ 20 mM.

To 1.9 mL of frap reagent was added 0.1 mL of solvent to perform the blank, or of extracted sample.

Measurements were carried on at λ_{max} = 593 nm with a spectrophotometer (Beckman Coulter ™, DU® 530, Life Science UV-Vis Spectrophotometer).

The standard used to prepare the calibration curve is Trolox, and the results are given in μmol Trolox/g.

10.2. Dermatophytes Experimental Protocols

The dermatophytes used in this study were:

1. *Microsporum gypseum* (Iran) CBS 130948 strain
2. *Microsporum canis* (Iran) CBS 131110 strain
3. *Trichophyton violaceum* (Africa) CBS 459.61 strain
4. *Trichophyton mentagrophytes* (Netherlands) CBS 160.66 strain
5. *Trichophyton tonsurans* (Netherlands) CBS 483.76 strain
6. *Trichophyton rubrum* (Turkey) CBS 132252 strain
7. *Epidermophyton floccosum* var. floccosum (Netherlands) CBS 358.93 strain
8. *Arthroderma cajetani* (Netherlands), CBS 495.70 strain

The cell cultures were stored in agar's slants or in an appropriate culture medium (SDA, Difco).

In order to evaluate the antifungal activity of the compounds herein presented, cells cultures of each fungus were obtained after transplanting mycelium disks, 10 mm in diameter, from a single culture on a stationary phase. Consequently, these were incubated at 26 ± 1 °C on the appropriate medium (SDA), on thin sterile sheets of cellophane, until the logarithmic phase of growth was reached. The grown fungi were transferred then to Petri supports containing the medium loaded with the test compound. Each molecule was dissolved into dimethyl sulfoxide (DMSO), and a proper dilution in order to reach a final concentration of 20, or 100 μg/mL was aseptically added to the medium at 45 °C. In the final solutions the concentration of DMSO was adjusted to 0.1%. Controls were set up with equivalent quantities (0.1%) of DMSO. Determination of growth rate was achieved by registering the daily modifications in the colony diameter for a period of 7 days after the transport of the fungus onto supports containing the substance under investigation. At day 7^{th} the Δd (difference in colony diameter between day 7 and control) in comparison with the control was evaluated for each fungus in order to evaluate the percentage values of growth inhibition on all the dermatophytes considered. The experiments were run in duplicates for each concentration considered. The growth inhibition values were expressed as the mean of values obtained in two independent experiments.

The relative inhibition rate of the circle mycelium compared to the blank assay was calculated by means of Equation 10.2.1.

$$\textbf{Relative inhibition rate (\%)} = [(dex - dex')/dex] \times 100\%$$

Equation 10.2.1 *Equation for the relative inhibition rate.*

In Equation 10.2.1**Error! Reference source not found.** dex represents the extended diameter of the circle mycelium during the blank assay, whereas dex' the extended diameter of the circle mycelium during testing.

10.3. 5-Lipooxygenase Protocols

10.3.1. *Human Recombinant 5-LO Expression and Purification*

E. coli Bl21 (DE3) cells were transformed with pT3–5LO plasmid, lysed in a solution 50 mM triethanolamine/HCl at pH 8.0 with addition of EDTA (5 mM), then soybean trypsin inhibitor (60 μg/mL), phenylmethanesulphonyl fluoride (1 mM), dithiothreitol (1 mM) and lysozyme (1 mg/mL) and were added and the mixture was subsequently sonicated (3 × 15 sec). The homogenate was centrifuged at 10,000 × g for 15 min and the remaining supernatant at 40,000 × g for 70 min at 4 °C. 5-LO in the supernatant was partially purified by affinity chromatography on an ATP-agarose column as described by Fisher et al. in 2003.[125] The resulting semi-purified 5-LO was diluted in PBS containing EDTA (1 mM) and ATP (1 mM) and immediately used for activity assays.

10.3.2. *Activity Assay for Human Recombinant 5-LO*

Human recombinant 5-LO was pre-incubated with the test compounds for 10 min at 4 °C and pre-warmed for 30 s at 37 °C. 5-LO product formation was initiated by addition of 2 mM $CaCl_2$ and 20 μM arachidonic acid. After 10 min at 37 °C, the reaction was terminated by addition of 1 mL ice-cold methanol. Formed 5-LO metabolites (all-trans isomers of LTB4 and 5-H(P)ETE) were analysed by means of RP-HPLC as described by Koeberle et al. in 2009.[126]

10.3.3. *Determination of 5-LO Product Formation in Neutrophils*

Freshly isolated neutrophils (1×10^7/mL) were pre-incubated with the test compounds for 15 min at 37 °C. 5-LO product formation was then started by addition of 2.5 μM Ca^{2+}-ionophore A23187. The reaction was stopped after 10 min at 37 °C with 1 mL of methanol. Major 5-LO metabolites (LTB4 and its all-trans isomers and 5-H(P)ETE) were extracted and analysed by HPLC as described by Werz et al.[127] Cysteinyl-LTs C4, D4 and E4 and oxidation products of LTB4 were not determined.

10.4. Cytotoxicity assays

U937 (ATCCCRL1593.2) cell line, derived from malignant cells of a pleural effusion of 37 year old Caucasian male with diffuse histiocytic lymphoma, was grown in RPMI 1640 (Gibco) added with 10% FBS (Foetal Bovine Serum), 10% Hepes Buffer, 5% penicilin\strepatamicin at 37 °C in a humidified 5% CO_2 atmosphere for 72 hours. 100 μL

of cells at the density of 1×10^6/mL were seaded into 96-well plates (Nunc) and added with the different compounds at different concentrations (Caffeic acid at 1, 10, 20 µM; **8a, 8d, 8e,8f, 9,10** at 3, 10, 20 µM) and analysed by MTT assay (Sigma-Aldrich) after 24 hrs incubation. MTT stock solution (5 mg/mL) was added to each culture being assayed to equal one-tenth the original culture volume and incubated for 4 hr. At the end of the incubation period, we added acidic isopropanol (100 µL of 0.04 N HCl in absolute isopropanol). Absorbance of converted dye was measured at a wavelength of 570 nm with background subtraction at 630–690 nm using ELISA-reader (Victor, Perkin-Elmer). We expressed the effect on cell viability as EC_{50}, which is the concentration required to inhibit MTT-reducing mitochondrial dehydrogenase activity by 50%. The absorbance of untreated cells (RPMI+DMSO) was taken as 100% viability to calculate cytotoxicity.

10.5. General Synthetic Procedures and Compounds Characterisation

All solvents were used as supplied unless otherwise stated.

Flash column chromatography (FCC) was performed using Breckland Scientific silica gel 60, particle size 40-63 nm under air pressure. Analytical thin layer chromatography (TLC) was performed using silica gel 60 F254 pre-coated glass backed plates and visualised by ultraviolet radiation (254 nm) and/or potassium permanganate or ammonium molybdate as appropriate. Isolated yields are reported to 0 decimal places and "quant." signifies a yield of 99.5% or higher. ^{1}H NMR spectra were recorded on Bruker DRX-400 (400MHz) or DRX-600 (600 MHz) spectrometer. Chemical shifts are reported in ppm with the resonance resulting from incomplete deuteration of the solvent as the internal standard ($CDCl_3$: 7.26 ppm, or DMSO-*d*$_6$: 2.54 ppm, q). ^{13}C NMR spectra were recorded on Bruker DRX-400 (100 MHz) or DRX-600 (150 MHz) spectrometer with complete proton decoupling. Chemical shifts are reported in ppm with the solvent resonance as the internal standard ($CDCl_3$: 77.0 ppm, t or DMSO-*d*$_6$: 30.73, ep.). Data are reported as follows: chemical shift δ/ppm , multiplicity (s = singlet, d = doublet, t = triplet, q = quartet, br = broad, m = multiplet or combinations thereof. ^{13}C signals are singlets unless otherwise stated), coupling constants J Hz, integration (^{1}H only). ^{1}H NMR signals are reported to 2 decimal places and ^{13}C signals to 1 decimal place unless rounding would produce a value identical to another signal. In this case, an additional decimal place is reported for both signals concerned. ^{19}F NMR signals are reported to 2 decimal places and trifluoro-toluene (BTF) was used as internal standard. High resolution mass spectrometry (HRMS) was performed on a Waters Micromass LCT spectrometer using electrospray ionization, time-of-flight analysis and Micromass MS

software HRMS signals are reported to 4 decimal places and are within ±5 ppm of theoretical values. Infrared spectra were recorded neat as thin films on a Perkin-Elmer Spectrum One FTIR spectrometer and only selected peaks are reported (s = strong, m = medium, w = weak, br = broad). Melting points were collected using a Stanford Research Systems Optimelt automated melting point system using a gradient of 1 °C per min.

Purity was checked by elemental analysis or by HPLC traces using a C18 waters bondapak .10 μm*125Å, 3.9*150 mm.

10.5.1. *Di-acetylation General Procedure*

To caffeic acid in pyridine (1.00 eq.) was added acetic anhydride (5.00 eq.) under magnetic stirring until the reaction was complete. The reaction mixture was then diluted with DCM and consequently washed three times with 3 M HCl and three times with brine, it was then dried over $MgSO_4$ and concentrated to dryness to afford the pure product.

10.5.2. *Esters Derivatives Synthesis: Method A.*

A mixture of diacetylcaffeic acid or 3,4 di-fluoro cinnamic acid (1.00 eq.), thionyl chloride (25.0 eq), a catalytic amount of DMF in dry benzene (1.00 mL each mmol of diacetyl-caffeic acid) was refluxed for 4 hours. The excess of thionyl chloride was removed *in vacuo*. The residue was dissolved in dry benzene (4 mL for each mmol of diacetylcaffeic acid) before pyridine (0.001 eq.) was added drop-wise followed by the appropriate alcohol derivatives was added (1.2 eq.). The mixture was stirred at room temperature overnight under an atmosphere of argon. The resulting mixture was dried *in vacuo*, the residue re-dissolved in DCM (10 mL) and the organics washed with water (3 × 10 mL), washed with brine (3 × 10 mL), dried over $MgSO_4$ and solvents were removed *in vacuo* to afford the crude material. The crude was purified by column chromatography EtOAc/petroleum ether in the appropriate ratio according to the compound polarity.

10.5.3. *Esters Derivatives Synthesis: Method B*

To 6-acetyl-2,5,7,8-tetramethylchromane-2-carboxylic acid (Acetyl-Trolox 1.00 eq.), prepared following the literature,[5] in DCM was added DCC (1.00 eq.) and DMAP (1.00eq.). The mixture was allowed to stir for 10 minutes at room temperature before the azide or alcohol (1.00 eq.) was added. The mixture was stirred at room temperature overnight under an atmosphere of argon. The resulting mixture was filtered, washed with a 10% solution of

$KHSO_4$ three times and dried over $MgSO_4$ before the solvent removed *in vacuo* to afford the crude material.[6]

(*E*)-4-(3-(But-3-yn-1-yloxy)-3-oxoprop-1-en-1-yl)-1,2-phenylene diacetate (3a)

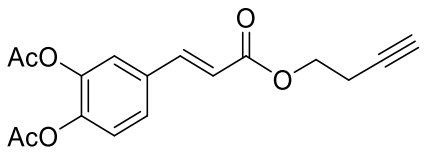

According to the general esterification procedure method A, a solution of di-acetyl-caffeic-acid (166 mg, 0.6 mmol, 1.0 eq) in $SOCl_2$ (2.5 mL), DMF (44 µL) and dry benzene (1 mL) was refluxed for 4 hours. The mixture was then concentrated *in vacuo*. The residue was re-dissolved in dry benzene (4 mL) before pyridine was added drop-wise followed by 3-butyn-1-ol (52.98 mg, 0.75mmol, 1.2 eq). The reaction was allowed to stir for 12 hours at room temperature under an atmosphere of argon. The resulting mixture was concentrated *in vacuo* re-dissolved in DCM (10 mL) washed with water (3 × 10 mL), washed with brine (3 × 10 mL), dried over $MgSO_4$ and concentrated *in vacuo*.

The crude material was purified by column chromatography (EtOAc/petroleum ether 30:70). Recrystallised from EtOAc/hexanes (10:90) to give a white solid (176 mg, 0.56 mmol, 93%).

MP: 82 °C. R_f 0.23 (EtOAc/petroleum ether 30:70). ^{1}H NMR (600 MHz, $CDCl_3$) δ 7.65 (d, J = 16.0 Hz, 1H), 7.41 (dd, J = 8.4, 1.9 Hz, 1H), 7.36 (d, J = 2.0 Hz, 1H), 7.23 (d, J = 8.4 Hz, 1H), 6.40 (d, J = 16.0 Hz, 1H), 4.32 (t, J = 6.8 Hz, 2H), 2.61 (m, J = 6.8, 2.7 Hz, 2H), 2.31 (s, 3H), 2,30 (s, 3H), 2.03 (t, J = 2.7 Hz, 1H). ^{13}C NMR (150 MHz, $CDCl_3$) δ 168.0, 167.9, 166.2, 143.6, 143.3, 142.4, 133.2, 126.4, 123.9, 122.8, 118.8, 80.0, 70.0, 62.3, 20.7, 20.6, 19.1. FT-IR (Neat, υ_{max} cm^{-1}) 3272, 1765, 1714, 1638. HRMS *m/z* calculated for $C_{17}H_{17}O_6$ $[M+H]^+$ 317.1020, found 317.1016. Elemental analysis calculated for $C_{17}H_{16}O_6$ found C 64.26 %, H 5.12%, requires C 64.55%, 5.10%.

(*E*)-4-[3-(Hex-5-yn-1-yloxy)-3-oxoprop-1-en-1-yl]-1,2-phenylene diacetate (3b)

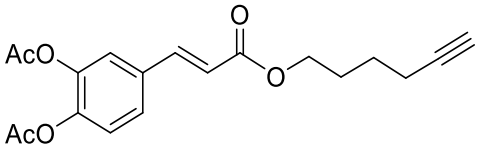

According to the general esterification procedure method A, a solution of di-acetyl-caffeic-acid (1.0 g, 3.8 mmol, 1.0 eq) in $SOCl_2$ (5 mL), DMF (280 µL) and dry benzene (4 mL) was refluxed for 4 hours. The mixture was then concentrated *in vacuo*. The residue was then re-dissolved in dry benzene (12 mL) before pyridine was added drop-wise followed by 5-hexyn-1-ol (445 mg, 4.54 mmol, 1.2 eq). The reaction was allowed to proceed for 12 hours at room temperature under an atmosphere of argon. The resulting mixture was concentrated *in vacuo*, re-dissolved in DCM (10 mL) washed with water (3 × 10 mL), washed with brine (3 × 10 mL), dried over $MgSO_4$ and concentrated *in vacuo*.

The crude material was purified by column chromatography (EtOAc/petroleum ether 30:70). Recrystallised from hexanes (100%) to give a white solid (900 mg, 2.6 mmol, 69%). MP: 48 °C. R_f 0.35 (EtOAc/petroleum ether 30:70). ^{1}H NMR (400 MHz, $CDCl_3$) δ 7.58 (d, J = 16.0 Hz, 1H), 7.36 (d, J = 8.5 Hz, 1H), 7.33 (overlapping, br, s, 1H), 7.18 (d, J = 8.3 Hz, 1H), 6.35 (d, J = 16.0 Hz, 1H), 4.19 (t, J = 6.3 Hz, 2H), 2.26 (s, 3H), 2.25 (s, 3H), 2.22 (overlapping m, 2H), 1.96 (s, 1H), 1.86 – 1.73 (m, 2H), 1.65 – 1.58 (m, 2H). ^{13}C NMR (100 MHz, $CDCl_3$) δ 167.7, 167.6, 166.2, 143.2, 142.5, 142.2, 133.0, 126.1, 123.7, 122.5, 119.0, 83.7, 68.7, 64.0, 27.6, 24.8, 20.50, 20.46, 18.0. FT-IR (Neat, υ_{max} cm^{-1}) 3290, 2933, 2864, 1762, 1707, 1638, 1507. HRMS *m/z* calculated for $C_{19}H_{21}O_6$ $[M+H]^+$ 345.1338, found 345.1347. Elemental analysis calculated for $C_{19}H_{20}O_6$ found C 66.23%, H 5.87%, requires C 66.27%, 5.85%.

(*E*)-4-[3-(Hept-6-yn-1-yloxy)-3-oxoprop-1-en-1-yl]-1,2-phenylene diacetate (3c)

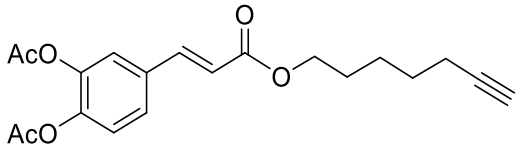

According to the general procedure method A, a solution of Di-acetyl-caffeic-acid (1.5 g, 5.6 mmol, 1 eq) in $SOCl_2$ (10 mL), DMF (1 mL) and dry benzene (6 mL) was refluxed for 4h. The mixture was then concentrate *in vacuo*. The residue was then re-dissolved in dry benzene (24 mL), pyridine was added drop-wise followed by 6-heptyn-1-ol (763.5 mg, 6.72 mmol, 1.2 eq). The reaction was allowed to proceed for 12 hours at room temperature under an atmosphere of argon. The resulting mixture was concentrated *in vacuo* re-dissolved in DCM (10 mL) washed with water (3 × 10 mL), washed with brine (3 × 10 mL), dried over $MgSO_4$ and concentrated *in vacuo*.

The crude material was purified by column chromatography (EtOAc/petroleum ether 30:70). Recrystallised from hexanes (100%) to give a white solid (823 mg, 2.29 mmol, 41%). MP: 68 °C. R_f 0.23 (EtOAc/petroleum ether 30:70). ^{1}H NMR (400 MHz, $CDCl_3$) δ 7.59 (d, J = 16.0 Hz, 1H), 7.37 (d, J = 8.4 Hz, 1H), 7.34 (br, s, 1H), 7.19 (d, J = 8.3 Hz, 1H), 6.36 (d, J = 16.0 Hz, 1H), 4.18 (t, J = 6.6 Hz, 2H), 2.272 (s, 3H), 2,266 (s, 3H), 2.19 (td, J = 6.6, 2.3 Hz, 2H), 1.94 (t, J = 2.4 Hz, 1H), 1.76 – 1.64 (m, 2H), 1.62 – 1.43 (m, 4H). ^{13}C NMR (100 MHz, $CDCl_3$) δ 167.9, 167.8, 166.4, 143.3, 142.6, 142.3, 133.2, 126.2, 123.8, 122.6, 119.2, 84.1, 68.4, 64.4, 28.1, 27.9, 25.0, 20.48, 20.45, 18.2. FT-IR (Neat, υmax cm^{-1}) 3294, 2940, 2861, 1764, 1705, 1638. HRMS *m/z* calculated for $C_{20}H_{23}O_6$ [M+H]+ 359.1489, found 359.1479. Elemental analysis calculated for $C_{20}H_{22}O_6$ found C 66.99%, H 6.24%, requires C 67.03%, H 6.19%.

(*E*)-4-[3-(Dec-9-yn-1-yloxy)-3-oxoprop-1-en-1-yl]-1,2-phenylene diacetate (3d)

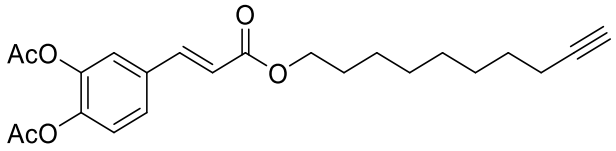

According to the general procedure method A, a solution of di-acetyl-caffeic-acid (1.0 g, 3.8 mmol, 1.0 eq) in $SOCl_2$ (5 mL), DMF (1 mL) and dry benzene (4 mL) was refluxed for 4 hours. The mixture was then concentrated *in vacuo*. The residue was then re-dissolved in dry benzene (12 mL) before pyridine was added drop-wise followed by 9-decyn-1-ol (703.4 mg, 5 mmol, 1.2 eq). The reaction was allowed to stir for 12 hours at room temperature under an atmosphere of argon. The resulting mixture was concentrated *in vacuo* re-dissolved in DCM (10 mL) washed with water (3 × 10 mL), washed with brine (3 × 10 mL), dried over $MgSO_4$ and concentrated *in vacuo*.

The crude material was purified by column chromatography (EtOAc/petroleum ether 30:70). Recrystallised from hexanes (100%) to give a white solid (669.58 mg, 1.7 mmol, 44%). MP: 49 °C. R_f 0.43 (EtOAc/petroleum ether 30:70). ^{1}H NMR (400 MHz, $CDCl_3$) δ 7.61 (d, J = 16.0 Hz, 1H), 7.40 (dd, J = 8.4, 1.9 Hz, 1H), 7.36 (d, J = 1.8 Hz, 1H), 7.22 (d, J = 8.4 Hz, 1H), 6.38 (d, J = 16.0 Hz, 1H), 4.19 (t, J = 6.7 Hz, 2H), 2.31 (s, 3H), 2.30 (s, 3H), 2.21 – 2.15 (m, 3H), 1.94 (t, J = 2.6 Hz, 1H), 1.74 – 1.64 (m, 2H), 1.59 – 1.46 (m, 4H), 1.38 (m, 7H). ^{13}C NMR (100 MHz, $CDCl_3$) δ 168.34, 168.26, 167.0, 143.7, 142.9, 142.7, 133.7, 126.6, 124.2, 123.0, 119.8, 85.0, 68.4, 65.1, 29.4, 29.3, 29.0, 28.9, 28.7, 26.2, 21.0, 20.9, 18.7. FT-IR (Neat, υ_{max} cm^{-1}) 3303, 2932, 2862, 1764, 1709, 1638. HRMS *m/z* calculated for $C_{23}H_{29}O_6$ $[M+H]^+$ 401.1959, found 401.1956. Elemental analysis calculated for $C_{23}H_{28}O_6$ found C 68.87%, H 7.03%, requires C 68.98%, H 7.05%.

(*E*)-4-(3-(But-3-yn-1-ylamino)-3-oxoprop-1-en-1-yl)-1,2-phenylene diacetate (3e)

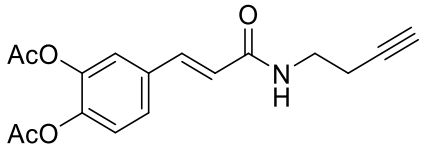

According to the general esterification procedure method A, a solution of di-acetyl-caffeic-acid (264.23 mg, 1 mmol, 1.0 eq) in $SOCl_2$ (2 mL), DMF (300 µL) and dry benzene (1 mL) was refluxed for 4 hours. The mixture was then concentrated *in vacuo*. The residue was re-dissolved in dry benzene (4 mL) before pyridine was added drop-wise followed by 1-amino-3-butyne (82.93 mg, 1.2 mmol, 1.2 eq). The reaction was allowed to stir for 12 hours at room temperature under an atmosphere of argon. The resulting mixture was concentrated *in vacuo* re-dissolved in DCM (10 mL) washed with water (3 × 10 mL), washed with brine (3 × 10 mL), dried over $MgSO_4$ and concentrated *in vacuo*.

The crude material was purified column chromatography (EtOAc/petroleum ether 60:40). Recrystallised from EtOAc/hexane (90:10) to give a white solid (254 mg, 0.8 mmol, 80%). MP: 143 °C. R_f 0.32 (EtOAc/petroleum ether 60:40). ^{1}H NMR (600 MHz, $CDCl_3$) δ 7.57 (d, J = 15.6 Hz, 1H), 7.37 (dd, J = 8.4, 1.7 Hz, 1H), 7.34 (d, J =1.6 Hz, 1H), 7.19 (d, J = 8.3 Hz, 1H), 6.33 (d, J = 15.5 Hz, 1H), 5.97 (s, 1H), 3.54 (q, J = 6.3 Hz, 2H), 2.47 (td, J = 6.3, 2.5 Hz, 2H), 2.301 (s, 3H), 2.296 (s, 3H), 2.04 (t, J = 2.5 Hz, 1H). ^{13}C NMR (150 MHz, $CDCl_3$) δ 168.09, 168.07, 165.4, 142.9, 142.3, 139.2, 133.7, 126.2, 123.7, 122.2, 121.7, 81.5, 70.1, 38.2, 20.58, 20.55, 19.4. HRMS *m/z* found 316.1191 requires 316.1185. FT-IR (Neat, υ_{max} cm^{-1}) 3274, 3241, 3073, 1755, 1658, 1614, 1569. HRMS *m/z* calculated for $C_{17}H_{18}NO_5$ $[M+H]^+$ 316.1191, found 316.1185. Elemental analysis calculated for $C_{17}H_{17}NO_5$ found C 64.37%, H 5.38%; N 4.30%, requires C 64.75%, H 5.43%, N 4.44%

But-3-yn-1-yl (*E*)-3-(3,4-difluorophenyl) acrylate (3f)

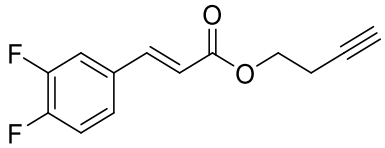

According to the general esterification procedure method A, a solution of 3-4 di-fluoro cinnamic acid (3.0 g, 16 mmol, 1.0 eq) in $SOCl_2$ (30 mL), DMF (1.5 mL) and dry benzene (16 mL) was refluxed for 4 hours. The mixture was then concentrated *in vacuo*. The residue was re-dissolved in dry benzene (50 mL) before pyridine was added drop-wise followed by 3-butyn-1-ol (1.36 mg, 19.5 mmol, 1.2 eq). The reaction was allowed to stir for 12 hours at room temperature under an atmosphere of argon. The resulting mixture was concentrated *in vacuo* re-dissolved in DCM (10 mL) washed with water (3 × 10 mL), washed with brine (3 × 10 mL), dried over $MgSO_4$ and concentrated *in vacuo*.

The crude material was purified by column chromatography (EtOAc/petroleum ether 10:90). Recrystallised from petroleum ether (100%) to give a white solid (2.2g, 9.3 mmol, 58%). MP: 48 °C. R_f 0.4 (EtOAc/petroleum ether 10:90). ^{1}H NMR (400 MHz, $CDCl_3$) δ 7.61 (d, *J* = 16.0 Hz, 1H), 7.40 – 7.30 (m, 1H), 7.28 – 7.23 (m, 1H), 7.18 (dt, *J* = 16.6, 8.2 Hz, 1H), 6.37 (d, *J* = 16.0 Hz, 1H), 4.32 (t, *J* = 6.8 Hz, 2H), 2.61 (td, *J* = 6.8, 2.6 Hz, 2H), 2.03 (t, *J* = 2.6 Hz, 1H). ^{13}C NMR (100 MHz, $CDCl_3$) δ 166.2 , 152.9 , 151.9 (d, *J* = 13.2 Hz), 150.3 (d, *J* = 12.9 Hz), 149.4 (d, *J* = 13.2 Hz), 142.9 , 124.9 (dd, *J* = 6.6, 3.6 Hz), 118.9 , 117.9 (dd, *J* = 17.8, 0.7 Hz), 116.5 (dd, *J* = 17.7, 0.9 Hz), 80.2 , 77.5 , 77.2 , 76.8 , 70.1 , 62.6 , 19.3 . ^{19}F NMR (376 MHz, $CDCl_3$) δ -63.61 (d, *J* = 3.5 Hz), -134.83 (d, *J* = 20.9 Hz), -137.41 (d, J = 20.8 Hz). FT-IR (Neat, υ_{max} cm^{-1}) 3296, 1710, 1640, 1612, 1602, 1513. HRMS *m/z* calculated for $C_{13}H_{11}F_2O_2$ $[M+H]^+$ 237.0722, found 237.0710. Elemental analysis calculated for $C_{13}H_{10}F_2O_2$ found C 66.07%, H 4.30%, requires C 66.10%, H 4.27%.

(*E*)-Dec-9-yn-1-yl-3-(3,4-difluorophenyl)acrylate (3g)

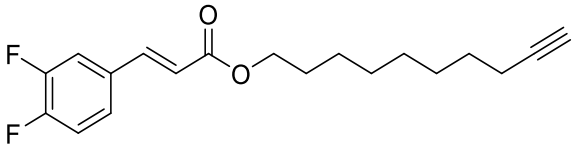

White solid (70%). MP 34 °C. Purified by column chromatography (EtOAc/hexane 10:90). Recrystallised from EtOAc/hexane (10:90). R_f 0.4 (EtOAc/hexane 10:90). ^{1}H NMR (600 MHz, $CDCl_3$) δ 7.58 (d, *J* = 16.0 Hz, 1H), 7.34 (ddd, *J* = 10.8, 7.6, 2.0 Hz, 1H), 7.28 – 7.24 (m, 1H), 7.18 (dt, *J* = 9.9, 8.2 Hz, 1H), 6.36 (d, *J* = 15.9 Hz, 1H), 4.21 (t, *J* = 6.7 Hz, 2H), 2.19 (td, *J* = 7.1, 2.6 Hz, 2H), 1.95 (br s, 1H), 1.78 – 1.67 (m, 2H), 1.54 (m, 2H), 1.47 – 1.28 (m, 8H). ^{13}C NMR (150 MHz, $CDCl_3$) δ 166.5, 151.8 (dd, *J*= 130.0, 13.0 Hz), 150.2 (dd, *J* = 126.3, 13.0 Hz), 142.1 (t, *J*= 2.1 Hz), 131.7 (dd, J = 6.0, 4.0 Hz), 124.7 (dd, *J* = 6.5, 3.4 Hz), 119.4 (d, *J* = 2.5 Hz), 117.8 (d, *J* = 17.7 Hz), 116.3 (d, *J* = 17.6 Hz), 84.7, 68.1, 64.8, 29.1, 28.9, 28.6, 28.6, 28.4, 25.9, 18.3 . ^{19}F NMR (376 MHz, $CDCl_3$) -135.33 (d, *J* = 20.8 Hz), -137.67 (d, *J* = 20.9 Hz). FT-IR (Neat, υ_{max} cm^{-1}) 3298, 2936, 2925, 2853, 1712, 1639, 1516, 1272, 1179, 828, 666. HRMS *m/z* calculated for $C_{19}H_{23}F_2O_2$ $[M+H]^+$ 321.1666, found 321.1657. Elemental analysis calculated for $C_{19}H_{22}F_2O_2$: C 71.23, H 6.92; found: C 71.25, H 6.88.

(*E*)-4-(3-(3-Azidopropoxy)-3-oxoprop-1-en-1-yl)-1,2-phenylene diacetate (5)

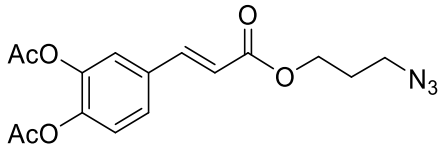

According to the general esterification procedure method A, a solution of di-acetyl-caffeic-acid (2.0 g, 7.5 mmol, 1.0 eq) in $SOCl_2$ (10 mL), DMF (550 µL) and dry benzene (8 mL) was refluxed for 4 hours. The mixture was then concentrated *in vacuo*. The residue was re-dissolved in dry benzene (24 mL) before pyridine was added drop-wise followed by 3-azidopropan-1-ol (918.4 mg, 9.08 mmol, 1.2 eq). The reaction was allowed to stir for 12 hours at room temperature under an atmosphere of argon. The resulting mixture was concentrated *in vacuo* re-dissolved in DCM (10 mL) washed with water (3 × 10 mL), washed with brine (3 × 10 mL), dried over $MgSO_4$ and concentrated *in vacuo*.

The crude material was purified by column chromatography (EtOAc/petroleum ether 40:60) to give a yellow oil (1.88 g, 5.4 mmol, 72%). R_f 0.28 (EtOAc/petroleum ether 30:70). ^{1}H NMR (400 MHz, $CDCl_3$) δ 7.58 (d, J = 16.0 Hz, 1H), 7.36 (dd, J = 8.4, 1.9 Hz, 1H), 7.33 (d, J = 1.8 Hz, 1H), 7.17 (d, J = 8.3 Hz, 1H), 6.34 (d, J = 16.0 Hz, 1H), 4.23 (t, J = 6.2 Hz, 2H), 3.38 (t, J = 6.7 Hz, 2H), 2.25 (s, 3H), 2.24 (s, 3H), 1.96 – 1.88 (m, 2H). ^{13}C NMR (100 MHz, $CDCl_3$) δ 168.35, 168.25, 166.7, 143.9, 143.5, 142.8, 133.4, 126.7, 124.3, 123.1, 119.2, 61.9, 48.5, 28.5, 20.93, 20.89. FT-IR (Neat, υ_{max} cm^{-1}) 2096, 2933, 2864, 1770, 1710, 1639. HRMS *m/z* calculated for $C_{16}H_{18}N_3O_6$ $[M+H]^+$ 348.1190, found 348.1189

3-Azidopropyl 6-acetoxy-2,5,7,8-tetramethylchromane-2-carboxylate (7)

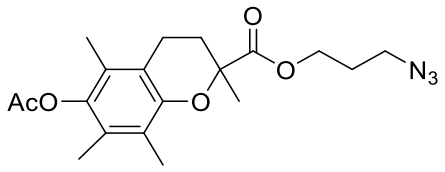

According to general esterification procedure method B, to a solution of 6-acetyl -2,5,7,8-tetramethylchromane-2-carboxylic acid (Acetyl-Trolox 1.00 g, 3.4 mmol, 1.0 eq.) in DCM (15 mL) DCC (701 mg, 3.4 mmol, 1.00 eq.) and DMAP (415 mg, 3.4 mmol, 1.0 eq.) were added. The mixture was allowed to stir for 10 minutes before 3-azidopropan-1-ol (356 mg, 3.4 mmol, 1.0 eq.) was added and the mixture was stirred at room temperature overnight under an atmosphere of argon. The resulting mixture was filtered, washed with a 10% solution of $KHSO_4$ three times, dried over $MgSO_4$ and the solvents removed *in vacuo* to afford the crude material.

The crude material was purified by column chromatography (EtOAc/petroleum ether 40:60). R_f 0.24 (EtOAc/petroleum ether 60:30) to give a colourless oil (1.0 g, 2.6 mmol, 78%). ^{1}H NMR (400 MHz, DMSO-d_6) δ 4.13 (m, 1H), 3.97–4.03 (m, 1H), 3.10–3.03 (m, 2H), 2.68 – 2.56 (m, 1H), 2.50 – 2.32 (m, 2H), 2.29 (s, 3H), 2.09 (s, 3H), 1.96 (s, 3H), 1.87 (s, 3H), 1.86-1.77 (m, 1H), 1.75 – 1.65 (m, 2H), 1.57 (s, 3H). ^{13}C NMR (100 MHz, DMSO-*d6*) δ 172.4, 168.8, 148.7, 140.9, 126.5, 124.9, 121.7, 117.0, 77.00, 61.8, 47.2, 29.9, 27.5, 25.1, 20.24, 20.20, 12.7, 11.8, 11.6. FT-IR (Neat, υ_{max} cm^{-1}) 2934, 2097, 1731, 1752. HRMS *m/z* calculated for $C_{19}H_{25}N_3O_5Na$ $[M+Na]^+$ 398.1705, found 398.1692

10.5.4. *Synthesis of Triazole Derivatives:*

To a stirred solution of azide analogues (1.0 eq.) and terminal alkyne derivatives (1.2 eq.) in a 1:1 ratio of H_2O–*tert*-BuOH (4 mL for each mmol of alkyne derivative) was added copper(I) iodide (0.1 eq.). The mixture was heated at 125 °C for one hour until the limiting starting material disappeared (TLC 80% EtOAc-petroleum ether 20%). The reaction was allowed to cool to room temperature before the addition of water followed by extracted with DCM (3 × 10 mL), the organics separated and dried over $MgSO_4$, concentrated and purified by column chromatography with the appropriate eluent system to afford the pure triazole derivatives.

(*E*)-4-(3-(2-(1-(3-Hydroxypropyl)-1H-1,2,3-triazol-4-yl)ethoxy)-3-oxoprop-1-en-1-yl)-1,2-phenylene diacetate (8a)

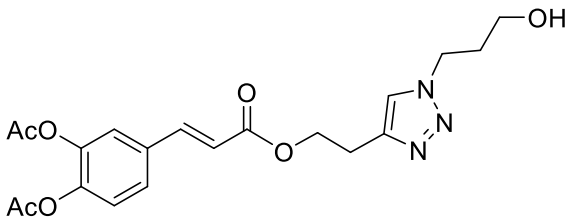

According to the general procedure for the copper catalysed 1,3 dipolar cycloaddition reaction, reported above, to 3-azidopropan-1-ol (286 mg, 2.83 mmol, 1.0 eq.) in (1:1) H_2O–*tert*-BuOH (7 mL) was added (*E*)-4-(3-(but-3-yn-1-yloxy)-3-oxoprop-1-en-1-yl)-1,2-phenylene diacetate (1.07 g, 3.4 mmol, 1.2 eq.). Then copper(I) iodide (54 mg, 0.283 mmol, 0.1 eq.) was added. The mixture was heated at 125 °C for one hour in a sealed tube. The reaction was then allowed to cool to room temperature than diluted with water, extracted with DCM (3 × 10 mL), dried over $MgSO_4$, concentrated and purified by column chromatography (EtOAc/petroleum ether 70:30) to give a yellow oil (0.87 g, 2.1 mmol, 74%). *Rf* 0.20 (EtOAc 100%). ^{1}H NMR (600 MHz, $CDCl_3$) δ 7.62 (d, *J* = 16.0 Hz, 1H), 7.45 (s, 1H), 7.40 (dd, *J* = 8.4, 1.8 Hz, 1H), 7.37 (d, *J* = 1.8 Hz, 1H), 7.23 (d, *J* = 8.4 Hz, 1H), 6.38 (d, *J* = 16.0 Hz, 1H), 4.52-4.48 (m, 4H), 3.64 (q, *J* = 5.6 Hz, 2H), 3.20 – 3.12 (m, 2H), 2.35 (s, 1H), 2.32 (s, 3H), 2.31 (s, 3H), 2.15 – 2.10 (m, 2H). ^{13}C NMR (150 MHz, $CDCl_3$) δ 168.3, 168.1, 166.5, 143.7, 143.3, 142.5, 133.3, 126.6, 124.1, 122.9, 122.3, 119.1, 63.5, 58.8, 47.0, 32.7, 31.1, 25.7, 20.77, 20.76. FT-IR (Neat, υ_{max} cm^{-1}) 2954 (br), 1771, 1710, 1638, 1505. HRMS *m/z* calculated for $C_{20}H_{24}O_7N_3$ $[M+H]^+$ 418.1609, found 418.1605.

(*E*)-4-(3-(4-(1-(3-Hydroxypropyl)-1H-1,2,3-triazol-4-yl)butoxy)-3-oxoprop-1-en-1-yl)-1,2-phenylene diacetate (8b)

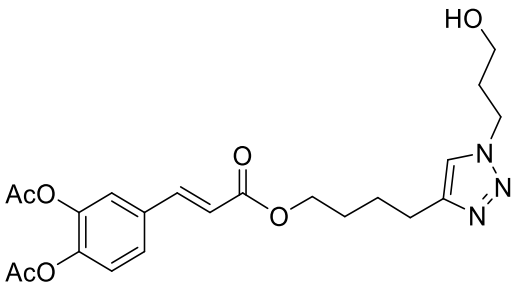

According to the general procedure for the copper catalysed 1,3 dipolar cycloaddition reaction, reported above, to 3-azidopropan-1-ol (25 mg, 0.25 mmol, 1.00 eq.) in (1:1) H_2O–*tert*-BuOH (2 mL) was added (*E*)-4-[3-(hex-5-yn-1-yloxy)-3-oxoprop-1-en-1-yl]-1,2-phenylene diacetate (106 mg, 0.3 mmol, 1.2 eq.). Copper(I) iodide (5 mg, 0.025 mmol, 0.1 eq.) was then added. The mixture was heated at 125 °C for one hour in a sealed tube. The reaction was then allowed to cool to room temperature before dilution with water. The reaction mixture was extracted with DCM (3 × 5 mL), dried over $MgSO_4$, and the volatiles removed *in vacuo* and the crude product purified by column chromatography (EtOAc/petroleum ether 70:30) to give a yellow oil (40%) *Rf* 0.22 (EtOAc 100%). ^{1}H NMR (400 MHz, $CDCl_3$) δ 7.59 (d, *J* = 16.0 Hz, 1H), 7.38 (d, *J* = 8.4 Hz, 1H), 7.35 (br, s, 2H), 7.20 (d, *J* = 8.3 Hz, 1H), 6.35 (d, *J* = 16.0 Hz, 1H), 4.46 (t, *J* = 6.7 Hz, 2H), 4.20 (t, *J* = 5.4 Hz, 2H), 3.61 (t, *J* = 5.6 Hz, 2H), 2.74 (t, *J* = 6.6 Hz, 2H), 2.29 (s, 3H), 2.28 (s, 3H), 2.10-2.07 (m, 2H), 1.82 – 1.71 (m, 4H). ^{13}C NMR (100 MHz, $CDCl_3$) δ 168.2, 168.1, 166.8, 147.7, 143.6, 142.9, 142.5, 133.4, 126.5, 124.0, 122.8, 121.4, 119.4, 64.5, 58.8, 46.9, 32.8, 28.3, 25.9, 25.3, 20.73, 20.70. FT-IR (Neat, υmax cm-1) 2948 (br), 1770, 1706, 1638, 1505 HRMS *m/z* calculated for $C_{22}H_{28}O_7N_3$ $[M+H]^+$ 446.1927, found 446.1927

(*E*)-4-(3-((5-(1-(3-Hydroxypropyl)-1H-1,2,3-triazol-4-yl)pentyl)oxy)-3-oxoprop-1-en-1-yl)-1,2-phenylene diacetate (8c)

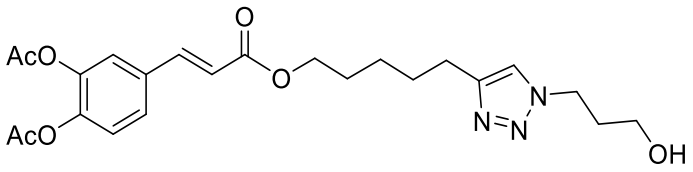

According to the general procedure for the copper catalysed 1,3 dipolar cycloaddition reaction, to 3-azidopropan-1-ol (141 mg, 1.4 mmol, 1.0 eq.) in (1:1) H_2O–*tert*-BuOH (12 mL) was added (*E*)-4-[3-(hept-6-yn-1-yloxy)-3-oxoprop-1-en-1-yl]-1,2-phenylene diacetate (600 mg, 1.7 mmol, 1.2 eq.). Copper(I) iodide (31 mg, 0.14 mmol, 0.1 eq.) was then added. The mixture was heated at 125 °C for one hour in a sealed tube. The reaction was then allowed to cool to room temperature before dilution with water. The reaction mixture was extracted with DCM (3 × 5 mL), dried over $MgSO_4$, and the volatiles removed *in vacuo* and the crude product purified by column chromatography (EtOAc/petroleum ether 70:30) to give a yellow oil (390 mg, 0.85 mmol, 61%). R_f 0.22 (EtOAc 100%). ^{1}H NMR (600 MHz, $CDCl_3$) δ 7.56 (d, *J* = 16.0 Hz, 1H), 7.36 (dd, *J* = 8.4, 1.9 Hz, 1H), 7.33 (d, *J* = 1.9 Hz, 1H), 7.31 (s, 1H), 7.18 (d, *J* = 8.4 Hz, 1H), 6.34 (d, *J* = 16.0 Hz, 1H), 4.41 (t, *J* = 6.9 Hz, 2H), 4.15 (t, *J* = 6.6 Hz, 2H), 3.57 (t, *J* = 5.8 Hz, 2H), 3.12 (s, 1H), 2.69 (t, *J* = 7.6 Hz, 2H), 2.26 (s, 3H), 2.25 (s, 3H), 2.07 – 2.01 (m, 2H), 1.73 – 1.63 (m, 4H), 1.47 – 1.37 (m, 2H). ^{13}C NMR (150 MHz, $CDCl_3$) δ 168.0, 167.9, 166.5, 147.7, 143.3, 142.6, 142.3, 133.1, 126.3, 123.8, 122.6, 121.1, 119.2, 64.4, 58.4, 46.7, 32.6, 28.8, 28.2, 25.4, 25.3, 20.48, 20.45. FT-IR (Neat, υ_{max} cm^{-1}) 2939, 2860, 1770, 1707, 1639, 1505. HRMS *m/z* calculated for $C_{23}H_{30}O_7N_3$ $[M+H]^+$ 460.2071, found 460.2084

(*E*)-4-(3-((8-(1-(3-Hydroxypropyl)-1H-1,2,3-triazol-4-yl)octyl)oxy)-3-oxoprop-1-en-1-yl)-1,2-phenylene diacetate (8d)

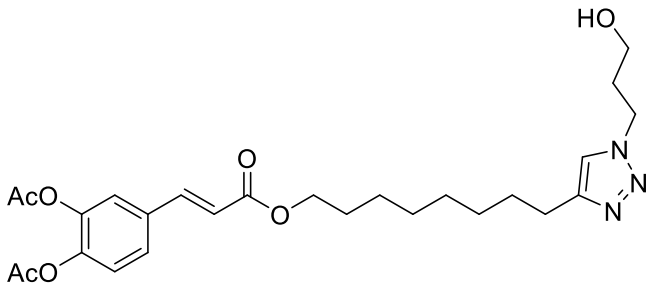

According to the general procedure for the copper catalysed 1,3 dipolar cycloaddition reaction, to 3-azidopropan-1-ol (41 mg, 0.42 mmol, 1.0 eq.) in (1:1) H_2O–*tert*-BuOH (3 mL) was added (*E*)-4-[3-(dec-9-yn-1-yloxy)-3-oxoprop-1-en-1-yl]-1,2-phenylene diacetate (200 mg, 0.5 mmol, 1.2 eq.). Copper(I) iodide (8 mg, 0.04 mmol, 0.1 eq.) was then added. The mixture was heated at 125 °C for one hour in a sealed tube. The reaction was then allowed to cool to room temperature before dilution with water. The reaction mixture was extracted with DCM (3 × 5 mL), dried over $MgSO_4$, and the volatiles removed *in vacuo* and the crude product purified by column chromatography (EtOAc/petroleum ether 70:30) to give a white solid (130 mg, 0.26 mmol, 62%) MP: 73 °C. Recrystallised from hexanes (100%). R_f 0.25 (EtOAc 100%). ^{1}H NMR (400 MHz, $CDCl_3$) δ 7.60 (d, *J* = 16.0 Hz, 1H), 7.40 (d, *J* = 8.4 Hz, 1H), 7.36 (s, 1H), 7.29 (s, 1H), 7.21 (d, *J* = 8.4 Hz, 1H), 6.38 (d, *J* = 16.0 Hz, 1H), 4.47 (t, *J* = 6.7 Hz, 2H), 4.18 (t, *J* = 6.6 Hz, 2H), 3.63 (t, *J* = 5.8 Hz, 2H), 2.70 (t, *J* = 7.6 Hz, 2H), 2.30 (s, 3H), 2.29 (s, 3H), 2.13-2.07 (m, 2H), 1.70-1.65 (m, 4H), 1.40-1.30 (m, 8H). ^{13}C NMR (100 MHz, $CDCl_3$) δ 168.0, 167.9, 166.6, 143.3, 142.5, 142.3, 133.3, 126.3, 123.8, 122.6, 120.9, 119.4, 77.14, 64.7, 58.8, 46.6, 32.6, 29.3, 29.1, 29.00, 28.99, 28.6, 25.8, 25.5, 20.6, 20.5. FT-IR (Neat, υ_{max} cm^{-1}) 3460, 2920, 2853, 1760, 1731, 1702, 1635, 1504. HRMS (ESI^+) calculated for $C_{26}H_{36}O_7N_3$ *m/z* 502.2567, found 502.2553 Elemental analysis calculated for $C_{26}H_{35}O_7N_3$ requires C 62.11%, H 7.00%, N 8.38% found C 62.12%, H 6.97%, N 8.30%.

(*E*)-4-(3-((2-(1-(3-Hydroxypropyl)-1H-1,2,3-triazol-4-yl)ethyl)amino)-3-oxoprop-1-en-1-yl)-1,2-phenylene diacetate (8e)

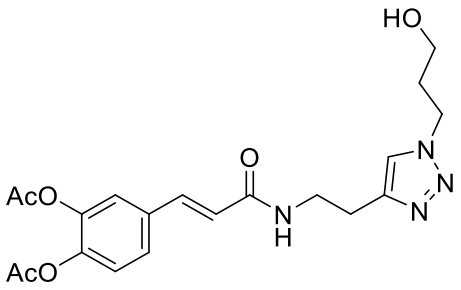

According to the general procedure for the copper catalysed 1,3 dipolar cycloaddition reaction, reported above, to 3-azido-1-propanol (32 mg, 0.32 mmol, 1.0 eq.) in (1:1) H_2O–*tert*-BuOH (4 mL) was added (*E*)-4-(3-(but-3-yn-1-ylamino)-3-oxoprop-1-en-1-yl)-1,2-phenylene diacetate (120 mg, 0.38 mmol, 1.2 eq.). Copper(I) iodide (6 mg, 0.03 mmol, 0.1 eq.) was added. The mixture was heated at 125 °C for one hour in a sealed tube. The reaction was then allowed to cool to room temperature before dilution with water. The reaction mixture was extracted with DCM (3 × 10 mL), dried over $MgSO_4$, and the volatiles removed *in vacuo* and the crude product purified by column chromatography (MeOH/DCM 5:95), recrystallised from EtOAc/ hexanes (20:80) to give a white solid (155 mg, 0.29 mmol, 76%). MP: 84°C. R_f 0.25 (MeOH/DCM 10:90). ^{1}H NMR (600 MHz, $CDCl_3$) δ 7.54 (d, J = 15.6 Hz, 1H), 7.45 (s, 1H), 7.37 (dd, J = 8.4, 2.0 Hz, 1H), 7.33 (d, J = 2.0 Hz, 1H), 7.21 (d, J = 8.2 Hz, 1H), 6.48 (m, 1H), 6.33 (d, J = 15.6 Hz, 1H), 4.51 (t, J = 6.7 Hz, 2H), 3.78-3.75 (m, 2H), 3.64-3.61 (m, 2H), 2.99 (t, J = 6.3 Hz, 2H), 2.32 (s, 3H), 2.31 (s, 3H), 2.19 (s, 1H), 2.16 – 2.10 (m, 2H), 1.97 (t, J = 4.9 Hz, 1H). ^{13}C NMR (150 MHz, $CDCl_3$) δ 168.18, 168.15, 165.7, 142.9, 142.31, 142.29, 139.0, 133.8, 126.2, 123.8, 122.3, 122.0, 58.6, 46.9, 38.8, 32.4, 29.7, 25.5, 20.64, 20.60. FT-IR (Neat, υ_{max} cm^{-1}) 3348, 3243, 3060, 2933, 2256, 1768, 1663.21, 1620, 1574, 1505. HRMS *m/z* calculated for $C_{20}H_{25}O_6N_4$ $[M+H]^+$ 417.1778, found 417.1774 . Elemental analysis calculated for $C_{20}H_{24}O_6N_4$ requires C 57.69%, 5.81%, N 13.45% found C 58.19 %, H 6.04%, N 10.25%.

2-(1-(3-Hydroxypropyl)-1H-1,2,3-triazol-4-yl)ethyl (*E*)-3-(3,4-difluorophenyl)acrylate (8f)

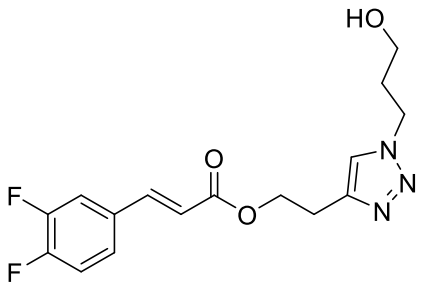

According to the general procedure for the copper catalysed 1,3 dipolar cycloaddition reaction, to 3-azido-1-propanol (178 mg, 1.8 mmol, 1.0 eq.) in (1:1) H_2O–*tert*-BuOH (12 mL) was added but-3-yn-1-yl (*E*)-3-(3,4-difluorophenyl) acrylate (500 mg, 2.11 mmol, 1.2 eq.). Copper(I) iodide (34 mg, 0.18 mmol, 0.1 eq.) was then added. The mixture was heated at 125 °C for one hour in a sealed tube. The reaction was then allowed to cool to room temperature before dilution with water. The reaction mixture was extracted with DCM (3 × 10 mL), dried over $MgSO_4$, and the volatiles removed *in vacuo* and the crude product purified by column chromatography (EtOAc/petroleum ether 70:30), recrystallised from petroleum ether to give a white solid (637 mg, 1.88 mmol, quantitative). MP: 82 °C. R_f 0.11 (EtOAc/petroleum ether 80:20). ^{1}H NMR (400 MHz, $CDCl_3$) δ 7.53 (d, *J* = 16.0 Hz, 1H), 7.47 (s, 1H), 7.34 – 7.27 (m, 1H), 7.20 (s, 1H), 7.16 – 7.06 (m, 1H), 6.30 (d, *J* = 16.0 Hz, 1H), 4.46 (dt, *J* = 13.2, 6.6 Hz, 4H), 3.62 (t, *J* = 5.5 Hz, 2H), 3.10 (t, *J* = 6.2 Hz, 2H), 2.14 – 2.01 (m, 2H). ^{13}C NMR (100 MHz, $CDCl_3$) δ 165.9 (s), δ 152.0 (dd, *J* = 96.8, 13.0 Hz), 149.5 (d, *J* = 79.7 Hz) 143.7 (s), 142.6 – 142.3 (m), 131.2 (dd, *J* = 6.0, 4.1 Hz), 124.5 (dd, *J* = 6.6, 3.5 Hz), 121.7 (s), 118.6 (d, J = 2.3 Hz), 117.5 (d, *J* = 17.8 Hz), 116.0 (d, *J* = 17.7 Hz), 63.2 (s), 58.6 (s), 46.7 (s), 32.4 (s), 25.4 (s). ^{19}F NMR (376 MHz, CDCl3) δ -62.75 (s), -133.92 (s), -133.98 (s), -136.52 (d, J = 20.9 Hz). FT-IR (Neat, υ_{max} cm-1) 3328, 3124, 3055, 2962, 2885, 1712, 1638, 1600, 1516. HRMS *m/z* calculated for $C_{16}H_{18}O_3N_3F_2$ $[M+H]^+$ 338.1316, found 338.1316. Elemental analysis calculated for $C_{16}H_{17}N_3O_3F_2$ requires C 56.97%, H 5.08%, N 12.46% found C 56.97%, H 5.19%, N 12.16%.

(*E*)-8-[1-(3-Hydroxypropyl)-1H-1,2,3-triazol-4-yl]octyl-3-(3,4-difluorophenyl)acrylate. (8g)

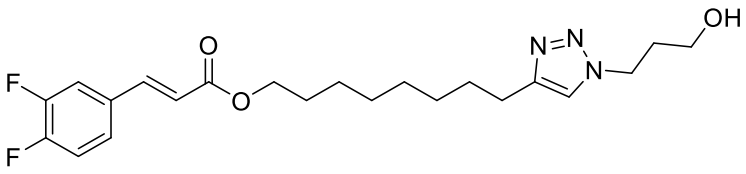

White solid (75%). MP 62 °C. Purified by crystallisation (EtOAc/hexane 10:90). R_f 0.4 (EtOAc/hexane 10:90). ^{1}H NMR (400 MHz, $CDCl_3$) δ 7.55 (d, *J* = 16.0 Hz, 1H), 7.36 – 7.32 (m overlapping s at 7.32 ppm, 1H), 7.32 (s, 1H), 7.25 – 7.20 (m, 1H), 7.16 (td, *J* = 9.7, 8.3 Hz, 1H), 6.34 (d, *J* = 16.1 Hz, 1H), 4.47 (t, *J* = 6.8 Hz, 2H), 4.17 (t, *J* = 6.7 Hz, 2H), 3.63 (t, *J* = 5.83 Hz, 1H), 2.69 (t, *J* = 7.7 Hz, 1H), 2.14 – 2.08 (m, 2H), 1.70 – 1.63 (m, 4H), 1.39 – 1.33 (m, 8H). ^{13}C NMR (150 MHz) δ 166.6, 151.8 (dd, *J* = 131.6, 13.0 Hz), 150.2 (dd, *J* = 127.9, 13.1 Hz), 142.2 (br s), 131.7 (dd, *J* = 5.9, 4.0 Hz), 124.8 (dd, *J* = 6.5, 3.5 Hz), 119.40, 119.39, 116.3, 117.8 (d, *J* = 17.7 Hz), 116.3 (d, *J* = 17.6 Hz), 64.8, 58.7, 46.8, 32.7, 29.4, 29.2, 29.1, 28.6, 25.9, 25.6. ^{19}F NMR (376 MHz, $CDCl_3$) -135.35 (d, *J* = 20.9 Hz), -137.71 (d, J = 20.8 Hz). FT-IR (Neat, υ_{max} cm^{-1}) 3337, 3063, 2920, 2853, 1714, 1516, 1272, 1179, 1044, 818. HRMS *m/z* calculated for $C_{22}H_{29}F_2N_3O_3$ $[M]^+$ 422.2177, found 422.2165. Elemental analysis calculated for $C_{22}H_{29}F_2N_3O_3$: C 62.69, H 6.94, N 9.97; found: C 61.89, H 6.83, 9.84.

(*E*)-4-(3-(3-(4-(2-Hydroxyethyl)-1H-1,2,3-triazol-1-yl)propoxy)-3-oxoprop-1-en-1-yl)-1,2-phenylene diacetate (8h)

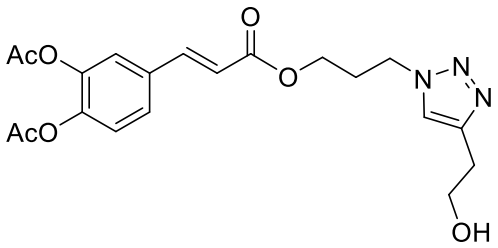

According to the general procedure for the copper catalysed 1,3 dipolar cycloaddition reaction, to (*E*)-4-(3-(3-azidopropoxy)-3-oxoprop-1-en-1-yl)-1,2-phenylene diacetate (1.0 g, 2.89 mmol, 1.0 eq.) in (1:1) H_2O–*tert*-BuOH (10 mL) was added 3-butyn-1-ol (242 mg, 3.5 mmol, 1.2 eq.). Copper(I) iodide (55 mg, 0.289 mmol, 0.1 eq.) was then added. The mixture was heated at 125 °C for one hour in a sealed tube. The reaction was then allowed to cool to room temperature before dilution with water. The reaction mixture was extracted with DCM (3 × 10 mL), dried over $MgSO_4$, and the volatiles removed *in vacuo* and the crude product purified by column chromatography (EtOAc 100%) to give a white solid (554 mg, 1.3 mmol, 46%). MP: 78 °C. R_f 0.14 (EtOAc 100%). Recrystallised from EtOAc (100%). ^{1}H NMR (400 MHz, $CDCl_3$) δ 7.60 (d, *J* = 16.0 Hz, 1H), 7.44 (s, 1H), 7.40 (dd, *J* = 8.5, 1.9 Hz, 1H), 7.37 (d, *J* = 1.7 Hz, 1H), 7.22 (d, *J* = 8.3 Hz, 1H), 6.35 (d, *J* = 16.0 Hz, 1H), 4.46 (t, *J* = 6.9 Hz, 2H), 4.23 (t, *J* = 5.9 Hz, 2H), 3.92 (t, *J* = 5.8 Hz, 2H), 2.93 (t, *J* = 5.9 Hz, 2H), 2.34-2.31 (m, overlapping s, 2H), 2.30 (s, 3H), 2.29 (s, 3H). ^{13}C NMR (100 MHz, $CDCl_3$) δ 168.2, 168.1, 166.5, 143.8, 143.6, 142.6, 133.1, 126.61, 126.60, 124.1, 122.9, 122.1, 118.7, 61.7, 61.3, 47.3, 29.6, 28.8, 20.8, 20.7. FT-IR (Neat, υ_{max} cm^{-1}) 2933, 2099, 1770, 1710, 1639, 1505. HRMS m/z calculated for $C_{20}H_{23}O_6N_3$ $[M+H]^+$ 359.1501, found 4359.1495.

4-((*E*)-3-(3-(4-(2-(((*E*)-3-(3,4-Diacetoxyphenyl)acryloyl)oxy)ethyl)-1H-1,2,3-triazol-1-yl)propoxy)-3-oxoprop-1-en-1-yl)-1,2-phenylene diacetate (9)

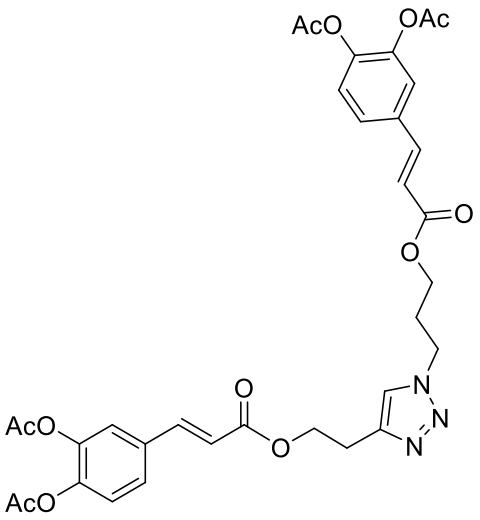

According to the general procedure for the copper catalysed 1,3 dipolar cycloaddition reaction, to (*E*)-4-(3-(3-azidopropoxy)-3-oxoprop-1-en-1-yl)-1,2-phenylene diacetate (347 mg, 0.6 mmol, 1.0 eq.) in (1:1) H_2O–*tert*-BuOH (8 mL) was added (*E*)-4-(3-(but-3-yn-1-yloxy)-3-oxoprop-1-en-1-yl)-1,2-phenylene diacetate (380 mg, 0.72 mmol, 1.2 eq.). Copper (I) iodide (19 mg, 0.06 mmol, 0.1 eq.) was then added. The mixture was heated at 125 °C for one hour in a sealed tube. The reaction was then allowed to cool to room temperature than before dilution with water. The reaction mixture was extracted with DCM (3 × 10 mL), dried over $MgSO_4$, and the volatiles removed *in vacuo* and the crude product purified by column chromatography (EtOAc 100%) and recrystallised from EtOAc/hexanes (20:80) to give a white solid (155 mg, 0.23 mmol, 40%). MP: 125 °C. R_f 0.27 (EtOAc/petroleum ether 80:20). ^{1}H NMR (400 MHz, $CDCl_3$) δ 7.61 (dd, *J* = 16.0, 2.3 Hz, 2H), 7.43 (s, 1H), 7.40 (dd, *J* = 8.4, 2.2 Hz, 2H), 7.37 (s, 2H), 7.23 (d, *J* = 8.4 Hz, 1H), 7.21 (d, *J* = 8.5, 1H), 6.40-6.34 (m, 2H), 4.50-4.47 (m, 4H), 4.25 (t, *J* = 5.9 Hz, 2H), 3.20 – 3.10 (m, 2H), 2.37 – 2.33 (m, 2H), 2.31 (s, 3H), 2.30 (s, 3H), 2.29 (s, 3H), 2.29 (s, 3H). ^{13}C NMR (100 MHz, $CDCl_3$) δ 168.20, 168.16, 168.08, 168.06, 166.5, 166.4, 144.4, 143.8, 143.7, 143.6, 143.3, 142.62, 142.59, 133.3, 133.2, 126.6, 124.1, 124.07, 122.95, 122.89, 121.96, 119.1, 118.7, 63.5, 61.3, 47.3, 29.7, 25.74, 25.66, 20.78, 20.77, 20.74, 20.73. FT-IR (Neat, υ_{max} cm^{-1}) 2962, 1768, 1708, 1638, 1504. HRMS *m/z* calculated for $C_{33}H_{34}O_{12}N_3$ $[M+H]^+$ 664.2137, found 664.2130 Elemental analysis calculated for $C_{33}H_{33}O_{12}N_3$ requires C 59.73%, H 5.01%, N 6.33% found C 59.06%, H 4.97%, N 6.02%.

(*E*)-4-(3-(2-(1-(3-((6-Acetoxy-2,5,7,8-tetramethylchromane-2-carbonyl)oxy)propyl)-1H-1,2,3-triazol-4-yl)ethoxy)-3-oxoprop-1-en-1-yl)-1,2-phenylene diacetate (10)

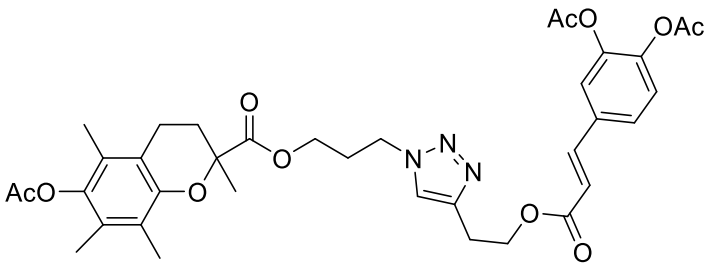

According to the general procedure for the copper catalysed 1,3 dipolar cycloaddition reaction, to 3-azidopropyl 6-acetoxy-2,5,7,8-tetramethylchromane-2-carboxylate (500 mg, 1.3 mmol, 1.0 eq.) in H_2O–*tert*-ButOH (10 mL) was added (*E*)-4-(3-(but-3-yn-1-yloxy)-3-oxoprop-1-en-1-yl)-1,2-phenylene diacetate (506 mg, 1.6 mmol, 1.2 eq.). Copper(I) iodide (25 mg, 0.13 mmol, 0.1 eq.) was then added. The mixture was heated at 125 °C for one hour in a sealed tube. The reaction was then allowed to cool to room temperature before dilution with water. The reaction mixture was extracted with DCM (3 × 10 mL), dried over $MgSO_4$, and the volatiles removed *in vacuo* and the crude product purified by column chromatography (EtOAc/petroleum ether 20:80) to give a white solid (3274 mg, 0.4 mmol 30%).MP: 56-60 °C. R_f 0.44 (EtOAc/petroleum ether 30:70). Recrystallised hexanes (100%). ^{1}H NMR (600 MHz, DMSO) δ 7.75 (s, 1H), 7.69-7.65 (m, 1H), 7.64 (d, *J* = 15.5 Hz, 2H), 7.31 (d, *J* = 8.3 Hz, 1H), 6.63 (d, *J* = 16.0 Hz, 1H), 4.38 (t, *J* = 6.2 Hz, 2H), 4.22 – 4.07 (m, 2H), 4.04 – 3.88 (m, 2H), 3.02 (t, *J* = 6.1 Hz, 2H), 2.67 – 2.33 (m, 4H), 2.28 (d, *J* = 3.6 Hz, 8H), 2.09 (s, 3H), 2.04 (s, 2H) 1.93 (s, 3H), 1.86 (s, 3H), 1.85 – 1.76 (m, 2H), 1.55 (s, 3H). ^{13}C NMR (150 MHz, DMSO) δ 173.0, 169.5, 168.6, 168.5, 166.4, 149.3, 144.0, 143.6, 143.4, 142.8, 141.4, 133.3, 127.4, 127.1, 125.5, 124.6, 123.6, 123.0, 122.2, 119.4, 117.7, 77.5, 63.6, 62.2, 46.3, 30.3, 29.2, 25.5, 25.4, 20.8, 20.73, 20.68, 20.64, 13.2, 12.3, 12.1. FT-IR (Neat, υ_{max} cm^{-1}) 2935, 1749, 1712, 1638, 1505. HRMS *m/z* calculated for $C_{36}H_{42}O_{11}N_3$ $[M+H]^+$ 692.2814, found 692.2823 Elemental analysis calculated for $C_{36}H_{41}N_3O_{11}$ requires C 62.51%, H 5.97%, N 6.07 % found C 61.76%, H 5.90%, N 5.92.

11. Spectral Data for Synthesised Compounds

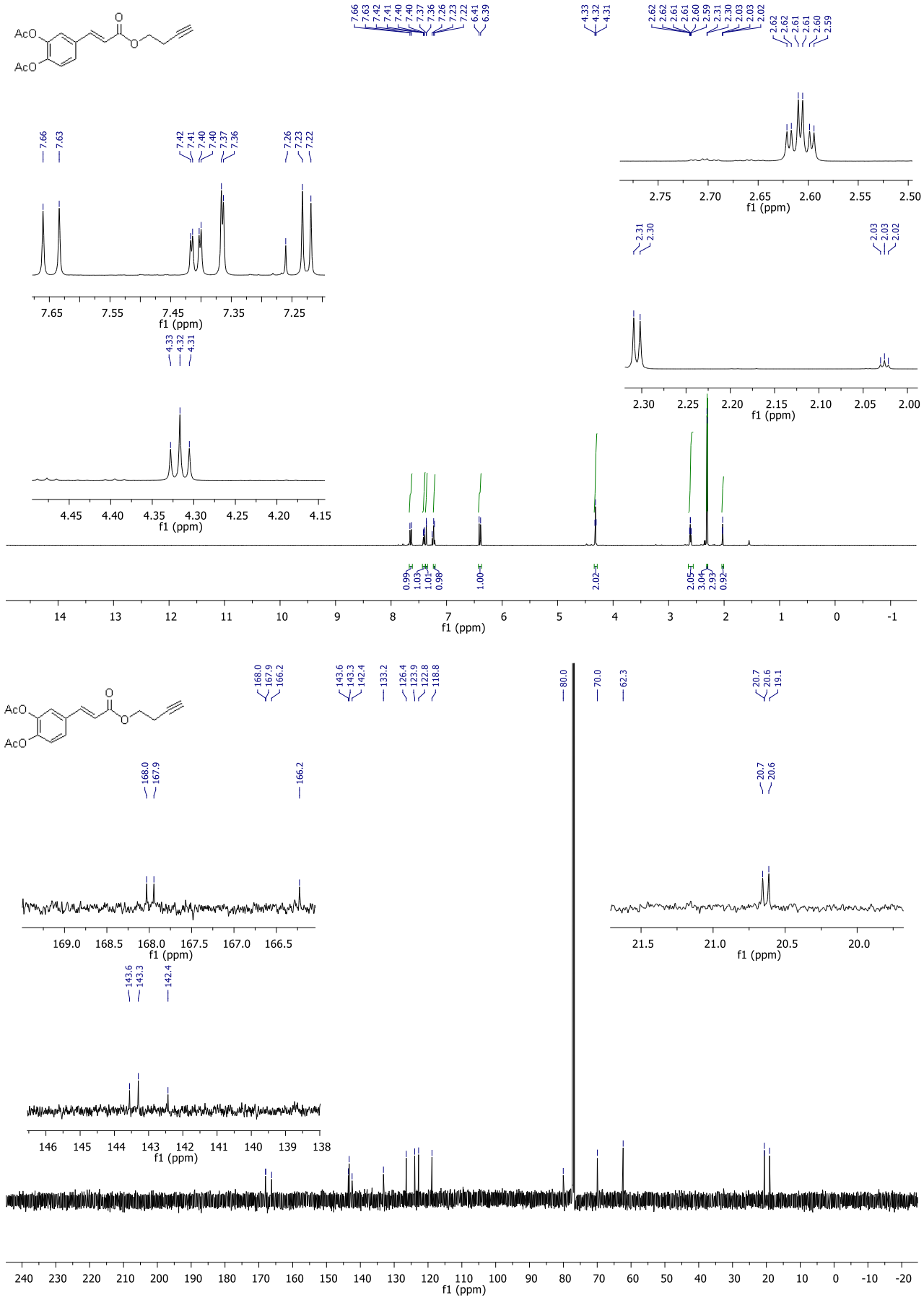

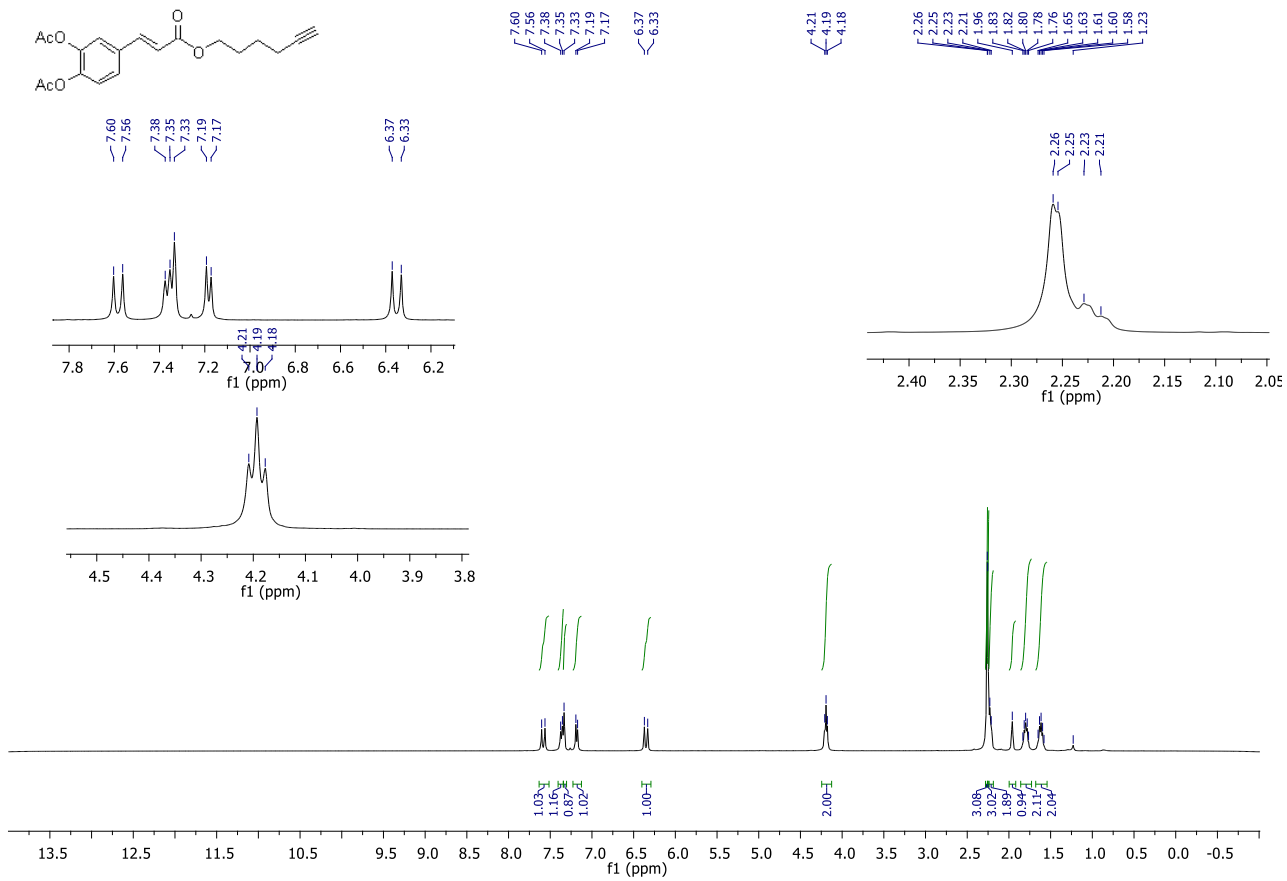
AcO
AcO
O
O
7.60
7.56
7.38
7.35
7.33
7.19
7.17
6.37
6.33
4.21
4.19
4.18
2.26
2.25
2.23
2.21
1.96
1.83
1.82
1.80
1.78
1.76
1.65
1.63
1.61
1.60
1.58
1.23
f1 (ppm)
1.03
1.15
0.87
1.02
1.00
2.00
3.08
3.02
1.89
0.94
2.11
2.04

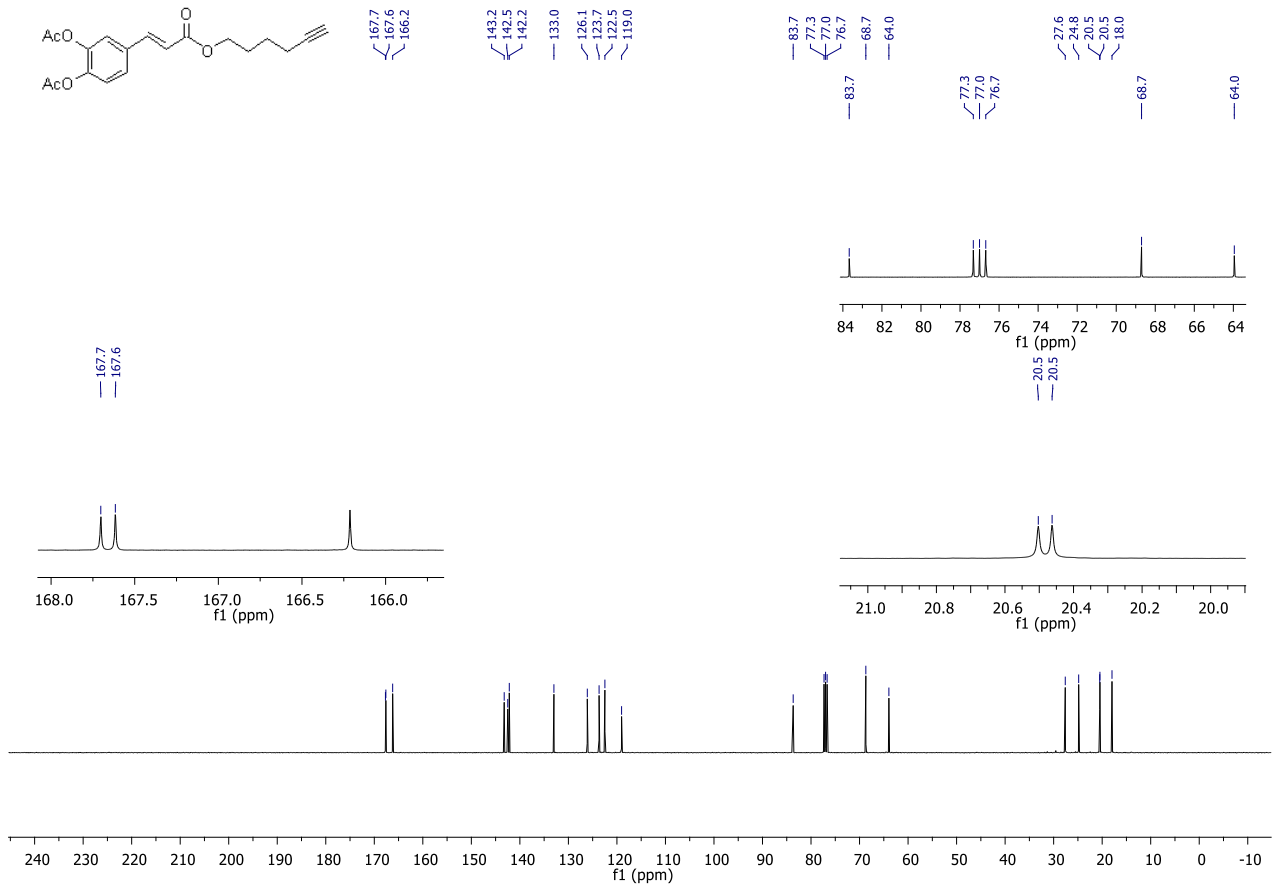
AcO
AcO
O
O
167.7
167.6
166.2
143.2
142.5
142.2
133.0
126.1
123.7
122.5
119.0
83.7
77.3
77.0
76.7
68.7
64.0
27.6
24.8
20.5
20.5
18.0
f1 (ppm)

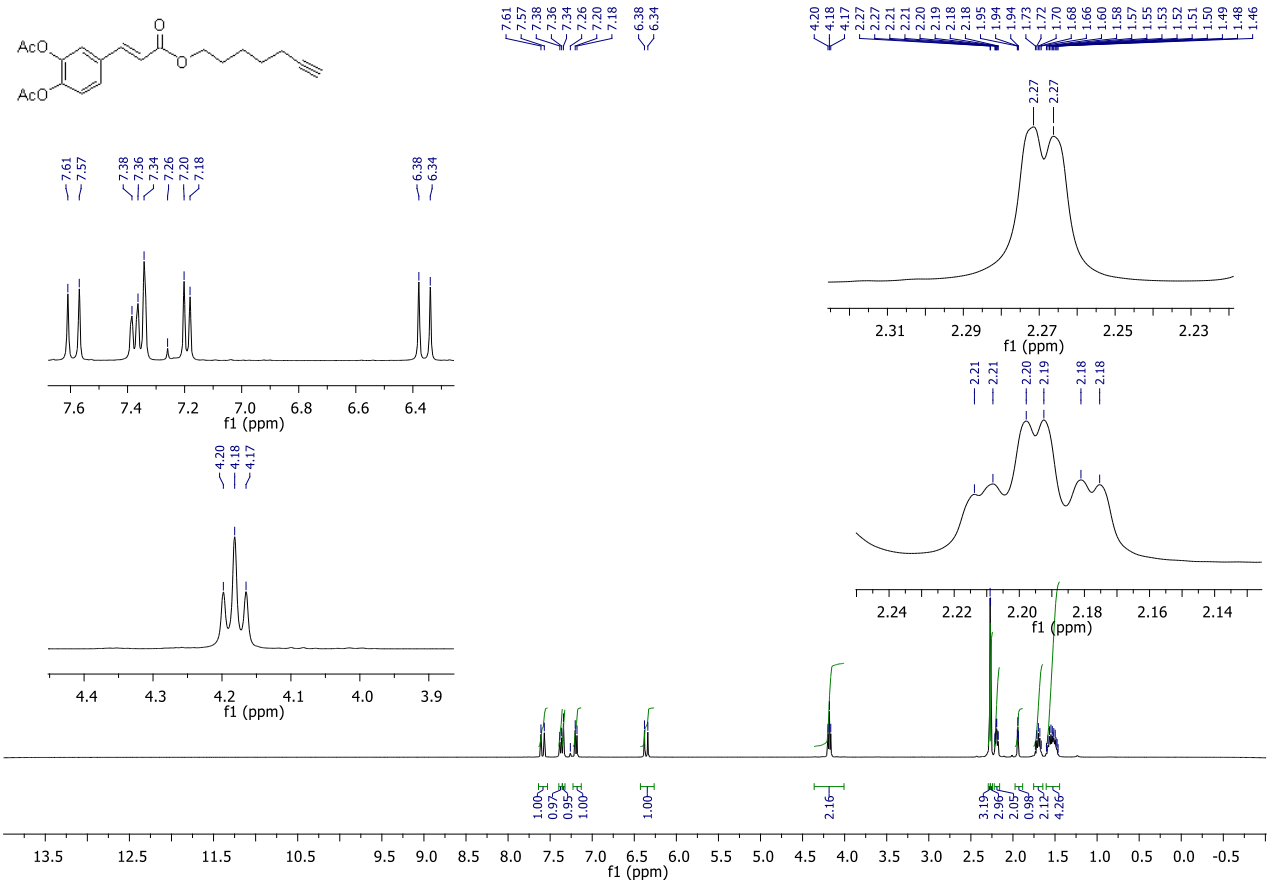
AcO
AcO
O
O
f1 (ppm)

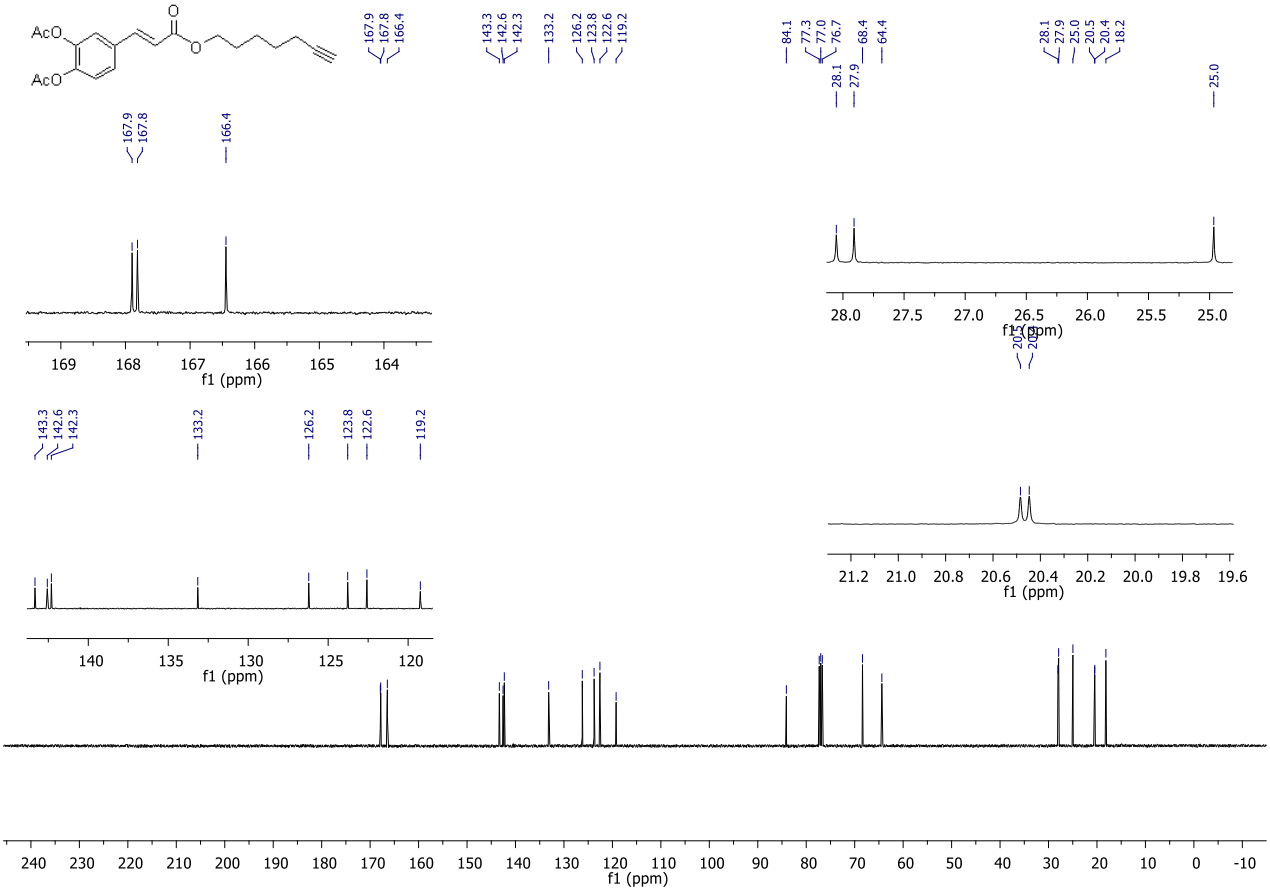
AcO
AcO
O
O
f1 (ppm)

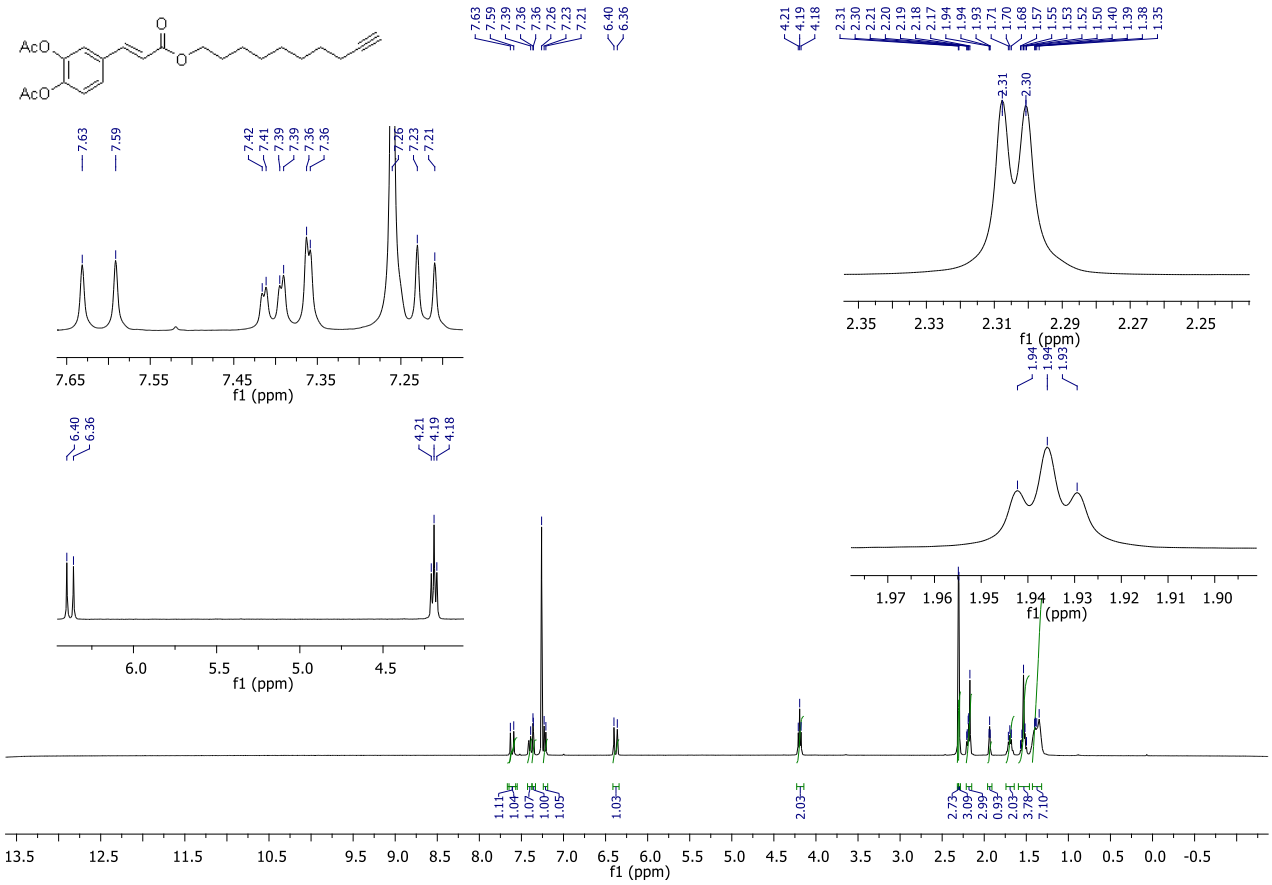
AcO
AcO
O
O
7.63
7.59
7.42
7.41
7.39
7.39
7.36
7.36
7.26
7.23
7.21
6.40
6.36
4.21
4.19
4.18
2.31
2.30
2.31
2.30
1.94
1.94
1.93
f1 (ppm)

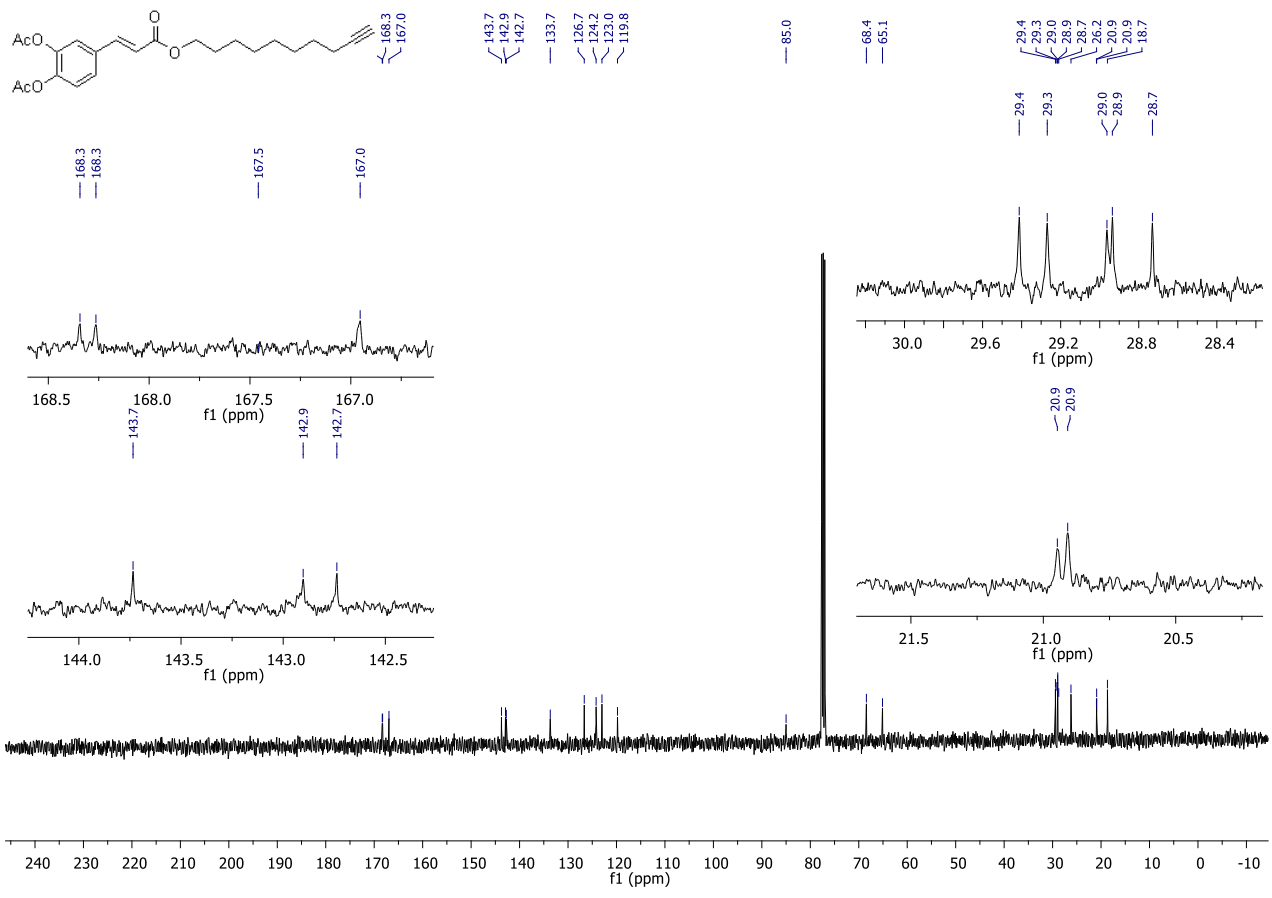
AcO
AcO
O
O
168.3
167.0
143.7
142.9
142.7
133.7
126.7
124.2
123.0
119.8
85.0
68.4
65.1
29.4
29.3
29.0
28.9
28.7
26.2
20.9
20.9
18.7
f1 (ppm)

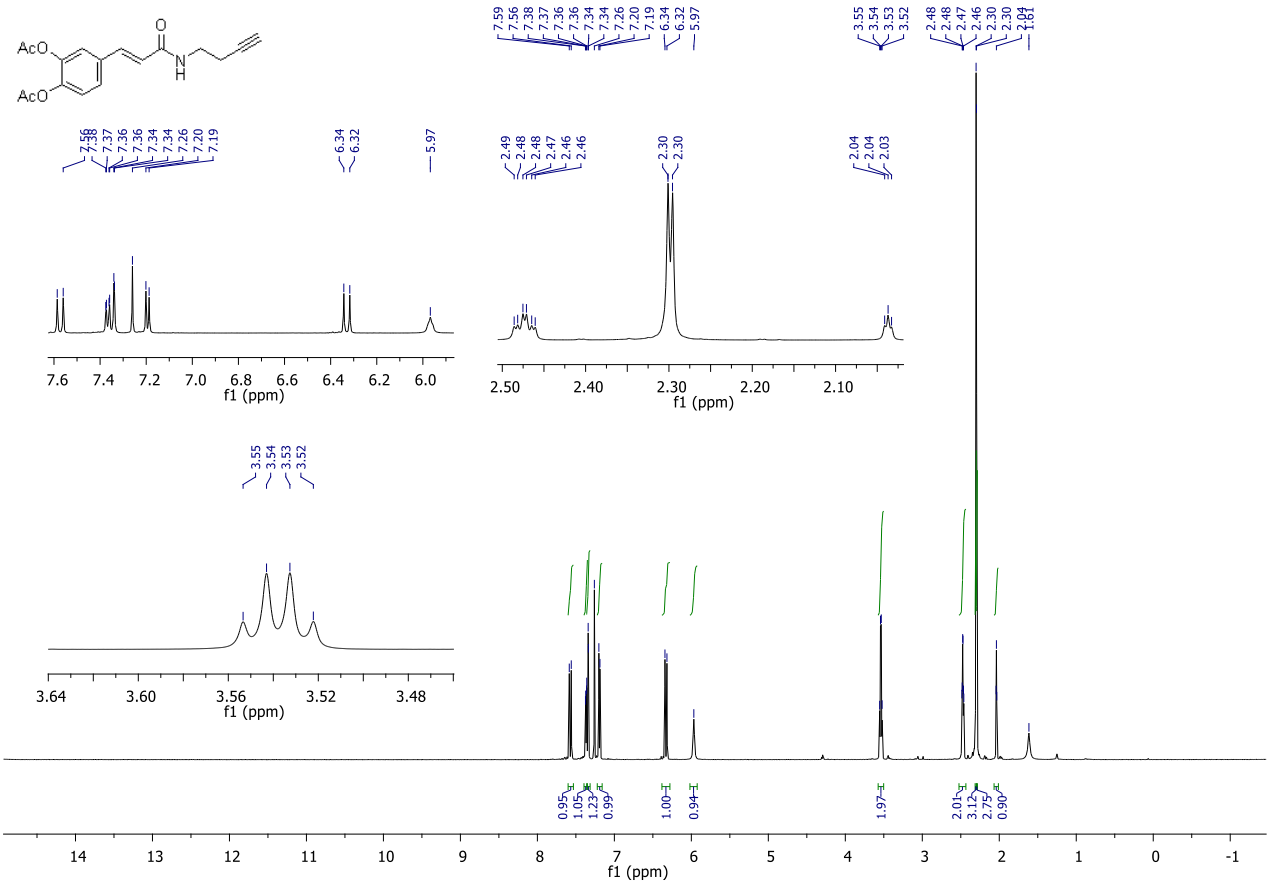
AcO
AcO
O
N
H
f1 (ppm)

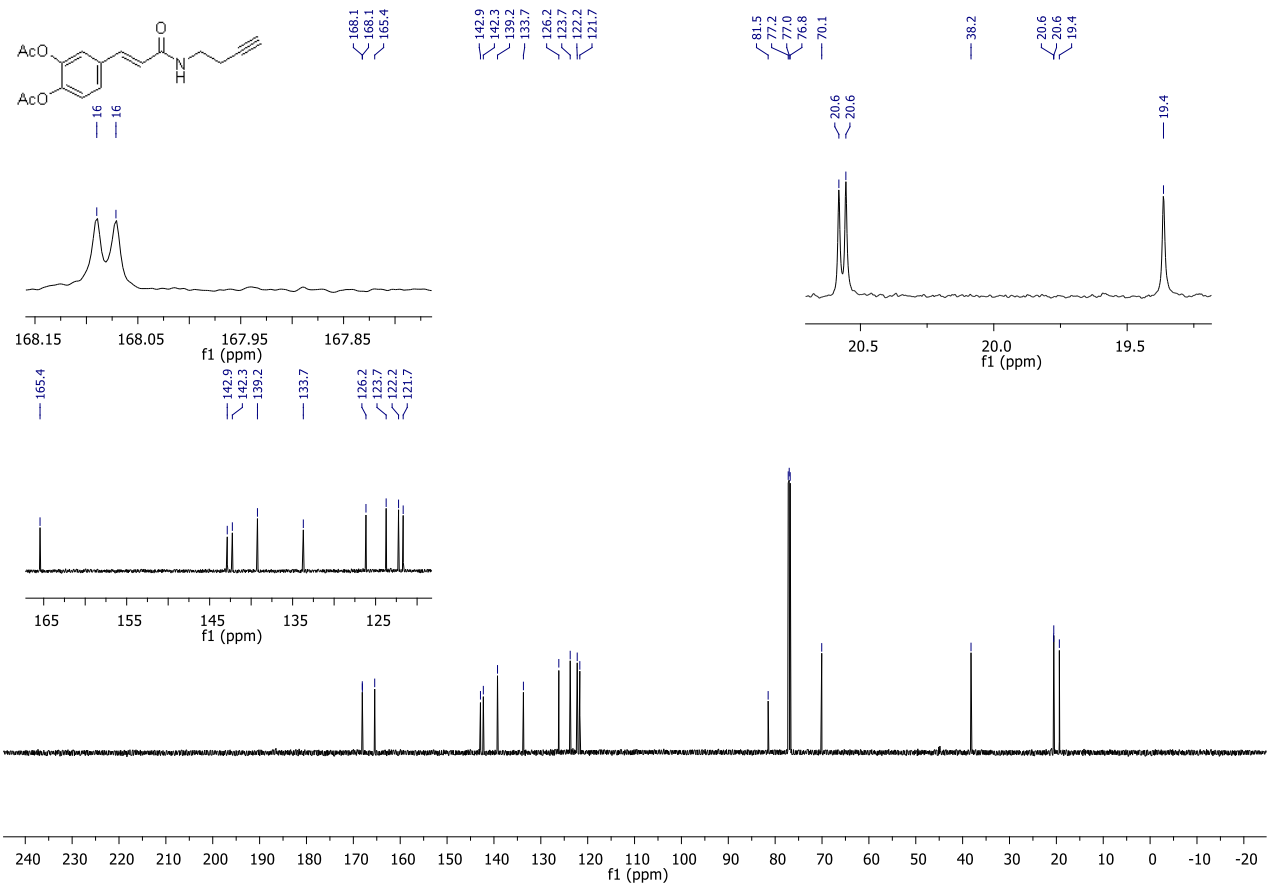
AcO
AcO
O
N
H
f1 (ppm)

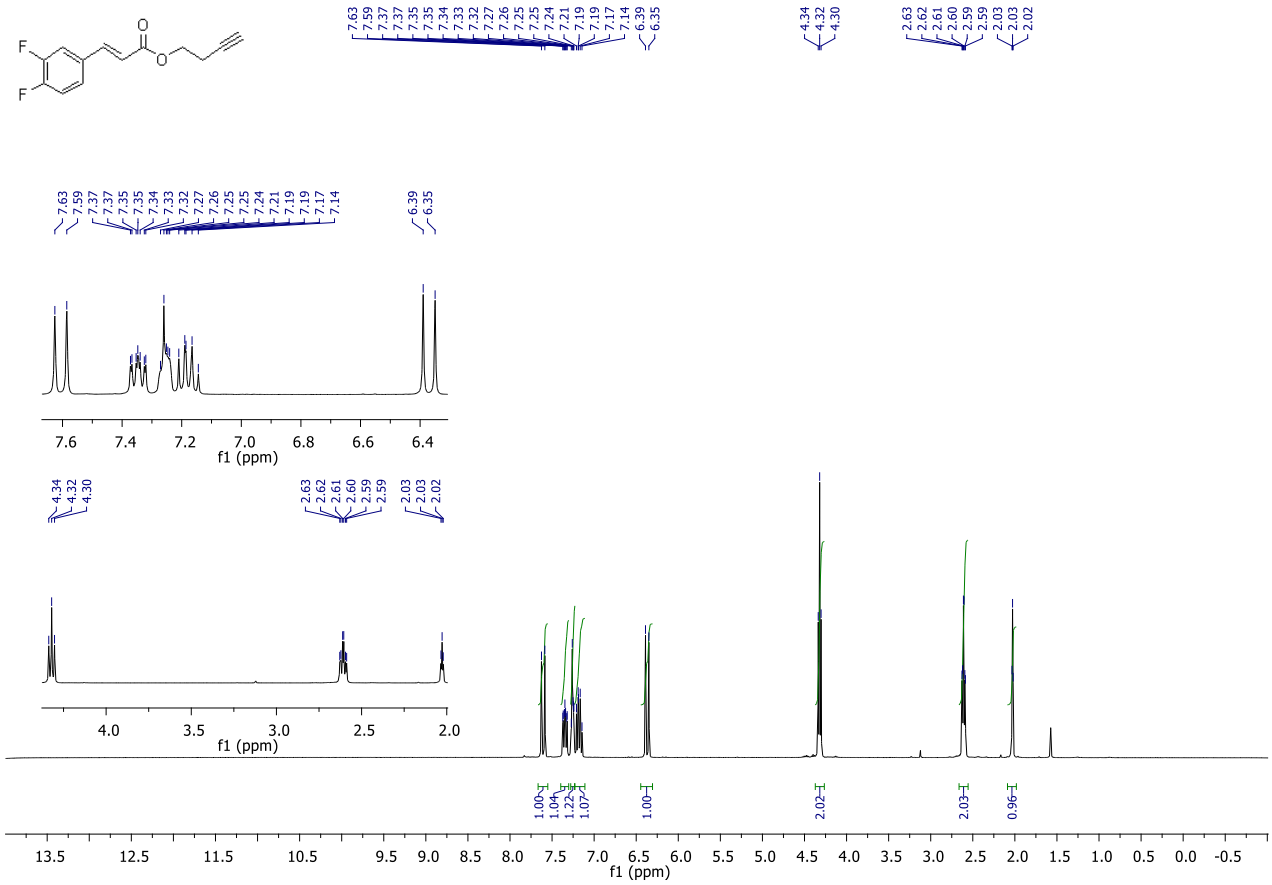
F
F
O
O
f1 (ppm)

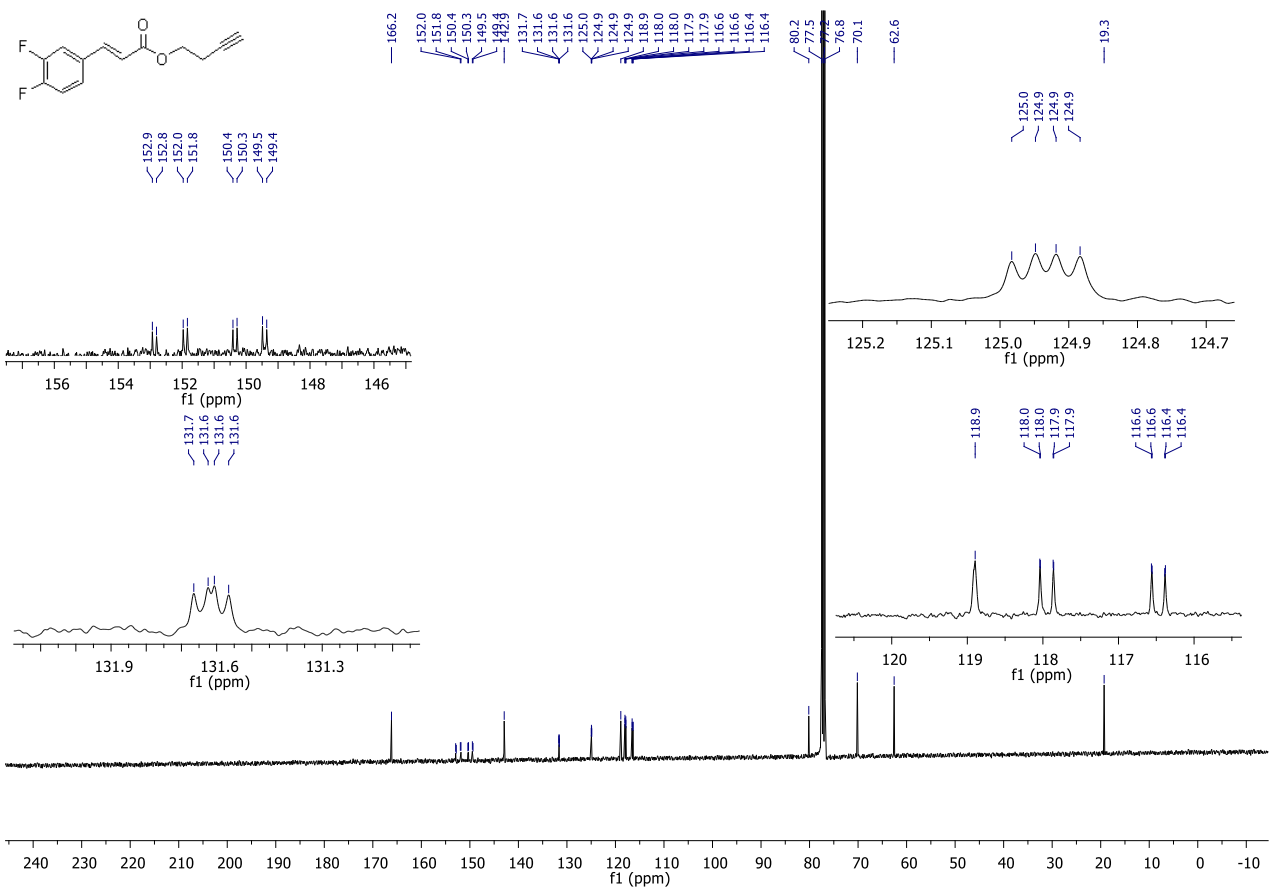
F
F
O
O
f1 (ppm)

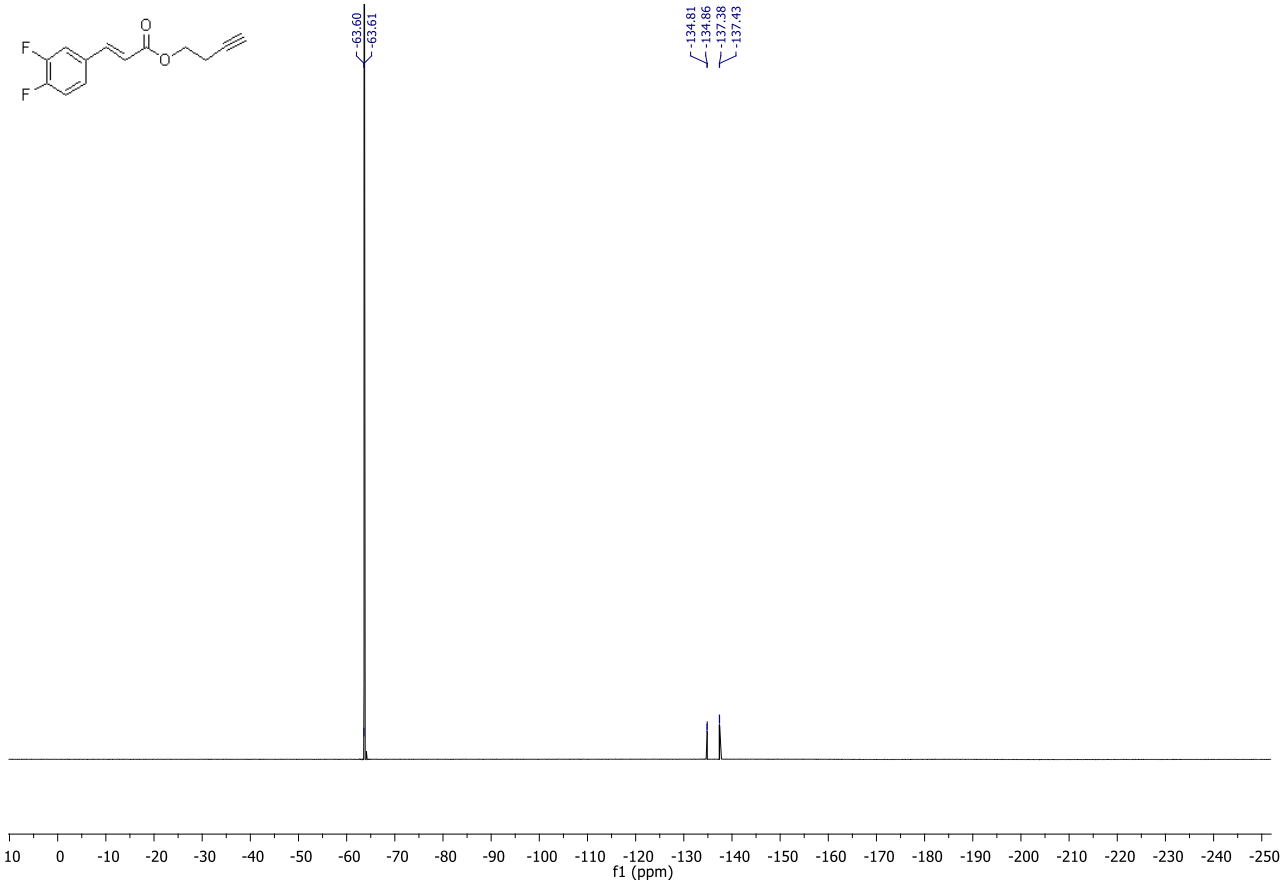
-63.60
-63.61
-134.81
-134.86
-137.38
-137.43
f1 (ppm)

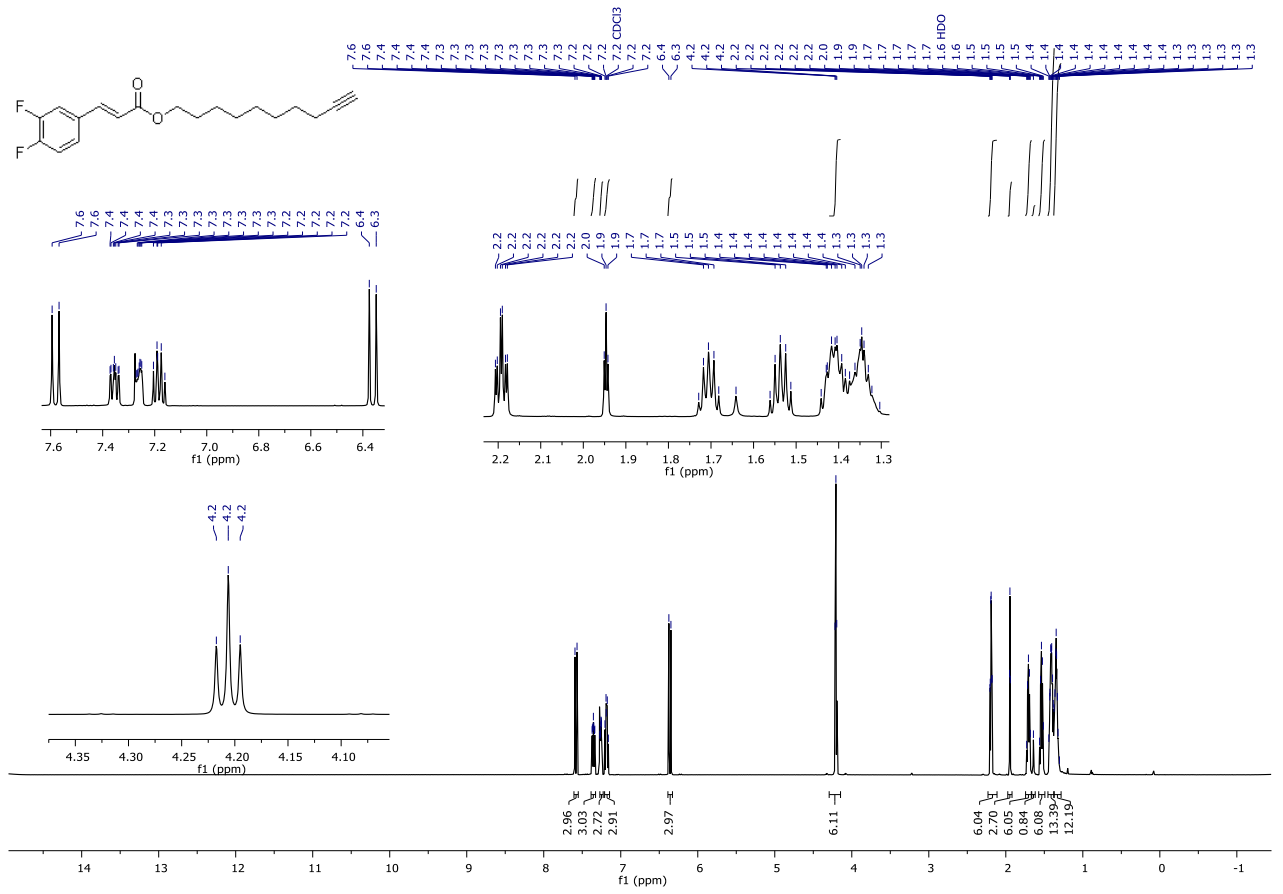
CDCl3
HDO
f1 (ppm)

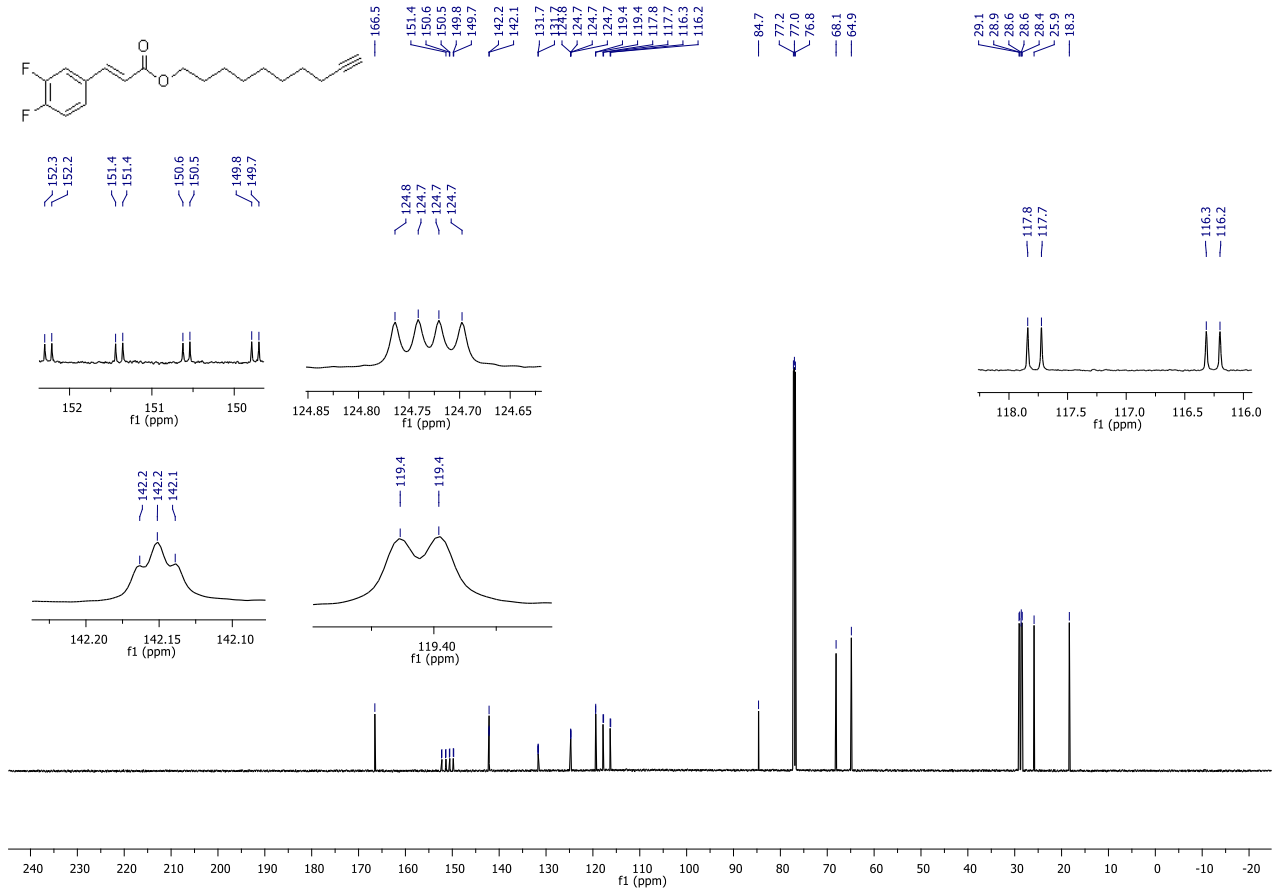
F
F
O
O
166.5
151.4
150.6
150.5
149.8
149.7
142.2
142.1
131.7
131.6
124.8
124.7
124.7
124.7
119.4
119.4
117.8
117.7
116.3
116.2
84.7
77.2
77.0
76.8
68.1
64.9
29.1
28.9
28.6
28.6
28.4
25.9
18.3
152.3
152.2
151.4
151.4
150.6
150.5
149.8
149.7
124.8
124.7
124.7
124.7
117.8
117.7
116.3
116.2
142.2
142.2
142.1
119.4
119.4
f1 (ppm)

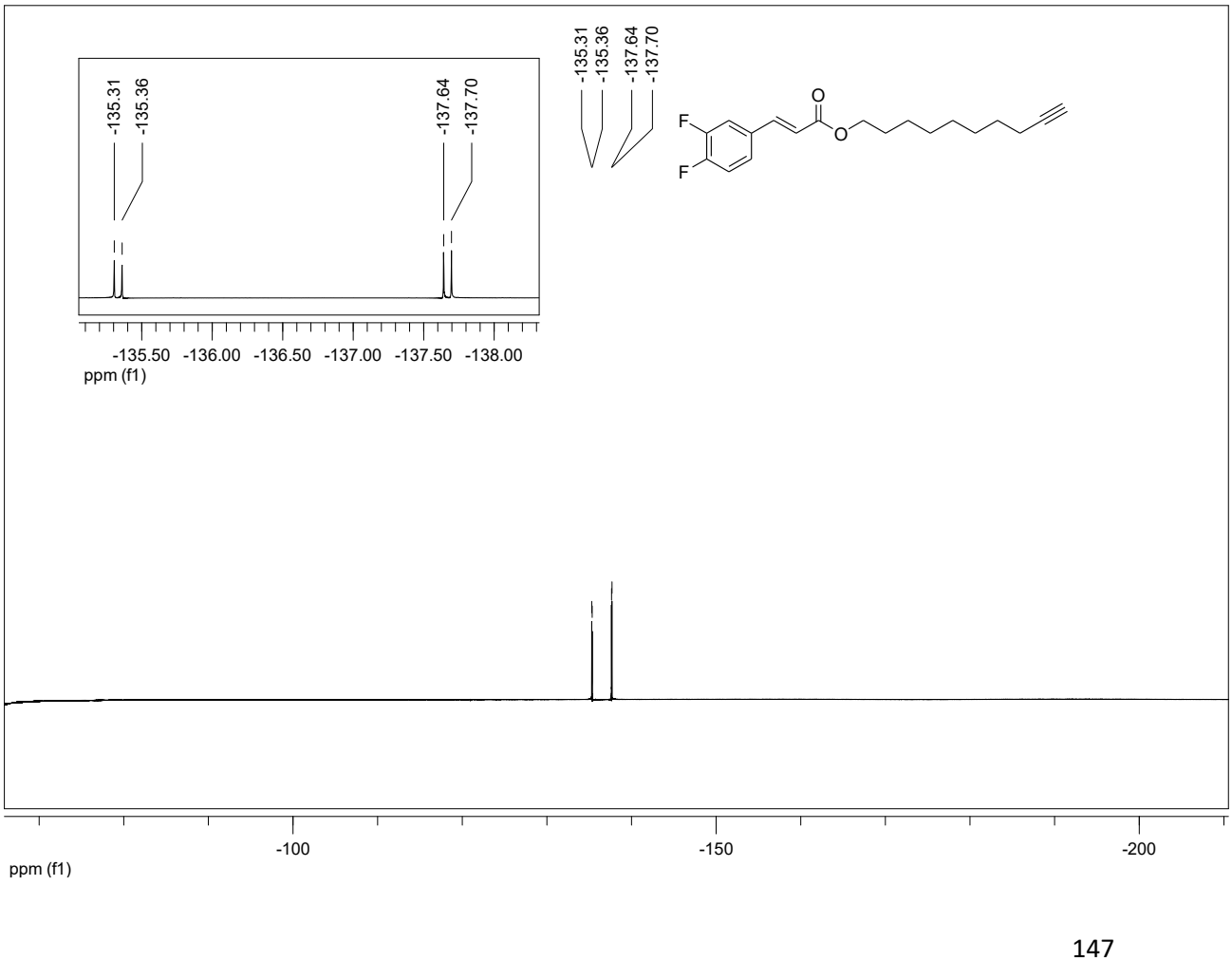
-135.31
-135.36
-137.64
-137.70
-135.50
-136.00
-136.50
-137.00
-137.50
-138.00
ppm (f1)
F
F
O
O
-100
-150
-200
ppm (f1)

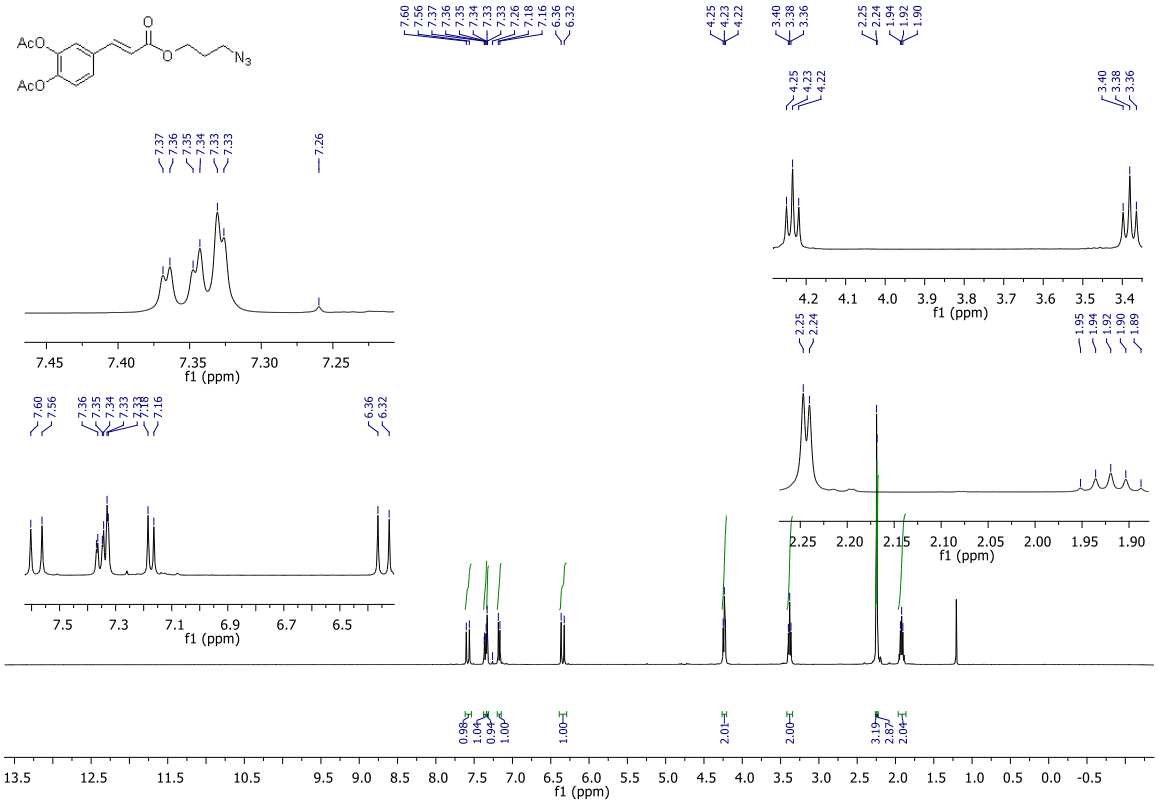
AcO
AcO
O
O
N3
f1 (ppm)

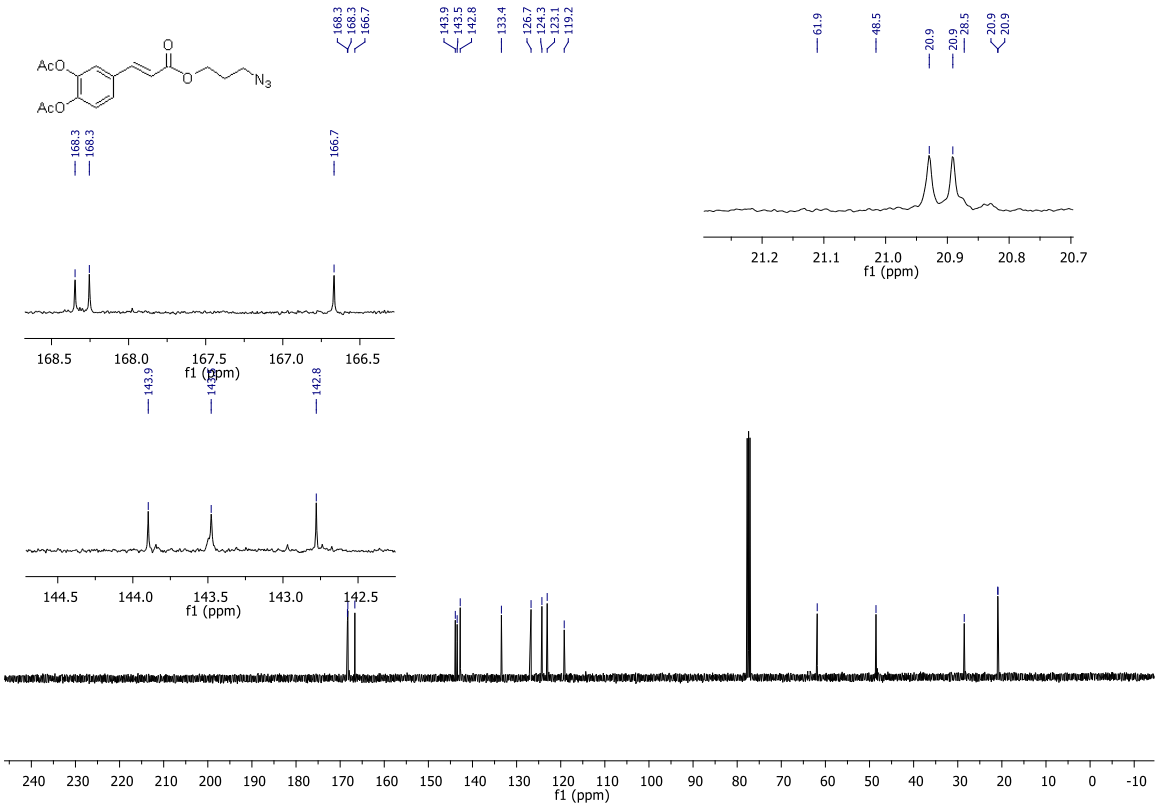
AcO
AcO
O
O
N3
f1 (ppm)

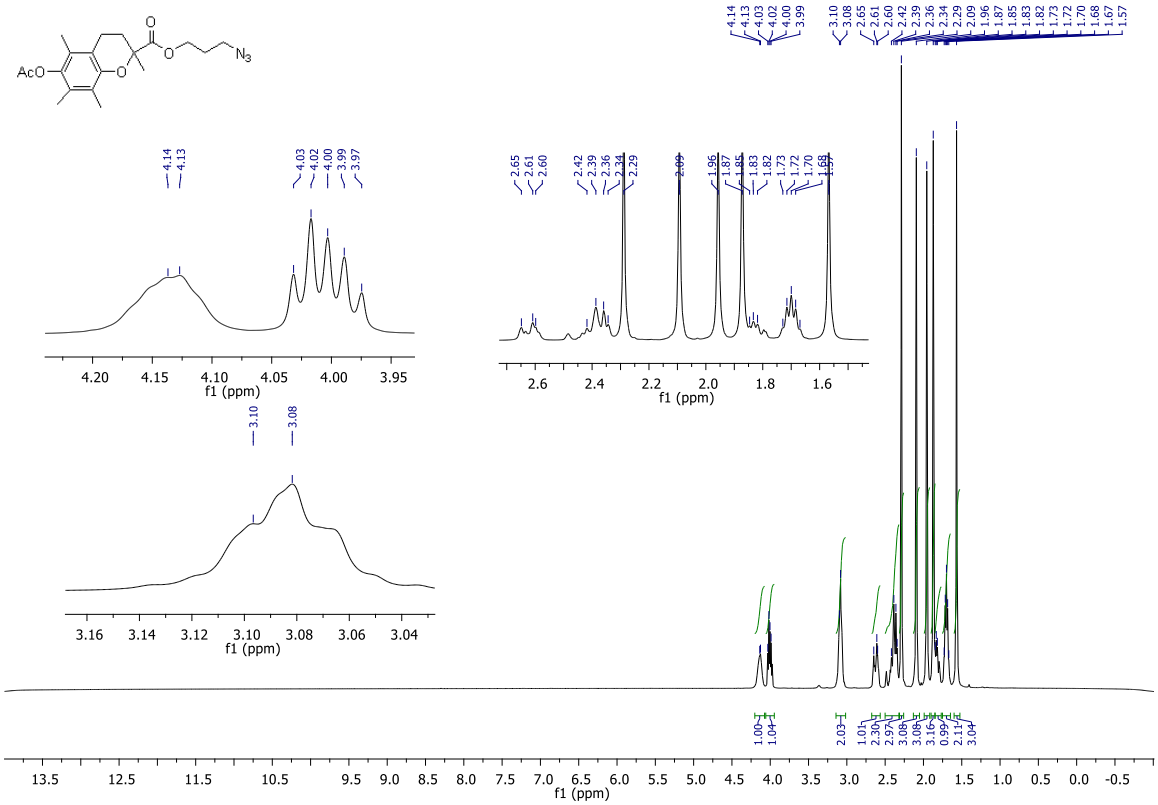
AcO
O
O
O
N3
4.14
4.13
4.03
4.02
4.00
3.99
3.97
2.65
2.61
2.60
2.42
2.39
2.36
2.34
2.29
2.09
1.96
1.87
1.85
1.83
1.82
1.73
1.72
1.70
1.68
3.10
3.08
f1 (ppm)

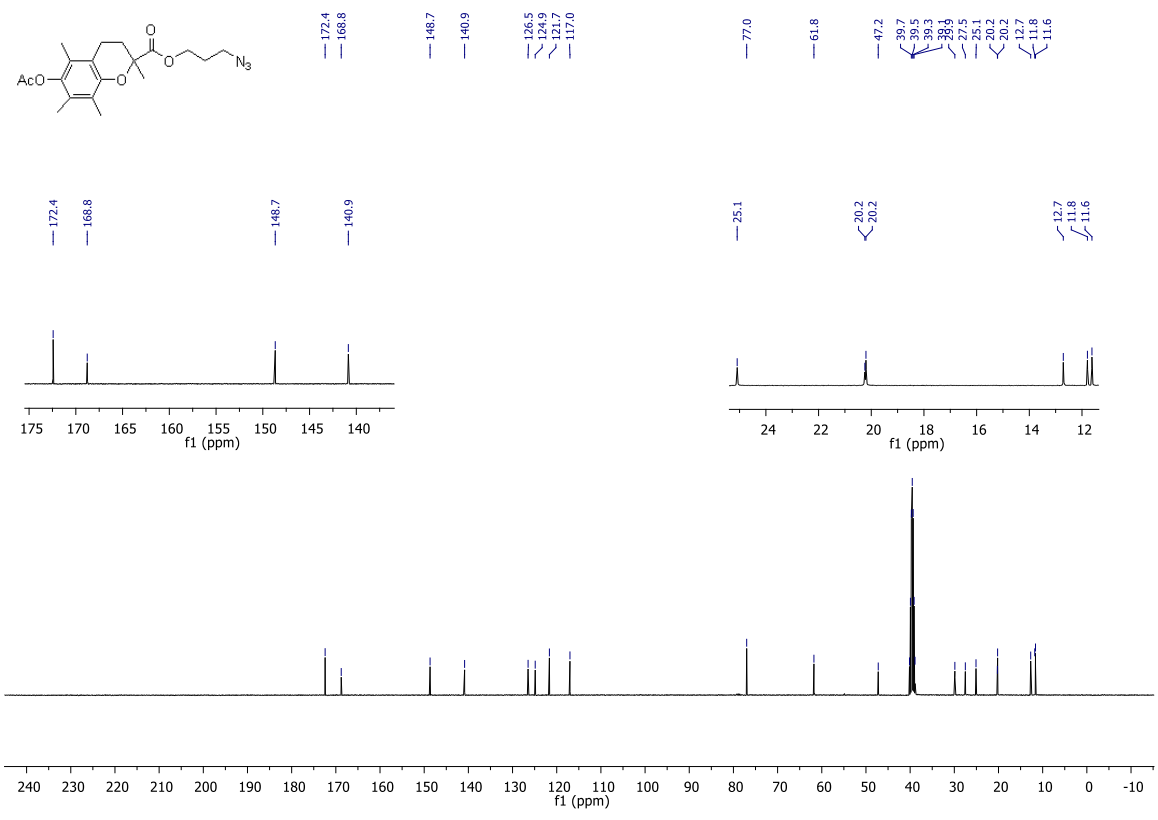
AcO
O
O
O
N3
172.4
168.8
148.7
140.9
126.5
124.9
121.7
117.0
77.0
61.8
47.2
39.7
39.5
39.3
39.1
38.9
27.5
25.1
20.2
20.2
12.7
11.8
11.6
f1 (ppm)

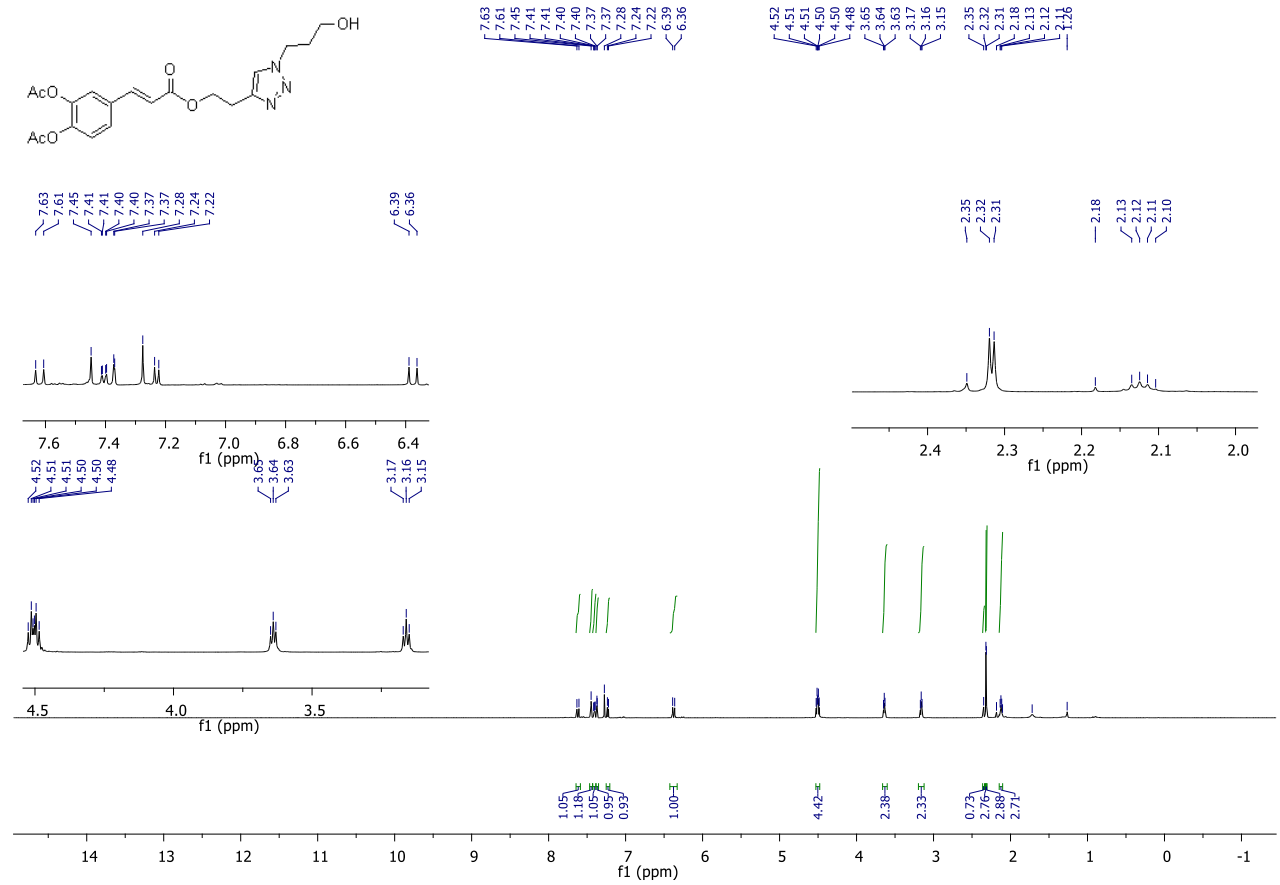
OH
AcO
AcO
O
O
N
N
N
7.63
7.61
7.45
7.41
7.41
7.40
7.40
7.37
7.37
7.28
7.24
7.22
6.39
6.36
4.52
4.51
4.51
4.50
4.50
4.48
3.65
3.64
3.63
3.17
3.16
3.15
2.35
2.32
2.31
2.18
2.13
2.12
2.11
2.10
1.26
f1 (ppm)

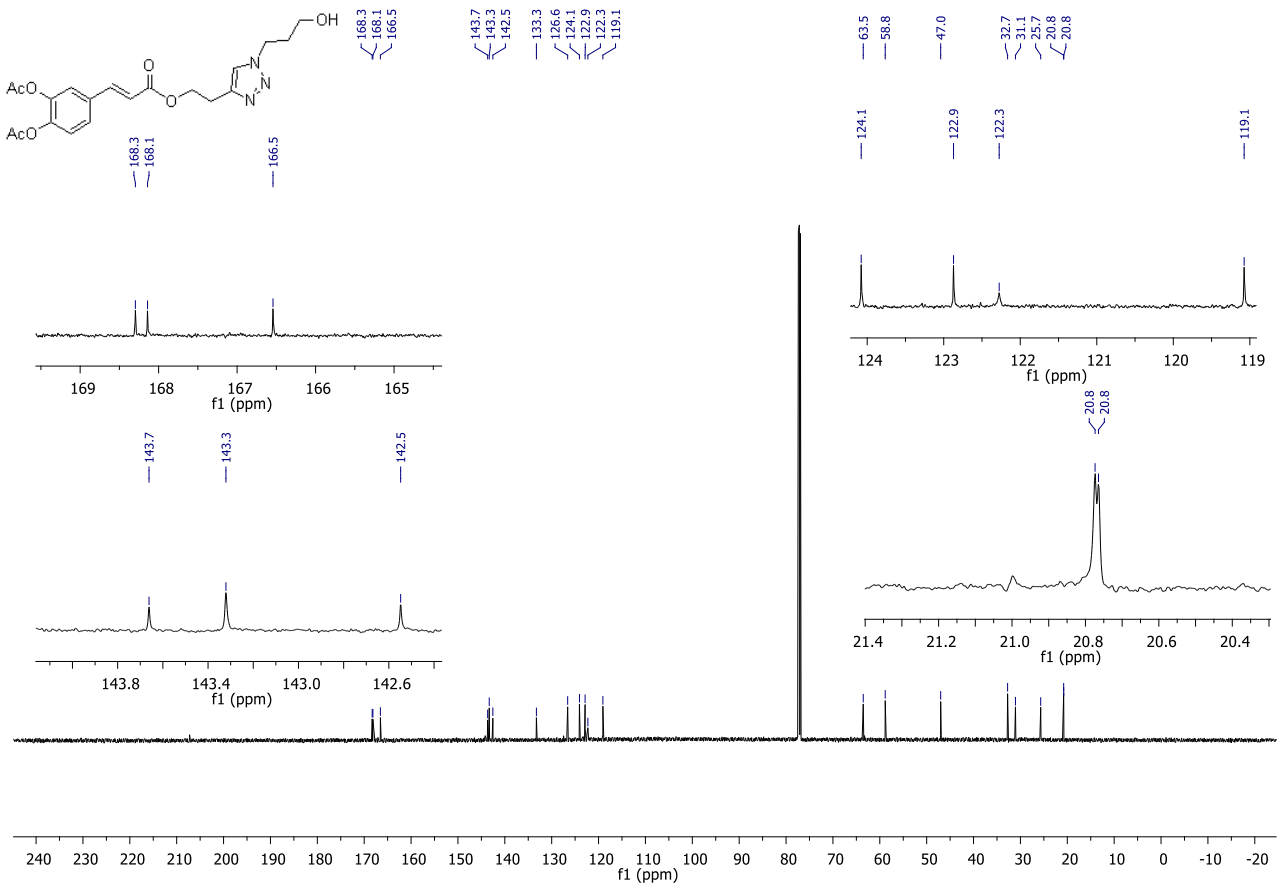
OH
AcO
AcO
O
O
N
N
N
168.3
168.1
166.5
143.7
143.3
142.5
133.3
126.6
124.1
122.9
122.3
119.1
63.5
58.8
47.0
32.7
31.1
25.7
20.8
20.8
f1 (ppm)

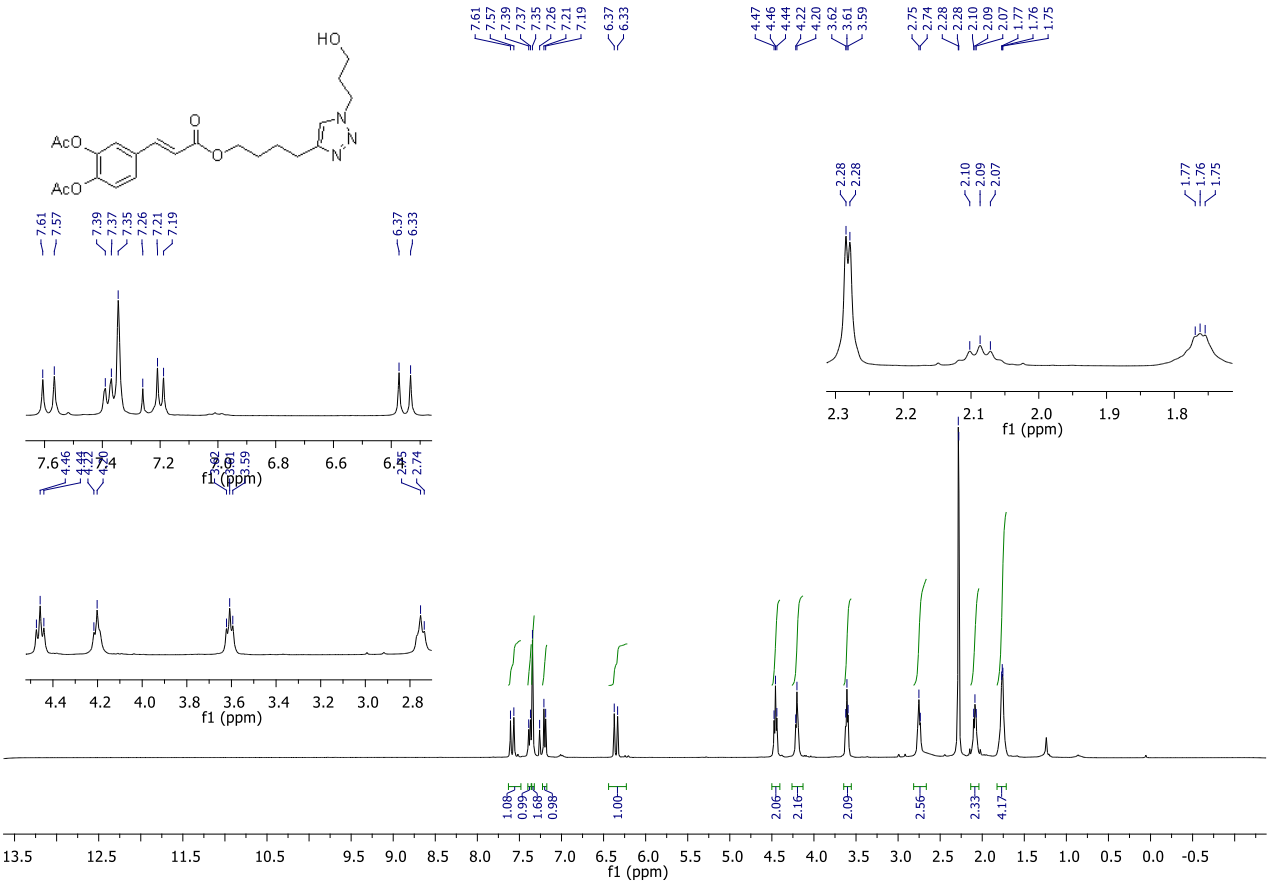
HO
AcO
AcO
O
O
N
N
N
f1 (ppm)

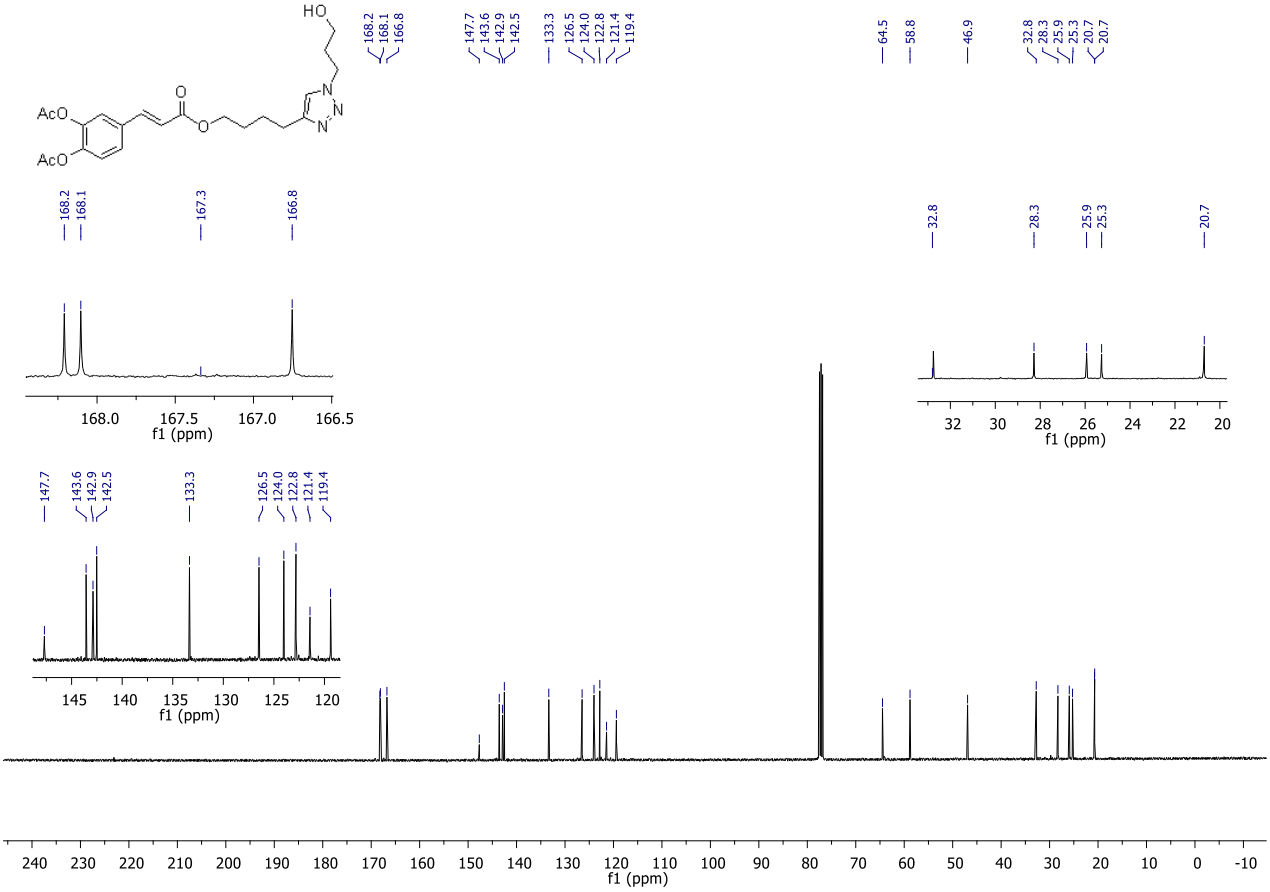
HO
AcO
AcO
O
O
N
N
N
f1 (ppm)

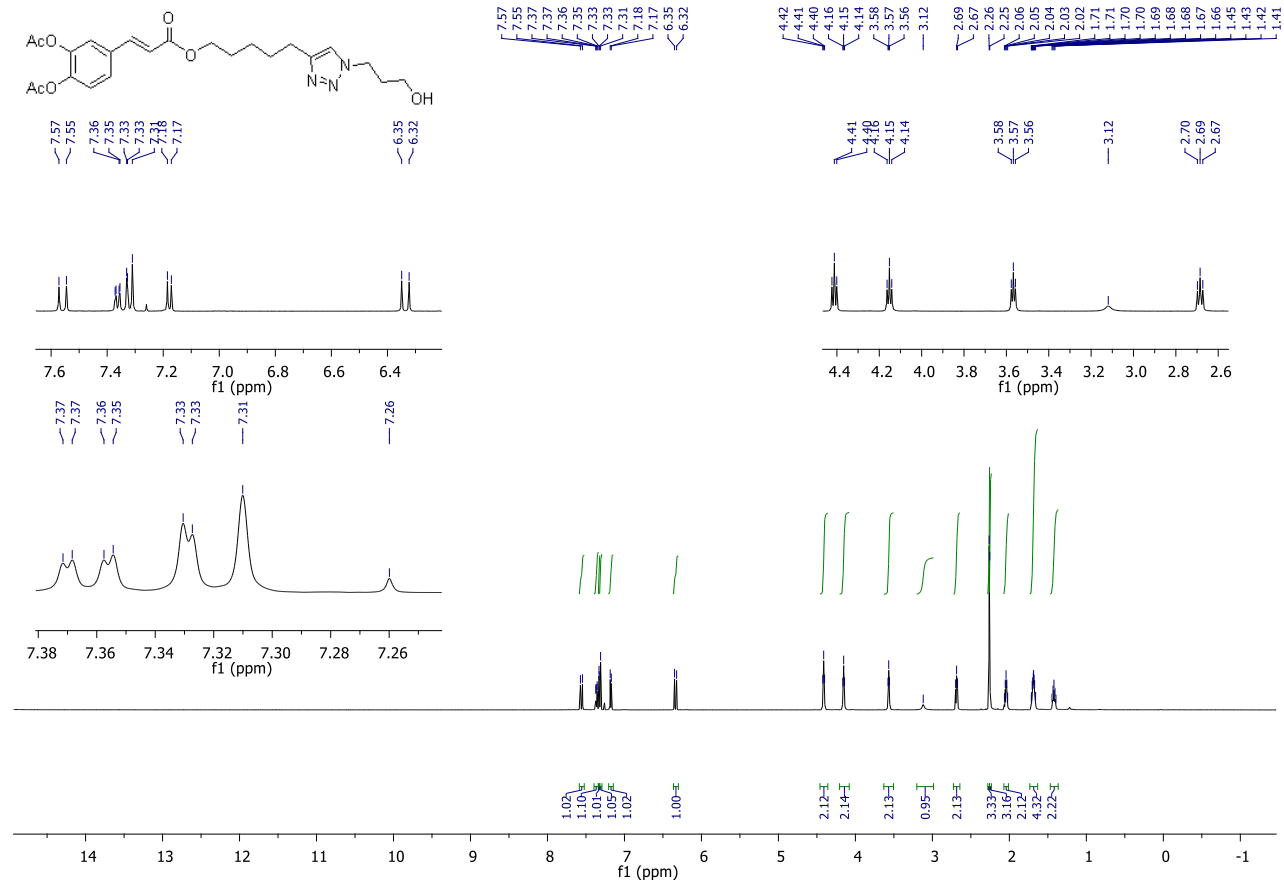
AcO
AcO
O
O
N
N
N
OH
f1 (ppm)

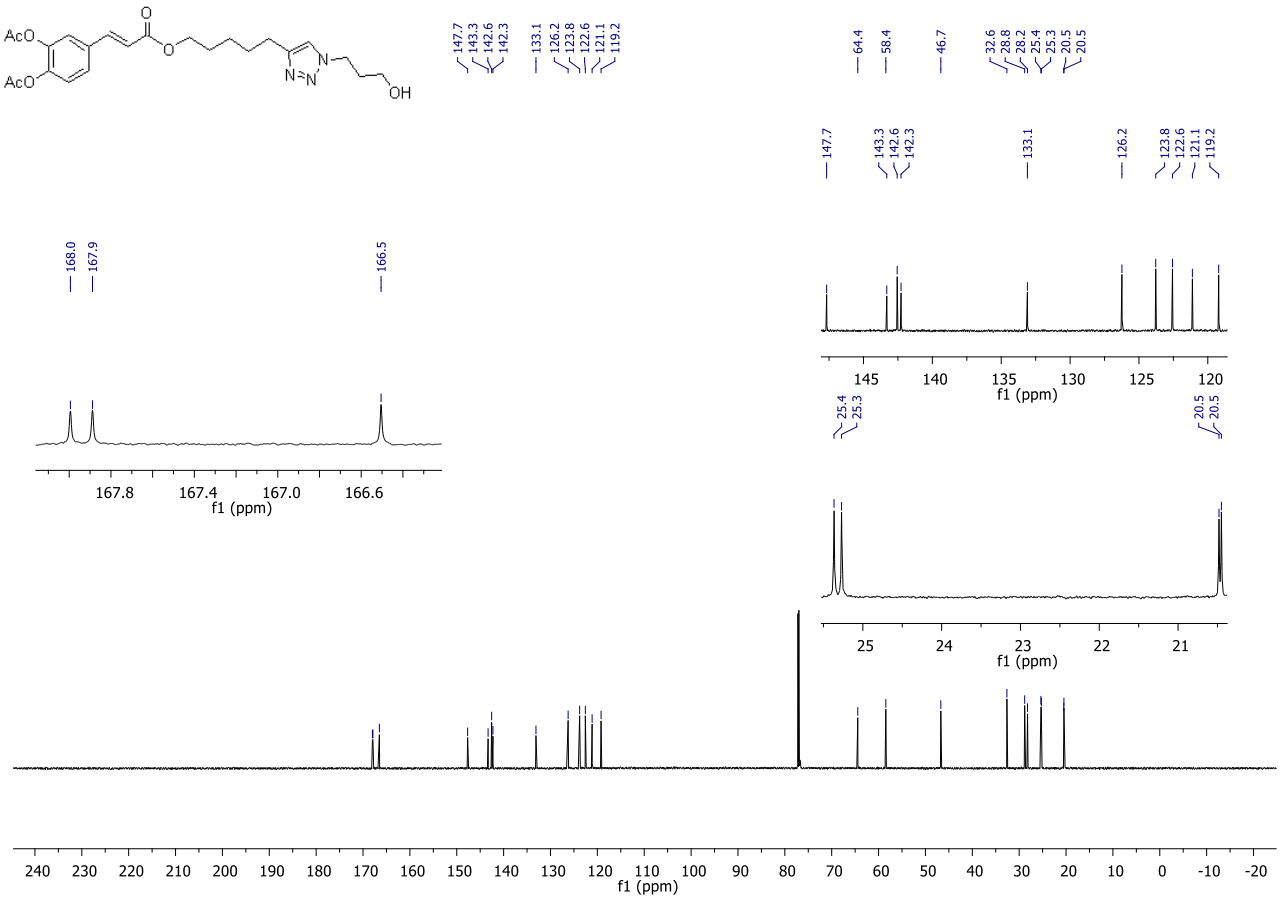
AcO
AcO
O
O
N
N
N
OH
f1 (ppm)

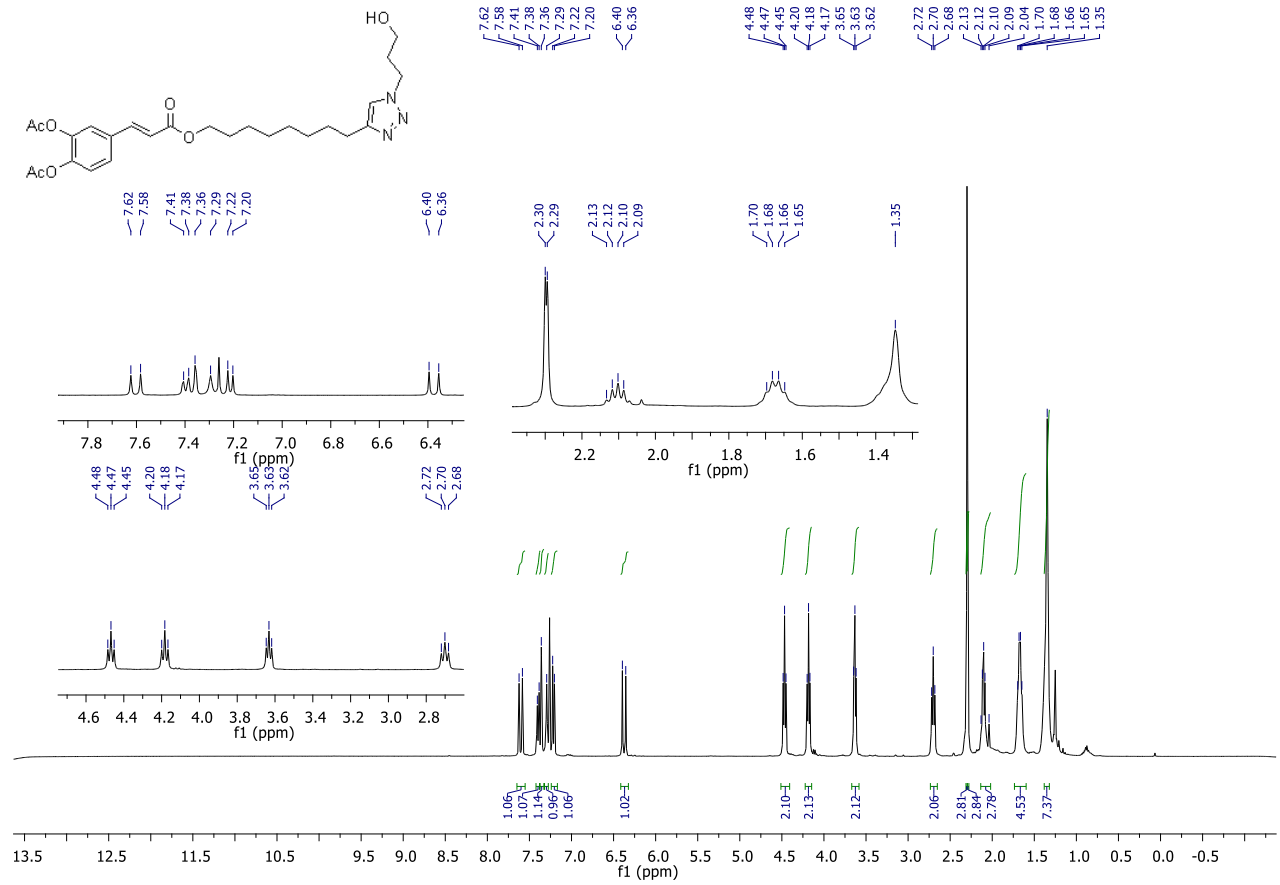
HO
AcO
AcO
O
O
N
N
N
f1 (ppm)

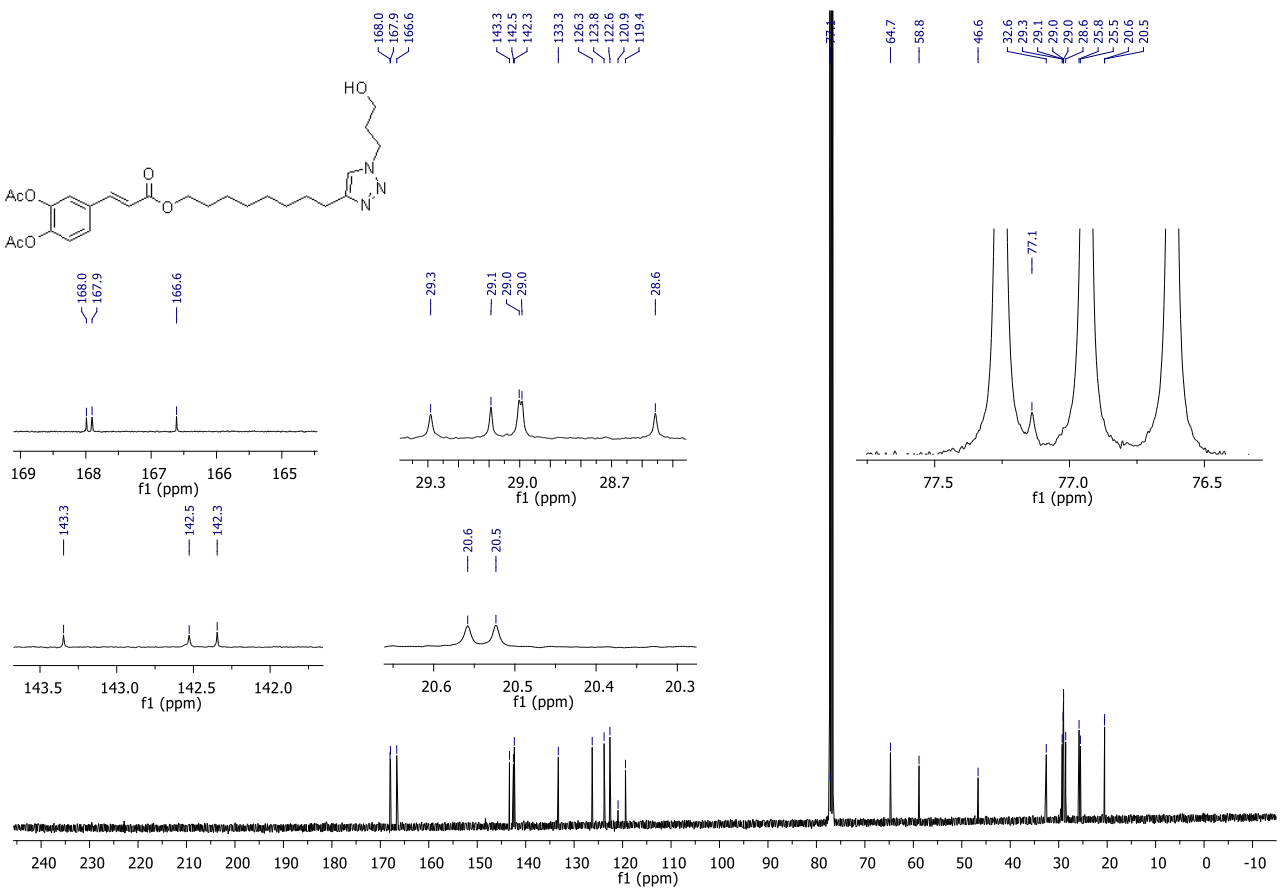
HO
AcO
AcO
O
O
N
N
N
f1 (ppm)

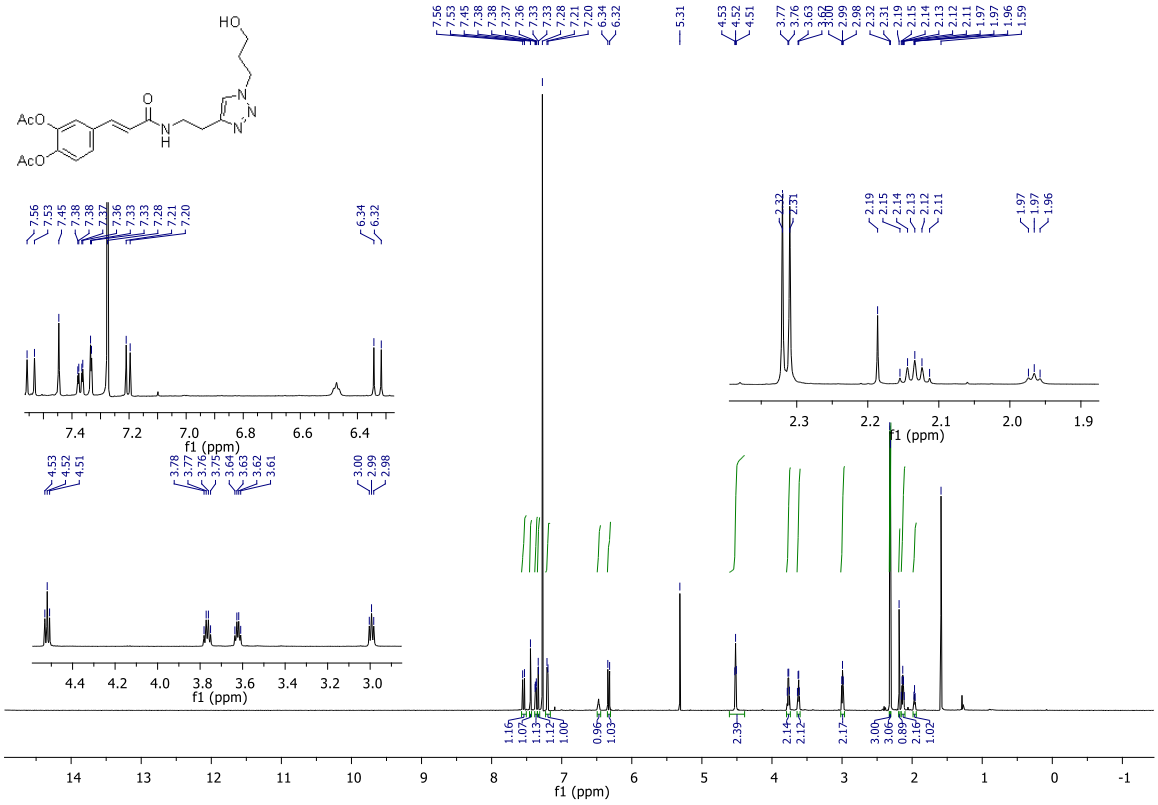
HO
AcO
AcO
O
N
H
N
N
N
f1 (ppm)

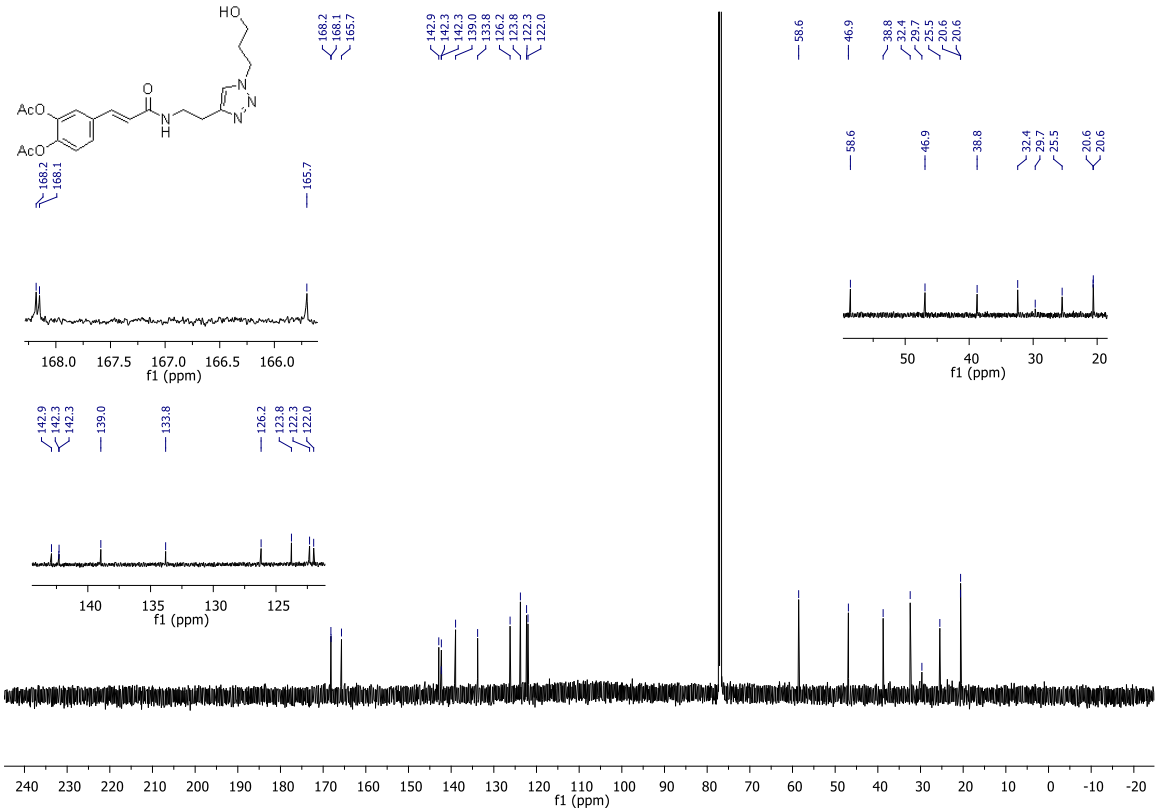
HO
AcO
AcO
O
N
H
N
N
N
f1 (ppm)

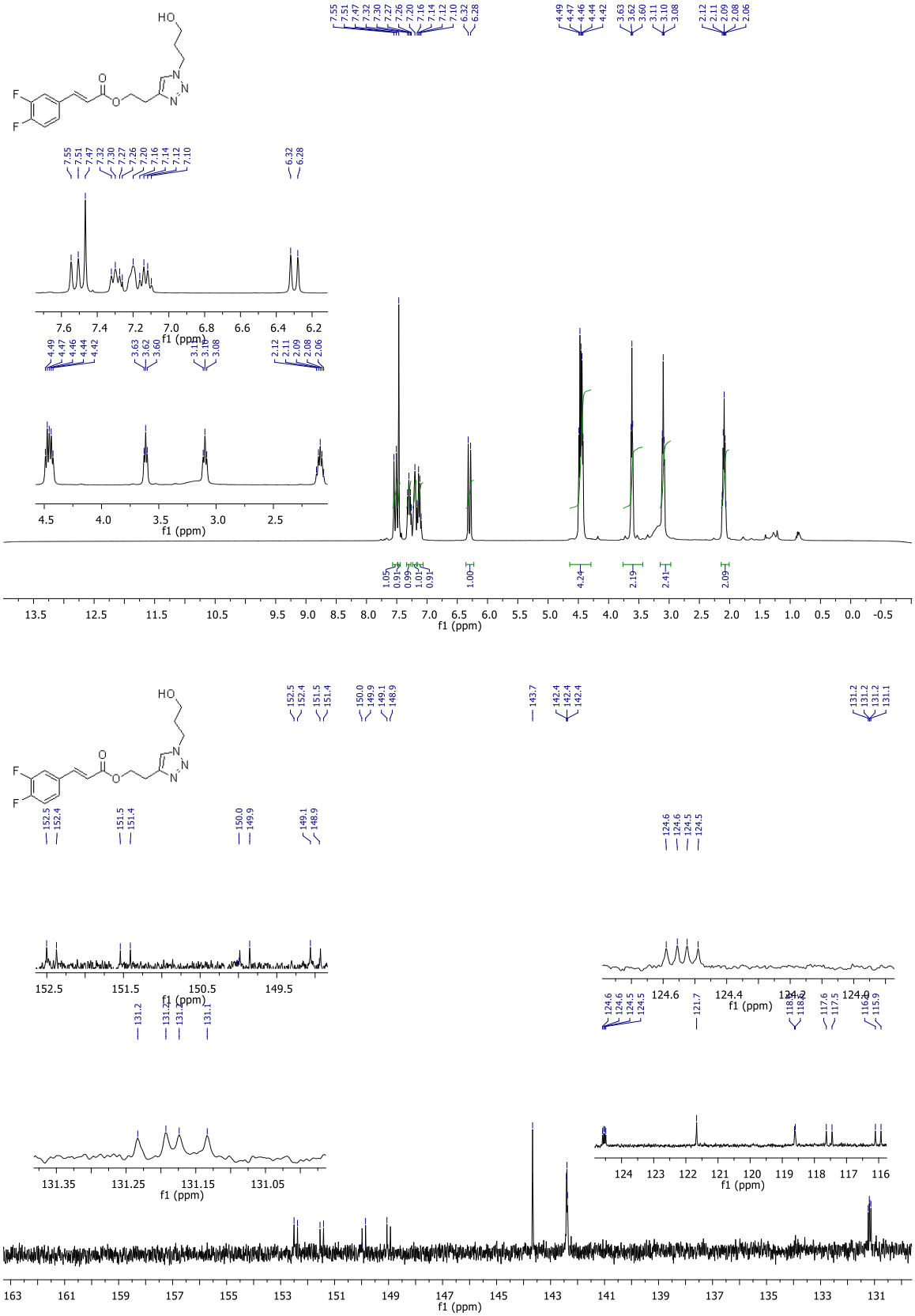

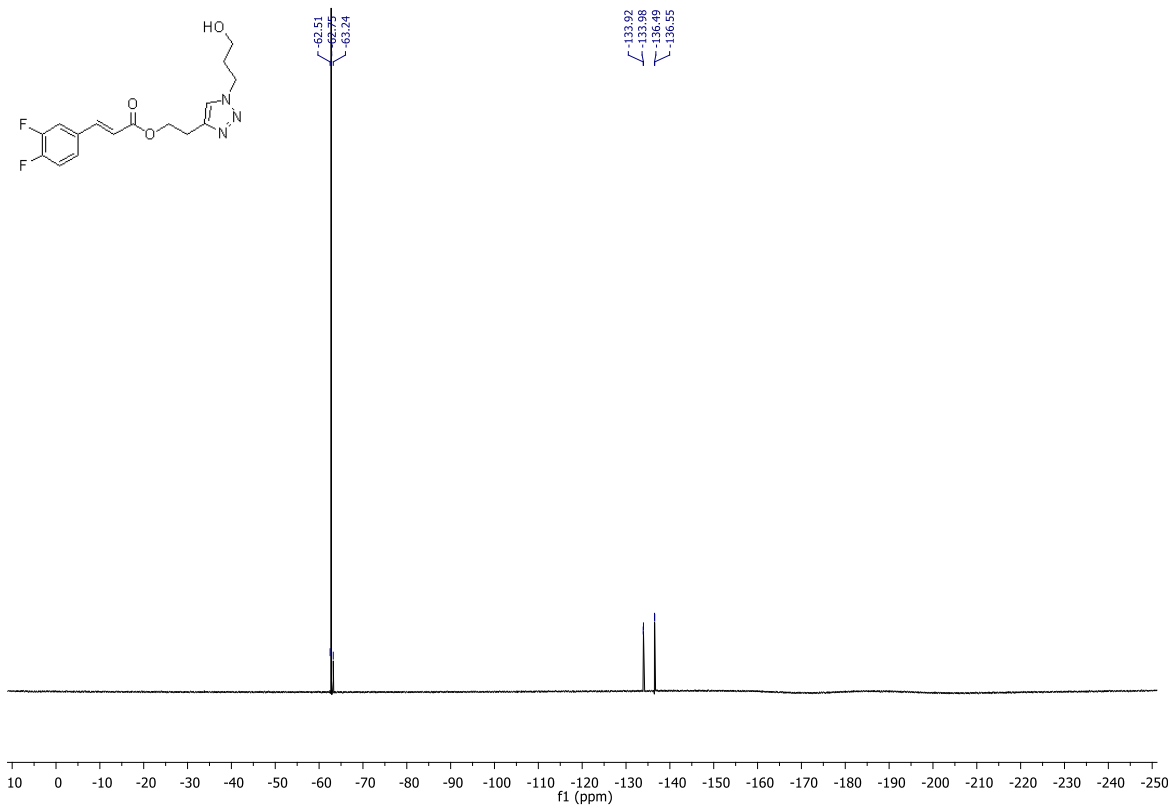
HO
O
O
N
N
N
F
F
-62.51
-62.75
-63.24
-133.92
-133.98
-136.49
-136.55
f1 (ppm)

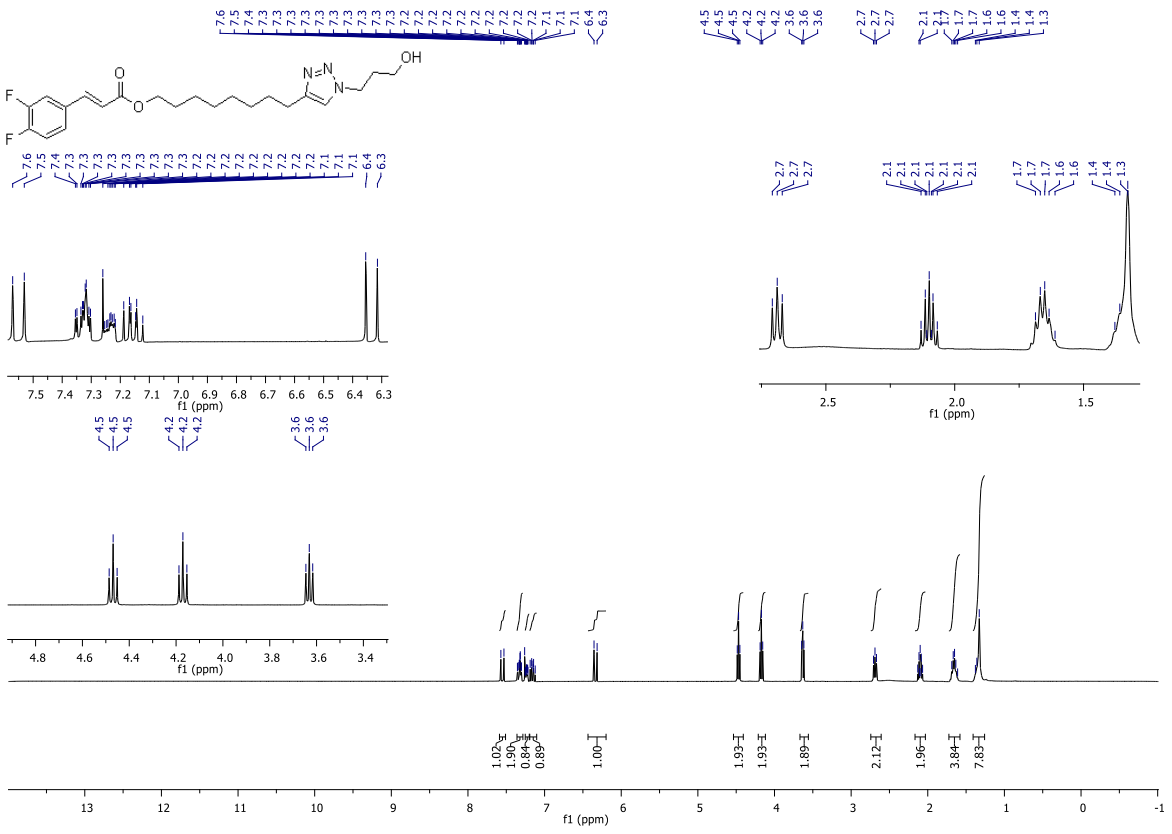
OH
O
O
N
N
N
F
F
f1 (ppm)

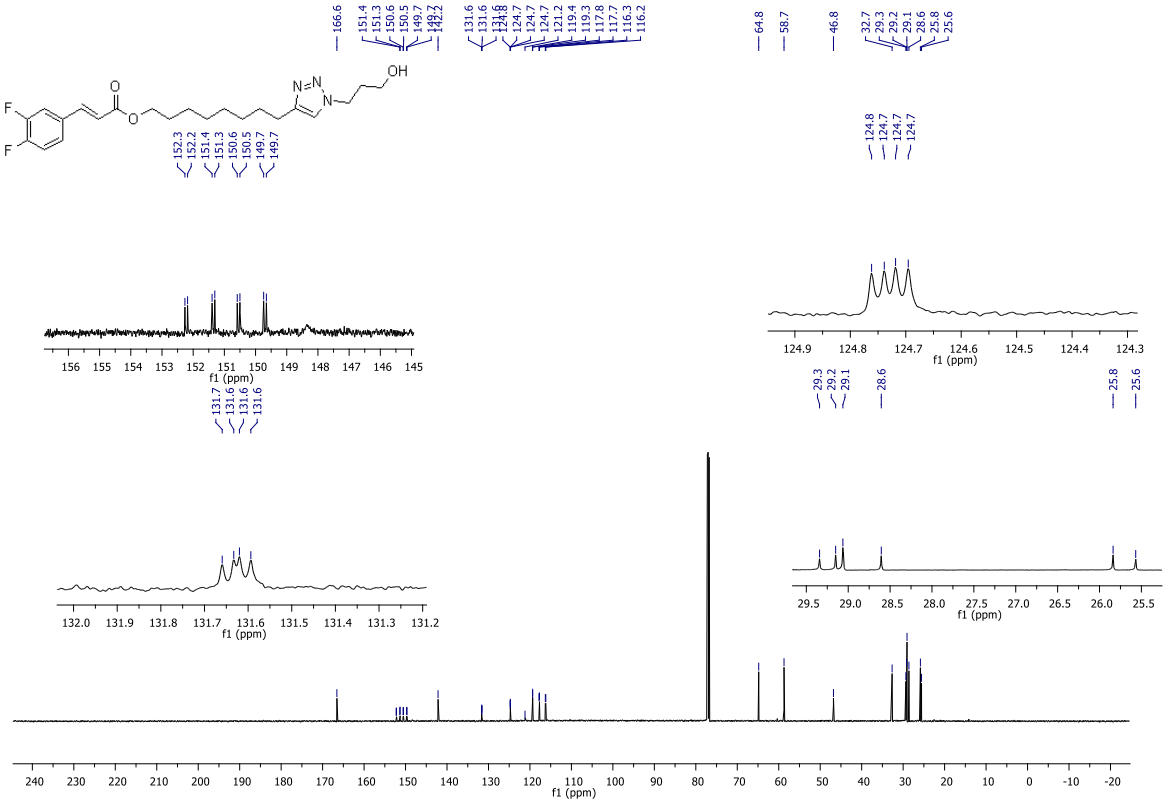
166.6
151.4
151.3
150.6
150.5
149.7
149.2
131.6
131.6
124.8
124.7
124.7
121.2
119.4
117.8
117.7
116.3
116.2
64.8
58.7
46.8
32.7
29.3
29.2
29.1
28.6
25.8
25.6
124.8
124.7
124.7
124.7
O
O
N=N
N
OH
F
F
152.3
152.2
151.4
151.3
150.6
150.5
149.7
149.7
f1 (ppm)
131.7
131.6
131.6
131.6
29.3
29.2
29.1
28.6
25.8
25.6

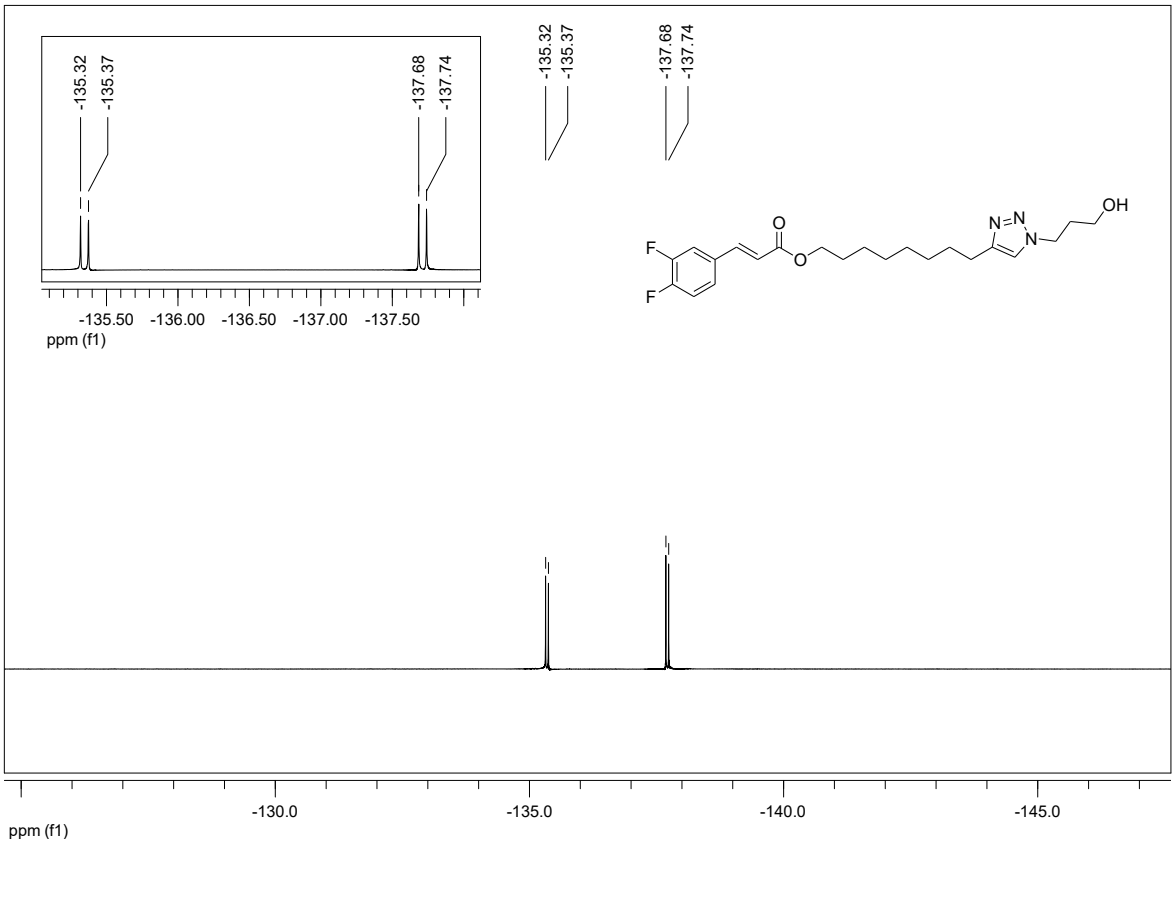
-135.32
-135.37
-137.68
-137.74
-135.50
-136.00
-136.50
-137.00
-137.50
ppm (f1)
-130.0
-135.0
-140.0
-145.0
ppm (f1)
O
O
N=N
N
OH
F
F

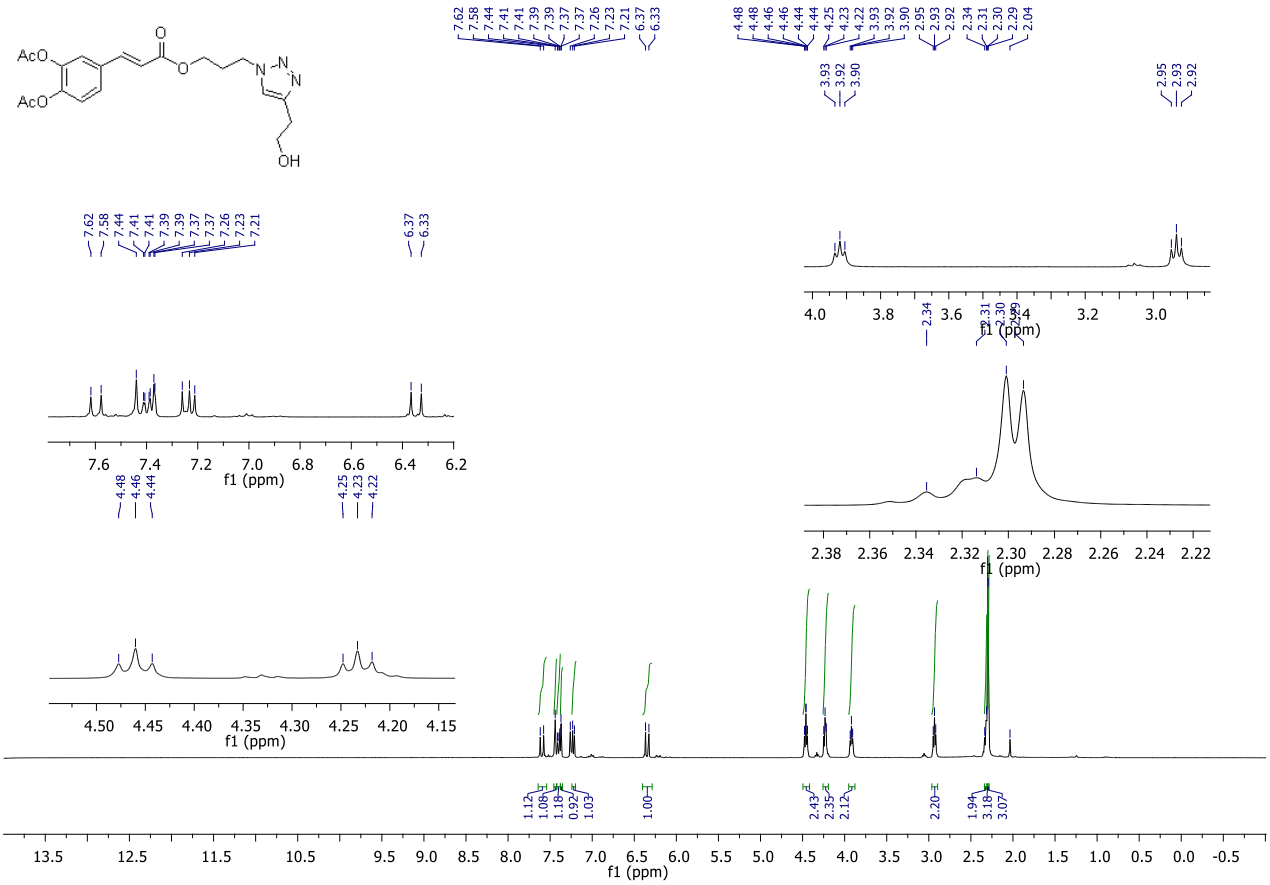
AcO
AcO
O
N
N
N
OH
f1 (ppm)

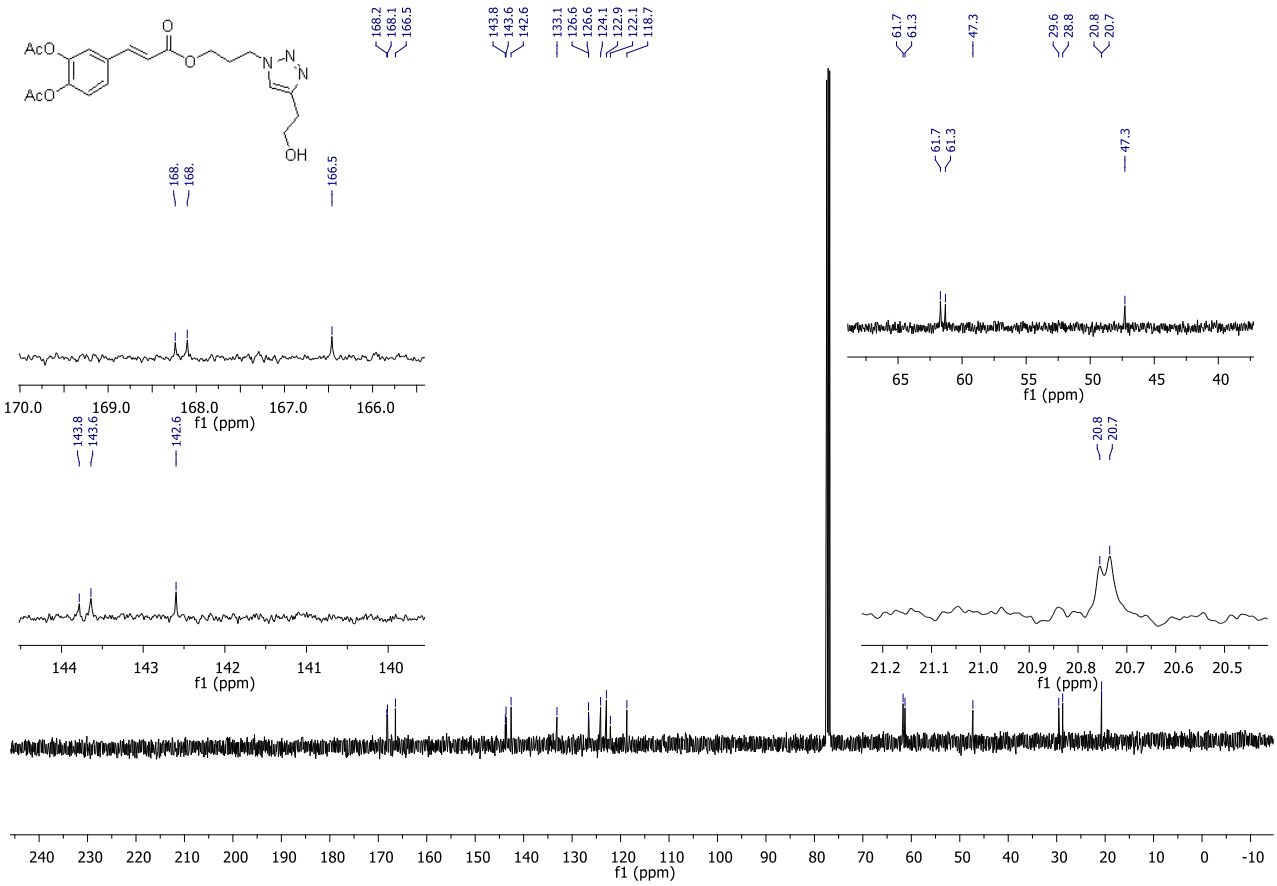
AcO
AcO
O
N
N
N
OH
f1 (ppm)

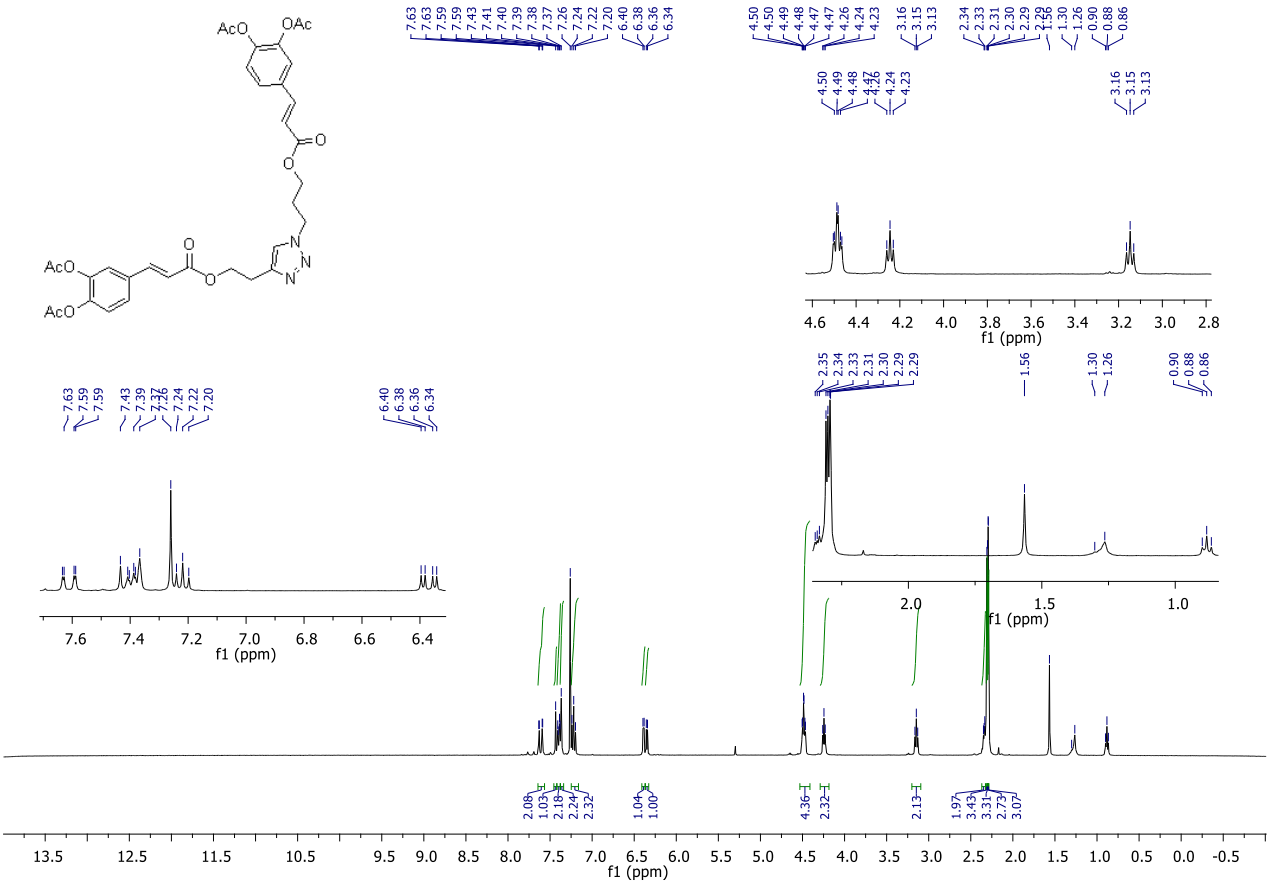
AcO
OAc
AcO
AcO
f1 (ppm)

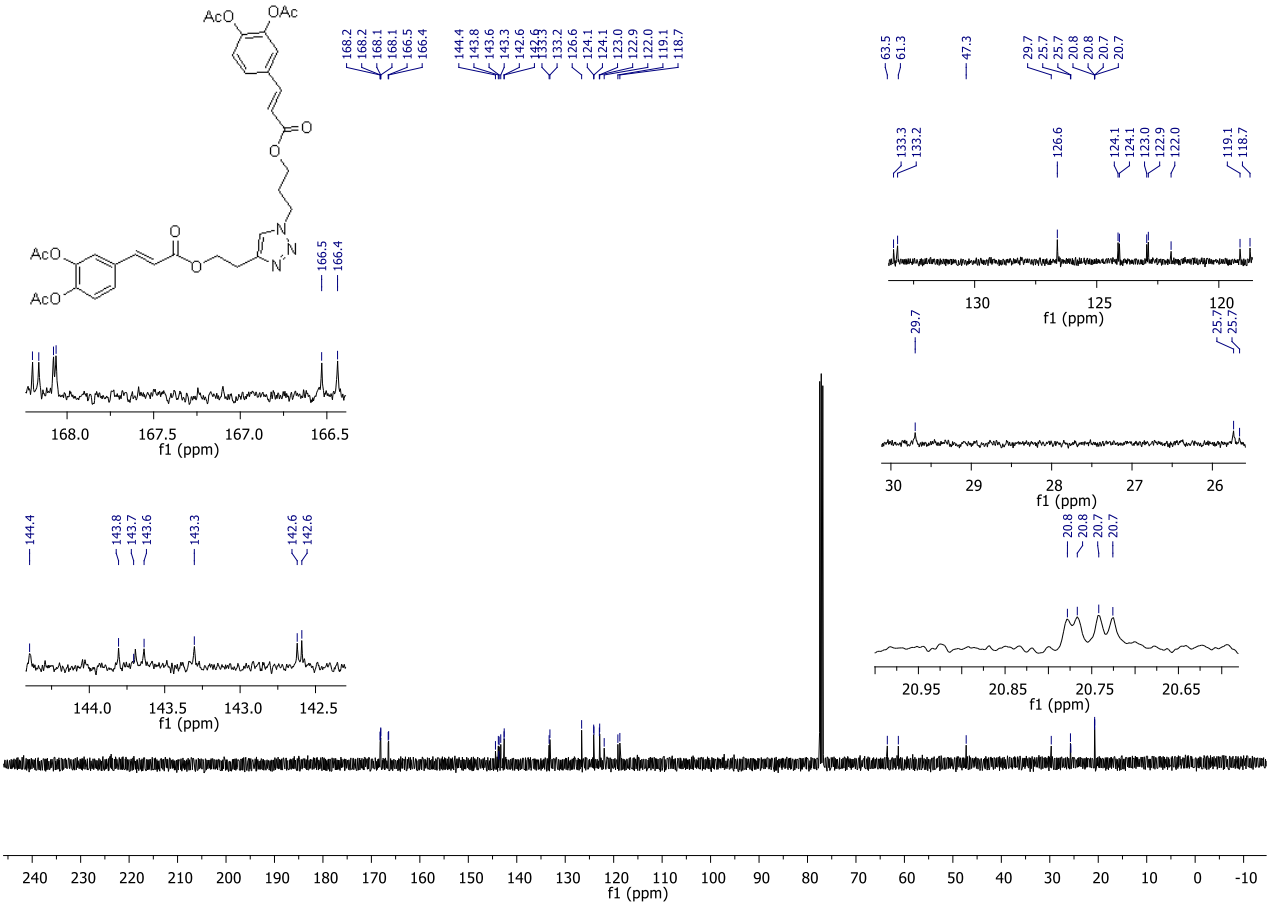
AcO
OAc
AcO
AcO
f1 (ppm)

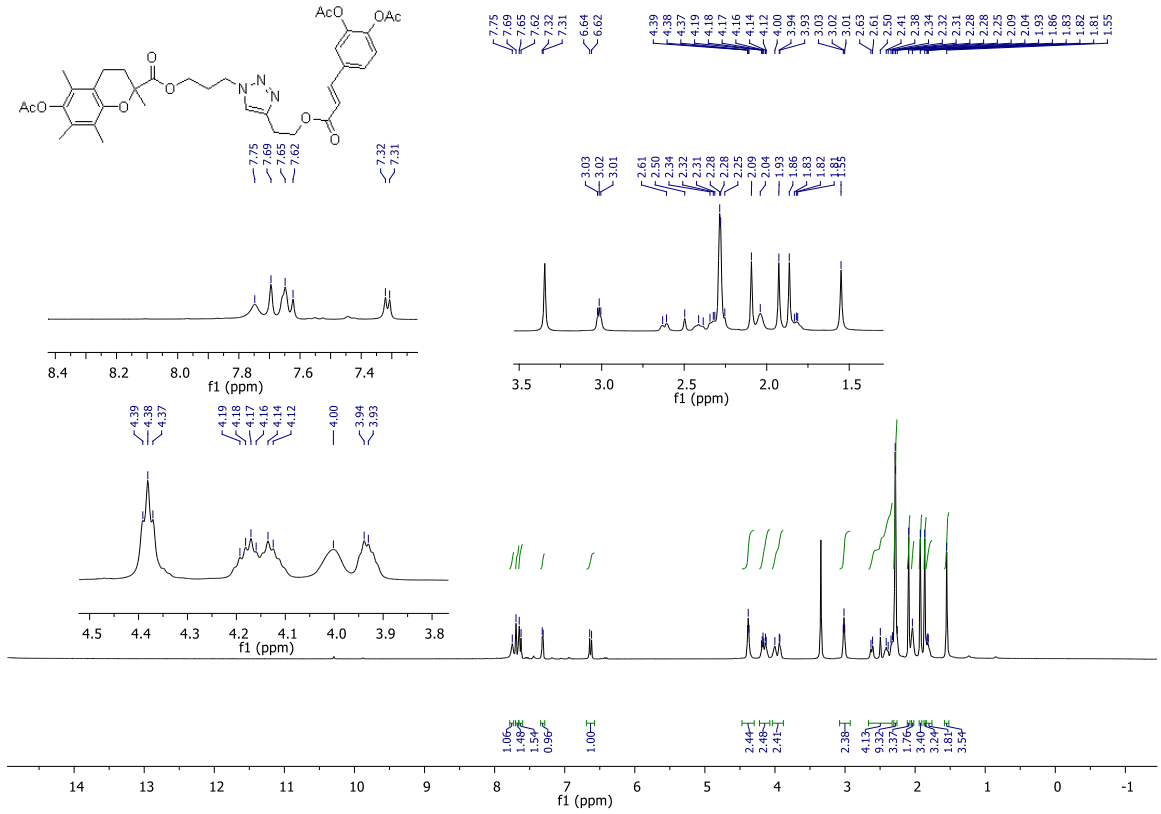
AcO
OAc
f1 (ppm)

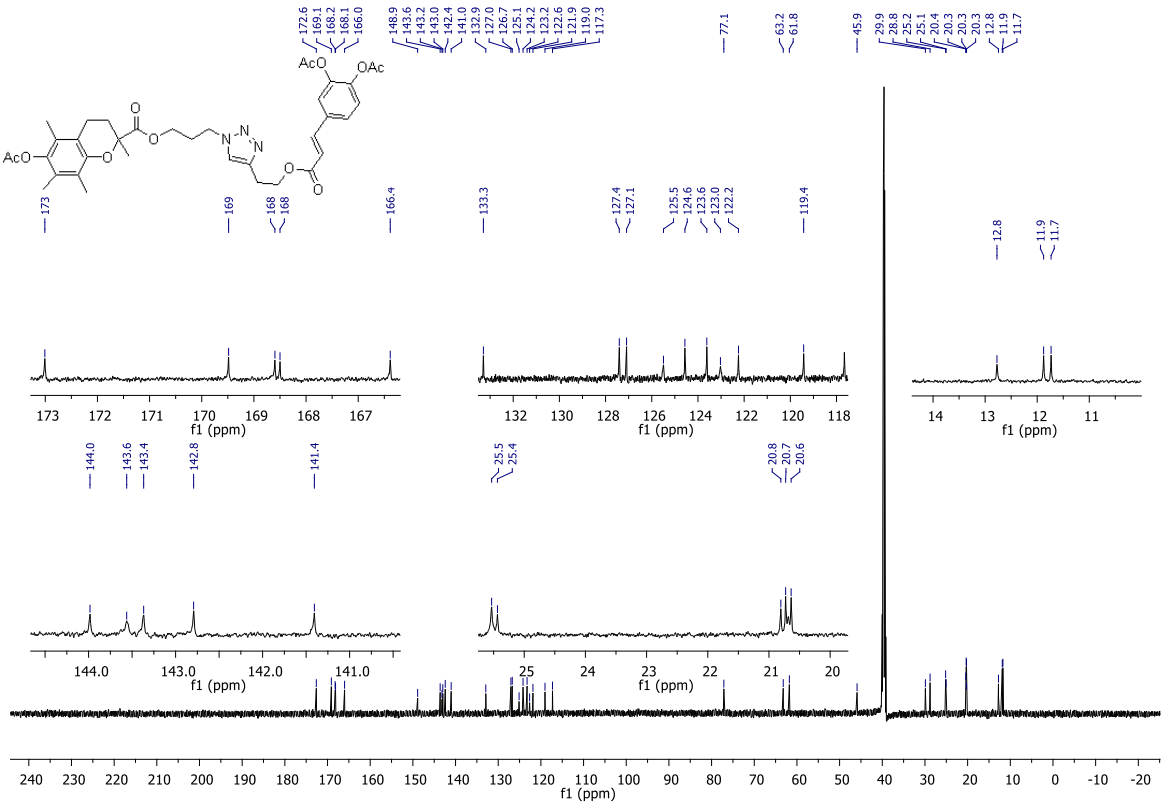
AcO
OAc
f1 (ppm)

12. Appendix Log P

The partition coefficient (Log P[128]) describes the ratio of a compounds between two immiscible phases, generally *n*-octanol and water. It gives a measure of the hydrophilicity of the molecule. It is important to understand that the Log P value is a valid indicator of the hydrophilicity of a molecule for non-dissociated species at neutral pH, if working with ionisable species the Log D (pH-dependent lipophilicity descriptor) must be used. It is a fundamental parameter in medicinal chemistry and its one of the points of the rule of 5.[129]

The Lipinsky rule of 5 was initially meant to predict cell permeability and adsorption of compounds in the body but has been used for more than twenty years now to predict drug likeness.

The rule of 5 states that potential drugs should follow the parameters listed below, to increase their possibility of success:

1. MW lower than 500[§§§§,130]
2. Log P less than 5 (–0.4 to +5.6 accepted range)
3. Number of H-Bond donors (HBD) is less than 5
4. Number of H-Bond acceptors (HBA) is less than 10

The rule was based on the 90 percentile values of the physic-chemical properties distribution of more than 2000 drug molecules.

Log P is often considered the most important parameter to judge drug likeness this because it affects adsorption, membrane permeability, metabolism, promiscuity, toxicity and survival of the drug in the pipeline.[131]

The reference compounds zileuton for anti-inflammatory activity and fluconazole for antimycotic activity possess Log P of 1.77 and 1.81 respectively. In Table 10.5.1 the Log P of the library of compounds herein presented are reported and are all in the acceptable range described by Lipinski (exception made for **8e** that was anyway inactive).

[§§§§] This cut out has been questioned, and it has been more recently evidenced that the number of rotatable bonds and the polar surface area are more useful to discriminate between compounds orally active, in particular they should have less than 10 rotatable bonds and polar surface area not higher than 140 Å.^{2}

Table 10.5.1 *Table of Log P of synthesised compounds calculated with Marvin Sketch 5.4.1.1 method KLOP Marvin Sketch software ver. 5.4.1.1.*[132, 133]

Compound	***Log P***
3a	1.99
3b	2.93
3c	3.40
3d	4.80
3e	1.08
3f	3.07
5	1.50 ionic species
7	1.63 on ionic species 4.16 ionic species 4.30 non-ionic species
8a	1.01
8b	1.77
8c	2.24
8d	3.65
8e	0.10
8f	2.09
8h	1.01
9	3.04
10	5.70

13. References

[1] Ahmad M.F., Ashraf S.A., Ahmad F. A., Ansari J.A., Siddiquee M.R.A.; Nutraceutical market and its regulation. *Am. J. Food Technol*. **2011,** 6:342-347

[2] Bower V., Nutraceuticals: Poised for a healthy slice of the healthcare market? *Nat. Biotech*. **1998**, 16:728-730

[3] Gutiérrez N.L., González R.R., Bolaños P.P., Martínez Vidal J.L., Frenich A.G.; Identification and quantification of phytochemicals in nutraceutical products from green tea by UHPLC–Orbitrap-MS. *Food Chem*. **2015**, 607-618

[4] Consden R., Gordon A.H., Martin A.J.; Qualitative analysis of proteins: a partition chromatographic method using paper. *Biochem J.* **1944**;38(3):224–232

[5] Snyder LR., Principles of Adsorption Chromatography: Apparatus, Theory and Applications. New York: Marcel Dekker.**1968**

[6] Soczewinski E.; Solvent composition effects in thin layer chromatography systems of the type of silica gel-electron donor solvent. *Anal. Chem*. **1969**; 41:179-182

[7] Scott R.P.W., Kucera P.; Solute –solvent interactions on the surface of silica gel. *J.Chromatogr*. A 1978; 149: 93-110

[8] Kaiser R. E., Planar Chromatography, Volume I, Huethig, **1986**

[9] Yrjönen T., Extraction and Planar Chromatographic Separation *Techniques in the Analysis of Natural Products*, **2004**

[10] Handbook of Thin – Layer Chromatography, volume 55, edited by Joseph Sherma & Bernard Fried, MARCEL DEKKER, INC, **1991**

[11] Friedrich Geiss, Fundamentals of Thin Layer Chromatography (Planar Chromatography), Hüethig, **1987**

[12] Douglas A. Skoog, James J. Leary, Chimica analitica strumentale, EdiSES, **1995**

[13] John Burke, Solubility Parameters: Theory and Application, The Oakland Museum of California, August 1984 (Appeared in the *AIC Book and Paper Group Annual*, Volume 3, **1984**, Craig Jensen Editor)

[14] Snyder – Kirkland, Itroduction to modern liquid Chromatography, 2nd edition, **1980**

[15] Friedrich Geiss, Fundamentals of Thin Layer Chromatography (Planar Chromatography), Hüethig, **1987**

[16] P. Kulbeka, F. Munk, Z. Techn. Physik, 12, **1931**,593

[17] P. Kulbeka, J. Opt. Soc. Am.,38,**1948**, 448

[18] Brady O; The characterisation and bioactivity determination of Adansonia digitata L. Baobab fruit pulp, for commercial product development. **2011**, Dissertation, Dublin Institute of Technology, Ireland

[19] FAO Traditional food plants. FAO *Food Nutr Pap* **1988,** 42:63–67

[20]Vertuani S., Braccioli E., Buzzoni V., Manfredini S.; Antioxidant capacity of Adansonia digitata fruit pulp and leaves. *Acta Phytother*. **2002**, 5:2–7.

[21] Airan TW, Desai RM Sugars and organic acids in Adansonia digitata. *J. of University of Bombay,* **1954**, 22:23–27

[22] Amaretti A., Tamburini E., Bernardi T., Pompei A., Zanoni S., Vaccari G., Matteuzzi D., Rossi M. ; Substrate preference of Bifidobacterium adolescentis MB 239: compared growth on single and mixed carbohydrates. *Appl Microbiol Biotechnol* **2006**, 73:654–662

[23] Gibson GR, Roberfroid MB; Dietary modulation of the colonic microbiota: introducing the concept of prebiotics. *J*

Nutr **1995**, 125:1401–1412

[24] Roberfroid M.; Prebiotics: the concept revisited. *J Nutr* , **2007**, 137:830S–837S

[25] De Caluwé E., Halamová K., Van Damme P.; Adansonia digitata L.—a review of traditional uses, phytochemistry and pharmacology. *Afrika Focus* **2010,** 23:11–51

[26] Aachary A.A., Prapulla S.G.; Xylooligosaccharides (XOS) as an Emerging Prebiotic: Microbial Synthesis, Utilization, Structural Characterization, Bioactive Properties, and Applications. *Compr Rev Food Sci F*, **2011**, 1-16

[27] De Caluwé E., Halamová K., Van Damme P., Adansonia digitata – A review of traditional uses, phytochemistry and pharmacology. *Afrika Focus* **2010,** 23:11–51

[28] FAO Traditional food plants. FAO **1988** *Food Nutr Pap* 42:63–67

[29] Vertuani S. , Braccioli E. , Buzzoni V. , Manfredini S.; Antioxidant capacity of Adansonia digitata fruit pulp and leaves. *Acta Phytother.* **2002,** 5:2–7

[30] Davis F., Terry L.A., Chope G.A., Faul C.F.J., Effect of extraction procedure on measured sugar concentrations in onion (Allium cepa L.) bulbs. *J Agric Food Chem* **2007,** 55:4299–4306

[31] Wei L.Y., Wang J.H., Zheng X.D., Teng D., Yang Y.L., Cai C.G., Feng T.H., Zhang F.; Studies on the extracting technical conditions of inulin from Jerusalem artichoke tubers. **2007** *J Food Eng* 79:1087–1093

[32] Jaime L., Martınez F., Martın-Cabrejas M.A., Molla E., Lopez-Andreu F.J., Waldron K.W., Esteban R.M.; Study of total fructan and fructooligosaccharide content in different onion tissues. *J Sci Food Agr* **2001,** 81:177–182

[33] Casterline J.L., Oles C.J., Ku Y.O., Measurement of sugars and starches in foods by a modification of the AOAC total dietary fiber method. *J AOAC Int* **1999,** 82:759–765

[34] Vaccari G., Lodi G., Tamburini E., Bernardi T., Tosi S. ; Detection of oligosaccharides in sugar products using planar chromatography. *Food Chem* **2001**, 74:99–110

[35] Bernardi T., Tamburini E.; An HPTLC-AMD method for understanding the metabolic behaviour of microorganisms in the presence of mixed carbon sources. The case of Bifidobacterium adolescentis MB 239. *J Planar Chromatogr-Mod TLC* **2009**, 22:321–325

[36] Parkar S.G., Stevenson D.E., Skinner M.A.; The potential influence of fruit polyphenols on colonic microflora and human gut health. *Int J Food Microbiol* **2008**, 124:295–298

[37] Tzounis X., Vulevic J., Kuhnle G.G.C., George T., Leonczak J., Gibson G.R., Kwik-Uribe C., Spencer J.P.E.;Flavanol monomer-induced changes to the human faecal microflora. *Br J Nutr* **2008**, 99:782–792

[38] Icumsa Method GS4/3-7 "The determination of Total Reducing Sugars in Molasses and Refined syrups after Hydrolysis" *by the Lane & Eynon Constant Volume Procedure Official*. **1994,** pp 1–4.

[39] Jork H., Funk W., Fischer W., Wimmer H.;*thin layer chromatography, Reagents and detection methods*, Vol 1a, Weinheim, VCH, **1990**, pp 325–328

[40] Landete, J. M**.;** Updated Knowledge about Polyphenols: Functions, Bioavailability, Metabolism, and Health.*Critical Reviews in Food Science and Nutrition*, **2012**, 52, 936–948.

[41] C. Manach, A. Scalbert, C. Morand, C. Remesy, L. Jimenez, Polyphenols: food sources and bioavailability *Am. J. Clin. Nutr.* **2004**, *79*, 724-727

[42] Prasain J.K., Barnes S.; Metabolism and Bioavailability of Flavonoids in Chemoprevention: Current Analytical Strategies and Future Prospectus. *Molecular Pharmaceutics* **2007** VOL. 4, NO. 6, 846–864

[43]Huang D., Ou B., Prior R.L.; The Chemistry behind Antioxidant Capacity Assays *, J.Agric.Food Chem*. **2005**, 53:1841-1856

[44] Valko M., Leibfritz D., Moncola I. , Cronin M.T.D., Mazura M., Telser J., Free radicals and antioxidants in normal physiological functions and human disease. *Int. J. Biochem. Cell Biol.* **2007***,* 39:44–84

[45] Draper H., Hadley M.; "A review of recent studies on the metabolism of exogenous and endogenous malondialdehyde"; *Xenobiotica*, **1990**, 20:901-910

[46] Peterson D.R., Doorn J.A.; Reactions of 4-hydroxynonenal with proteins and cellular targets. *Free Radical Biol. Med.* **2004**, 37, 7:937-934

[47] Buettner GR. The pecking order of free radicals and antioxidants: Lipid peroxidation, α-tocopherol, and ascorbate. *Arch Biochem Biophy.* **1993**, 300:535-543

[48] Hummel G.S., Fischer A:J., Martin S.M.,Schafer F.Q., Buettner G.R.; Nitric oxide as a cellular antioxidant: A little goes a long way. Free Radical Biol. Med **2006,** 40: 501 – 506

[49] Benzie I:F:F., Strain J.J.; Ferric reducing /antioxidant power assay: direct measure of total antioxidant activity of biological fluids and modified version for simultaneous measurement of total antioxidant power and ascorbic acid concentration. *Methods Enzymol.* **1999**, 299,15-27

[50] Hong J., Bose M., Ju J., Ryu J.H., Chen X., Sang S., Lee M.J., Yang C.S.;Modulation of arachidonic acid metabolism by curcumin and related β-diketone derivatives: effects on cytosolic phospholipase A2, cyclooxygenases and 5-lipoxygenase. *Carcinogenesis*, **2004**, 25, 1671-1679

[51] Koeberle A., Northoff H., Werz O.; Curcumin blocks prostaglandin E2 biosynthesis through direct inhibition of the microsomal prostaglandin E2 synthase-1. *Mol. Cancer Ther*. **2009**, 8, 2348–2355

[52] Padhye S., Chavan D., Pandey S.,Deshpande J.,Swamy K. V.,Sarkar F. H.; Perspectives on Chemopreventive and Therapeutic Potential of Curcumin Analogs in Medicinal Chemistry. *Mini Rev. Med Chem*. **2010**, 10 (5) 372-387.

[53] Boudreau L. H.; Picot N.; Doiron J.; Villebonnet B.; Surette M. E.; Robichaud A. G.; Touaibia M.; Caffeoyl and cinnamoyl clusters with anti-inflammatory and anti-cancer effects. Synthesis and structure-activity relationship; New J. Chem. 2009, 33, 1932-1940.

[54] Prasad N.R., Karthikeyan, Karthikeyan S., Reddy B. V.; Inhibitory effect of caffeic acid on cancer cell proliferation by oxidative mechanism in human HT-1080 fibrosarcoma cell line. *Mol. Cell. Biochem.* **2011,** 349:11-19

[55] http://www.ars.usda.gov/is/AR/archive/oct06/nuts1006.htm

[56] Anighoro, A;, Bajorath, J; Rastelli, G; Polypharmacology: Challenges and Opportunities in Drug Discovery, *J.Med.Chem* **2014.** 57, 19, 7874-7887

[57] Koeberle A, Munoz E., Appendino G.B., Minassi A., Pace S., Rossi A., Weinigel C., Barz D., Sautebin L., Caprioglio D., Collado J.A., Werz O.; SAR Studies on Curcumin's Pro-inflammatory Targets: Discovery of Prenylated Pyrazolocurcuminoids as Potent and Selective Novel Inhibitors of 5-Lipooxygenase, *J.Med.Chem.* **2014**, 57, 5638-5648

[58] Samuelsson, B.; Dahlen, S.; Lindgren, J. A. N. A.; Rouzer, C. A.; Serhan, C. N.; *Science*, **1987**, 237, 1171–1176.

[59] Steinhilber, D.; Hofmann, Recent advances in the Search of Novel 5-Lipoxygenase Inhibitors B.; *Basic Clin. Pharmacol. Toxicol*. **2014**, 114, 70–77.

[60] Osburn W.O.; Kensler T. W.; *Mutation Research* 659 **2008** , 31-39

[61] Stables M.J., Gilroy D.W.; Old and new generation lipid mediators in acute inflammation and resolution. *Prog. Lipid. Research* **2011**, 50: 35-51

[62] Koeberle A., Werz O.; Multi-Target approach for natural products in inflammation. *Drug Discovery Today* **2014,** 19: 1871-1882

[63] Steinhilber, D.; Hofmann, B. Basic *Clin. Pharmacol. Toxicol*. **2014**, 114, 70–77.

[64] Hwang S.H., Wecksler A.T., Wagner K. and Hammock B.D.; Rationally Designed Multitarget Agents Against Inflammation and Pain. *Curr. Med. Chem.***2013**, 20: 1783-1799

[65] Rouzer, C.A.; Kargman, S. Translocation of 5-lipoxygenase to the membrane in human leukocytes challenged with ionophore A23187. *J. Biol. Chem.,* 1988, 263, 10980-10988.

[66] Radmark O., Samuelsson B. 5-Lipooxygenase: mechanism of regulation. *J. Lip. Res*., **2009** , S40-45

[67] Ford-Hutchinson, A.W. FLAP: a novel drug target for inhibiting the synthesis of leukotrienes. *Trends Pharmacol. Sci*., **1991**, 12, 68- 70

[68] Haeggstrom, J.Z.; Funk, C.D. Lipoxygenase and leukotriene pathways: biochemistry, biology, and roles in disease. *Chem. Rev.,* **2011**, 111, 5866-5898.

[69] Du L., Zhang Z., Luo X., Chen K., Shen X., Jiang H.; Binding Investigation of Human 5-Lipooxygenase with ist Inhibitors by SPR Technology Correlating with Molecular Docking Simulation. *J.Biochem*. **2006**, 139, 715-723

[70] Fischer L., Steinhilber D., Werz O.; Molecular pharmacological profile oft he non –redox type 5-lipooxygenase inhibitor CJ-13, 610.

[71] Meirer K., Steinhilber D. and Proschak E.; Inhibitors of the Arachidonic Acid Cascade : Interfering with Multiple Pathways. *Basic Clin Pharmacol Toxicol.***, 2014,** 114 : 83-91

[72] Fisher L., Hornig M., Pergola C., Meindl N., Franke L., Tanrikulu, Dodt G., Schneider G., Steinhilber D., Werz O.; The molecular mechanism oft he inhibition by licofelone oft he biosynthesis of 5-lipooxygenase produts: *Br. J. Pharmacol.*, **2007** ,152:471-480

[73] Werz O., Steinhilber D. Therapeutic options for 5-lipoxygenase inhibitors. *Pharmacol Ther.* **2006**, 122: 701-718

[74] Levy, R. M.; Saikovsky, R.; Shmidt, E.; Khokhlov, A.; Burnett, B. P. *Nutr. Res*. **2009**, 29, 298–304.

[75] Ding C., Cicuttini F.; Licofelone (Merckle). *IDrugs* **2003**, 6:802-808

[76] Hay, R. J., Fungal skin infections.; *Arch. Dis. Child.* **1992**, 67:1065–1067

[77] Rippon, J. W.. Medical mycology: the pathogenic fungi and the pathogenic actinomycetes, 3rd ed., **1988**, p. 169–275. The W. B. Saunders Co., Philadelphia, Pa.

[78] Cohn MS. Superficial fungal infections: topical and oral treatment of common types. *Postgrad Med.* 1992;91:239-52.

[79] Weitzman, I., and R. C. Summerbell.; The dermatophytes. *Clin. Microbiol*. *Rev*. **1995**, 8:240–259.

[80] Alley R.K.M., Baker S.J., Beutner K.R., Plattner J.; Recent progress on the topical therapy of onychomychosis. **2007,** *Exp.Opin.Investig. Drugs* **2007,** 16, 2: 157-167

[81] Ryley J.F.; Chemotherapy of Fungal Diseases, Springer-Verlag **1990**

[82] D. Kerridge, The plasma membrane of Candida albicans and its role in the action of antifungal drugs, in The Eukaryotic Microbial Cell. *Advances in Microbial Physiology*, Society for General Microbiology Symposium,vol. 27 eds. B.A. Haddock and W.A. Hamilton

[83] Williams D.A., Lemke T.L.; Foye's principi di chimica farmaceutica; **2005,** Ed.Piccin

[84] C. A. Hitchcock, K. Dickinson, S. B. Brown, Purification and properties of cytochrome P-450 dependent 14 alpha-sterol demethylase from Candida albicans. *Biochem. J*. **1990,** 266, 475-480

[85] J. Li, Y. Wang, C. Yang, P. Wang, D.K. Oelschlager, Y. Zheng, D.-A. Tian, W.E. Grizzle, D.J. Buchsbaum, M. Wan, Polyethylene glycosylated curcumin conjugate inhibits pancreatic cancer cell growth through inactivation of Jab1 *Mol. Pharmacol.* **2009,** 76, 81-90.

[86] K. Mohoi, Y. Watanabe, Y. Yoshida, M. Satoh, K. Isobe, N. Sugimoto, Y. Tsuda; Synthesis of Glycosylcurcuminoids *Chem. Pharm. Bull,* **2003**, 51,1268-1272.

[87] L. Biasutto, E. Marotta , A. Bradaschia, M. Fallica, A. Mattarei, S. Garbisa , M.Zoratti , C.Paradisi, Soluble polyphenols: synthesis and bioavailability of 3,4',5-tri(alpha-D-glucose-3-O-succinyl) resveratrol. , *Bioorg. Med. Chem. Lett.,* **2009,** *19*, 6721–6724.

[88] C. Manach, A. Scalbert, C. Morand, C. Remesy, L. Jimenez, Polyphenols: food sources and bioavailability *Am. J. Clin. Nutr.* **2004**, *79*, 724-727.

[89] Agalave S.G., Maujan R.S., Pore S.V.; Click Chemistry: 1,2,3-Triazoles as Pharmacophores, *Chem.Asian.J.***2011**, 6, 2696-2718

[90] Jiang B.,Huang X., Yao H., Jiang J., Wu X., Jiang S., Wang Q., Lu T, Xu J.; Discovery of potential anti-inflammatory drugs: diaryl-1,2,4-triazoles bearing *N*-hydroxyurea moiety as dual inhibitors of cyclooxygenase-2 and 5-lipoxygenase, *Org.Biomol. Chem.,* **2014**, 12, 2114-2127

[91] Kolb H. C., Finn M. G., Shrpless K. B. ; Click Chemistry: Diverse Chemical Function from a Few Good Reactions, *Angew. Chem. Int. Ed.* **2001** , *40*, 2004-2021

[92] Anighoro, A;, Bajorath, J; Rastelli, G; Polypharmacology: Challenges and Opportunities in Drug Discovery, *J.Med.Chem* **2014.** 57, 19, 7874-7887

[93] Koeberle A, Munoz E., Appendino G.B., Minassi A., Pace S., Rossi A., Weinigel C., Barz D., Sautebin L., Caprioglio D., Collado J.A., Werz O.; SAR Studies on Curcumin's Pro-inflammatory Targets: Discovery of Prenylated Pyrazolocurcuminoids as Potent and Selective Novel Inhibitors of 5-Lipooxygenase, *J.Med.Chem.* **2014**, 57, 5638-5648

[94] Samuelsson, B.; Dahlen, S.; Lindgren, J. A. N. A.; Rouzer, C. A.; Serhan, C. N.; *Science*, **1987**, 237, 1171–1176.

[95] Steinhilber, D.; Hofmann, Recent advances in the Search of Novel 5-Lipoxygenase Inhibitors B.; *Basic Clin. Pharmacol. Toxicol*. **2014**, 114, 70–77.

[96] Osburn W.O.; Kensler T. W.; *Mutation Research* 659 **2008** , 31-39

[97] Cohn MS. Superficial fungal infections: topical and oral treatment of common types. *Postgrad Med.* 1992;91:239-52

[98] Suntres Z.E.; Liposomal antioxidants for protection against oxidant-induced damage, *Journal of Toxicology,* **2011**, 1–16

[99] Regev-Shoshani G., Shoseyov O., Bilkis I., Kerem Z.; Glycosylation of resveratrol protects it from enzymic oxidation. *Biochem.J.* **2003**, 374 : 157-163

[100] Ronald R.C., Lansinger J. L., Lillie T.S., Wheeler C.J.; Total Synthesis of Frustulosin and Aurocitrin. *J.Org. Chem.* **1982**, 47, 2541-2549

[101] Schmidt F., Rosnizeck I.C: Spoerner M., Kalbitzer H.R., Konig B.; Zinc(II)cyclen–peptide conjugates interacting with the weak effector binding state of Ras. Inorg. Chim. Acta **2011**, 38-48

[102] Suzuki A. Z., Watanabe T., Kawamoto M., Nishiyama K.,Yamashita H., Ishii M., Iwamura M., Furuta T.; Coumarin-4-ylmethoxycarbonyls as Phototriggers for Alcohols and Phenols. *Org. Let,t* **2003**, 5, 25, 4867-4870

[103] Samioto H., Kusano Y., Hiyama T., *Tetrahedron Lett.*, A mild procedure for hydrolysis of alkoxymethyl aryl ethers to give hydroxyarenes. A rational synthesis of ascofuranone. **1986,** 27, 14, 1607-1610

[104] Williams D. A.; Lemke T.L., Foye's Principi di chimica farmaceutica; IV Ed. Piccin, **2005**, 891-903

[105] Kolb H. C., Finn M. G., Shrpless K. B.; Click Chemistry: Diverse Chemical Function from a Few Good Reactions, *Angew. Chem. Int. Ed.* **2001** , *40*, 2004-2021

[106] Sanner M. F.; Python: a programming language for software integration and development. *J. Mol. Graphics Modell*. **1999**, 17, 57-61.

[107] Trott, O.; Olson, A. J., AutoDock Vina: Improving the speed and accuracy of docking with a new scoring function, efficient optimization, and multithreading. *J. Comput. Chem*. **2010**, 31, 455-461.

[108] Charman W. N. ; Lipids, Lipophilic drugs and oral drug delivery. Some emerging concepts. *J. Pharm. Sci.* **2000**, 89, 8, 967-975.

[109] Nassar A. F., Kamel A. M., and Clarimont C. ; Improving the decision-making process in the structural modification of drug candidates: enhancing metabolic stability. *Drug discovery today* **2004**, 9, 1020-1028

[110] Purser S., Moore P. R.,, Swallow S., Gouverneur V. ; Fluorine in medicinal chemistry; *Chem. Soc. Rev.,* **2008**, 37, 320–330

[111] Ojima I.; Exploration of Fluorine Chemistry at the Multidisciplinary Interface of Chemistry and Biology; *J.Org.Chem* **2013**, 78(13), 6358-6383.

[112] Boudreau L. H.; Picot N.; Doiron J.; Villebonnet B.; Surette M. E.; Robichaud A. G.; Touaibia M.; Caffeoyl and cinnamoyl clusters with anti-inflammatory and anti-cancer effects. Synthesis and structure-activity relationship; *New J. Chem.* **2009**, 33, 1932-1940.

[113] Evens R. A. ; The rise of Azide-Alkyne 1,3-Dipolar 'Click' Cycloaddition and its application to Polymer Science and Surface Modification; *Aust. J. Chem.*, **2007**, 60, 384-395

[114] Encyclopedia of Polymer Science and Technology. Copyright 2009, Jhon Wiley & Sons, Inc.

[115] Werz O., Planta Med. **2007,** 73, 1331-1357.

[116] Hanke T., Dehm F., Liening S., Popella S.D., Maczewsky J., Pillong M., Kunze J., Weinigel C., Barz D., Kaiser A., Wurglics M., Lämmerhofer M., Schneider G., Sautebin L., Zsilavecz M.S., Werz O. ; Aminothiazole-Featured Pirinixic Acid Derivatives As Dual 5-Lipoxygenase and Microsomal Prostaglandin E2 Synthase-1 Inhibitors with Improved Potency and Efficiency in Vivo. *J. Med. Chem.*, **2013**, *56*, 22: 9031–9044

[117] Pergola C., Dodt G., Rossi A., Neunhoeffer E., Lawrenz B., Northoffer H., Samuelsson B., Rådmark O., Sautebin L., Werz O.; ERK-mediated regulation of leukotriene biosynthesis by androgens: A molecular basis for gender differences in inflammation and asthma. PNAS **2008,** 105, *50*, 19881-19886

[118] Biasutto L., Marotta E., De Marchi U., Zoratti M., Paradisi C.; Ester-Based Precursors to Increase the Bioavailability of Quercetin**.** *J. Med. Chem.* **2007,** *50,* 241-253

[119] Fisher L., Hornig M., Pergola C., Meindl N, Franke L, Tanrikulu, Dodt G., Schneider G., Steinhilber D., Werz O.; The molecular mechanism of the inhibition by licofelone of the biosynthesis of 5-lipoxygenase products. *Br. J. Pharmacol.***2007,** *152*, 471-480

[120] Moon J.K. , Shibamoto T., Antioxidant Assays for Plant and Food Components. *J. Agric. Food Chem.* **2009,** *57,* 1655–1666

[121] Sanchez M.C; Review: Methods used to evaluate the free radical scavenging activity in foods and biological systems. *Food Sci. Technol. Int.* **2002**, *8*, 121–137.

[122] Wang M, Li J. , Rangarajan M.,‡ Shao Y., LaVoie E.J., Huang T.C., Ho C.T., *J. Agric. Food Chem.* **1998,** *46,* 4869□4873

[123] Benzie I.F.F., Strain J.J.; The ferric reducing ability of plasma as a measure of antioxidant power: the FRAP assays. Analytical Biochemistry, 1996, 239: 70-76

[124] Xu G., Ye X., Chen J., Liu D.; Effect of Heat Treatment on the Phenolic Compounds and Antioxidant Capacity of Citrus Peel Extract *J. Agric. Food Chem.* **2007**, 55, 330−335

[125] Fischer L, Szellas D, Rådmark O, Steinhilber D, Werz O., Phosphorylation- and stimulus-dependent inhibition of cellular 5-lipoxygenase activity by nonredox-type inhibitors. FASEB J. **2003**;*17*:949–951.

[126] Koeberle A., Northoff H., Werz O. Identification of 5-lipoxygenase and microsomal prostaglandin E2synthase-1 as functional targets of the anti-inflammatory and anti-carcinogenic garcinol, Biochem. Pharmacol. **2009,** 77:1513–1521

[127] Werz O., Burkert E., Samuelsson B., Radmark O., and Steinhilber D. Activation of 5-lipoxygenase by cell stress is calcium independent in human polymorphonuclear leukocytes. *Blood* **2002**, 99: 1044–1052.

[128] Leo A., Hansch C. , Elkins D. ; Partition coefficients and their uses. *Chem. Rev.*, **1971,** 71, 6: 526-616

[129] Lipinski, C. A., Lombardo, F., Dominy, B. W., & Feeney, P. J.; Experimental and computational approaches to estimate solubility and permeability in drug discovery and development settings. *Advanced Drug Delivery Reviews*, **1997**, 23 (1 -3), 3 -25.

[130] Veber D.F., Johnson R.S., Cheng H.Y., Smith B.R., K.W., Kopple K.D.; Molecular Properties That Influence the Oral Bioavailability of Drug Candidates. *J.Med.Chem* **2002,** 2615-2623

[131] Wenlock M.C., Austin R.P., Barton P., Davis A.M., Leeson P.D.; A comparison of physiochemical property profiles of development and marketed oral drugs. *J.Med.Chem* **2003,** 27, 46, 7:1250-6

[132] http://www.chemaxon.com

[133] Klopman G., Li J.Y. , Wang S., Dimayuga M.; Computer Automated log P Calculations Based on an Extended Group Contribution Approach. *J. Chem. Inf. Comput. Sci.*, **1994**, 34, 4:752–781